B Cell Perturbations in HIV-1 Infection

Dissertation

zur

Erlangung der naturwissenschaftlichen Doktorwürde
(Dr. sc. nat.)

vorgelegt der

Mathematisch-naturwissenschaftlichen Fakultät

der

Universität Zürich

von

Thomas Andreas Liechti

von

Landiswil BE

Promotionskommission

Prof. Dr. Alexandra Trkola (Leitung der Dissertation)
Prof. Dr. Huldrych F. Günthard
Prof. Dr. Annette Oxenius
Prof. Dr. Heribert Stoiber

Zürich, 2017

Table of Contents

1. Research Summary

HIV-1 infection is accompanied by profound B cell alterations that impede responsiveness to novel antigens. Disease progression leads to loss of lymphoid architecture affecting the development of high-affinity antibody responses, polyclonal B cell activation, hypergammaglobulinemia and increased frequencies of activated (AM) and exhausted tissue-like (TLM) memory B cells. Despite these severe perturbations the elicitation of potent broadly neutralizing antibodies (bnAbs) against HIV-1 depends on years of exposure to HIV-1. Definition of why bnAbs preferentially develop in a stage where B cell responses generally are impaired is of outmost importance as current vaccine development struggles to elicit bnAb responses.

The aim of my thesis was to provide the basis for future research aiming to resolve the evolution of bnAb responses by establishing a comprehensive phenotypic map of peripheral B cell subsets in healthy and HIV-1 infected individuals that can be utilized to reveal B cell signatures related to HIV-1 infection that may be associated with the induction of potent neutralizing antibody responses.

The first experimental chapter of my thesis (Chapter 2.1) describes the development of a 16 color flow cytometry panel that was developed to define phenotypic alterations. To obtain insights into the dynamics of B cell repertoire alterations in HIV-1 infection I analyzed the composition of the B cell population during acute and chronic HIV-1 infection and assessed the effect of antiretroviral treatment (ART) in work described in Chapters 2.2. and 2.3.

Chapter 2.2 describes the emergence of $CD21^{neg}$ naïve and $CD21^{neg}$ marginal zone (MZ) B cells during HIV-1 infection. These subsets are characterized by altered chemokine receptor signatures switching their migration potential from lymphoid tissues to sites of inflammation. Functional analysis suggests that $CD21^{neg}$ naïve and $CD21^{neg}$ MZ B cells are activated and anergic based on increased CD95 and FcRL4 expression, increased frequency of proliferating cells and impaired response to BCR-mediated stimulation. Collectively the data suggest that HIV-1 infection leads to the accumulation of large fractions of anergic naïve and MZ B cells that are impaired in responding to their cognate antigen. The identification of these subsets highlights that even antigen-inexperienced B cells are affected by HIV-1 infection and with this a crucial cell population required for elicitation of *de novo* responses is impaired in HIV-1 infection.

Chapter 2.3 describes a detailed analysis of the memory B cell and plasmablast compartment in the same patient cohort. Using computational algorithms for dimensionality reduction (t-SNE) and clustering (SPADE/Ward's hierarchical clustering) to process the high-content cytometry data, the study revealed a previously underappreciated phenotypic diversity of memory B cells beyond subsets stratified for expression of B cell receptor isotype and classification by CD21/CD27 expression. Likewise, I identified a phenotypic variability among plasmablasts. Importantly, the newly defined clusters of memory B cells and plasmablasts show unique dynamics during HIV-1 infection and some alterations are not reversed when ART is initiated late highlighting the complexity of HIV-1 dependent B cell alterations. Surprisingly, t-SNE analysis revealed that $IgG3^{pos}$ memory B cells contain the highest levels of AM and TLM B cells compared to IgA- and IgG1-expressing memory B cell subsets in healthy and HIV-1 infected individuals. Furthermore $IgG3^{pos}$ resting memory B cells are characterized by expression of chemokine receptor signature associated with activation suggesting that induction of IgG3 responses have distinct requirements in terms of activation or characteristics of antigen resulting in more pronounced activation phenotype.

In summary, I established in my thesis an in-depth phenotypic analysis of the peripheral B cell compartment that revealed a highly complex landscape of B cell subsets both in healthy donors and HIV-1 infection. Dynamics of these subsets at different disease stages that my studies revealed will aid future functional studies aiming to define relevant B cell subsets that are linked with the development of bnAbs.

2. Zusammenfassung

Die HIV-1 Infektion führt zu ausgeprägten B Zell-Veränderungen, die eine Beeinträchtigung der Antikörperantwort gegen neue Antigene zur Folge hat. Im Verlauf der Krankheit wird die Architektur der Lymphorgane beschädigt und dadurch die Entwicklung hoch-affiner Antikörper gestört. Zusätzlich treten polyklonale B–Zell-Aktivierung, Hypergammaglobulinämie und vermehrt aktivierte (AM) und erschöpfte Gewebe-ähnliche (TLM) Gedächtnis-B Zellen auf. Trotz dieser Veränderungen bilden sich in manchen HIV-1 infizierten Patienten potente breit-neutralisierende Antikörper (bnAbs) gegen HIV-1 aus. Die Entwicklung dieser bnAbs benötigt jedoch mehrere Jahre aktive HIV-1 Infektion. BnAbs treten demnach mehrheitlich in einem Stadium der Infektion auf, welches von Beeinträchtigung der B Zellen geprägt ist. Es ist von speziellem Interesse, die Gründe dafür zu definieren, da es Ziel der HIV-Impfstoffentwicklung ist, solche bnAbs zu induzieren, dies sich aber als äusserst schwierig erwiesen hat.

Das Ziel meiner Dissertation bestand darin, eine umfangreiche phänotypische Analyse der peripheren B Zell-Subtypen in gesunden und HIV-1 infizierten Menschen zu erstellen, welche die zukünftige Erforschung der Entwicklung von bnAbs unterstützt. Fokus meiner Untersuchungen war es B Zell-Signaturen zu definieren, welche charakteristisch für eine HIV-1 Infektion sind und dadurch möglicherweise mit der Entwicklung von potenten Antikörperantworten gegen HIV-1 assoziiert sein könnten.

Im ersten Kapitel der Resultate meiner Dissertationsarbeit (Kapitel 2.1) wird die Entwicklung eines 16-Farben Durchflusszytometrie-Färbepanels beschrieben, das ich speziell entwickelt habe um phänotypische Veränderungen an B Zellen bestimmen zu können. Mit diesem Panel habe ich in Folge B Zellen während der akuten und chronischen Phase der HIV-1 Infektion analysiert, um die B Zell-Dynamik während der HIV-1 Infektion zu bestimmen und mit gesunden Spendern verglichen. Zusätzlich habe ich die Wirksamkeit der anitretroviralen Therapie (ART), HIV-1 abhängige B Zell-Veränderungen zu normalisieren, ermittelt. Diese Analysen sind in Kapitel 2.2 und 2.3 beschrieben.

Kapitel 2.2 beschreibt das Auftreten von $CD21^{neg}$ naiven und $CD21^{neg}$ Marginalzonen (MZ) B Zellen. Diese B Zell-Subtypen zeigen eine veränderte Expression von Chemokinrezeptoren auf, welche die Migration zu Lymphorganen reduziert und stattdessen die Migration zu Entzündungsorten fördert. Funktionelle Analysen zeigten, dass $CD21^{neg}$ naive und $CD21^{neg}$ MZ B Zellen eine erhöhte Expression von CD95 und FcRL4, erhöhte Häufigkeit an proliferierenden

Zellen und beeinträchtigte Reaktion auf Stimulierung aufweisen. Dies deutet darauf hin, dass, diese Zellen aktiviert und anergisch sind. Eine HIV-1 Infektion scheint daher zu einem Auftreten von $CD21^{neg}$ naiven und $CD21^{neg}$ MZ B Zellen, die in ihrer Funktion gestört sind, zu führen. Dadurch sind im HIV-1 infizierten Menschen ein grosser Teil von antigen-unerfahrenen B Zell-Subtypen beeinträchtigt, welche eine wichtige Rolle für *de novo* Antikörperantworten spielen.

Kapitel 2.3 beschreibt eine detaillierte Analyse der Gedächtnis-B Zellen und Plasmablasten innerhalb der gleichen Patienten. Dabei wurden mittels automatisierten Algorithmen zur Dimensionsreduktion (t-SNE) und Clusteranalyse (SPADE/Ward-basierende hierarchische Clusteranaylse) die multidimensionalen Durchflusszytometrie-Daten analysiert. Die Analysen zeigten, dass Gedächtnis-B Zellen eine hohe Diversität aufweisen, die über die Definition von Subtypen über exprimierte B Zellrezeptor-Isotypen und der Klassifizierung basierend auf CD21/CD27 hinausgeht. In ähnlicher Weise konnte ich eine phänotypische Diversität von Plasmablasten aufzeigen. Die in dieser Studie neu definierten Cluster von Gedächtnis-B Zellen und Plasmablasten zeigen unterschiedliche Dynamiken während der HIV-1 Infektion auf. Zudem konnten einige HIV-1 induzierte Veränderungen mittels ART nicht normalisiert werden, wenn die Therapie zu einem späten Zeitpunkt der HIV-1 Infektion begonnen wurde, was die Komplexität der HIV-1 abhängigen B Zell-Veränderungen weiter unterstreicht. Interessanterweise zeigte die t-SNE Analyse, dass $IgG3^{pos}$ Gedächtnis-B Zellen in gesunden und HIV-1 infizierten Personen im Vergleich zu IgA- und IgG1-exprimierenden B Zellen die höchsten Werte an AM und TLM B Zellen aufweisen. Zusätzlich zeigen ruhende $IgG3^{pos}$ Gedächtnis-B Zellen ein Expressions-muster von Chemokinrezeptoren, welches mit B Zell-Aktivierung assoziiert ist. Dies deutet darauf hin, dass es Unterschiede in der Entwicklung der verschiedenen Isotypen-Antworten gibt und IgG3 Antikörperantworten eventuell andere Voraussetzungen in Bezug auf Aktivierung oder Antigene benötigt, die auch den Phänotyp mitbestimmen.

Zusammenfassend habe ich im Rahmen dieser Dissertation eine vertiefte phänotypische Analyse der peripheren B Zellen durchgeführt, welche die Komplexität der B Zellen in gesunden und HIV-1 infizierten Patienten aufzeigt. Die in dieser Arbeit beschriebenen HIV-1 abhängigen Dynamiken dieser B Zell-Subtypen, können zukünftige Studien unterstützen, die zum Ziel haben, die für die Entwicklung von bnAbs relevanten B Zell-Subtypen zu untersuchen.

3. Introduction

3.1 B cell biology

3.1.1 B cell development

The development of mature B cells from hematopoietic stem cells (HSC) is a complex process taking place in the bone marrow where B cell progenitors transit several developmental stages associated with a tightly regulated program with the goal to acquire a functional and diverse yet not autoreactive B cell receptor [reviewed in (LeBien and Tedder 2008; Melchers 2015)]. The transition from HSC to early B cell progenitors is characterized by expression of enzymes such as RAG1/2 and TdT important for V(D)J recombination, an important step resulting in the unique diversity of B cell receptors (LeBien 2000; LeBien and Tedder 2008; Schatz and Ji 2011). The human immunoglobulin loci contains multiple genes for V (variable), D (diversity) and J (joining) elements resulting in a first line of B cell receptor diversity (Lefranc 2001; Watson, Steinberg et al. 2013). The enzyme TdT randomly extends the DNA double breaks initiated during V(D)J recombination by randomly adding and removing nucleotides, which ensures an additional level of B cell receptor (BCR) diversity [reviewed in (Schatz and Ji 2011; Schatz and Swanson 2011)]. During the development to mature B cells the D-J and subsequent V-D-J recombination happens in early and pro-B cells, respectively [reviewed in (LeBien 2000; LeBien and Tedder 2008)]. These two subsets are the earliest committed to the B cell fate and include important steps to guarantee the expression of the pre-BCR receptor [reviewed in (LeBien 2000; Monroe 2006; LeBien and Tedder 2008)]. This receptor is composed of a mature heavy chain associated with a surrogate light chain (SLC) containing the λ5 and VpreB proteins [reviewed in (Monroe 2006)]. It has been shown that mice lacking the SLC have a dramatically delayed development of mature B cells pinpointing to an important function of a proper pre-BCR (Kitamura, Kudo et al. 1992). The pre-BCR supports the development of B cell progenitors into mature cells by providing tonic BCR signaling, an important survival and proliferation signal (Monroe 2006; Nemazee 2006). The pre-B cell subsets, divided in subsets I and II, initiate VJ recombination of the light chain and as these cells become immature B cells they express a functional mature BCR (LeBien 2000; LeBien and Tedder 2008). However, a high fraction of these cells express autoreactive BCR and could be potentially harmful when leaving the bone marrow [reviewed in (Pillai, Mattoo et al. 2011; Melchers 2015)]. In order to eliminate or edit autoreactive BCR several immune tolerance mechanisms occur which involve deletion by apoptosis, receptor editing or anergy [reviewed in (Meffre and Wardemann 2008; Meffre 2011; Melchers 2015)]. The fate of an autoreactive B cell is determined by its affinity to the autoantigen (Lang, Jackson et al. 1996; Nemazee 2006).

Strong affinity results in apoptosis whereas intermediate affinity initiates the process of receptor editing [reviewed in (Nemazee 2006)]. In case of cells with low affinity the state of unresponsiveness defined as anergy can be induced and these B cells egress from bone marrow [reviewed in (Nemazee 2006)]. Receptor editing includes the exchange of the light chain or the replacement of the V_H element altering the specificity of the BCR [reviewed in (Nemazee 2006)]. *In vivo* studies in mice support the high efficiency of receptor editing in altering autoreactive BCR and that the majority of autoreactive B cells are edited rather than deleted (Halverson, Torres et al. 2004). Dysregulated immune tolerance can result in the emergence of autoreactive naïve B cells as observed for autoimmune and inflammatory diseases such as systemic lupus erythematodes (SLE) and rheumatoid arthritis (RA) [reviewed in (Meffre and Wardemann 2008)]. Impaired BCR signaling and dysregulated soluble factors regulating B cell survival such as B cell-activating factor of the tumor-necrosis family (BAFF) are observed among these diseases and are thought to contribute to the survival and egress of autoreactive mature B cells into the periphery [reviewed in (Meffre and Wardemann 2008; Meffre 2011)]. Edited immature B cells egress the bone marrow and are defined as transitional B cells developing into mature naïve B cells in the periphery (Chung, Silverman et al. 2003; Sims, Ettinger et al. 2005).

3.1.2 B cell activation and Germinal center reaction

In order to scan the environment for antigens naïve B cells shuttle constantly between the periphery and lymphoid tissues such as lymph nodes or the spleen (von Andrian and Mempel 2003; Coelho, Natale et al. 2013). Lymph nodes are highly specialized tissues to guarantee optimal and efficient immune responses and contain areas designated for B and T cells called B cell follicle and T cell area, respectively [reviewed in (von Andrian and Mempel 2003; Lederman and Margolis 2008; Batista and Harwood 2009)]. B cell follicles are adjacent to T cell areas and the subcapsular sinus (SCS) (Junt, Moseman et al. 2007; Phan, Grigorova et al. 2007; Kuka and Iannacone 2014). The location of these areas guarantees efficient drainage of antigens from the SCS and close proximity of T cells in T cell area, respectively, to initiate optimal B cell responses [reviewed in (Batista and Harwood 2009; Roozendaal, Mempel et al. 2009; Gonzalez, Degn et al. 2011)]. The B cell follicles contain mostly mature B cells and a network composed of follicular dendritic cells (FDC) whereas the T cell area is characterized by fibroblastic reticular cells (FRC) [reviewed in (von Andrian and Mempel 2003)]. The latter express CCL19 and CCL21, which are important chemokines attracting CCR7-expressing cells such as B cells, T cells and dendritic cells (DC) (Link, Vogt et al. 2007; Fletcher, Acton et al. 2015). B cells are usually entering the lymph node via high endothelial venules (HEV) by attaching to the endothelial cells via L-selectin (CD62L) and

LFA-1, a process which requires CCR7 signaling (von Andrian and Mempel 2003; Park, Hwang et al. 2012; Coelho, Natale et al. 2013). B cells in the lymph node move along the FRC network in a CXCR5- and LFA-1-dependent manner towards B cell follicles in mice (von Andrian and Mempel 2003; Coelho, Natale et al. 2013). The FDC in the follicles produce CXCL13 which results in a gradient from the follicle into the T cell area attracting B cells known to express high levels of CXCR5, the receptor for CXCL13, to the follicle (Ansel, Ngo et al. 2000; Heesters, Myers et al. 2014). The CXCL13/CXCR5 axis plays a crucial role in attracting B and T cells to and allowing entrance into B cell follicles in order to optimally induce germinal center reaction (Cyster 2010; Griffith, Sokol et al. 2014).

FDC express high levels of complement receptor 1 (CR1; CD35) and 2 (CR2; CD21) and show the ability to retain and present complement-opsonized antigens and immune complexes to B cells in the follicle (Roozendaal and Carroll 2007; Heesters, Chatterjee et al. 2013; Heesters, Myers et al. 2014). Interestingly, FDC show the ability to present the antigens for prolonged time in the range of weeks to months (Heesters, Chatterjee et al. 2013; Heesters, Myers et al. 2014). The prolonged retention of antigens ensures the maintenance of the GC and GC-associated processes such as SHM to improve antibody responses (Heesters, Chatterjee et al. 2013; Heesters, Myers et al. 2014). Since antigens are derived from afferent lymphatic vessels and only antigens with less than 70 kDa can diffuse through the porous layer of SCS macrophages it was for a long time puzzling how bigger antigens can reach the follicles (Kuka and Iannacone 2014). It has been shown that SCS macrophages can take up antigens in a complement- and Fc receptor-dependent manner and present them on the basal site adjacent to the follicles (Junt, Moseman et al. 2007; Batista and Harwood 2009; Gonzalez, Degn et al. 2011; Kuka and Iannacone 2014). Naïve B cells can shuttle the opsonized antigens from the SCS macrophages to FDC transferring the antigens to sites of antigen presentation in the follicle (Phan, Grigorova et al. 2007; Cinamon, Zachariah et al. 2008). Although antigen presentation via FDC is thought to be the main mechanism of B cell activation there are others such as capturing of dendritic cell (DC)-derived antigens in the T cell area or soluble small antigens diffusing into the follicles [reviewed in (Batista and Harwood 2009)]. The former requires that DC do not digest the antigens since B cells can recognize the antigens in their native form [reviewed in (Batista and Harwood 2009)]. T cell area-resident DC are shown to present antigens to B cells through several mechanisms such as on FcRγIIB or DC-SIGN (DC-specific ICAM-3 grabbing non-integrin; CD209), both receptors inducing internalization into compartments not associated with protein denaturation and digestion (Bergtold, Desai et al. 2005; Batista and Harwood 2009). While Fc receptors can only bind immune complexes through the Fc region of the antibodies, DC SIGN is a type II C-type lectin receptor and can bind carbohydrate moieties of antigens directly [reviewed in (Svajger, Anderluh et al. 2010)]. B cells recognizing

antigens via their BCR become activated and migrate towards the border of the T and B cell area (Figure 1A) (Liu, Zhang et al. 1991; Okada, Miller et al. 2005). Activated B cells present antigen via MHCII to interact with antigen-specific T cells for prolonged time and to thereby receive T-cell help that supports B cell proliferation and differentiation into GC B cells or short-lived plasmablasts (Figure 1A) (Parker 1993; Okada, Miller et al. 2005). The decision between differentiation towards GC B cells or plasmablasts is affinity-dependent with high-affinity antigen binding associated with differentiation towards extrafollicular plasmablasts (Mills and Cambier 2003; Paus, Phan et al. 2006; Schwickert, Victora et al. 2011). Interestingly, extrafollicular plasmablasts further divide and express activation-induced deaminase, an important enzyme for somatic hypermutation (SHM) [reviewed in (Zhang, Garcia-Ibanez et al. 2016)]. This suggests that extrafollicular plasmablasts known to be important for the early antibody response possess the ability to adapt and improve the early antibody response although excluded from the GC (Toellner, Jenkinson et al. 2002; MacLennan, Toellner et al. 2003). However, extrafollicular plasmablasts are shown to only slightly increase mutations in the variable regions (Toellner, Jenkinson et al. 2002; Zhang, Garcia-Ibanez et al. 2016). Interestingly, antibody responses against Salmonella have been shown to develop extrafollicularly emphasizing that dependent on the antigen different mechanism of antibody response maturation can occur (Di Niro, Lee et al. 2015).

The T:B cell interaction clusters can be observed within 1-2 days after antigen administration and subsequently a fraction of activated B cells differentiating into GC B cells migrate back to the follicle where they build a foci close to the FDC network characterized by proliferating blasts [reviewed in (De Silva and Klein 2015)]. During the T:B cell interactions class-switch recombination (CSR) occurs highlighting that switching to another isotype can occur early and before affinity maturation [reviewed in (Toellner, Gulbranson-Judge et al. 1996; Toellner, Luther et al. 1998; Zhang, Garcia-Ibanez et al. 2016)].

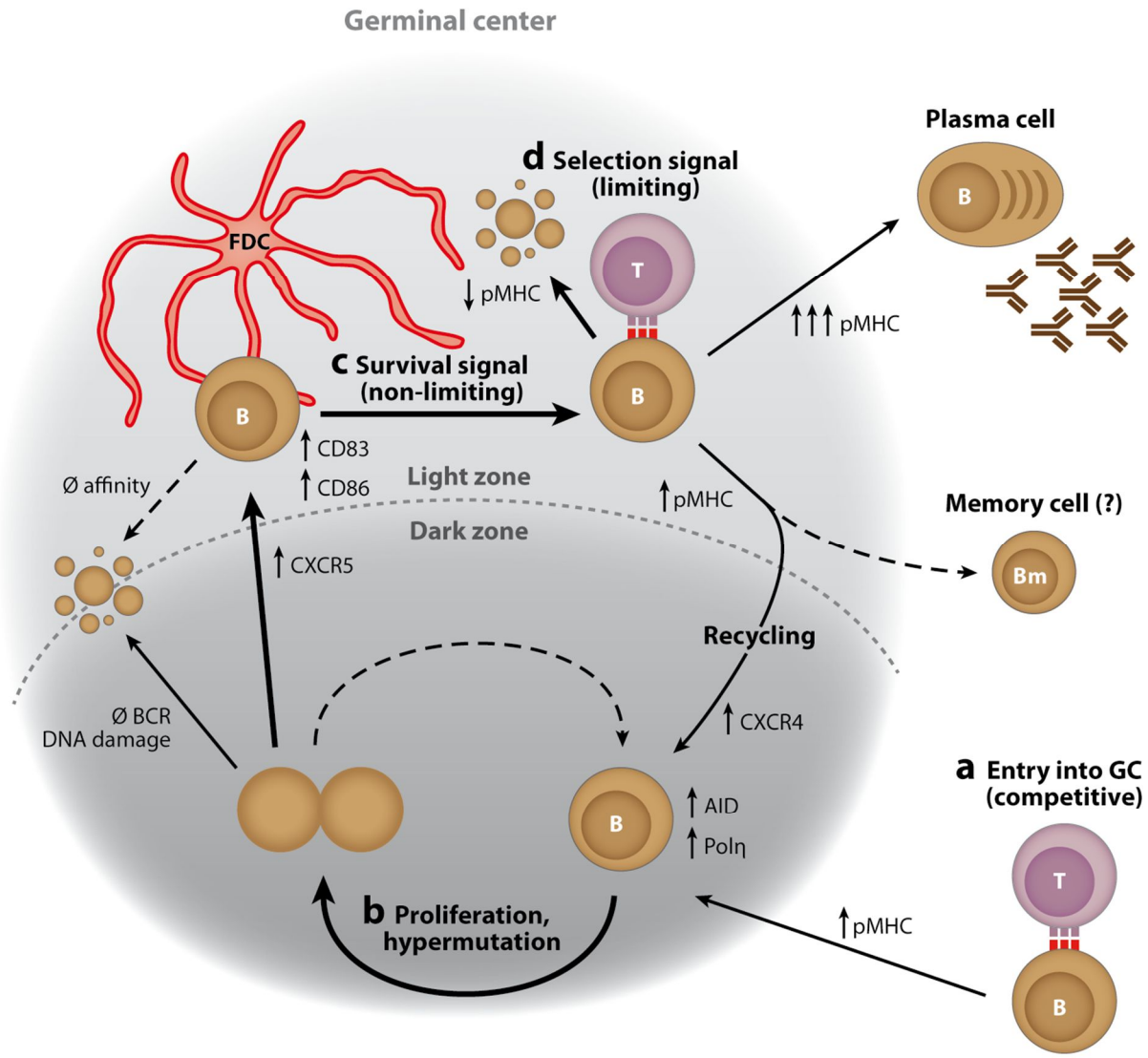

Figure 1: Germinal center (GC) reaction and development of high-affinity antibodies

(A) T:B cell interaction results in full activation of B cells and differentiation to GC B cells, migration to B cell follicle and GC formation. *(B)* GC B cells proliferate in the dark zone of the GC. During this process somatic hypermutation (SHM) occurs. *(C)* After several rounds of proliferation and SHM GC B cells migrate to the light zone, capture antigens presented on the surface of FDC, process and present the antigens via MHC II to T_FH cells. *(D)* GC B cells receiving sufficient T cell help re-enter the dark zone by up-regulating CXCR4 while GC B cells lacking T cell help undergo apoptosis. After several rounds of proliferation and SHM and selection based on T_FH cell help GC B cells leave the GC and become either memory B cells or plasma cells. Reprinted by permission from Annual Reviews: *Annual Reviews Immunology* 30: 429-457. © 2012.

The activated T cells can further differentiate into follicular helper T cells (T_FH) characterized by expression of CXCR5, PD-1, ICOS and the master regulator bcl-6 and secretion of IL-4 and IL-21 [reviewed in (De Silva and Klein 2015; Vinuesa, Linterman et al. 2016)]. IL-21 is

known to support a plethora of pathways of T cell-dependent B cell responses (Ettinger, Sims et al. 2005; Good, Bryant et al. 2006; Ettinger, Kuchen et al. 2008; Linterman, Beaton et al. 2010; Zotos, Coquet et al. 2010; Crotty 2011; Eto, Lao et al. 2011; Lee, Rigby et al. 2011; Deenick, Avery et al. 2013; Moens and Tangye 2014; Spolski and Leonard 2014; Tangye 2015). This differentiation results in the re-location of T_FH cells into the B cell follicle [reviewed in (De Silva and Klein 2015; Vinuesa, Linterman et al. 2016)]. After 5-7 days the follicle is highly expanded due to the rapid proliferation of GC B cells and a polarization of the GC occurs with the dark zone characterized by proliferating B cells and the light zone where FDC and T_FH cells are located [reviewed in (Victora and Nussenzweig 2012; Victora and Mesin 2014; De Silva and Klein 2015)]. The dark zone is characterized by a network of reticular cells expressing CXCL12 [reviewed in (Victora and Nussenzweig 2012; Victora and Mesin 2014; De Silva and Klein 2015)]. Proliferating B cells in the dark zone express high levels of CXCR4 and are therefore attracted to this site (Victora, Schwickert et al. 2010; Victora, Dominguez-Sola et al. 2012), where they undergo SHM resulting in randomly distributed mutations and diversification of the BCR (Figure 1B). GC B cells in the dark zone down-regulate CXCR4 and up-regulate co-stimulatory molecules CD80 and CD86 and transit to the light zone of the GC where selection of B cell clones with the highest affinity for antigens occur (Figure 1C and D) (Victora, Schwickert et al. 2010; Victora and Nussenzweig 2012; Victora and Mesin 2014; De Silva and Klein 2015). B cells are shuttling between light and dark zone of the GC in a CXCR4-dependent manner and undergo several cycles of affinity-based selection and proliferation before leaving the GC.

What factors limit selection of B cells with highest affinity has been debated for long [reviewed in (Victora and Nussenzweig 2012)]. One possibility is that the antigen presented by FDC is limiting and therefore only high-affinity clones can capture, process and present a sufficient amount of antigen via MHC class II to T_FH cells [reviewed in (Victora and Nussenzweig 2012)]. However, others reported that the availability of antigens on FDC may not be limited. Therefore high-affinity B cell clones can process and present more antigens and thus are more likely to receive sufficient T cell help in the light zone from the limited numbers of T_FH cells and as a result continue to migrate to the dark zone for further proliferation and SHM instead of undergoing apoptosis due to “death-by-neglect” (Figure 1C and D) (Victora, Schwickert et al. 2010; Victora and Nussenzweig 2012). The strength of the T cell help in the light zone determines the proliferation rate and SHM of GC B cells highlighting that high-affinity B cell clones undergo an enhanced selection and maturation resulting in large clonal families within the GC (Gitlin, Mayer et al. 2015; Mesin, Ersching et al. 2016; Tas, Mesin et al. 2016). Interestingly the existing antibody repertoire can compete with the B cell clones for antigens in the GC and therefore support affinity maturation by

outcompeting B cells with lower affinity than the antibody repertoire [reviewed in (Zhang, Garcia-Ibanez et al. 2016)].

GC B cells differentiate into memory B cells and plasma cells after undergoing GC reaction [reviewed in (De Silva and Klein 2015)]. Memory B cells are characterized by long persistence in the body and the unique ability to respond to re-occurring antigens with fast kinetics and potency (Amanna, Carlson et al. 2007; Kurosaki, Kometani et al. 2015). The determinants of the memory B cell or plasma cell fate are less well known than the GC reaction and is partially due to technical limitations foremost the accessibility of these cells [reviewed in (Mesin, Ersching et al. 2016)]. There are several factors known to contribute to plasma cell differentiation which are in agreement with T cell help such as CD40:CD40L interaction, IL-21 and PD-1 resulting in a dramatic change of transcriptional signature [reviewed in (Nutt, Hodgkin et al. 2015)]. CD40 ligation is associated with increased expression of the transcription factor IRF4 which results in down-regulation of Bcl-6, the master transcriptional factor for GC B cells. In addition differentiation of plasma cells is associated with up-regulation of the transcription factors Blimp-1 and XBP-1, which coincides with down-regulation of Bcl-6 and up-regulation of IRF4 (Klein, Casola et al. 2006; Todd, McHeyzer-Williams et al. 2009; Victora and Nussenzweig 2012; Nutt, Hodgkin et al. 2015; Minnich, Tagoh et al. 2016). Although the mechanisms of memory B cell and plasma cell differentiation are well characterized it is poorly understood what the decisive factors are that induce differentiation into the different post-GC subsets (Good-Jacobson and Shlomchik 2010; Shlomchik and Weisel 2012). It has been shown that memory B cells and plasma cells can derive from the same GC B cell clone suggesting that descendants of naïve B cells can differentiate into distinct subsets and that naïve B cells can reconstitute a variety of different subsets as elegantly shown by *in vivo* limiting dilution studies in mice (Taylor, Pape et al. 2015). The kinetics of GC egress shows that cells leaving GC early are committed to the memory B cell fate whereas plasma cells occur at later stages during the GC maturation (Shlomchik and Weisel 2012; Weisel, Zuccarino-Catania et al. 2016). This is supported by *in vivo* experiments with impaired functions of important GC-related molecules resulting in premature termination of the GC reaction. As a consequence the formation of plasma cells was abrogated whereas the memory B cell differentiation remained intact [reviewed in (Good-Jacobson and Shlomchik 2010; Shlomchik and Weisel 2012)]. Isotype switching and differentiation of plasma cells are thought to be stochastic processes linked to number of divisions suggesting that B cell-intrinsic mechanism can determine memory B cell and plasma cell differentiation (Hasbold, Corcoran et al. 2004). Interestingly cytokines can influence the division numbers necessary to differentiate into plasma cells *in vitro* suggesting that many factors play a role and that the differentiation between memory B cells and plasma cells is tightly regulated (Hasbold, Corcoran et al. 2004). In contrast to plasma cells, memory

B cells are able to re-enter the GC reaction during secondary immune responses resulting in further diversification of their BCR which allows the maturation of memory B cells towards higher affinities (Bende, van Maldegem et al. 2007; McHeyzer-Williams, Milpied et al. 2015).

3.1.3 T cell-independent B cell responses

Antibody responses against highly ordered repetitive antigens can be induced without T cell help (Bachmann, Rohrer et al. 1993; Mond, Lees et al. 1995; Vos, Lees et al. 2000). These T cell-independent (TI) antigens can be divided in two subgroups. TI-1 antigens are mitogenic interacting through antigen-unspecific mechanism whereas TI-2 antigens are repetitive and highly-ordered as seen for bacterial polysaccharides or viral particles (i.e. vesicular stomatitis virus) (Bachmann, Rohrer et al. 1993; Zinkernagel 1996; Mond and Brunswick 2003; Hangartner, Zinkernagel et al. 2006). T cell-independent B cell responses require multivalent B cell receptor cross-linking and cluster formation in combination with additional stimulation such as Toll-like receptor signaling [as reviewed in (Vos, Lees et al. 2000)]. An additional signal for T cell-independent responses can be provided by the CD19/CD21 complex, which has been shown to modulate the threshold of B cell activation enhancing stimulation (Vos, Lees et al. 2000; Cherukuri, Cheng et al. 2001; Roozendaal and Carroll 2007). T cell-independent B cell responses have been proven to be important for vaccines against polysaccharides such as *Streptococcus pneumoniae* although their efficiency could be improved when switched to T cell-dependent immune responses by conjugating polysaccharides to proteins [reviewed in (Avci and Kasper 2010; Nuccitelli, Rinaudo et al. 2015)].

Two major B cell subsets are described with the ability to undergo T cell-independent B cell responses, namely B1 and marginal zone (MZ) B cells (Martin, Oliver et al. 2001). B1 cells were first described in mice and are thought to act as a first line of defense through secretion of natural polyreactive IgM and are therefore sometimes referred as innate-like B cells (Baumgarth 2013). However, although B1 cells can be readily detected in the peritoneal and pleural cavities of mice the identification of this subset in human is controversial (Descatoire, Weill et al. 2011; Griffin, Holodick et al. 2011; Griffin, Holodick et al. 2011; Covens, Verbinnen et al. 2013; Tangye 2013). Therefore this introduction focuses on marginal zone B cells, known to be relevant in humans and key players of T cell-independent antibody responses against bacterial polysaccharides (Martin, Oliver et al. 2001). Their crucial role in T cell-independent responses is supported by the fact that infants aged under 2 years who lack T cell-independent B cell responses through a suggested immaturity of Spleen and MZ B cells as well as patients who underwent splenectomy harbor reduced levels of MZ B cells

and have been shown to be at higher risk to acquire bacterial infections (Kruetzmann, Rosado et al. 2003; Weill, Weller et al. 2009).

Human MZ B cells can be found in the blood and the marginal zone of the spleen. MZ B cells from both compartments show a similar surface marker phenotype of $IgM^{high}IgD^{low}CD27^{+}CD21^{+}CD23^{-}CD1c^{+}$ and are therefore likely circulating between those two compartments (Weller, Braun et al. 2004; Weill, Weller et al. 2009). The spleen is an important immune organ connected to blood circulation playing a crucial role in defense against encapsulated microorganisms [reviewed in (Mebius and Kraal 2005; Cerutti, Cols et al. 2013)]. The origin and function of peripheral MZ B cells, often referred as $IgD^{+}IgM^{+}CD27^{+}$ memory B cells, is still a matter of debate due to the fact that these cells share many features with classical memory B cells and it has therefore been proposed that MZ B cells could originate from classical GC-dependent reactions but leave the GC early as IgM-producing early effector cells (Tangye and Good 2007; Seifert and Kuppers 2009; Seifert, Przekopowitz et al. 2015). Although sharing many similarities there are substantial differences between human memory B cells and MZ B cells [reviewed in (Weill, Weller et al. 2009)]. MZ B cells show a different immunoglobulin repertoire compared to classical memory B cells analyzed by deep-sequencing and therefore it is supposed that MZ B cells undergo a distinct developmental path (Wu, Kipling et al. 2010). Strong evidence that MZ B cells emerge through a distinct pathway can be observed in patients with hyper-IgM syndrome (HIGM) due to CD40L deficiency resulting in the absence of GC (Weller, Faili et al. 2001; Jesus, Duarte et al. 2008; Berkowska, Driessen et al. 2011). These patients show almost no classical memory B cells although MZ B cells are still detectable in the periphery albeit at reduced frequencies highlighting their independence of GC reaction (Weller, Faili et al. 2001; Berkowska, Driessen et al. 2011). However the reduced levels of MZ B cells suggest that at least a fraction of MZ B cells arise from GC-dependent pathways (Berkowska, Driessen et al. 2011). Interestingly, MZ B cells in HIGM patients show mutated B cell receptors emphasizing that MZ B cell diversify their BCR in a GC-independent manner (Weller, Faili et al. 2001; Weller, Braun et al. 2004). In addition it has been shown that MZ B cell pre-diversify their BCR in an antigen-independent manner within the first month of life although T cell-independent MZ B cell responses against encapsulated bacteria are absent (Weller, Faili et al. 2001; Weller, Braun et al. 2004; Weller, Mamani-Matsuda et al. 2008; Weill, Weller et al. 2009). In favor of this, the mutated MZ B cell repertoire emerging during T cell-independent responses is elicited early during infection and precedes the emergence of mutated GC-dependent B cells and therefore supporting the notion that MZ B cells contain a pre-diversified BCR repertoire [reviewed in (Weill, Weller et al. 2009)].

As a further prove of pre-diversification, a study identified an ancestor MZ B cell clone carrying mutations in the variable loop prior to polysaccharide-based vaccination, which was

clonally related to the major MZ B cell clone emerging upon vaccination emphasizing that pre-diversified MZ B cells are optimally equipped to quickly respond to T cell-independent antigens (Weller, Braun et al. 2004; Weill, Weller et al. 2009).

3.2 B cell alterations during HIV-1 infection

3.2.1 HIV-1 dependent changes in lymphoid organs

HIV-1 infection is associated with remarkable changes of lymphoid organs resulting in inflammatory lymphadenopathy already at early stage of the infection [reviewed in (Lederman and Margolis 2008; Estes 2013)]. The increased size of lymph nodes is associated with follicular hyperplasia as a result from massive activation and proliferation of B cells [reviewed in (Lederman and Margolis 2008; Estes 2013)]. Fibrosis occurs in lymph nodes as a consequence of maintained inflammation and therefore impairs the migration and communication between immune cells important for the induction of efficient antibody responses [as reviewed in (Estes, Haase et al. 2008; Estes 2013)]. In certain circumstances follicular involution can occur resulting in the disappearance of GC. During acute HIV-1 infection structural alterations and loss of GC in lymphoid tissues of intestinal mucosa was observed suggesting that GC damage occurs early during HIV-1 infection (Levesque, Moody et al. 2009). During acute HIV-1 infection a massive depletion of CD4+ T cells occurs in the intestinal mucosa and/or gut-associated lymphoid tissue (GALT) and therefore the lack of CD4 T cells might impair T:B cell interaction and B cell survival [reviewed in (Grossman, Meier-Schellersheim et al. 2006; Brenchley and Douek 2008)]. Interestingly, massive cell death of B cells occurred in the GC most likely due to the lack of appropriate T cell help (Levesque, Moody et al. 2009). Although some HIV-1 dependent lymph node pathologies such as lymphadenopathy can be reversed with highly active anti-retroviral therapy (ART) many abnormalities persist such as follicular hyperplasia and reduced levels of $CD4^+$ T cells in the lymph node. Considering that ART reduced the viral load and elevated peripheral CD4 counts in these patients underlines that the damage of lymphoid tissue is irreversible and therefore supports recent recommendations to induce ART early to prevent continuous deterioration of the immune system (Bucy, Hockett et al. 1999; Schacker, Nguyen et al. 2002; Lederman and Margolis 2008; Estes 2013; Gunthard, Saag et al. 2016).

During acute HIV-1 infection cytotoxic $CD8^+$ T cells can be observed within the GC of mucosal tissues and may contribute to the massive cell death in lymph nodes (Levesque, Moody et al. 2009). However, in non-human primate studies rhesus monkeys with the ability to control SIV, so-called elite controllers, showed efficient extrafollicular $CD8^+$ T cell responses capable of maintaining low viral loads [reviewed in (Deeks and Walker 2007; Walker and Yu 2013)]. Nevertheless T_FH cells which constitute a main target cell of HIV-1, are productively infected in B cell follicles and spread is not restricted by cytotoxic T cells as only low levels of $CD8^+$ T cells are able to enter the follicle due to the lack of CXCR5 expression (Connick, Mattila et al. 2007; Tjernlund, Zhu et al. 2010; Perreau, Savoye et al. 2013; Fukazawa, Lum et al. 2015; Banga, Procopio et al. 2016; Pallikkuth, Sharkey et al.

2016). Recently, the emergence of cytotoxic CXCR5$^+$ CD8 T cells in lymph nodes of HIV-1 infected individuals was reported (He, Hou et al. 2016). Of particular note, the frequency of peripheral HIV-1 specific CXCR5$^+$ CD8$^+$ T cells inversely correlated with viral load emphasizing that a population of cytotoxic CD8$^+$ T cells possess the capability to enter B cell follicles and presumably eliminate HIV-1 infected T cells (He, Hou et al. 2016). While these CXCR5$^+$ CD8$^+$ T cells are highly intriguing, their effect on the HIV-1 infected T_FH cell pool yet has to be determined.

3.2.2 Direct interactions between HIV-1 and B cells

The devastating damage of lymphoid tissues, the preferred infection of T_FH cells, which play a crucial role in the process of eliciting high-affinity antibodies in the GC, and the lack of CD8$^+$ T cell response in B cell follicles likely lay the foundation for the impaired B cell responses observed in HIV-1 infection. However, HIV-1 does not only affect immune cells and lymphoid tissues important for high-affinity B cell responses but can impair B cells via direct and indirect mechanisms. HIV-1 dependent alterations of B cells were recognized already early during HIV-1 epidemics (Lane, Masur et al. 1983; Schnittman, Lane et al. 1986; Yarchoan, Redfield et al. 1986). Initial observations showed increased levels of immunoglobulin known as hypergammaglobulinemia as well as hyperactivity and polyclonal activation of B cells characterized by spontaneous secretion of immunoglobulins (Lane, Masur et al. 1983; Schnittman, Lane et al. 1986; Yarchoan, Redfield et al. 1986; Shirai, Cosentino et al. 1992; Morris, Binley et al. 1998; De Milito, Nilsson et al. 2004). Hypergammaglobulinemia and peripheral antibody-secreting cells are reduced upon ART highlighting that their emergence is associated with viremia and associated immune activation (Morris, Binley et al. 1998). However, the etiology of hypergammaglobulinemia and polyclonal B cell stimulation is still not completely resolved and involves likely a range of contributing factors (Haas, Zimmermann et al. 2011).

In accordance with the CD4 T cell decline and increased immune activation, alterations in the B cell compartment increase during the progression of HIV-1 infection. Several factors are associated with B cell hyperactivity including a range of cytokines. Elevated levels of TNF-α, IFN-α, IL-10, soluble CD40L and BAFF can be observed in viremic patients and these factors are known to directly influence B cells [as reviewed in (Moir and Fauci 2009; McMichael, Borrow et al. 2010; Moir and Fauci 2013)]. However, virus-derived proteins themselves can also directly influence B cells. Gp120 can bind to α4β7 on naïve B cells and initiate an abortive proliferation response rendering B cells less permissive to T cell-dependent stimulation (Jelicic, Cimbro et al. 2013). In addition, the co-stimulatory molecule CD80 is up-

regulated to a lower magnitude upon stimulation and therefore these B cells are less likely to provide co-stimulatory signals to T cells (Jelicic, Cimbro et al. 2013). Integrin α4β7 engagement by gp120 on B cells leads to the production of the anti-inflammatory cytokine TGF-β1 highlighting that HIV-1 can directly influence B cells and their responsiveness to stimulation (Jelicic, Cimbro et al. 2013). HIV-1 and in particular gp120 are associated with induction of B cell stimulation and proliferation and can potentially act as a superantigen (Schnittman, Lane et al. 1986; Patke and Shearer 2000). However, this activity was found to be restricted to a population of B cells expressing members of the V_H3 family (Berberian, Goodglick et al. 1993; Goodglick, Zevit et al. 1995; Neshat, Goodglick et al. 2000). The HIV-1 accessory protein Nef shows divergent effects on B cells. It was reported to have the ability to inhibit class-switching in lymphoid tissues and has also been indicated to induce the secretion of ferritin from macrophages which can support polyclonal activation of B cells by inducing proliferation of resting B cells (Swingler, Zhou et al. 2008; Xu, Santini et al. 2009). In addition, Nef has been shown to induce the expression of inflammatory chemokines MIPα and β (CCL3 and CCL4, respectively) which can influence immune regulation and therefore presumably also B cell activation (Swingler, Mann et al. 1999). Although only a minority of peripheral B cells express CCR1 and CCR5, the receptors for CCL3 and CCL4, these receptors are up-regulated in B cells in tonsils and lymph nodes and show migration upon MIPα stimulation suggesting that CCL3 and CCL4 can have direct effects on B cells (Schall, Bacon et al. 1993; Buri, Korner et al. 2001; Corcione, Tortolina et al. 2002; Trentin, Cabrelle et al. 2004; Ehrhardt, Hsu et al. 2005; Henneken, Dorner et al. 2005; Griffith, Sokol et al. 2014). In addition, the viral Tat protein impairs proliferation upon BCR-mediated stimulation but increased responsiveness to CD40/IL-4 mediated stimulation, emphasizing that Tat can modulate the pathways of B cell activation (Lefevre, Krzysiek et al. 1999).

The interaction of B cells with HIV-1 virions is multifold and B cells can capture virions through several mechanisms. DC-SIGN is known to bind gp120 resulting in internalization, transfer of virions to and infection of $CD4^+$ T cells. This *trans* infection mechanism is a mode for highly efficient HIV-1 infection of $CD4^+$ T cells as the virions are protected intracellularly in the DC-SIGN bearing cells and presented to $CD4^+$ T cells that attach to these cells (Geijtenbeek, Kwon et al. 2000; Kwon, Gregorio et al. 2002). The DC-SIGN trans-infection mechanism was originally described for myeloid DC but was later also identified to be relevant in the interaction of DC-SIGN expressing B cells and $CD4^+$ T cells (Geijtenbeek, Kwon et al. 2000; Kwon, Gregorio et al. 2002; Rappocciolo, Piazza et al. 2006). DC-SIGN itself is not sufficient for HIV-1 entry, thus the DC-SIGN bearing cells that do not express CD4 and coreceptors may remain uninfected. In DC however, which express the HIV-1 entry receptors, DC-SIGN trapped virus can engage CD4 on DC and therefore support productive infection of DC (Geijtenbeek, Kwon et al. 2000; Kwon, Gregorio et al. 2002; Burleigh, Lozach

et al. 2006). Resting B cells do not express DC-SIGN but DC-SIGN can be induced through B cell stimulation as demonstrated *in vitro* and is highly efficient in *trans* infection of $CD4^+$ T cells (Rappocciolo, Piazza et al. 2006). In addition the complement receptor 2 (CR2; CD21), known to capture complement-opsonized pathogens or immune complexes, is highly expressed on B cells and can trap replication-competent HIV-1 on the surface of B cells (Moir, Malaspina et al. 2000; Roozendaal and Carroll 2007). *In vitro* studies confirmed that only HIV-1 immune complexes in combination with complement efficiently bind to B cells in a process that depends on CD21 (Jakubik, Saifuddin et al. 1999; Doepper, Stoiber et al. 2000; Jakubik, Saifuddin et al. 2000). HIV-1 envelope glycoproteins can also directly activate the complement cascade (Solder, Schulz et al. 1989; Ebenbichler, Thielens et al. 1991; Spear, Jiang et al. 1991; Stoiber, Thielens et al. 1994; Ji, Gewurz et al. 2005; Stoiber 2009). While this also leads to HIV-1 trapping to B cells via CD21 the efficiency of trapping of immune complexed and complement opsonized particles is markedly higher (Jakubik, Saifuddin et al. 1999; Doepper, Stoiber et al. 2000; Jakubik, Saifuddin et al. 2000). The interaction between CD21-dependent HIV-1 bearing B cells and $CD4^+$ T cells results in efficient infection of T cells emphasizing that B cells can enhance infection of $CD4^+$ T cells with HIV-1 through a complement-dependent pathway (Doepper, Stoiber et al. 2000; Jakubik, Saifuddin et al. 2000; Moir, Malaspina et al. 2000; Doepper, Wilflingseder et al. 2003).

3.2.3 B cell exhaustion in HIV-1 infection

It has been long realized that HIV-1 infection leads to the emergence of $CD21^{neg}$ B cells that form several different subsets (Benedetto, Di Caro et al. 1992; Moir, Malaspina et al. 2000; Moir, Malaspina et al. 2001; Moir and Fauci 2008; Moir, Ho et al. 2008; Moir and Fauci 2009; Moir and Fauci 2013). The first indication for a shift towards $CD21^{neg}$ B cell subsets stems from a study published in 1987 by Martínez-Maza et al. describing elevated frequencies of B cells expressing CD10 and Plasma cell antigen-1 (CD203a) suggesting that immature transitional B cells and plasmablasts/plasma cells are increased in HIV-1 infection, respectively, both of which are known to lack CD21 expression (Martinez-Maza, Crabb et al. 1987; Moir and Fauci 2009; Moir and Fauci 2013).

Further studies confirmed the increased frequency of $CD10^+$ transitional B cells in viremic individuals and showed that their frequencies correlated inversely with $CD4^+$ T cell counts and positively with serum IL-7 concentration and viral load (Figure 2) (Malaspina, Moir et al. 2006). IL-7 plays a crucial role in T cell homeostasis and increased levels of IL-7 in HIV-1 infection is thought to be mechanism to counteract T cell loss (Napolitano, Grant et al. 2001; Bradley, Haynes et al. 2005). Interestingly, idiopathic $CD4^+$ T cell lymphocytopenia, a disease with unknown etiology manifested by dramatically reduced $CD4^+$ T cell numbers, is

also characterized by elevated IL-7 and transitional B cell levels supporting the notion that the relevant factor in HIV-1 infection are solely the reduced $CD4^+$ T cell numbers which prompt increases in IL-7 levels and result in elevated frequencies of transitional B cells independent of viral load (Malaspina, Moir et al. 2007; Zonios, Sheikh et al. 2012).

A further $CD21^{neg}$ subset elevated in HIV-1 infection are $CD10^-CD27^{high}CD38^{high}$ plasmablasts which may be upregulated due to the polyclonal hyperactivation of B cells (Figure 2) (Lane, Masur et al. 1983; Shirai, Cosentino et al. 1992; Morris, Binley et al. 1998; Moir, Malaspina et al. 2001). Seminal studies on the dysregulation of B cell subsets in HIV-1 infection in viremic patients revealed that several distinct populations of $CD21^{neg}$ B cells exists that are phenotypically distinct from classical transitional B cells and plasmablasts (Moir, Malaspina et al. 2001; Moir, Malaspina et al. 2004; Malaspina, Moir et al. 2006). These cells were found to belong to memory B cell subsets either expressing or lacking CD27 and were defined as activated memory (AM) B cells and tissue-like memory (TLM) B cells, respectively (Figure 2) (Moir, Ho et al. 2008). AM B cells are characterized by high expression of CD80 and CD95, two important activation marker (Moir, Malaspina et al. 2004; Moir, Ho et al. 2008; Moir and Fauci 2013). The classical $CD21^+CD27^+$ resting memory (RM) B cell subset representing the major memory B cell subset in healthy individuals was found to be dramatically reduced during HIV-1 infection whereas AM and TLM B cell frequencies are increased (Moir, Ho et al. 2008). The processes that lead to CD21 downregulation in HIV-1 infection are not well understood. A mechanism of CD21 downregulation on B cells upon binding of immune complexes was proposed but may not be the sole component as CD21 mRNA transcription is also dramatically reduced in $CD21^{neg}$ B cells (Moir, Malaspina et al. 2000; Moir, Malaspina et al. 2001).

The $CD21^-CD27^-$ TLM B cells express Fc receptor-like 4 (FcRL4), which is known to bind IgA and functions as an inhibitory receptor (Ehrhardt, Davis et al. 2003; Wilson, Fuchs et al. 2012). This cell type was first described for a tonsil B cell population that lacked CD27 and had reduced CD21 levels (Ehrhardt, Hsu et al. 2005) and peripheral $CD21^-CD27^-$ memory B cells are thought to share a common phenotype with tissue-resident memory B cells (Moir, Ho et al. 2008). Emergence of TLM B cells has been observed in other chronic diseases such as malaria and hepatitis C virus infection supporting the notion that they result from a continuous stimulation (Oliviero, Mantovani et al. 2015; Portugal, Tipton et al. 2015; Sullivan, Kim et al. 2015). Phenotypic and functional analysis of TLM B cells in HIV-1 infection revealed that these cells up-regulate inhibitory receptors such as CD22, CD85j, LAIR-1 and CD72 and FcRL-4 (Moir, Ho et al. 2008; Moir and Fauci 2014). These inhibitory receptors contain immunoreceptor tyrosine-based inhibitory motifs (ITIM) which recruit protein tyrosine phosphatase SHP-1 resulting in inhibition of BCR-mediated activation [reviewed in (Nitschke 2005)]. TLM B cells further show an increased expression of CXCR3, the receptor for the

inflammatory chemokines CXCL9-11 secreted at sites of inflammation, whereas CD62L and CXCR5, two chemokine receptors important for lymph node and B cell follicle entry, respectively, are down-regulated suggesting that these TLM B cells show a distinct migratory potential and that their responsiveness is likely to be impaired by the inhibitory receptors (Moir, Ho et al. 2008; Weiss, Crompton et al. 2009; Groom and Luster 2011; Dauby, Kummert et al. 2014; Griffith, Sokol et al. 2014). Although TLM B cells proliferate *in vivo* they were shown to have a reduced diversity of the BCR variable genes and an impaired responsiveness both BCR-dependent and -independent stimulation compared to classical memory B cells assessed for proliferation or differentiation to antibody-secreting cells *in vitro* (Moir, Ho et al. 2008; Moir and Fauci 2013; Meffre, Louie et al. 2016). Therefore TLM B cells which can be a large fraction of memory B cells are defined as exhausted (Moir, Ho et al. 2008). Interestingly their exhausted state can be reversed by knocking down inhibitory receptors such as FcRL4 or SIGLEC-6 by small interfering RNA highlighting that indeed part of their exhaustion is determined by the expression of these inhibitory receptors (Kardava, Moir et al. 2011).

Noteworthy, $CD21^{neg}$ B cells have been also observed in autoimmune diseases such as SLE and RA and common variable immunodeficiencies (CVID). These cells show phenotypic and functional similarities with TLM B cells found in HIV-1 infection although some of these populations express IgM and IgD and are therefore thought to be naïve B cells (Rakhmanov, Keller et al. 2009; Isnardi, Ng et al. 2010; Saadoun, Terrier et al. 2013; Tipton, Fucile et al. 2015; Flint, Gibson et al. 2016). It is therefore thought that $CD21^{neg}$ B cells that express IgM and IgD and lack CD27 resemble recently activated naïve B cells in SLE (Tipton, Fucile et al. 2015). The $CD21^{neg}$ B cell populations are enriched for autoreactive BCR in autoimmune diseases and CVID emphasizing that activation due to the cognate self-antigen results in exhaustion in autoimmune disease and that immune tolerance breakdown results in the increased frequencies of exhausted autoreactive B cells (Meffre and Wardemann 2008; Rakhmanov, Keller et al. 2009; Isnardi, Ng et al. 2010; Saadoun, Terrier et al. 2012; Tipton, Fucile et al. 2015).

Exhaustion is a state induced by chronic activation due to persistent antigen exposure and therefore it is tempting to speculate that a high fraction of HIV-1 specific B cells should be found within the TLM B cell subset in viremic individuals. Indeed this was confirmed by flow cytometry in several studies (Wherry 2011; Kardava, Moir et al. 2014; Wherry and Kurachi 2015). In addition a high frequency of HIV-1 specific memory B cells resembled AM and TLM B cells but only few HIV-1 specific RM B cells could be found (Kardava, Moir et al. 2014). These observations confirm that chronic exposure of B cells to its cognate antigen is contributing to the exhausted state of HIV-1 specific B cells. Interestingly in chronically HIV-1 infected individuals, influenza and tetanus-specific B cells showed decreased and increased

levels of TLM and RM B cells, respectively, compared to HIV-1 specific B cells (Kardava, Moir et al. 2014). A recent study revealed that RM B cells in HIV-1 infection harbor elevated frequencies of BCR mutations compared to TLM B cells and express BCR with neutralizing activity against HIV-1 whereas TLM B cells showed dramatically reduced frequencies of clones with neutralization activity. These observations strongly suggest that TLM B cells are impaired in the development towards high-affinity antibodies due to their exhausted state (Meffre, Louie et al. 2016).

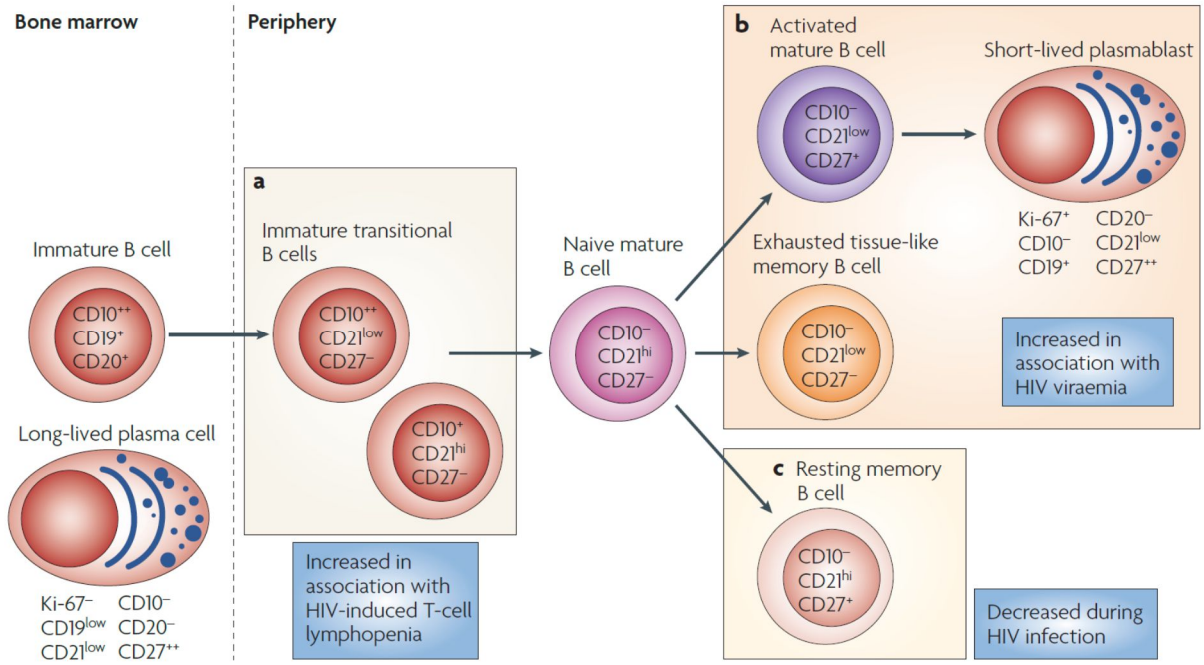

Figure 2: B cell alterations in HIV-1 infection

HIV-1 infection results in elevated transitional B cells dependent on low $CD4^+$ T cell levels and elevated IL-7 concentrations. Due to chronic polyclonal and antigen-specific activation memory B cells with an activated ($CD21^-CD27^+$) and exhausted tissue-like ($CD21^-CD27^-$) phenotype emerge while classical memory B cells ($CD21^+CD27^+$) are reduced compared to healthy individuals. Due to polyclonal activation short-lived antibody-secreting B cells emerge contributing to hypergammaglobulinemia. Reprinted by permission from Macmillan Publishers Ltd: *Nature Reviews Immunology* 9: 235-245. © 2009.

3.2.4 Highly active anti-retroviral therapy and restoration of B cell alterations

Since many of the B cell alterations that accompany HIV-1 infection appear to be driven by virus replication it has been hoped that inhibiting virus replication by ART leads to a complete normalization of the B cell compartment. Indeed, the HIV-1 induced elevated frequency of plasmablasts and hypergammaglobulinemia normalize during ART (Morris, Binley et al. 1998; Moir, Buckner et al. 2010). In addition ART restores the perturbations observed amongst B cells by decreasing frequencies of transitional, AM and TLM B cells, while at the same time increasing RM B cell frequencies (Moir, Malaspina et al. 2008). However, a recent study challenges the notion that ART can fully restore the B cell compartment. Particularly when ART is initiated at later stages of the disease, AM and TLM B cells remain elevated (Moir, Buckner et al. 2010). It has been hypothesized that these sustained B cell alterations might be a consequence of residual virus replication despite ART (Pallikkuth, Sharkey et al. 2015; Banga, Procopio et al. 2016; Lorenzo-Redondo, Fryer et al. 2016) but causes have not been fully unraveled. Of note, it has been long realized that also a low level of T cell activation is sustained during ART (Corbeau and Reynes 2011; Hatano, Jain et al. 2013; Wilson and Sereti 2013; Cobos Jimenez, Wit et al. 2016; Fromentin, Bakeman et al. 2016) supporting the notion that ART cannot fully restore a normal (non-activated) immune system. Early initiation of ART is thus recommended to limit irreversible alterations of the immune system and has been shown to be effective in restoring the B cell compartment to a close to normal setting (Moir, Buckner et al. 2010; Gunthard, Saag et al. 2016).

3.2.5 B cell alterations and HIV-1 – What are the implications for neutralizing antibody responses?

The impaired B cell compartment has implications for B cell responses against HIV-1 but also for antibody responses to co-infections and the efficacy of vaccines. The envelope (Env) specific antibody response against HIV-1 is the most intensely studied as Env antibodies are the only ones that can neutralize the virus by blocking entry into target cells. The Env antibody response is characterized by a first wave of antibodies against immunodominant epitopes within gp41 followed by antibodies against the variable loop 3 (V3) of the viral envelope protein (Tomaras, Yates et al. 2008; Tomaras and Haynes 2009). These first antibodies commonly are not neutralizing. Neutralizing antibodies emerge only after several weeks to months after infection, (Wei, Decker et al. 2003; Haynes, Moody et al. 2011; Overbaugh and Morris 2012). The prototypic first neutralizing antibodies to appear are V3-directed, type specific (neutralize only the autologous strain) and are subject to rapid escape (Wei, Decker et al. 2003; Bunnik, Pisas et al. 2008; Davis, Gray et al. 2009; Tomaras and

Haynes 2009; Tang, Robinson et al. 2011; Overbaugh and Morris 2012). Interestingly, several studies suggest that the initial B cell response to gp41 is derived from preexisting cross-reactive memory B cells reacting with diverse antigens including commensal bacteria raising the possibility that at least certain HIV-1 specific antibodies are not elicited *de novo* by activation of naïve B cells (Haynes, Moody et al. 2011; Liao, Chen et al. 2011; Trama, Moody et al. 2014). While neutralizing antibodies emerge essentially in all HIV-1 infected individuals and the antibody response continuously adapts to the emerging virus escape variants, the virus stays always ahead of the antibody response in this cat and mouse game. Whether this is due to particulars of the virus or whether the impaired B cell responses are the underlying reason for the inefficacy of antibodies to control HIV-1 infection has not been fully resolved (Ferreira, Merino-Mansilla et al. 2013; Derdeyn, Moore et al. 2014; Meffre, Louie et al. 2016). While B cell responses are sustained, it has been suggested that the multifaceted B cell alterations contribute to a delayed emergence of HIV-1 neutralizing antibodies [reviewed in (Haynes, Moody et al. 2011)].

The neutralizing antibodies to HIV-1 are to a large extent type specific, i.e. they only neutralize the patient's own isolates. The capacity to centralize also heterologous viruses (referred to as cross-reactivity) develops later but not in all individuals (Simek, Rida et al. 2009; Doria-Rose, Klein et al. 2010; Rusert, Kouyos et al. 2016). Greater breadth (signified by the capacity to neutralize HIV-1 strains of divergent subtypes) and so called elite neutralizing capacity (signified by high breadth and potency) develop only in 10-25% and 1% of individuals, respectively ((Doria-Rose, Klein et al. 2010; Rusert, Kouyos et al. 2016). These so called broadly neutralizing antibodies (bnAbs) are often characterized by unusual sequence features such as long CDRH3 and high frequency of somatic hypermutations emphasizing that B cell clones undergo extensive selection until they gain breadth [reviewed in (Mascola and Haynes 2013; Burton and Hangartner 2016)].

Considering the severe dysregulation of the immune system in HIV-1 infection and in particular the perturbation of the B cell repertoire, it is striking that nevertheless a highly functional envelope-specific B cell response emerges and continuously adapts. Interestingly, amongst the factors that influence the development of bnAbs most potently are high viral loads and infection length suggesting that exposure to high antigen levels is key (Gray, Moore et al. 2007; Sather, Armann et al. 2009; Moore, Williamson et al. 2015; Rusert, Kouyos et al. 2016). The prolonged co-evolution of HIV-1 and the B cell response further exposes the immune system to an ever increasing diversity of envelope antigen that results from the continuous evolution of the virus and its escape from the neutralizing antibody pressure (Liao, Lynch et al. 2013; Moore, Williamson et al. 2015) and diversity has been shown to be a critical factor in shaping bnAb responses (Liao, Lynch et al. 2013; Moore, Williamson et al. 2015; Rusert, Kouyos et al. 2016). Current HIV-1 vaccine design thus

focuses on developing antigens for sequential immunization to mimic the diversity of the naturally evolving Env quasispecies that lead to bnAb evolution (Haynes, Kelsoe et al. 2012; Mascola and Haynes 2013; Escolano, Steichen et al. 2016).

HIV-1 infection has also been described to have profound effects on pre-existing memory B cells resulting in the loss immunological memory for a variety of pathogens such as *Streptococcus pneumoniae*, influenza and measles (Titanji, De Milito et al. 2006; Wheatley, Kristensen et al. 2016). HIV-1 infection also is associated with impaired antibody responses against co-infections with other pathogens as described for HCV, *Salmonella* and malaria (MacLennan, Gilchrist et al. 2010; Chang, Crane et al. 2013). The same is true for antibody responses against vaccines as shown for vaccine responses to influenza, tetanus and pneumococcal antigens (Ballet, Sulcebe et al. 1987; Kroon, Vandissel et al. 1994; Kroon, van Dissel et al. 1997; Malaspina, Moir et al. 2005; Crum-Cianflone and Wallace 2014; Kerneis, Launay et al. 2014; Mena, Garcia-Basteiro et al. 2015).

In sum these studies highlight that B cell alterations during HIV-1 infection can result in profound impairments in clearing co-infections or inducing protection with vaccines. A rapid restoration of B cell responses by initiating ART early after infection to prevent permanent B cell is thus key to ensure immunity against co-infections.

3.3 Single cell analysis technologies

Flow cytometry is a widely used technology that allows the analysis of several fluorescence parameters on single cells and has been instrumental in shaping our understanding of the cellular networks that form the immune system (Roederer 2002; Perfetto, Chattopadhyay et al. 2004; Bendall, Nolan et al. 2012). The principle of flow-based analysis was the first time commercially implemented in the 1950's from Wallace Coulter when the principle of an impedance-based hemocytometer was described (Coulter 1956). About the same time fluorescence activation cell sorting (FACS) was invented by Mack Fulwyler in 1964 and further developed by Leonard Herzenberg in Stanford (Fulwyler 1965; Hulett, Bonner et al. 1969). The group of Leonard Herzenberg started combining the technologies of hybridoma and flow cytometry to characterize immune cells (Herzenberg, Parks et al. 2002). Ever since flow cytometry has become a widely used technology.

In particular due to the emergence of the HIV-1 epidemics the technical development of flow cytometry was boosted [reviewed in (Roederer 2002; Kestens and Mandy 2016)]. Monitoring of HIV-1 infection requires a tight control of the CD4 T cell counts in peripheral blood as important clinical parameter for disease progression (Kestens and Mandy 2016). Beyond this flow cytometry gain tremendous importance in deciphering the alteration of the immune system that occur in HIV-1 infection [as reviewed in (Roederer 2002; Cossarizza, De Biasi et al. 2013; Kestens and Mandy 2016)].

The technical and optical development as well as the ever-increasing number of available fluorochromes allows nowadays the measurement of 18 fluorescence parameters simultaneously. Most recent developments allow the analysis of 28 colors with the goal to reach 50 parameters [as reviewed in (Perfetto, Chattopadhyay et al. 2004; Bendall, Nolan et al. 2012)]. A drawback of these high numbers of parameters is that the development of multicolor panels is technically challenging, labor-intensive and increases the complexity of data analysis (Mahnke and Roederer 2007; Saeys, Van Gassen et al. 2016).

Flow-cytometry analyses with high dimensionality is thus mostly restricted to dedicated research groups due to both, the need for highly advanced cytometers and cytometry experts. Recent years have highlighted the immense potential of the technology as it allowed the identification of new immune cell types. For example, flow cytometry has shed light on the phenotypic diversity of T cells and proven to be valuable in detecting very rare cell populations such as antigen-specific T and B cells in addition to determining their phenotype (Gattinoni, Lugli et al. 2011; Bacher and Scheffold 2013; Kardava, Moir et al. 2014; Wei, Feng et al. 2015). In addition to surface markers, the stimulation and the subsequent production of cytokines in T cells were analyzed intracellularly to elucidate correlates of vaccine protection or disease progression (Seder, Darrah et al. 2008; Lin, Finak et al. 2015).

While the technology is powerful in detecting specificities of single-cells, machine settings and parameters need to be carefully validated and standardized to allow comparisons. This is particularly critical in large multicenter flow cytometry projects or longitudinal studies. Among the most common variations are reagents, sample processing and storage, protocols, instrument configurations and performance and analysis, which have to be standardized in order to allow comparability of data among different research centers or in longitudinal studies according to guidelines from different flow cytometry consortia (Maecker, Rinfret et al. 2005; Kalina, Flores-Montero et al. 2012; Maecker, McCoy et al. 2012; Kalina, Flores-Montero et al. 2015; Finak, Langweiler et al. 2016). These guidelines propose to use the same reagents, same protocol for staining and sample preparation and cryopreservation, regular optimizing and monitoring of instrument performance across multiple centers and automated data analysis to avoid analysis variation.

Due to the increasing number of parameters measured simultaneously and large sample numbers that need to be processed, manual analysis of flow cytometry data has become difficult. As a consequence a range of algorithms for automated gating algorithms, clustering of cells into subsets with similar phenotypes, dimensionality reduction to visualize cell population heterogeneity, determining trajectories of cell development and even tools to estimate cell populations differing between study groups have been developed (Qiu, Simonds et al. 2011; Amir, Davis et al. 2013; Bruggner, Bodenmiller et al. 2014; Lin, Finak et al. 2015; Verschoor, Lelic et al. 2015; Anchang, Hart et al. 2016; Mair, Hartmann et al. 2016; Saeys, Van Gassen et al. 2016; Setty, Tadmor et al. 2016). These algorithms allowed the identification of new subsets, correlation of subsets with clinical outcome of diseases or treatments and provide an unprecedented resolution of cell subsets (Aghaeepour, Chattopadhyay et al. 2012; Newell, Sigal et al. 2012; Bruggner, Bodenmiller et al. 2014; Gaudilliere, Fragiadakis et al. 2014; Lin, Finak et al. 2015).

In parallel to the advance of flow cytometry new technologies are emerging allowing the measurement of more parameters per cell. A technology similar to flow cytometry is mass cytometry or CyTOF (Cytometry time-of-flight). The CyTOF technology uses metal isotype-tagged antibodies and stained cells are introduced into a plasma mass spectrometer (Bendall, Nolan et al. 2012). A big advantage of the CyTOF technology is that there is no spectral overlap which limits the resolution in flow cytometry (Mahnke and Roederer 2007; Bendall, Nolan et al. 2012). To date panels can analyze up 37 parameters (Bendall, Nolan et al. 2012). The disadvantage of mass cytometry is the irreversible loss of cells, the lower sample throughput, lower sampling efficiency and lower per-channel sensitivity [reviewed in (Bendall, Nolan et al. 2012; Chattopadhyay, Gierahn et al. 2014)].

A further technology that allows single-cell analysis is single-cell RNA sequencing which allows the analysis of the whole transcriptomics as reviewed in (Kolodziejczyk, Kim et al. 2015; Gawad, Koh et al. 2016).

Collectively these new single cell technologies have a tremendous capacity to measure even high numbers of parameters that will allow unprecedented insight into the diversity of the immune system and the hope is that this will allow a targeted identification of correlates of disease control, progression or vaccine efficacy, areas which are under high investigation in the setting of HIV-1 infection (Seder, Darrah et al. 2008; Chattopadhyay, Gierahn et al. 2014).

3.4 Aim of this study

Despite a wealth of knowledge on B cell alterations in HIV-1 infection a detailed delineation of perturbations in B cell subsets as possible through multidimensional cytometry analysis has thus far not been accomplished. Such a fine-mapping of the B cell landscape across different disease stages of HIV-1 infection could however have a tremendous potential in aiding our understanding which components of the B cell population are affected and at which stages of the infection. This information is particular important to understand the limitations in restoring the B cell compartment to normal function by ART and the consequence of permanent alterations for common immune responses to infections and vaccination.

In my thesis I therefore aimed to reveal the phenotypic landscape of B cells at different stages of HIV-1 infection using multiparametric flow cytometry. In the first experimental part of my thesis (Chapter 4) I describe the development of a 16-color flow cytometry panel to phenotypically characterize B cells. The panel includes staining for classical B cell marker such as CD10, CD19, CD27, CD38 and IgD allowing the identification of main B cell subsets, different isotypes like IgA, IgG1, IgG3 to study different memory B cell subsets and phenotypic marker such as chemokine receptors (CCR7, CXCR3, CXCR4 and CXCR5), IL-21R and proliferation marker Ki-67 in order to determine phenotypic differences and migratory potential of the several B cell subsets.

In Chapters 5 and 6 I applied this 16-color B cell phenotyping panel to analyze the landscape of B cells in HIV-1 infected and healthy donors. Using peripheral mononuclear blood samples (PBMC) from patients enrolled in Zurich Primary HIV Infection (ZHPI) cohort study I studied the B cell repertoire during acute and chronic infection and the capacity of antiretroviral treatment (ART) in reversing HIV-1 inflicted perturbations of the B cell population.

Chapter 5 summarizes my findings on the naïve and marginal zone (MZ) B cell population in HIV-1 infection. Using multidimensional flow cytometry I discovered the presence of two previously unidentified subsets, namely $CD21^{neg}$ naïve B cells and $CD21^{neg}$ MZ B cells. These subsets emerge alongside with the rise in of the $CD21^{neg}$ memory B cell populations highlighting that also antigen-inexperienced B cells are affected by HIV-1 infection. This finding raises the possibility that alterations in the naïve repertoire could contribute to the decreased antibody responses observed to co-infections and vaccines in HIV-1 infected individuals. Noteworthy my analyses further reveal that frequencies of $CD21^{neg}$ naïve and $CD21^{neg}$ MZ B cells are restored by ART to levels observed for healthy donors. To understand the potential impact of the $CD21^{neg}$ naïve and $CD21^{neg}$ MZ B cell subtypes on B cell functionality, the phenotypic analysis was followed by a functional analysis of these B cell subsets. By monitoring the proliferative state, expression of activation and exhaustion

marker, frequency of apoptotic cells and BCR-mediated phosphorylation upon BCR-mediated stimulation clear functional differences of $CD21^{neg}$ naïve and $CD21^{neg}$ MZ B cells and their $CD21^{+}$ counterparts became evident. I found that a large fraction of $CD21^{neg}$ naïve and $CD21^{neg}$ MZ B cells that emerge during chronic HIV-1 infection are activated and anergic and thus may be a driving reason why *de novo* induction of antibody responses is impaired.

In Chapter 6 I used the 16-color B cell phenotyping panel to analyze the memory B cell compartment in the same patient cohort to retrieve a fine-mapping of the subset diversification amongst memory B cells that are inflicted by HIV-1 infection. Using dimensionality reduction analysis t-SNE I obtained intriguing novel insights on the composition of the main memory B cell subsets. Memory B cells grouped based on CD21 and CD27 expression into the four known subsets, namely intermediate (IM; $CD21^{+}CD27^{-}$), resting (RM; $CD21^{+}CD27^{+}$), activated (AM; $CD21^{-}CD27^{+}$) and tissue-like (TLM; $CD21^{-}CD27^{-}$) memory B cells, proved to contain distinct distributions of IgA-, IgG1- and IgG3-expressing B cells with TLM B cells containing the highest frequency of $IgG3^{+}$ cells. In line with this, $IgG3^{+}$ B cells express higher levels of CXCR3, known to be expressed on activated and exhausted memory B cells. Interestingly, the elevated CXCR3 expression observed on several memory B cell subsets was not reduced to healthy donor levels when ART was initiated late - in the chronic stage of HIV-1 infection - compared to patients with early ART who initiated treatment during the acute phase. Although the functional consequences of the sustained phenotypic alterations of AM and TLM B cell still need to be unraveled, that fact that these perturbations are not fully restored when ART is initiated at later disease stages highlights the importance of early onset of ART. To provide a basis for future phenotypic and functional characterization of the memory B cell subsets in HIV-1 infection, I subjected the data obtained in my study to the cluster analysis SPADE in combination with hierarchical clustering to obtain a fine-mapping of the memory B cell phenotypes. This analysis revealed a high diversity of memory B cells that go well beyond the classically defined subsets that are solely based on CD21/CD27 and isotype expression. My data highlight that our current view of the memory B cell compartment is limited to only few categories that do not fully appreciate the diversity of the memory B cell network. The drivers of this diversification and the functional properties of the individual memory B cell species thus need to be unraveled to understand their impact in health and disease.

In the frame of my thesis I conducted a thorough analysis of the B cell compartment in HIV-1 infection which provides a starting point for an in depth analysis of the B cell landscape in both healthy and compromised immune systems.

4. Optimized Multicolor Immunofluorescence Panel (OMIP): High-dimensional characterization of human B cells

Manuscript in preparation. My contributions include designing the flow cytometry panel, generating, analyzing and plotting all data. I prepared all figures and wrote the manuscript which was commented on by the coauthors.

Optimized Multicolor Immunofluorescence Panel (OMIP): High-dimensional phenotypic characterization of B cells

Thomas Liechti[1], Alexandra Trkola[1]

[1]Institute of Medical Virology, University of Zurich, Switzerland

Cytometry Part A (Online ISSN: 1552-4930)

4.1 Purpose and appropriate sample type

The present panel was designed to allow a detailed dissection of human B cell subsets and their phenotype in peripheral blood mononuclear cells in both healthy donors and in the context of chronic diseases such as infection with Human Immunodeficiency Virus (HIV)-1. The panel encompasses a range of backbone markers that ensure accurate definition of common B cell subsets in combination with diverse phenotypic markers (chemokine receptors, cytokine receptor, B cell receptor isotypes, and proliferation marker) that allow highly detailed phenotypic and functional investigations of B cell subsets. The panel was validated and used for cryopreserved peripheral blood mononuclear cells (PBMC) from healthy and HIV-1 infected donors (Table 1).

4.2 Background

Chronic viral diseases such as HIV and HCV result in dramatic perturbations of the B cell compartment, most strikingly a shift towards mature and exhausted phenotypes and increased levels of immature $CD10^+$ transitional B cells (1, 2). As a consequence B cell responses in HIV-1 infection are frequently impaired resulting in delayed and in part insufficient humoral responses to diverse infectious agents and vaccines (3-9).

B cells can be defined by expression of the canonical marker CD19. We used a Dump channel including CD3, CD14, CD16 and a Live/Dead dye to achieve an optimal resolution between $CD19^+$ and $CD19^-$ cell types and dead cells to allow definition and inclusion of $CD19^{dim}$ plasmablasts into the analysis (Figure 1A).

For detection of transitional B cells CD10 was included in the panel. While transitional B cells can also be defined by the classical Bm1-Bm5 classification of B cells according to their CD38 and IgD expression (10), we found that the relying on the latter separation is usually less pronounced compared to inclusion of CD10 (10, 11). Inclusion of CD38 and IgD in the panel allowed a dissection of $CD10^-$ mature B cells in IgD^+ unswitched B cells ($CD38^+IgD^+$), class-switched memory B cells ($CD38^{dim}IgD^-$) and plasmablasts ($CD38^{++}IgD^-$) based on the expression pattern of CD38 and IgD (Figure 1B).

IgD^+ unswitched B cells encompass antigen-inexperienced naïve B cells and marginal zone (MZ) B cells (12, 13) which can be distinguished by the differential expression of the memory B cell marker CD27. Naïve B cells do not express CD27 but express high levels of IgD whereas IgD on MZ B cells is lower and paired with expression of CD27 (12).

IgD is a well-established marker to define the B cell population which underwent class-switching (14) as the majority of memory B cells lose IgD expression and only low frequencies of IgD^+ memory B cells in the periphery have been described (15, 16).

Analysis of B cell subsets based on CD21 and CD27 expression has been frequently used in the literature but bears a limitation as naive B cells with a phenotype of $CD21^+CD27^-$ are commonly not distinguished from memory B cells with the same expression profile (4, 7, 8, 17). The present OMIP panel defines the naïve B cell population separately based on IgD and CD27 expression which allows to exclude this subset from the analysis of memory B cells and to define so-called intermediate memory B cells characterized by $CD21^+CD27^-$ expression (17). The differential expression of CD21 and CD27 allows the definition of resting memory B cells (RM, $CD21^+CD27^+$), activated memory B cells (AM, $CD21^-CD27^+$) and tissue-like memory B cells (TLM, $CD21^-CD27^-$) as described (Figure 1C) (17, 18). To obtain a refined dissection of phenotypic differences amongst the memory B cell subsets our staining panel monitors IgA, IgG1 and IgG3 B cell receptor isotypes (Figure 1C).

To provide insight into the potential tissue destination and migratory profiles of the diverse B cell subsets chemokine receptors CCR7, CXCR3, CXCR4 and CXCR5 are monitored by our

panel (Figure 1C-E). CCR7 plays an important role to guide cells to the T cell area in secondary lymph organs (SLO). In B cell follicles follicular dendritic cells secrete high levels of CXCL13, which attract CXCR5-expressing B cells towards the GC. CXCR3 binds to CXCL9 and CXCL10. Both chemokines are secreted in inflamed tissues and attract B cells to these sites with ongoing immune activation. CXCR4, the chemokine receptor for CXCL12, is important for homing of B cells to bone marrow and lymphoid organs including the spleen (19, 20).

A further marker included in our panel is IL-21R (Figure 1D). IL-21, mainly secreted by follicular helper T cells in the GC, supports SHM and isotype switching through signaling of the IL-21R and is crucial for the development of high-affinity antibody responses (21-25). Inclusion of IL-21R in the B cell panel allows analysis of the dynamics of IL-21R expression in order to define whether chronic viral infections manipulate the responsiveness of B cells to SHM and isotype class switching through regulation of IL-21R (22, 23, 26).

Inclusion of the proliferation marker Ki67, allows the characterization of recently activated B cells and their phenotype which allows insights in alterations of concurrent B cell phenotypes when performing longitudinal assessments of the B cell repertoire (Figure 1F) (27).

Combining classical lineage markers with a range of phenotypic parameters (Table 2) our comprehensive 16-parameter B cell panel provides the possibility for a highly detailed characterization of the B cell compartment in healthy individuals, as well as in response to infections or in autoimmune diseases.

4.3 Table and figure legends

Table 1: Summary table for application of OMIP.

Table 2: Reagents used for OMIP.

Figure 1: Characterization of B cell subsets by flow cytometry.

(A) A Time vs SSC-A gate was set to exclude fluorescence intensity fluctuations due to eventual irregular acquisition of the flow cytometer. Single cells were further defined based on SSC-A and FSC-A and a gate for doublet discrimination based on a FSC-H/FSC-A gate. B cells were defined as Dump-negative (Dump set as CD3, CD14, CD16 positive and, dead cells) and CD19-positive cells. A major B cell subset discrimination is based on CD10 and therefore B cells were divided in $CD10^-$ and $CD10^+$ subpopulations. **(B)** $CD10^+$ B cells can be further refined in transitional B cells ($CD38^+IgD^+$). $CD10^-$ B cells comprise IgD^+ unswitched B cells (IgD^+), class-switched B cells ($CD38^{low}IgD^-$) and plasmablasts ($CD38^{high}IgD^-$), which can be defined based on the surface expression pattern of CD38 and IgD. The unswitched IgD^+ fraction can be further divided in naïve ($CD27^-IgD^{high}$) and marginal zone B cells ($CD27^+IgD^+$). **(C)** To characterize memory B cell subsets based on their expressed B cell receptor isotype we included IgG1, IgG3 and IgA in our panel. To define memory B cell subsets based on their maturation state expression patterns of CD21 and CD27 were analyzed as described (17, 18, 28). Intermediate ($CD21^+CD27^-$) and resting memory ($CD21^+CD27^+$) memory B cells are defined as quiescent states, whereas activated memory B cells are $CD21^-CD27^+$. Tissue-like memory B cells, an exhausted subset, do not express CD21 and CD27. In HIV-1 infected patients the distribution is known to be skewed towards activated and tissue-like memory B cells (17, 18, 28). Analysis of cell samples from HIV-1 infection was thus useful to verify sufficient resolution of CD21 staining. **(D)** In order to characterize the potential migratory activity of B cell subsets, we included antibodies for the chemokine receptors CCR7, CXCR3, CXCR4 and CXCR5 in our panel. To measure responsiveness to IL-21, an important cytokine for development of high-affinity antibody responses, IL-21R levels were measured. The resolution of anti-CXCR4, -CXCR5 and –IL-21R antibodies was good as judged by staining differences between the full stained sample (blue) and the corresponding FMO control (grey). **(E)** Resolution of CCR7 proved high so that FMO was not necessary to define positive populations. **(F)** In healthy donors the frequency of CXCR3 and Ki67 expressing B cells is genuinely low necessitating FMO controls. FMO control and fully stained sample are shown as a dot plot in combination with CD27. Both markers show a sufficient separation in combination with full staining panel.

4.4 Tables and figures

Table 1

PURPOSE	B CELLS
Species	Human
Cell types	PBMC
Cross-reference	n.a.

Table 2

SPECIFICITY	CLONE	FLUOROCHROME	PURPOSE
CD3	SK7	APC-Cy7	Dump
CD14	HCD14	APC-Cy7	Dump
CD16	3G8	APC-Cy7	Dump
Dead cells	-	Near-infrared	Dump
CD19	SJ25C1	Brilliant violet 786	Lineage
CD10	HI10a	BV650	B cell subsets
IgD	IA6-2	PE-Cy5 *(in-house conjugation)*	B cell subsets
CD38	HIT2	AF700	B cell subsets
CD21	B-ly4	BV711	B cell subsets/Exhaustion
CD27	M-T271	PE-CF594	Differentiation, Memory
IgG1	HP6001	PE	IgG1 class-switched B cells
IgG3	Polyclonal Sheep IgG	FITC	IgG3 class-switched B cells
IgA	Polyclonal goat IgG	APC	IgA class-switched B cells
CCR7	G043H7	BV605	Migration pattern
CXCR3	G025H7	PE-Cy7	Migration pattern
CXCR4	12G5	PE-Cy5.5 *(in-house conjugation)*	Migration pattern
CXCR5	RF8B2	BV510	Migration pattern
IL-21R	2G1-K12	BV421	Cytokine receptor
Ki67	20Raj1	PerCP-eFluor710	Proliferation marker

Figure 1

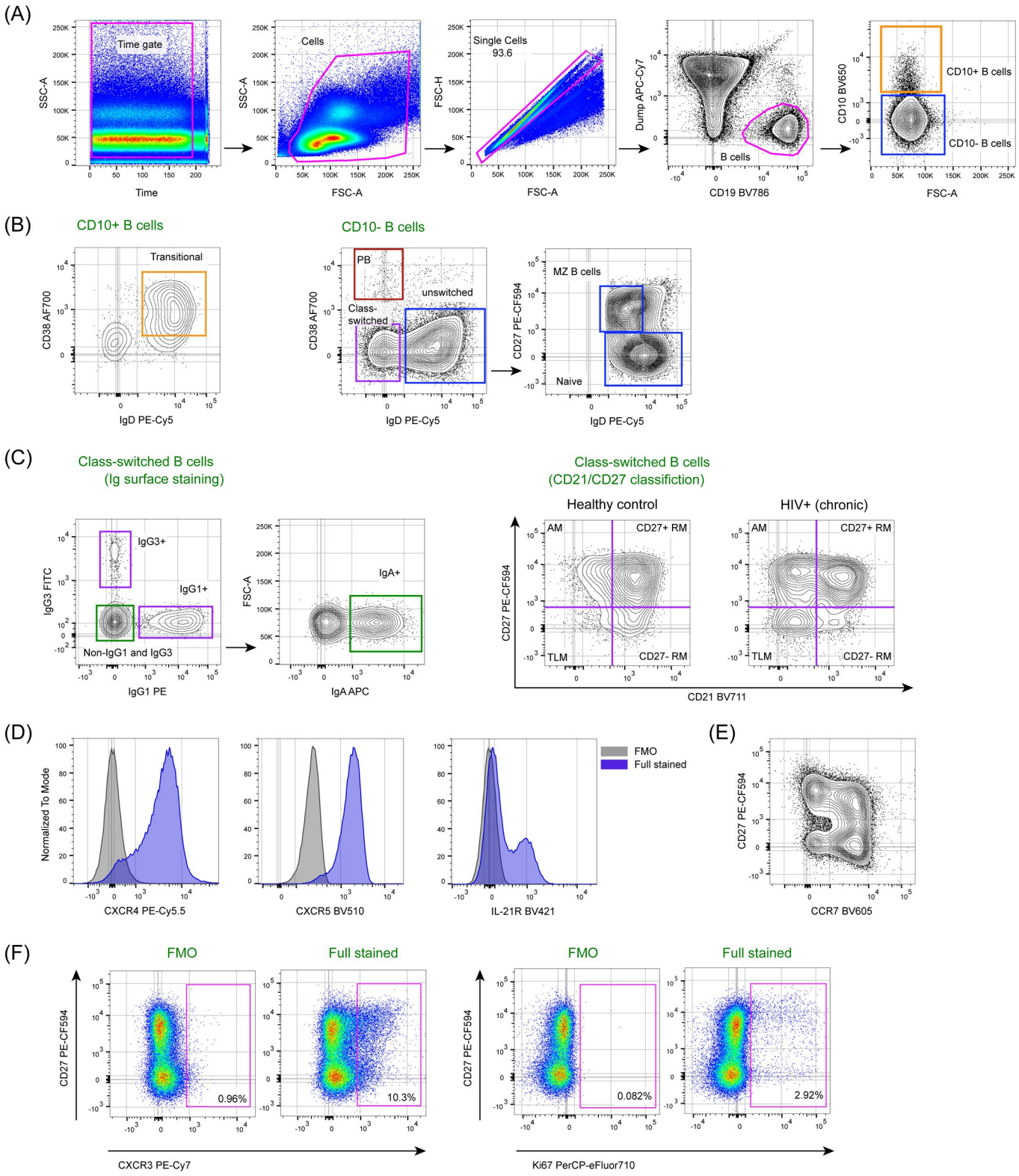
(A)
Time gate
SSC-A
Time
Cells
FSC-A
Single Cells
93.6
FSC-H
Dump APC-Cy7
B cells
CD19 BV786
CD10+ B cells
CD10- B cells
CD10 BV650
(B)
CD10+ B cells
CD10- B cells
Transitional
CD38 AF700
IgD PE-Cy5
PB
unswitched
Class-switched
MZ B cells
Naive
CD27 PE-CF594
(C)
Class-switched B cells (Ig surface staining)
Class-switched B cells (CD21/CD27 classifiction)
Healthy control
HIV+ (chronic)
IgG3+
IgG1+
Non-IgG1 and IgG3
IgG3 FITC
IgG1 PE
IgA+
IgA APC
AM
CD27+ RM
TLM
CD27- RM
CD21 BV711
(D)
Normalized To Mode
CXCR4 PE-Cy5.5
CXCR5 BV510
IL-21R BV421
FMO
Full stained
(E)
CCR7 BV605
(F)
FMO
Full stained
0.96%
10.3%
0.082%
2.92%
CXCR3 PE-Cy7
Ki67 PerCP-eFluor710

4.5 Supplementary info

4.5.1 Developmental strategy

The chosen markers were classified according priority, which includes the availability of fluorochromes as well as the allocation of bright fluorochromes to difficult to stain (e.g. low-level expressed) targets such as IL-21 receptor and some of the chemokine receptors (Supplementary table 1). For chemokine receptors and B cell subset markers different fluorochromes are available, which allows testing several reagent combinations and optimization. The panel was optimized for a BD Fortessa cytometer with the specifications listed in supplementary table 2.

All reagents were carefully titrated (Supplementary table 3 and 4 and Supplementary figure 1). Most markers were tested in combination with the Dump channel reagents and the B cell lineage specific anti-CD19 antibody to estimate the optimal antibody concentration on B cells, especially when the target is expressed on only a small subset of cells (Supplementary figure 1B). The concentrations of antibodies used for the panel were estimated as the lowest concentration which had no effect on the negative population but provided staining of the positive population in the saturation range. Reagents tested but not included in the final panel are listed in supplementary table 5.

Since antibodies specific for IgD and CXCR4 conjugated with PE-Cy5 and PE-Cy5.5, respectively, were not commercially available, these antibodies had to be conjugated in-house. The Lightning-link kits from Innova Biosciences were used according to manufacturer's recommendations. After each new batch preparation coupled antibodies were titrated and compared with the previous batch in order to guarantee comparable staining intensities.

In few cases reagents (CD27 PE-CF594 and IgA APC) reagents were diluted below saturation to avoid excessive spreading error into other channels as further described below.

An initial 10 color B cell panel (Supplementary table 6, panel 1) was built using a progressive approach as described (29). The resolution of the chemokine receptors CXCR3 and CXCR4 was insufficient and needed further optimization. The resolution of CXCR4 PE-Cy5 was dramatically reduced due to spill-over from anti-IgA APC even though a good separation of CXCR4 was expected on B cells which highly express CXCR4 and therefore could potentially allow overcoming the spill-over dependent loss of resolution (Supplementary figure 2A and B). As this was not the case, several changes were implemented. IgD was switched to IgD PE-Cy5 because IgD and IgA are exclusively expressed on naïve B cells and a subset of memory B cells, respectively. Therefore it was expected that the large spill-over between PE-Cy5 and APC would not impair the definition of IgA^+ memory B cells and IgD^+ naïve B cells. Furthermore, due to good separation between negative and positive

population, the APC-conjugated anti-IgA antibody was used at lower concentrations as described in the initial 10 color panel. This further reduced the spill-over into the PE-Cy5 detector (Supplementary figure 3). The combination of IgD PE-Cy5 and IgA APC proved to be useful during the progressive panel design towards 16 markers.

The first 10-color panel included CXCR3 assigned to the fluorochrome PerCP-Cy5.5 (Supplementary table 6, Panel 1). However, the resolution was not acceptable due to tremendous spill-over from CD27 PE-CF594 and weak staining with CXCR3 PerCP-Cy5.5. In order to decrease the CD27 PE-CF594 dependent spill-over the antibody was used at concentrations below saturation (1:400-1:800), without significant loss of resolution between CD27 positive and negative events. However, the decreased staining showed a notable loss of spreading into the PerCP-Cy5.5 channel (Supplementary figure 4). Nevertheless, the CXCR3 staining remained insufficient to resolve $CXCR3^+$ B cells. Therefore CXCR3 was switched to the brighter fluorochrome PE-Cy7 to further increase the resolution (Supplementary figure 5A).

Since the spreading error into the PerCP-Cy5.5 was decreased after using CD27 PE-CF594 at a lower concentration and due to the high expression of CXCR4 on B cells, CXCR4 was switched to PerCP-Cy5.5 (Supplementary table 6, Panel 2).

Several further optimization measures were tested such as different incubation temperature, resting of cells overnight and the effect of cryopreservation on CXCR3 expression.

The staining of CXCR3 could not be improved by staining at 4°C or 37°C instead of room temperature (RT) (Supplementary figure 5B). Cryopreservation had only marginal effects on CXCR3 expression as shown by decreased detectable frequencies of $CXCR3^+$ B cells. Resting of B cells at 37°C overnight in complete RPMI medium could not recover the surface CXCR3 levels but lead to increased CXCR4 levels possibly due to relocation of intracellularly stored CXCR4 to the cell membrane during the incubation period (Supplementary figure 6). As expression pattern were thus altered compared to freshly isolated or thawed cells no resting steps were performed in further analyses (Supplementary figure 6).

As a next step the panel was expanded to 13 markers (Supplementary table 6, panel 3). One demand for our forthcoming studies was a refined discrimination of the IgG^+ B cell population into $IgG1^+$ and $IgG3^+$ memory B cells. Due to the fact that the range of commercially available IgG3-specific antibodies is limited we assigned this marker to the FITC fluorchrome and IgG1 to PE since the IgG1 antibody was only available conjugated with PE. As a consequence we had to omit CCR10 from the PE channel.

In addition, since IL-21R is a crucial molecule we tested sought to improve its staining resolution. IL-21R was consequently assigned to the brightest available fluorochrome (BV421) which finally allowed us to achieve a sufficient resolution to distinguish clearly IL-

21R expressing B cells (Figure 1D). In addition CCR7 BV605 and CXCR5 BV510 were included. Since CD19 BV510 showed limited resolution and therefore could not resolve CD19dim plasmablasts sufficiently we changed CD19 to the brighter BV711 and used CXCR5 BV510 as CXCR5 is highly expressed on B cells and consequently showed sufficient separation with the dim fluorochrome BV510 (figure 1D).

In a last round of adaptation the 13 color B cell panel was expanded to 16 markers to include CD10, CD21 and Ki67 (Supplementary table 6, panel 4). To achieve this the panel had to be rearranged. CD19 was changed to BV786 and CD21 was assigned to BV711 because this antibody was not available with the BV786 conjugate. In addition CD10 BV650 was used due to the fact that this channel was not used and suffers from limited spill-over from other fluorochromes. This was critical as CD10 is usually only weakly expressed on transitional B cells. Furthermore, since CXCR5 (BV510), CCR7 (BV605) and CD21 (BV711) can be expressed on the same B cell population it could affect the resolution of these markers if an additional marker expressed by the same cell would be stained with BV650 as these fluorochromes are close in their spectral behavior. By using BV650 for CD10 we avoided having BV650 on the main B cell populations of our interest in forthcoming studies such as naïve and memory B cells.

Our initial plan to change CCR10 from PE to PerCP was discarded as although we used the same antibody clone, and CCR10 PE resulted in a decent staining of $CCR10^+$ cells, CCR10 PerCP unfortunately showed insufficient resolution. When double-stainings were performed this was confirmed showing that cells with high CCR10 PE signal showed only low signal with CCR10 PerCP and were not resolved from the background noise (Supplementary figure 7).

The expansion of the panel from 13 to 16 color was again done in a progressive manner as described in the literature showing that none of the newly included markers had dramatic effects on other markers and that the populations defined by the newly included markers are well resolved (Supplementary figure 8) (29). Since the addition of the marker CD10 BV650, CD21 BV711 and CXCR4 PE-Cy5.5 did not affect the resolution in the PerCP-Cy5.5 channel we decided to use Ki67 PerCP-eFluor710 since this marker is highly expressed in proliferating cells and showed a sufficient resolution to resolve $Ki67^+$ B cells (figure 1F).
The final panel (Supplementary table 6, panel 4) showed sufficient separation to define the major B cell subsets and to assess the expression of phenotypic marker for characterizing B cell subsets of interest and is therefore suitable for our further studies.

4.5.2 Staining protocol

1. Thaw PBMC vial (approx. $5x10^6$ cells) gently in a water bath pre-warmed at 37°C.
2. Transfer cells to pre-warmed FACS buffer (37°C; PBS, 2% FCS, 2mM EDTA) containing 20µg/ml DNase.
3. Centrifuge cells 10' at 450g at RT.
4. Wash again with FACS buffer/DNase.
5. Centrifuge 10' at 450g at RT.
6. Stain cells with Live/Dead NIR at optimal concentration diluted in PBS and incubate for 30min.
7. Wash cells twice as described above with FACS buffer/DNase.
8. Resuspend cells in 50µl Brilliant violet stain buffer with 20µg/ml DNase containing cocktail of surface staining antibodies.
9. Incubate 30' at room temperature.
10. Wash cells three times as described above with FACS buffer/DNase and once with permeabilization buffer from the Foxp3 / Transcription Factor Staining Buffer Set according to manufacturer's description.
11. Fix cells with the 100µl Fixation/Permeabilization buffer from Foxp3 / Transcription Factor Staining Buffer Set as described in the manufacturer's protocol for 45 minutes at 4°C.
12. Without washing 150µl of permeabilization buffer was added and cells were centrifuged at 750g for 10 minutes at room temperature. These centrifugation settings were used for the entire protocol after the fixation step.
13. Wash cells twice with 200µl permeabilization buffer.
14. Resuspend cells with 50µl of permeabilization buffer containing anti-Ki67 PerCP-eFluor710 antibody at optimal concentration as determined by antibody titration.
15. Incubate cells for 30min at room temperature.
16. Wash cells two times with 200µl permeabilization buffer and once with FACS buffer.
17. Resuspend cells in FACS buffer and analyze with the flow cytometer.

4.5.3 Supplementary table and figure legends

Supplementary table 1: Priority characterization of reagents.

Supplementary table 2: Instrument configuration of the BD Fortessa cytometer used for establishing the B cell panel.

Supplementary table 3: Commercially available reagents included in the B cell panel.

Supplementary table 4: In house conjugated reagents with the corresponding labeling kit used. Unlabeled antibodies are listed on the left side and the corresponding fluorochrome-labeling kit on the right side.

Supplementary table 5: Reagents tested but not included in final panel.

Supplementary table 6: Step-wise panel design towards final 16 color B cell phenotyping panel.

Supplementary table 7: Reagents used for staining.

Supplementary figure 1: Antibody titrations and analysis on whole **(A)** PBMC or **(B)** on pre-gated viable $CD19^+$ B cells.

Supplementary figure 2: Resolution of CXCR4 PE-Cy5 is impaired by spill-over from IgA APC. **(A)** Dot plots of naïve (top row) and memory B cells (bottom row) are shown of FMO control for CXCR4 PE-Cy5 (left column) and fully stained sample (right column). IgA^+ memory B cells show dramatic spreading into the CXCR4 channel (lower right dot plot; FMO CXCR4 PE-Cy5) resulting in decreased resolution of CXCR4 staining on IgA^+ memory B cells. Naïve B cells do not express IgA and therefore resolution of CXCR4 PE-Cy5 staining is not affected by IgA APC. **(B)** In addition, memory B cells showed lower expression of CXCR4 compared to naïve B cells as indicated by the overlay histograms which demonstrate that an improved separation between negative and positive events must be found. Cells were stained with panel 1 listed in supplementary table 6 and pre-gated on viable $Dump^-CD19^+$ B cells.

Supplementary figure 3: Dilution of IgA APC below saturation concentration decreased spreading error from APC into PE-Cy5. As IgD^+ B cells showed unspecific IgA staining at high concentrations of anti-IgA APC, lower anti-IgA APC concentration as determined by titration was used. Cells were stained with panel 1 listed in supplementary table 6 and pre-gated on viable $Dump^-CD19^+$ B cells.

Supplementary figure 4: PE-CF594 conjugated anti-CD27 showed dramatic spill-over into the PerCP-Cy5.5 channel. Since PerCP-Cy5.5 was assigned to the dim marker CXCR3, CD27 PE-CF594 would mask the CXCR3 staining. Therefore CD27 PE-CF594 was titrated down below optimal saturating concentration showing dramatic improvement of the spill-over effect into the PerCP-Cy5.5 channel. A dilution of 1:800 shows dramatically reduced spreading and was therefore used. Cells were pre-gated on viable $CD19^+$ B cells stained with Panel 1 as indicated in supplementary table 6. Backbone staining contains all marker in Panel 1 without CD27 PE-CF594 and CXCR3 PerCP-Cy5.5

Supplementary figure 5: (A) Changing CXCR3 from PerCP-Cy5.5 to the brighter fluorochrome PE-Cy7 dramatically increased the resolution of CXCR3. The spill-over of PE-CF594, APC and PE-Cy5 into the PerCP-Cy5.5 channel resulted in spreading lowering the resolution of PerCP-Cy5.5 staining (left column). The spill-over into the PE-Cy7 channel was moderate without negative influence on the CXCR3 PE-Cy7 staining (right column). **(B)** To increase the resolution of CXCR3 PE-Cy7 cells were stained at different temperatures. As no temperature setting improved resolution all further stainings were performed at room temperature. Cells were stained with panel 1 in case of CXCR3 PerCP-Cy5.5 and panel 2 in case of CXCR3 PE-Cy7 as indicated in supplementary table 6. Cells were pre-gated on viable $CD19^+$ B cells.

Supplementary figure 6: Effect of cryopreservation on CXCR3 and CXCR4 expression on B cells was determined. CXCR3 and CXCR4 expression after isolation, after cryopreservation with resting overnight at 37°C in complete RPMI media and after cryopreservation without a resting phase was assessed. Dot plots showing CXCR3 expression and corresponding FMO control are shown in top two rows. $CXCR3^+$ B cells are gated and percentage is shown. Histogram overlay with CXCR4 expression (blue) and the corresponding FMO control (grey) at the different conditions are shown in bottom row. Expression was analyzed on viable $CD19^+$ B cells stained with Panel 2 listed in supplementary table 6.

Supplementary figure 7: Dual CCR10 staining with the same clone at equal concentrations derived from the same company labeled with PE and PerCP showed in CD4 T cells and B cells that CCR10 PerCP does not show sufficient separation of $CCR10^+$ events compared to the CCR10 PE antibody. Therefore CCR10 PerCP was omitted from the panel. CD4 T cells were gated as a control due to higher frequency of $CCR10^+$ events.

Supplementary figure 8: Progressive panel design from 13 to 16 colors by adding CD10 BV650, CD21 BV711 and CXCR4 PE-Cy5.5 sequentially showed no dramatic effect on the staining of all other markers and the additional markers exhibited sufficient separation between negative and positive events (red boxes). First column shows all cells gated by FSC and SSC. The subsequent columns are pre-gated on $Dump^-CD19^+$ B cells as they are the cell type of interest. No Ki67 staining was included to assess the spill-over into and the resolution of the PerCP-Cy5.5 channel showing the potential of using anti-Ki67 labeled with PerCP-eFluor710.

4.5.4 Supplementary tables and figures

Supplementary table 1

Priority ranking	*Category*	*Rationale for priority level*	*Reagents*
1	Dump channel	The dim fluorochrome APC-Cy7 requires highly expressed lineage markers to reach sufficient resolution. In addition, availability of reagents with APC-Cy7 is limited.	Live/Dead NIR, CD3, CD14 and CD16
2	B cell subset marker	Optimal separation of B cell subsets and reason for development	CD19, CD21, CD27, CD38, IgD,
3	Chemokine receptor	Further characterization of B cell subsets	CCR7, CXCR3, CXCR4, CXCR5
4	Luxury markers	Interesting markers which are only included when the magnitude of spill-over and the resolution are acceptable	IL-21R, Ki67

Supplementary table 2

Laser wavelength [nm]	Laser power [mW]	Laser type	Spectral range for detector [nm]	Optical filters		Fluorochrome
				Dichroic #1 [nm]	Band pass [nm]	
405nm	50	DPSS*	425-575	-	450/50	BV421
			500-550	505LP	525/50	BV510
			600-620	600LP	610/20	BV605
			655-685	630LP	670/30	BV650
			685-735	685LP	710/50	BV711
			775-825	735LP	800/50	BV786
488nm	50	DPSS*	515-545	505LP	530/30	FITC
			675-715	685LP	695/40	PerCP-eFluor710
561nm	50	DPSS*	578.5-593.5	-	586/15	PE
			600-620	600LP	610/20	PE-CF594
			655-685	635LP	670/30	PE-Cy5
			685-735	685LP	710/50	PE-Cy5.5
			750-810	750LP	780/60	PE-Cy7
640nm	40	DPSS*	663-677	-	670/14	APC
			707.5-752.5	690LP	730/45	AF700
			750-810	750LP	780/60	APC-Cy7

*Diode-pumped solid-state laser

Supplementary table 3

SPECIFICITY	CLONE	FLUOROCHROME	VENDOR	CATALOG NUMBER	DILUTION
CD3	SK7	APC-Cy7	Biolegend	344818	1:100
CD14	HCD14	APC-Cy7	Biolegend	325620	1:100
CD16	3G8	APC-Cy7	Biolegend	302018	1:100
Dead cells	-	Near-infrared	Life Technologies	L10119	1:1000
CD19	SJ25C1	Brilliant violet 786	BD Pharmingen	563326	1:10
CD10	HI10a	BV650	BD Pharmingen	563734	1:40
CD38	HIT2	AF700	Biolegend	303524	1:50
CD21	B-ly4	BV711	BD Pharmingen	563163	1:40
CD27	M-T271	PE-CF594	BD Pharmingen	562297	1:400
IgG1	HP6001	PE	Southern Biotech	9054-09	1:800
IgG3	Polyclonal Sheep IgG	FITC	AbD Serotec	OBT5096F	1:6400
IgA	Polyclonal goat IgG	APC	Jackson Immuno	109-135-011	1:6400
CCR7	G043H7	BV605	Biolegend	353224	1:10
CXCR3	G025H7	PE-Cy7	Biolegend	353719	1:100
CXCR5	RF8B2	BV510	BD Pharmingen	563105	1:50
IL-21R	2G1-K12	BV421	Biolegend	347809	1:10
Ki67	20Raj1	PerCP-eFluor710	eBiosciences	46-5699-42	1:40

Supplementary table 4

SPECIFICITY	CLONE	VENDOR	CATALOG NUMBER	FLUORO-CHROME	VENDOR	CATALOG NUMBER	DYE:AB RATIO	DILUTION
CXCR4	12G5	Biolegend	306502	PE-Cy5.5	Innova Biosciences	761-0010	1:1	1:80
IgD	IA6-2	Biolegend	348202	PE-Cy5	Innova Biosciences	760-0010	1:1	1:1600

Supplementary table 5

SPECIFICITY	CLONE	FLUOROCHROME	VENDOR	CATALOG NUMBER	DILUTION
CCR10	3143058 (25µg/ml)	PE	R&D systems	FAB3478P	1:20
CCR10	314305 (25µg/ml)	PerCP	R&D systems	FAB3478C	1:20
CD19	SJ25C1	BV510	BD Pharmingen	562947	1:50
CD19	SJ25C1	BV711	BD Pharmingen	563038	1:50
CXCR3	G025H7	PerCP-Cy5.5	Biolegend	353713	1:100
CXCR4	12G5	PE-Cy5	Biolegend	306507	1:200
CXCR4	12G5	PerCP-Cy5.5	Biolegend	306513	1:100
IgD	IA6-2	PE-Cy7	Biolegend	348209	1:200
IgG	Ploryclonal goat f(ab')2	FITC	Southern Biotech	2042-02	1:3200

Supplementary table 6

	Optical filters			Panel 1	Panel 2	Panel 3	Panel 4
Spectral range for detector [nm]	**Dichroic #1 [nm]**	**Band pass [nm]**	**Fluoro-chrome**				
425-575	-	450/50	BV421			IL-21R	IL-21R
500-550	505LP	525/50	BV510	CD19	CD19	CXCR5	CXCR5
600-620	600LP	610/20	BV605			CCR7	CCR7
655-685	630LP	670/30	BV650				CD10
685-735	685LP	710/50	BV711			CD19	CD21
775-825	735LP	800/50	BV786				CD19
515-545	505LP	530/30	FITC	IgG	IgG	IgG3	IgG3
675-715	685LP	695/40	PerCP-eFluor710	CXCR3 (PerCP-Cy5.5)	CXCR4 (PerCP-Cy5.5)	CXCR4 (PerCP-Cy5.5)	Ki67
578.5-593.5	-	586/15	PE	CCR10	CCR10	IgG1	IgG1
600-620	600LP	610/20	PE-CF594	CD27	CD27	CD27	CD27
655-685	635LP	670/30	PE-Cy5	CXCR4	IgD	IgD	IgD
685-735	685LP	710/50	PE-Cy5.5				CXCR4
750-810	750LP	780/60	PE-Cy7	IgD	CXCR3	CXCR3	CXCR3
663-677	-	670/14	APC	IgA	IgA	IgA	IgA
707.5-752.5	690LP	730/45	AF700	CD38	CD38	CD38	CD38
750-810	750LP	780/60	APC-Cy7	CD3, CD14, CD16, Live/Dead	CD3, CD14, CD16, Live/Dead	CD3, CD14, CD16, Live/Dead	CD3, CD14, CD16, Live/Dead

Supplementary table 7

REAGENT	VENDOR	CATALOG NUMBER
FoxP3/Transcription Factor staining kit	eBiosciences	00-5523
Brilliant violet stain buffer	BD Biosciences	563794
PBS	Life Technologies	14190-094
Heat-inactviated FCS	Life Technologies	10270-106
EDTA	Sigma Aldrich	E7889-100ML
Compensation beads Anti-mouse	BD Biosciences	552843
Compensation beads Anti-rat/hamster	BD Biosciences	552844
DNase	Sigma Aldrich	DN25-100MG

Supplementary figure 1

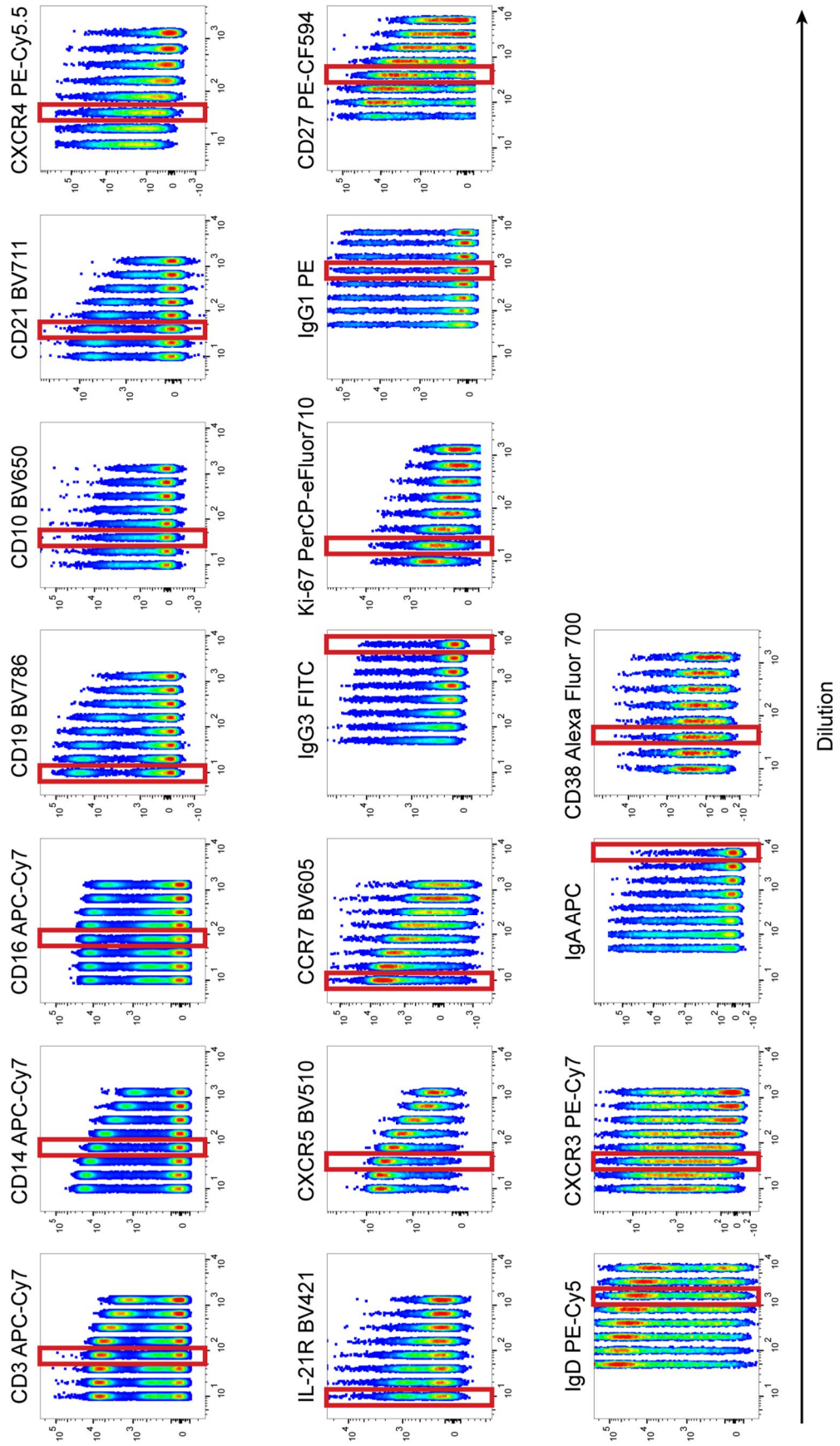

Supplementary figure 2

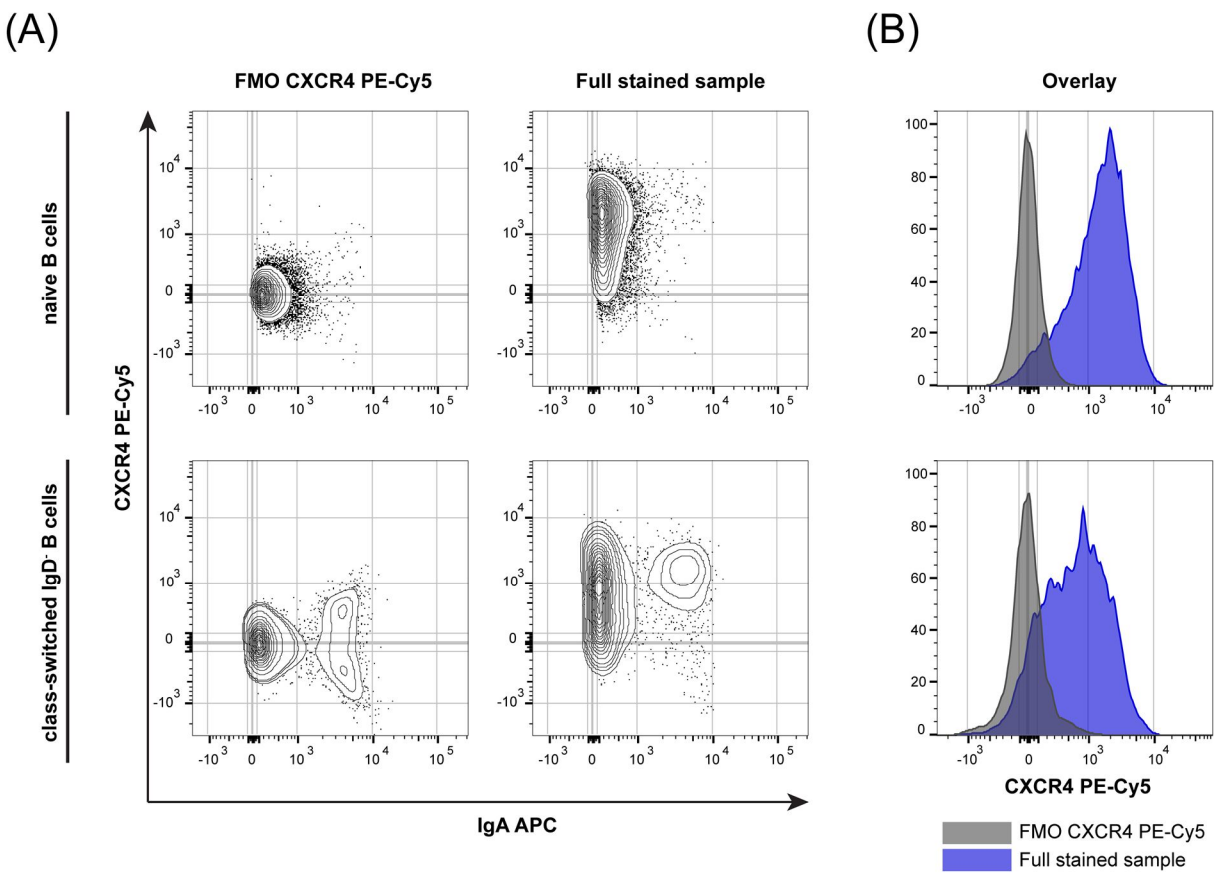

Supplementary figure 3

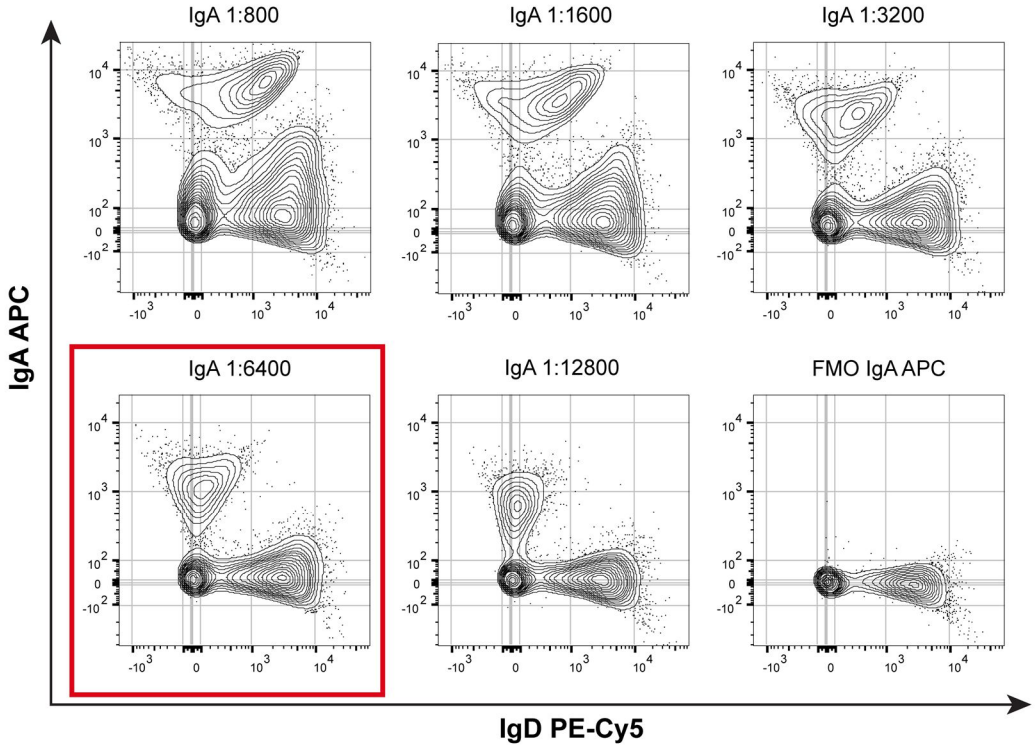

Supplementary figure 4

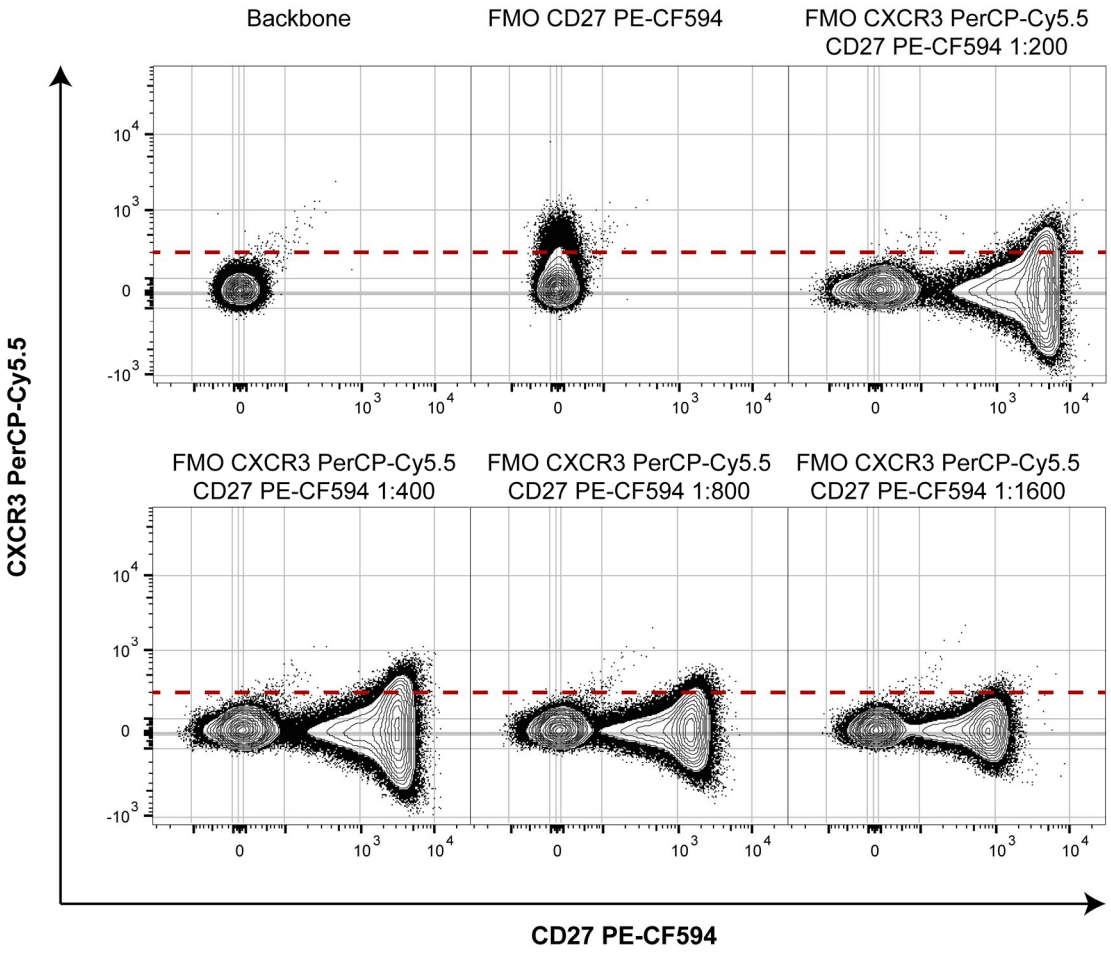

Supplementary figure 5

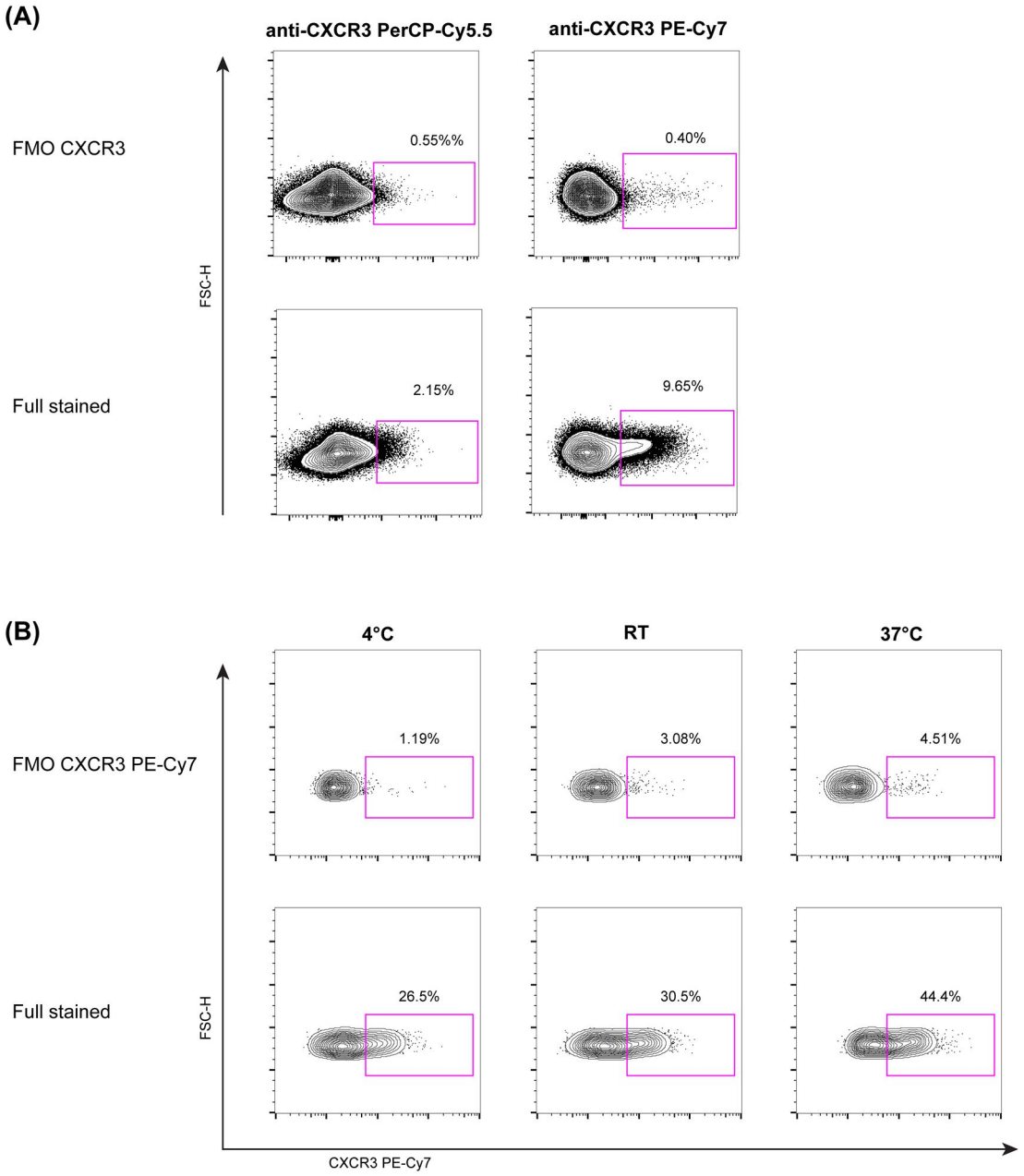

Supplementary figure 6

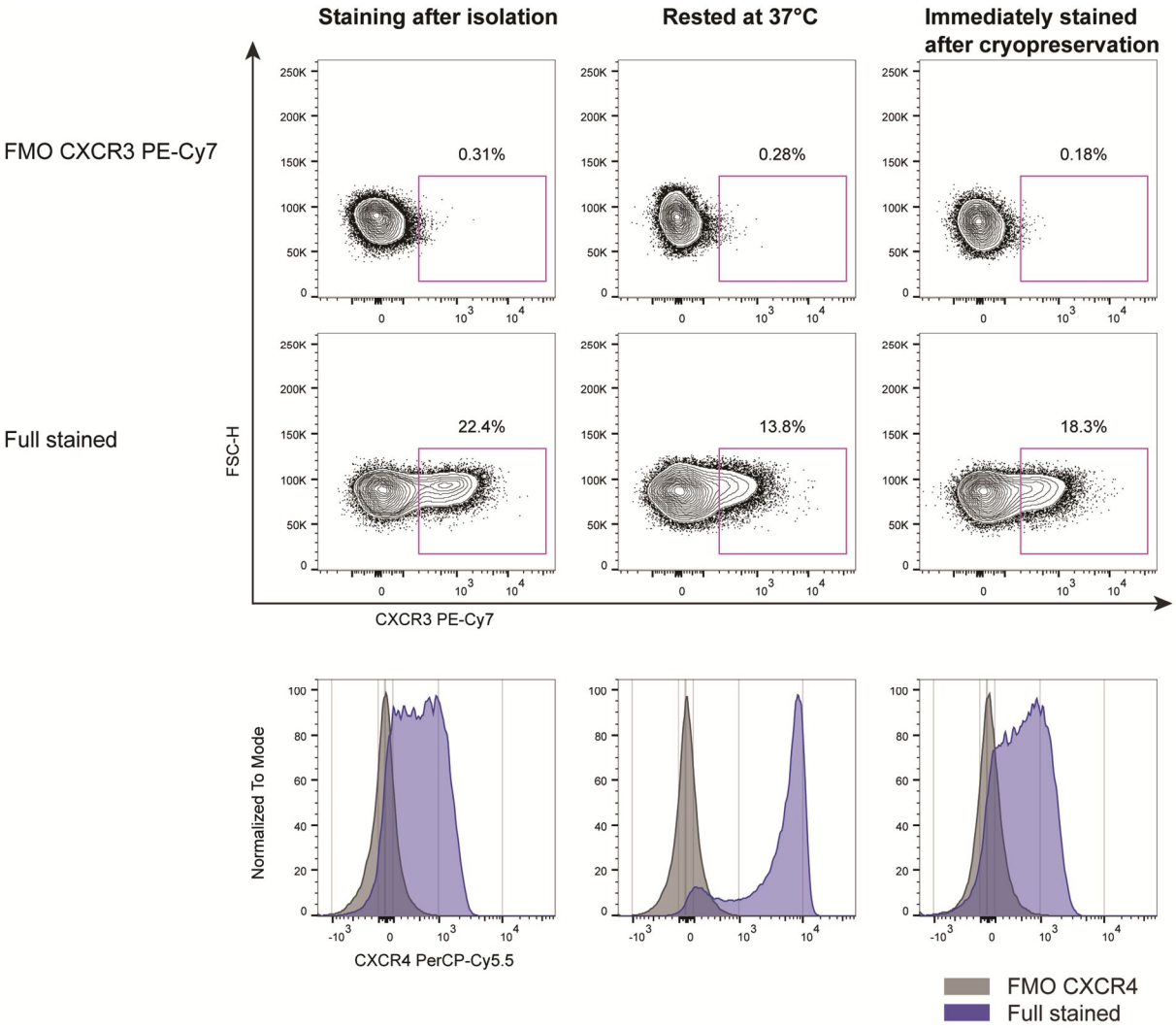

Supplementary figure 7

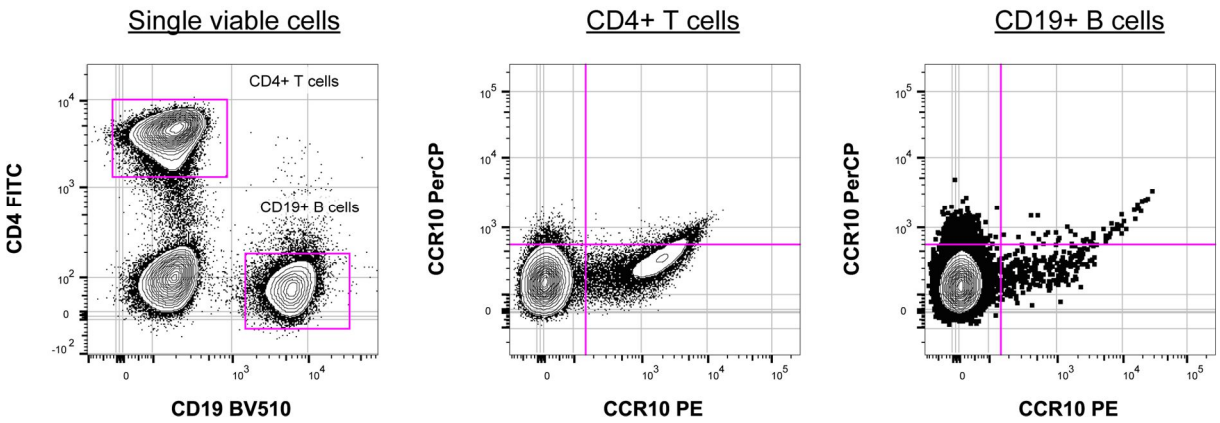

Supplementary figure 8

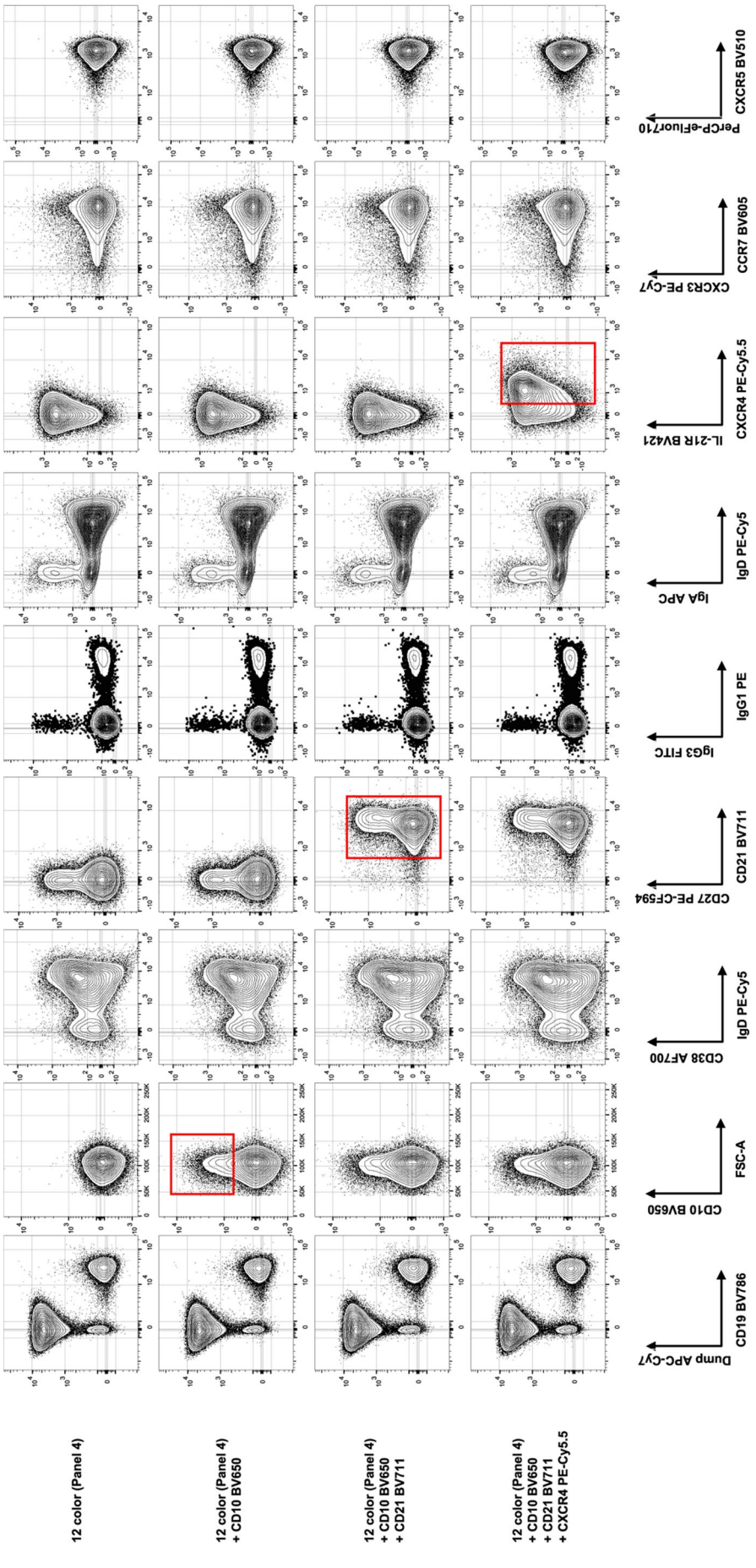

4.6 References

1. Malaspina, A., Moir, S., Ho, J., Wang, W., Howell, M.L., O'Shea, M.A., Roby, G.A., Rehm, C.A., Mican, J.M., Chun, T.W., et al. 2006. Appearance of immature/transitional B cells in HIV-infected individuals with advanced disease: correlation with increased IL-7. *Proc Natl Acad Sci U S A* 103:2262-2267.

2. Sugalski, J.M., Rodriguez, B., Moir, S., and Anthony, D.D. 2010. Peripheral Blood B Cell Subset Skewing Is Associated with Altered Cell Cycling and Intrinsic Resistance to Apoptosis and Reflects a State of Immune Activation in Chronic Hepatitis C Virus Infection. *Journal of Immunology* 185:3019-3027.

3. Doi, H., Tanoue, S., and Kaplan, D.E. 2014. Peripheral CD27-CD21- B-cells represent an exhausted lymphocyte population in hepatitis C cirrhosis. *Clin Immunol* 150:184-191.

4. Moir, S., Buckner, C.M., Ho, J., Wang, W., Chen, J., Waldner, A.J., Posada, J.G., Kardava, L., O'Shea, M.A., Kottilil, S., et al. 2010. B cells in early and chronic HIV infection: evidence for preservation of immune function associated with early initiation of antiretroviral therapy. *Blood*.

5. Moir, S., and Fauci, A.S. 2009. B cells in HIV infection and disease. *Nat Rev Immunol* 9:235-245.

6. Moir, S., and Fauci, A.S. 2008. Pathogenic mechanisms of B-lymphocyte dysfunction in HIV disease. *J Allergy Clin Immunol* 122:12-19; quiz 20-11.

7. Moir, S., Ho, J., Malaspina, A., Wang, W., DiPoto, A.C., O'Shea, M.A., Roby, G., Kottilil, S., Arthos, J., Proschan, M.A., et al. 2008. Evidence for HIV-associated B cell exhaustion in a dysfunctional memory B cell compartment in HIV-infected viremic individuals. *J Exp Med* 205:1797-1805.

8. Moir, S., Malaspina, A., Ho, J., Wang, W., Dipoto, A.C., O'Shea, M.A., Roby, G., Mican, J.M., Kottilil, S., Chun, T.W., et al. 2008. Normalization of B cell counts and subpopulations after antiretroviral therapy in chronic HIV disease. *J Infect Dis* 197:572-579.

9. Moir, S., Malaspina, A., Ogwaro, K.M., Donoghue, E.T., Hallahan, C.W., Ehler, L.A., Liu, S., Adelsberger, J., Lapointe, R., Hwu, P., et al. 2001. HIV-1 induces phenotypic and functional perturbations of B cells in chronically infected individuals. *Proc Natl Acad Sci U S A* 98:10362-10367.

10. Bohnhorst, J.O., Bjorgan, M.B., Thoen, J.E., Natvig, J.B., and Thompson, K.M. 2001. Bm1-Bm5 classification of peripheral blood B cells reveals circulating germinal center founder cells in healthy individuals and disturbance in the B cell subpopulations in patients with primary Sjogren's syndrome. *J Immunol* 167:3610-3618.

11. Sims, G.P., Ettinger, R., Shirota, Y., Yarboro, C.H., Illei, G.G., and Lipsky, P.E. 2005. Identification and characterization of circulating human transitional B cells. *Blood* 105:4390-4398.

12. Weller, S., Braun, M.C., Tan, B.K., Rosenwald, A., Cordier, C., Conley, M.E., Plebani, A., Kumararatne, D.S., Bonnet, D., Tournilhac, O., et al. 2004. Human blood IgM "memory" B cells are circulating splenic marginal zone B cells harboring a prediversified immunoglobulin repertoire. *Blood* 104:3647-3654.

13. Weill, J.C., Weller, S., and Reynaud, C.A. 2009. Human marginal zone B cells. *Annu Rev Immunol* 27:267-285.

14. Stavnezer, J., Guikema, J.E., and Schrader, C.E. 2008. Mechanism and regulation of class switch recombination. *Annu Rev Immunol* 26:261-292.

15. Xu, Z., Zan, H., Pone, E.J., Mai, T., and Casali, P. 2012. Immunoglobulin class-switch DNA recombination: induction, targeting and beyond. *Nat Rev Immunol* 12:517-531.

16. Chen, K., Xu, W., Wilson, M., He, B., Miller, N.W., Bengten, E., Edholm, E.S., Santini, P.A., Rath, P., Chiu, A., et al. 2009. Immunoglobulin D enhances immune surveillance by activating antimicrobial, proinflammatory and B cell-stimulating programs in basophils. *Nat Immunol* 10:889-898.

17. Kardava, L., Moir, S., Shah, N., Wang, W., Wilson, R., Buckner, C.M., Santich, B.H., Kim, L.J., Spurlin, E.E., Nelson, A.K., et al. 2014. Abnormal B cell memory subsets dominate HIV-specific responses in infected individuals. *J Clin Invest* 124:3252-3262.

18. Moir, S., and Fauci, A.S. 2013. Insights into B cells and HIV-specific B-cell responses in HIV-infected individuals. *Immunol Rev* 254:207-224.

19. Schulz, O., Hammerschmidt, S.I., Moschovakis, G.L., and Forster, R. 2016. Chemokines and Chemokine Receptors in Lymphoid Tissue Dynamics. *Annu Rev Immunol*.

20. Griffith, J.W., Sokol, C.L., and Luster, A.D. 2014. Chemokines and chemokine receptors: positioning cells for host defense and immunity. *Annu Rev Immunol* 32:659-702.

21. Crotty, S. 2011. Follicular helper CD4 T cells (TFH). *Annu Rev Immunol* 29:621-663.

22. Ettinger, R., Kuchen, S., and Lipsky, P.E. 2008. The role of IL-21 in regulating B-cell function in health and disease. *Immunol Rev* 223:60-86.

23. Ettinger, R., Sims, G.P., Fairhurst, A.M., Robbins, R., da Silva, Y.S., Spolski, R., Leonard, W.J., and Lipsky, P.E. 2005. IL-21 induces differentiation of human naive and memory B cells into antibody-secreting plasma cells. *J Immunol* 175:7867-7879.

24. Linterman, M.A., Beaton, L., Yu, D., Ramiscal, R.R., Srivastava, M., Hogan, J.J., Verma, N.K., Smyth, M.J., Rigby, R.J., and Vinuesa, C.G. 2010. IL-21 acts directly on B cells to regulate Bcl-6 expression and germinal center responses. *J Exp Med* 207:353-363.

25. Tangye, S.G. 2015. Advances in IL-21 biology - enhancing our understanding of human disease. *Curr Opin Immunol* 34:107-115.

26. Zotos, D., Coquet, J.M., Zhang, Y., Light, A., D'Costa, K., Kallies, A., Corcoran, L.M., Godfrey, D.I., Toellner, K.M., Smyth, M.J., et al. 2010. IL-21 regulates germinal center B cell differentiation and proliferation through a B cell-intrinsic mechanism. *J Exp Med* 207:365-378.

27. Scholzen, T., and Gerdes, J. 2000. The Ki-67 protein: from the known and the unknown. *J Cell Physiol* 182:311-322.

28. Moir, S., and Fauci, A.S. 2014. B-cell exhaustion in HIV infection: the role of immune activation. *Curr Opin HIV AIDS* 9:472-477.

29. Mahnke, Y.D., and Roederer, M. 2007. Optimizing a multicolor immunophenotyping assay. *Clin Lab Med* 27:469-485, v.

5. Wide spread perturbations of the B cell repertoire in HIV-1 infection afflict naïve and marginal zone B cells

Manuscript in preparation. My contributions include study design, generating, analyzing and plotting all data. Significant input for computational analysis and statistical analysis were provided by Claus Kadelka. I prepared all figures and wrote the manuscript which was commented on by the coauthors.

Wide spread perturbations of the B cell repertoire in HIV-1 infection afflict naïve and marginal zone B cells

Thomas Liechti[1], Claus Kadelka[1,2], Dominique L. Braun[1,2], Herbert Kuster[1,2], Jürg Böni[1], Huldrych F. Günthard[1,2], Alexandra Trkola[1].

[1]Institute of Medical Virology, University of Zurich, Switzerland

[2]Division of Infectious Diseases and Hospital Epidemiology, University Hospital Zurich, Zurich, Switzerland

5.1 Abstract

Perturbations of the B cell response including hypergammaglobulinemia and a diminished capacity to mount novel antibodies are a hallmark of HIV-1 infection. Alterations of the B cell repertoire are signified by increased numbers of activated memory B cells with a characteristic $CD21^{neg}$ exhausted phenotype that is thought to be a consequence of a continuous antigen-specific and bystander activation in HIV-1 infection. Using high-dimensional flow cytometric analysis we demonstrate here for the first time that the same exhausted phenotype is prevalent amongst antigen-inexperienced cells. We found that already in acute infection a substantial percentage of peripheral naïve and also marginal zone (MZ) B cells down-regulate CD21, and, in agreement with an exhausted phenotype, do not respond to B cell receptor-dependent stimulation. These $CD21^{neg}$ naïve and $CD21^{neg}$ MZ B cells differed from the respective $CD21^{pos}$ populations by an altered migratory capacity as evidenced by a distinct expression pattern of chemokine receptors CCR7, CXCR3, CXCR4 and CXCR5 that promote infiltration of inflamed tissues. In line with an HIV-dependent activation, $CD21^{neg}$ naïve and $CD21^{neg}$ MZ B cells showed increased expression of the proliferation marker Ki-67 and higher frequencies of apoptotic cells. This emergence of anergic $CD21^{neg}$ naïve and $CD21^{neg}$ MZ B cells is remarkable as it demonstrates a wider-spread impairment of B cells including antigen-inexperienced cells than previously appreciated. The reduced capacities of the exhausted, $CD21^{neg}$ naïve B cells population to respond to stimulation we demonstrate here is in line with the functional defects in mounting novel B cell responses in HIV-1 infection. Importantly, as we show here, successful antiretroviral treatment leads to a normalization of the peripheral naïve and MZ B population further underlining the importance of effective treatment.

5.2 Introduction

The humoral immune response against HIV-1 is characterized by a vigorous binding antibody response (1-3). Neutralizing antibodies appear within weeks to months but are subject to rapid escape by the virus (4-7). This sets the scene for a continuous interplay of virus and antibody co-evolution that leads to the evolution to neutralizing antibodies with improved potency and breadth (7-10). While the neutralizing antibody response to HIV-1 never succeeds in controlling virus replication and the virus even escapes the most potent antibodies known to date, the so-called broadly neutralizing antibodies (bnAbs) that develop in a fraction of individuals (9-14), this constant evasion suggests that their impact on controlling viral replication must be considerable. This is further substantiated by a recent report where B cell depletion during lymphoma treatment in an HIV-1 infected individual resulted in immediate increase of virus load (15). What effect B cell perturbation has on the development of HIV-1 neutralizing antibodies remains uncertain (16, 17). The neutralizing antibody response co-evolves with the virus until late disease stages (4, 8, 18). Yet, effective neutralizing responses, particularly bnAbs require prolonged times to develop. While a number of factors have been suggested that shape the development of bnAbs (19-22), disturbed functionality of the B cell population may be an additional reason why bnAbs develop late and only in a fraction of individuals (16, 17, 23). While the influence of B cell impairment on the autologous HIV-specific antibodies is difficult to assess due to the high variability of HIV and differential disease courses, HIV-1 infection has been shown to lead to impaired antibody responses against other pathogens and vaccines highlighting that general deficiency in mounting adequate antibody responses exists (24-34) .

HIV-1 infection is accompanied by massive bystander immune activation impairing many components of the innate and adaptive immune system including the B cell compartment (35-37). Perturbations of the B cell population have been in particular demonstrated for memory B cells (38-40). HIV-1 infection is accompanied with increased frequencies of activated (AM) and tissue-like (TLM) memory B cells (38, 39, 41, 42). TLM B cells exhibit an exhausted phenotype and are characterized by a reduced diversification of the variable regions of immunoglobulins and an impaired capacity to proliferate upon stimulation (38, 39, 41, 43). AM and TLM B cells are distinguished by the loss of the complement receptor 2 (CD21) expression, which supports B cell activation through binding of complement-opsonized antigens (38, 39, 41, 42, 44-47). In addition TLM B cells down-regulate the co-stimulatory molecule CD27, a canonical marker of memory B cells that provides crucial activating signal. Both AM and TLM B cells show different expression pattern of activation molecules and chemokine receptors as compared to resting memory B cells, the main memory B cell subset found in healthy subjects [reviewed in (38, 39, 48)]. CCR7 and CXCR5

chemokine receptors that are required to reach and enter T cell zones and B cell follicles in lymph nodes, respectively, and thus are required for B cells to enter GC reaction and to undergo class-switch recombination (CSR) and affinity maturation are downregulated in TLM B cells (38, 39, 41, 49-54). By losing the capacity to migrate towards B cell follicles and as a result to participate in GC reaction impairs TLM B cells in acquiring high-affinity B cell receptors [reviewed in (38)]. In contrast, CXCR3 expression is increased in TLM B cells suggesting that their migratory potential is orientated towards inflamed tissues where chemokines CXCL9-CXCL11 are secreted (38, 41) underlining that TLM B cells must partake in different type of immune interactions than conventional memory B cells (38, 55).

The highly elevated TLM B cells frequencies in HIV-1 infection are thought to be a result of the chronic activation (38, 40-42, 56). Owing to the inefficiency of TLM B cells to partake in GC reactions, substantial fraction of HIV-specific memory B cells are likely to be impaired in developing effective antibodies with high affinity by somatic hypermutation (17). Despite a wealth of information on the alteration in the memory B cell compartment in HIV-1 infection (38-40, 42, 57), it is currently not known if only memory B cells are compromised or if HIV-1 infection has even wider spread effects on the B cell population. Considering that de novo antibody responses to vaccine and other pathogens can be significantly reduced impairment beyond the memory B cell repertoire including antigen-inexperienced naïve B cells could be envisaged. In the current study we applied high-dimensional flow cytometry to assess the dynamics of B cell subsets during the course of HIV-1 infection using pheripheral blood mononuclear cell (PBMC) samples to obtain a comprehensive phenotypic analysis of a wide range of B cell subsets. Our analysis thereby sought to define the influence of HIV-1 infection on different B cell subsets at acute and chronic disease stages and the potential of antiretroviral therapy (ART) in reversing the alterations of the B cell population inflicted by the virus. Our results confirmed that the B cell signature in HIV-1 infected patients differs dramatically from healthy controls but revealed for the first time that these alterations are not restricted to shifts in the memory B cell subset frequencies and increased levels of transitional B cells but also include newly emerging $CD21^-$ naïve and $CD21^-$ marginal zone B cells. These cell types are phenotypically and functionally related to previously described anergic polyreactive naïve B cells in autoimmunity (58-61) raising the possibility that these cell populations may underlie the highly polyreactive HIV-1 specific antibody responses that are in part observed (62-64). Importantly, our results emphasize that HIV-1 influences B cell responses at early stages of B cell maturation and that their anergic state might be an explanation for the delayed and impaired antibody responses against co-infections and vaccines.

5.3 Results

5.3.1 Longitudinal changes of major B cell subsets in HIV-1 infection

The main intent of our study was to gain insight if perturbation of the B cell population in HIV-1 infection extend beyond the alterations known to occur amongst memory B cells (38, 39, 41) to enable an advanced understanding of the deficiencies observed in humoral responses in HIV-1 infection (24-32). To assess changes of B cell subsets during the course of HIV infection we analyzed peripheral blood from healthy controls and samples from HIV-1 infected individuals enrolled in the Zurich Primary HIV Infection Study (ZHPI) collected at different disease stages using multi-parametric flow cytometry. Patients were followed form acute to chronic infection stages and stratified into two groups – early and late ART, respectively, according to when they started therapy (Supplementary Table 1 and 2). Patients from the early ART group initiated ART in the acute infection stage, patients in the late ART group in the chronic infection stages. For each included individual three longitudinal PBMC samples encompassing acute infection, 2 years of chronic infection, and 1 year of ART were analyzed (Supplementary Table 1 and 2). Healthy donor controls were analyzed from single time points.

Using our 16-parameter B cell staining panel, our gating strategy allows the definition of major B cell subsets according to their maturation state, namely transitional, naïve, marginal zone and memory B cells, different memory B cell subsets including intermediate (IM), resting (RM), activated (AM) and tissue-like (TLM) memory B cells and plasmablasts (Supplementary figure 2). Interestingly, in addition to the these subsets, our multiparametric B cell staining panel revealed a $CD10^+$ B cell population with an unusual phenotype in both healthy and HIV-1 infected donors (Figure 1A and Supplementary figure 2A). CD10 is normally expressed on transitional B cells, germinal center B cells and B cell subsets associated with GC, the so-called GC founder B cells (65, 66). Whereas GC B cells are usually not detectable in the periphery, GC founder B cells are thought to be activated and migrate from the periphery towards lymphoid tissues while still exhibiting a phenotype similar to naïve B cells (65). Both, GC B cells and GC founder B cells express CD38 while GC B cells express CD27 and lack IgD (67-69). In contrast, GC founder B cells express high levels of IgD but do not express CD27 (65). The observed $CD10^+$ B cell subset in our study expresses only low levels of CD38 and no IgD (Supplementary figure 2A). Instead this $CD10^+$ B cell subset is characterized by the expression of CD27 and shows expression of IgG1, IgG3 and IgA as observed for classical memory B cells emphasizing that these cells are closely related to the maturation state of memory B cells (Supplementary figure 3A-C). Interestingly, although frequencies of IgA- and IgG3-expressing cells are comparable, $CD10^+$ memory B cells contain a higher frequency of IgG1-expressing cells compared to class-

switched B cells (Supplementary figure 3C). While the functional properties of these cells need to be defined, we refer to them based on their staining patterns as $CD10^+$ memory-like B cells.

Monitoring changes in the B cell subsets during HIV-1 infection we found that among the main B cell subsets (transitional, naïve, MZ and memory B cells and plasmablasts) only transitional B cells and plasmablasts showed increased frequencies in HIV-1 infected individuals compared to healthy donors. Transitional B cells had a peak frequency during the chronic phase of infection, whereas plasmablasts were highly increased during acute stage and declined during chronic progression (Figure 1A). Importantly, ART treatment reversed the elevated frequencies of transitional B cell and plasmablast levels to healthy donor levels showing that these cell types are not increased during therapy. Interestingly while frequency of classical memory B cells ($IgD^-CD27^+CD38^{low}$) were not affected, we observed decreased levels of $CD10^+$ memory-like B cells in the chronic phase (Figure 1A).

In line with the described B cell alterations in HIV-1 infection and effects of ART (41, 42, 56, 70), frequencies of memory B cell subsets were also distorted in our cohort showing increased levels of activated (AM) and tissue-like exhausted (TLM) memory B cells in contrast to decreased levels of intermediate (IM) and resting (RM) memory B cells during chronic HIV-1 infection (Figure 1B). A hallmark of activated and tissue-like memory B cells is the loss of CD21 expression (38, 39, 41, 71, 72). Most strikingly, we not only observed a down-regulation of CD21 on memory B cells in response to HIV-1 infection but also on naïve and marginal zone (MZ) B cells (Figure 1C). MZ B cells showed after 2 years of untreated HIV-1 infection a loss of CD21 in up to 70% (median 53.5%) of the cells. A significant loss of CD21 amongst naïve B cells was also evident compared to healthy controls (median 15.8%). As seen for the memory B cell subsets except for RM and TLM B cells, levels of $CD21^-$ naïve and $CD21^-$ MZ B cell levels reverted to healthy donor levels upon successful ART (Figure 1C).

5.3.2 Assessing B cell subset signature

To next we explored if B cell subsets in chronic HIV-1 infection form distinct signatures compared to healthy donors. When we subjected the B cell subsets transitional, naïve, MZ, $CD10^+$ memory and $CD10^-$ memory B cells, plasmablasts and the memory B cell subsets intermediate, resting, activated and tissue-like memory B cells measured in chronic infection and in healthy donors (Figure 1A-C) to a spearman correlation analysis we observed that most (15 of 21) chronically infected patients segregated into a separate cluster (Chronic Cluster) that was distinct from healthy donors (Figure 1D). Three HIV-1 infected individuals however clustered with the healthy donors (Healthy Cluster). Intriguingly, these patients had

significantly higher CD4 counts, lower viral load and lower plasma IgG levels highlighting that their infection was markedly less progressed which was linked with a normal B cell subset distribution (Figure 1E). A smaller third cluster (Intermediate Cluster) that formed contained healthy controls and HIV-1 infected patients with an intermediate B cell phenotype. Of note, HIV-1 infected patients within this cluster showed similar clinical parameters as patients within the Chronic Cluster, thus were equally far progressed.

5.3.3 Influence of ART initiation on B cell subset normalization

We next assessed the B cell subsets in the early and late ART initiation group separately to assess potential influences of the timing of ART initiation on B cell subset normalization. Interestingly, only few differences were observed between the two groups (Supplementary figure 4). Sampling time points for the acute, chronic 2 year and ART 1 year time points were matched as closely as possible in the early and late ART group. Owing to sample availability the acute infection sampling time point was earlier in the early ART group than in the late ART group (Supplementary table 1). This difference in sampling timing is likely to be the reason why we observed a lower MZ B cell frequency in the early compared to the late ART group (Supplementary figure 4A). Interestingly, plasmablasts frequencies were lower in the early ART group after two years of chronic infection following ART interruption which may suggest that early ART restores a B cell repertoire closer to healthy donors that is not rapidly distorted by the rebound of HIV-1 (Supplementary figure 4A).

The onset of ART made a notable difference only within the $CD10^{+}$ memory B cell subset which was reversed to normal levels by early but not late initiation of ART after one year of treatment (Supplementary figure 4D). While for the remaining B cell subsets, early and late ART had the same effect, ART was not able to fully restore normal B cell profiles as described (42). Even after 1 year of ART tissue-like memory (TLM) B cell frequencies remained increased compared to healthy controls with levels similar to frequencies found in the acute phase and remained elevated also during chronic infection. Likely as a consequence of these fluctuations RM B cells remained reduced after 1 year of ART compared to healthy controls (Figure 1B).

5.3.4 Appearance of $CD21^{neg}$ naïve and $CD21^{neg}$ MZ B cells is linked with clinical parameters of HIV-1 infection

The loss of CD21 on naïve and MZ B cells in HIV-1 infection revealed for the first time by our analysis emphasizes that B cell perturbations in HIV-1 infection go beyond memory B cells

and can even affect antigen-inexperienced B cells. This loss of CD21 may have implications for the efficacy in responding to antigen and could thus provide a further factor that attributes to the observed delayed capacity of HIV-1 infected individuals to mount high-affinity B cell responses to novel antigens (45, 46, 71, 73). To obtain insight to which HIV-1 associated factors drive the appearance of $CD21^-$ naïve and $CD21^-$ MZ B cells we explored their association with viral load, CD4 count and plasma IgG levels. While we observed no linear relationship of the magnitude of CD21 down-regulation on naïve B cells with either of the three parameters in acute or chronic infection, the emergence of $CD21^-$ MZ B cells was strongly linked with decreasing CD4 T cell counts and increases in viral load but not plasma IgG levels during the chronic phase (Figure 2). As shown in chapter 6 of this thesis, the emergence of activated and tissue-like memory B cells is also tightly linked with viral load and CD4 counts, underscoring strong effect of HIV-1 infection on antigen-experienced cells including both memory and MZ B cells.

5.3.5 Differential chemokine receptors and IL-21R expression of $CD21^{neg}$ and $CD21^{pos}$ naïve and $CD21^{neg}$ and $CD21^{pos}$ MZ B cell subsets in healthy and HIV-1 infected donors

$CD21^-$ B cell populations in autoimmune diseases and chronic viral diseases have been described to have a divergent surface expression profile (40, 58-61, 74-76) and therefore we analyzed the expression of chemokine receptors CCR7, CXCR3, CXCR4, CXCR5 and IL-21R on $CD21^-$ and $CD21^+$ naïve and $CD21^-$ and $CD21^+$ MZ B cells (Figure 3A-C and Supplementary figure 5A and B). Overall alterations in frequencies were linked with a general up- or down-regulation of the respective receptors in the naïve and MZ B cells populations (Figure 3D).

We found that $CD21^-$ naïve B cells in both, healthy donors and chronically HIV-1 infected patients, have decreased frequencies of cells expressing CCR7, CXCR5 and IL-21R with overall lower levels in HIV-1 infection for both $CD21^-$ and $CD21^+$ naïve B cells (Figure 3B and C and Supplementary figure 5B). In contrast $CD21^-$ naïve B cells showed higher frequencies of $CXCR3^+$ cells compared to $CD21^+$ naïve B cells in both healthy individuals and HIV-1 infection paired with a higher CXCR3 expression in both $CD21^+$ and $CD21^-$ naïve B cells in HIV-1 infection compared to healthy controls (Figure 3B and C and Supplementary figure 5B). Differences in receptor expression for MZ B cells were similar, with reduced frequencies of CCR7, CXCR5 and IL-21R in both $CD21^-$ MZ B cells healthy and HIV-1 infected donors. Alterations inflicted by HIV-1 infection where however in part less pronounced (Figure 3C). Unlike what we observed for naïve B cells, expression of IL-21R did not change in $CD21^-$ MZ

B cells in healthy controls but was elevated in CD21$^-$ MZ B cells from HIV-1 infected patients compared to CD21$^+$ MZ B cells possibly suggesting different requirements of IL-21R signaling for B cell responses induced by CD21$^-$ naïve and CD21$^-$ MZ B cells (Figure 3B). In HIV-1 infection CD21$^+$ MZ B cells further showed higher frequencies of CXCR3-expressing cells, while amongst CD21$^-$ MZ B cells more CCR7-bearing cells were detected (Figure 3C).

Most interestingly, CXCR4 expression proved to be differentially steered in healthy and HIV-1 infected individuals showing a decreased expression in CD21$^-$ naïve and CD21$^-$ MZ B cells in healthy donors whereas CXCR4 was not altered in CD21$^-$ naïve B cells and upregulated in CD21$^-$ MZ B cells in chronic HIV-1 infection (Figure 3B and D). This upregulation/preservation of CXCR4 in HIV-1 infection was accompanied by an overall increase in receptor expression (Figure 3D and Supplementary figure 5B). B cell exhaustion is known to be accompanied by an up-regulation of CD19 (58, 72). In line with this we observed increased CD19 expression levels CD21$^-$ naïve and CD21$^-$ MZ B cells of HIV-1 infected donors (Figure 3E and Supplementary figure 5B).

We next analyzed the longitudinal changes of phenotypic markers expressed on CD21$^-$ naïve and CD21$^-$ MZ B cells across different stages of HIV-1 infection covering acute, chronic infection and ART time points (Figure 4). Patients in the early ART initiation group started treatment during acute infection and interrupted after >1 year (Supplementary figure 1 and 2). Samples of chronic infection of these individuals were collected after 1 and 2 years after ART discontinuation. Patients in the late ART initiation group remained initially untreated and only started ART in their chronic infection phase. This setting allowed us to compare potential effects of early and late ART on the restoration of B cell phenotypes. Interestingly, we observed more longitudinal parameter changes in the early ART (Figure 4). As a comparison of the acute phase highlights, patients in the early ART group harbored CD21$^-$ naïve cells that expressed higher CCR7 and lower CD19 levels than patients in the late ART group (Figure 4). This suggests in line with the estimated infection dates (Supplementary figure 1 and 2) that patients in the late ART group were already more progressed at the available acute infection sample time point. Overall we observed with ongoing virus replication a gradual alteration in the parameters that were found to markedly differ in HIV-1 infection compared to healthy donors (Figure 3 and 4).

5.3.6 CD21^{neg} naïve B cells form a heterogeneous population

The high-dimensional parameter data we collected allowed us to explore the subset heterogeneity with using unsupervised clustering algorithms. We focused the analysis on CD21$^-$ naïve B cells as cell numbers of CD21$^-$ MZ B cells are too low to allow reliable

formation of clusters in this analysis. We used the recently described clustering algorithm spanning-tree progression analysis of density-normalized events (SPADE) (77, 78) and applied it to the data from $CD21^-$ naïve B cells from 17 HIV-1 infected patients including four time points of the different disease stages (acute infection, year 1 and 2 chronic infection and ART 1 year) and data from 15 healthy donors (Figure 5A). SPADE allows clustering similar cells based on multidimensional expression pattern of markers visualizing clusters in a tree-like structure (78). We used CCR7, CXCR3, CXCR5 and IL-21R for clustering. All four parameters were characterized by bimodal expression patterns to guarantee best possible cluster allocation. The generated SPADE trees showed a clear allocation of cells in clusters with specific expression patterns and provided an intriguing insight of the high diversity within $CD21^-$ naïve B cells (Figure 5A). In addition, CXCR4 and CD19 which both were not included in clustering, also showed areas with increased expression revealing a certain overlap of the expression pattern of different markers (Figure 5A and B). A drawback of clustering algorithms is the necessary over-clustering in order to be able to define rare B cell subsets. To verify the data obtained by SPADE further, we applied the individual SPADE clusters to a second hierarchical clustering by the Ward method that was based on the expression pattern of the clusters defined by SPADE (79). Using the Ward method we identified 10 different main clusters that portrayed distinct expression patterns of CCR7, CXCR3, CXCR5 and IL-21R (Figure 5C and Supplementary figure 6A). Of note, also the Ward analysis highlighted the overlap of CXCR4 and CD19 with other markers as observed within the SPADE trees (Figure 5B). We next analyzed interdependencies of the phenotypic marker expression intensities and clinical parameters in $CD21^-$ and $CD21^+$ naïve and MZ B cells in chronic HIV-1 infected patients (2 years of active infection). Interetsingly, CXCR3 and CXCR4 expression correlated with CD19 and IL-21R, respectively, on $CD21^-$ naïve B cells (Supplementary figure 7).

To verify the validity of the Ward analysis we performed a manual analysis of the 10 defined Ward clusters which confirmed distinct expression patterns for the majority of clusters (Supplementary figure 6B). We next analyzed the dynamics of these clusters during HIV-1 infection again stratifying HIV-1 infected individuals based on the two ART initiation groups and compared them with $CD21^-$ naïve B cell Ward clusters from healthy controls. Interestingly, differences compared to healthy controls were apparent in clusters 1-3, which increased and cluster 7 which decreased in HIV-1 infection (Figure 5D and Supplementary table 3). The clusters that increased were associated with either high IL-21R expression (cluster 1 and 2) and in addition with CXCR3 (cluster 3) whereas the decreased cluster 7 was characterized mainly by high expression of CCR7. As observed in the manual analysis (Figure 4), longitudinal changes of the identified Ward subsets were only apparent in the early ART group (Figure 5D). Interestingly, the increase of clusters expressing high levels of

CXCR3 and decreased frequencies of clusters with high CCR7 expression seem to develop longitudinally during ongoing viral replication and most pronounced differences occur at 2 years of chronic infection, the latest time point measured in our study. This again emphasizes that with prolonged HIV infection the already reduced CCR7 levels of $CD21^-$ naïve B cells decrease whereas clusters associated with markers expressed in inflammatory environment such as CXCR3, CXCR4, IL-21R as well as CD19 increase.

Importantly, the clustering analysis reveals that the altered expression of the markers is not evenly distributed but is linked to phenotypically distinct subsets of $CD21^-$ naïve B cells which emerge or decline during HIV-1 infection. These results highlight that within $CD21^-$ naïve B cells a high variability of different subsets exists. In this respect it is interesting to note that during HIV-1 infection $CD21^-$ naïve B cells with a phenotype of $CCR7^-CXCR3^{high}CXCR5^+IL\text{-}21R^-CXCR4^+CD19^{high}$ (cluster 5) and $CCR7^-CXCR3^+CXCR5^-IL\text{-}21R^+CXCR4^{high}CD19^{high}$ (cluster 3) emerge emphasizing that subpopulations within $CD21^-$ naïve B cells with the ability to migrate towards inflamed tissues but excluded from lymphoid tissues and to some extent with higher sensitivity to IL-21 and BCR signaling are developed. While the precise function of these subsets needs to be further investigated, their presence highlights that HIV infection results in emergence of unique $CD21^-$ naïve B cell subsets.

5.3.7 $CD21^{neg}$ naïve and $CD21^{neg}$ MZ B cells have distinct functional properties

The emergence of anergic naïve B cells with reduced responsiveness to activation has been documented in healthy donors but also in the context of autoimmunity, primary immunodeficiency or viral diseases (58-61). These cells are sometimes linked to reduced expression of CD21 and increased levels of CD19 along with other markers (58, 60, 72). One of these observed anergic naïve B cell populations is characterized by loss of surface IgM expression whether this is also linked with lower CD21 expression levels remains unclear (80). In order to probe if $CD21^-$ naïve B cells and $CD21^-$ MZ B cells share similarities with anergic B cells, we analyzed IgM, CD95 and FcRL4 expression in a set of chronically HIV-1 infected individuals (N= 7) and healthy controls (N= 29) (Figure 6A and B). $CD21^-$ naïve B cells showed low frequencies of IgM^{low} B cells and therefore can be classified as naïve B cells based on co-expression of IgD and the lack of CD27 (Figure 6A and B and Supplementary figure 2). Interestingly, healthy controls had higher levels of IgM^{low} cells within the $CD21^+$ naïve B cells compared to HIV-infection. CD95 expression is elevated in activated B cells and renders them permissive to cell death signals through Fas ligand (41, 81, 82). FcRL4 is reported to be up-regulated in exhausted memory B cells and widely used to determine exhausted B cells in the context of infectious diseases (38, 39, 41, 44). When we

examined the expression of these two markers on the different memory B cell subsets we observed, as expected, that CD95 and FcRL4 are highly expressed on AM and TLM and to lower extent on IM and RM B cells. However, only CD95 is upregulated with disease progression (Supplementary figure 8). $CD21^+$ and $CD21^-$ naïve and $CD21^-$ MZ B cells also showed elevated levels of CD95 compared to healthy controls already in acute HIV-1 infection, emphasizing that activation of naïve and MZ B cells must occur early after transmission. Similarly FcRL4 was s increased in $CD21^+$ and $CD21^-$ MZ B cells during the acute phase. Importantly, ART successfully reduced CD95 and FcRL4 to healthy donor levels.

Interestingly, FcRL4 was upregulated only on $CD21^-$ but not on CD21+ naïve B cells starting with the acute phase of HIV infection (Figure 6B). Comparisons of $CD21^+$ and $CD21^-$ naïve or $CD21^+$ and $CD21^-$ MZ B cells in healthy controls or at chronic stage of HIV disease further highlighted that CD95 and FcRL4 are expressed at higher levels in $CD21^-$ naïve and $CD21^-$ MZ B cells compared to the respective $CD21^+$ subsets (Figure 6C).

In sum our analyses highlighted that $CD21^-$ naïve B cells are classical naïve B cells based on their expression of IgD and IgM, but based on their increased expression levels of CD95 and FcRL4 emphasize that $CD21^-$ naïve B cells experienced recent activation events. The latter is also true for $CD21^-$ MZ B cells.

As dependent on the strength of the activation signal proliferation can be induced, we next probed whether $CD21^-$ naïve and $CD21^-$ MZ B cells entered cell cycling and proliferation. In line with their activation marker expression, $CD21^-$ naïve and $CD21^-$ MZ B cells showed significantly increased expression of the proliferation marker Ki-67 in healthy donors (Figure 6D and E). Interestingly though, the same was not true for HIV-1 infection likely due to the fact that there also $CD21^+$ subsets had elevated proliferation compared to healthy donors supporting the notion of a generalized immune activation.

Since $CD21^-$ naïve and $CD21^-$ MZ B cells showed an increased expression of CD95 rendering these cells sensitive to extrinsic pro-apoptotic signals we next investigated whether these cells are apoptotic *ex vivo*. To do this we analyzed two major events during apoptosis, the cleavage of caspase 3 and the exposure of phosphatidylserine on the outer leaflet of the cell membrane by flow cytometry. Indeed, $CD21^-$ naïve and $CD21^-$ MZ B cells showed higher frequencies of caspase 3^+Annexin V^+ apoptotic cells (Figure 6F and G). Interestingly, in chronic HIV-1 infection $CD21^-$ naïve B cells portrayed a higher frequency of apoptotic cells emphasizing that chronic HIV infection drives programmed cell death in naïve B cells (figure 6F and G).

5.3.8 Reduced potential for stimulation of CD21^{neg} naïve and CD21^{neg} MZ B cells

To probe if CD21$^-$ naïve and CD21$^-$ MZ B cells are anergic we next tested their potential to respond to B cell receptor-dependent stimulation. To do this we applied phosflow (83), to measure tyrosine phosphorylation on untreated or upon anti-IgA/-IgM/-IgG stimulation in CD21$^+$ and CD21$^-$ naïve and CD21$^-$ MZ B cells, as well as memory B cell subsets (IM, RM, AM, TLM) as defined by CD21 and CD27 expression (figure 7A-C). RM B cells, known to be in a quiescent state, had the highest potential to respond to stimulation (Fig 7B and C). As expected from their described exhausted phenotype TLM B cells (CD21$^-$CD27$^-$) showed in both, healthy controls and HIV-1 infection a decreased ability to respond to BCR cross-linking compared to other memory B cell subsets (Figure 7B and C). Of note basal phosphorylation levels were increased in the two activated and exhausted memory B cell subsets AM and TLM, proving that these cells experienced recent stimulation *in vivo* (Figure 7B and C). Similarly, compared to CD21$^+$ cells, CD21$^-$ naïve and CD21$^-$ MZ B cells showed increased basal phosphorylation in both, healthy and HIV-infected individuals emphasizing that these B cell subsets underwent recent activation-induced phosphorylation *in vivo* (Figure 7C). In line with this, CD21$^-$ naïve B cells had a diminished response to stimulation compared to CD21$^+$ naïve B cells, suggesting that CD21$^+$ naïve B cells are in an anergic state (Figure 7C). CD21$^-$ and CD21$^+$ MZ B cells were indistinguishable in their response to BCR triggering in healthy donors while in HIV-1 infected patients CD21$^-$ MZ B cells showed a reduced phosphorylation (Figure 7C). A direct comparison of the activation potential of memory B cell subsets healthy and HIV-1 infected donors confirmed that HIV-infection impaired the stimulation potential in memory B cell subsets with an activated phenotype, AM, TLM and CD21$^-$ MZ B cells but not in resting memory cells such as RM and IM B cells and CD21$^+$ MZ B cells(Figure 7D). Thus while the stimulation potential of CD21- naïve B cells is genuinely reduced, HIV-1 infection does not augment this deficiency.

5.4 Discussion

HIV-1 infection is accompanied by altered frequencies of B cell subsets with increased levels of transitional B cells and plasmablasts in addition to skewed memory B cell compartment towards activated and exhausted phenotypes (38, 41, 42, 70, 84, 85). In the present study we build on these observations by exploring to what extent perturbations in other B cell subsets exist. To do this we performed a detailed phenotypic analysis using multi-dimensional 16-parameter flow cytometry of peripheral B cells from 21 HIV-1 infected and 29 healthy donors. The comprehensive data on multiple parameters collected in these analyses enabled us to define B cell subset signatures associated with progressing HIV-1 infection (Figure 1D). Most importantly our high-content analysis revealed that the complexity of B cell subsets is higher than thus far appreciated (Figures 1A and Supplementary Figure 3). As we show here, amongst $CD10^+$ cells a memory B cell-like subsets exists that expresses CD27, IgG1, IgG3 and IgA but no IgD and only low levels of CD38 as classical memory B cells do (Figures 1A and Supplementary Figure 3A and B) suggesting that these cells are closely related to the maturation state of memory B cells.

Increased frequencies of $CD21^-$ activated (AM) and exhausted (TLM) memory B cells are considered a hallmark of HIV-1 infection (38-40, 42). As we show here for the first time, reduction of CD21 expression is not limited to these subsets, as in chronic HIV infection a substantial proportion of naïve and MZ B cells also lack CD21 (Figure 1B and C). Intriguingly increased frequencies of $CD21^-$ naïve B cells are described in common variable immunodeficiency (CVID) and different autoimmune disorders such as systemic lupus erythematosus, rheumatoid arthritis and thrombocytopenia but can also be found in healthy subjects at low frequencies (58-61). These cells are described to express high levels of activation markers such as CD95 and are characterized by decreased responses to B cell activation through BCR cross-linking *in vitro* with diminished calcium flux (58, 59). In contrast to their decreased proliferation upon stimulation *in vitro*, these $CD21^-$ naïve B cells have been shown to have an increased history of stimulation induced proliferation *in vivo* (58). The $CD21^-$ naïve B cells we identified in HIV infection resemble this pattern. They express high levels of activation and exhaustion marker CD95 and FcRL4, respectively, are characterized by altered chemokine receptor expression patterns with down-regulation of CCR7 and CXCR5 and increased levels of CXCR3 and show diminished phosphorylation upon BCR cross-linking compared to $CD21^+$ naïve B cells (Figure 3A and B and 7A-C). In healthy controls proliferating Ki-67^+CD21^- naïve B cells are increased (Figure 6D and E). Interestingly, in chronic HIV infection $CD21^+$ naïve B cells show increased frequencies of Ki-67-expressing cells to comparable levels as $CD21^-$ naïve and MZ B cells emphasizing that a fraction of classical $CD21^+$ naïve B cells get activated in chronic HIV infection and undergo proliferation.

Collectively thus, CD21$^-$ naïve B cells in HIV infection show high similarities with the CD21$^-$ naïve B cell subsets described in autoimmune diseases highlighting that this is a genuinely interesting B cell subset that needs to be considered in future studies. In this respect resolving whether or not CD21$^-$ naïve B cells evolve from classical CD21$^+$ naïve B cells upon a base level activation or have individual development paths will be of particular interest.

CD21$^-$ MZ B cells show a similar phenotype as observed for CD21$^-$ naïve B cells and are therefore likely to be activated and exhausted similar to CD21$^-$ naïve B cells and other CD21$^-$ memory B cell subsets (Figure 3). There are only few reports describing aberrant MZ B cell responses associated with a CD21$^-$ phenotype. In chronic Hepatitis C virus infection CD21$^-$ MZ B cell with similar impaired functional consequences as observed in CD21$^-$ naïve B cells were described (74). The strong association of CD21$^-$ MZ B cells with CD4 counts and viral load in chronic HIV infection we observed suggests that the activation and exhaustion state of these cells is directly linked with virus-induced immune activation (Figure 2). This is supported by the fact that human MZ B cells exhibit a memory B cell phenotype and likewise frequencies of the CD21$^-$ memory B cell subsets AM and TLM are highly associated with virus replication and CD4 T cell levels similar to CD21$^-$ MZ B cells ((86) and chapter 6). Interestingly, we found that in contrast the appearance of CD21$^-$ naïve B cells does not correlate with viral load, CD4 counts and plasma IgG concentration, possibly suggesting that the alterations in the naïve B cells happens early in HIV infection and is not linked with disease progression. HIV-1 infection is nevertheless a driving factor of increased CD21$^-$ naïve B cells as ART successfully restores healthy donor levels (Figure 1C).

CD21$^-$ naïve B cells show reduced levels of receptors for IL-21, a crucial cytokine for GC survival, retention and affinity maturation but also for the formation of memory B cells and plasmablasts (Figure 3A and B) (87-92). Decreased IL-21R levels thus should render CD21$^-$ naïve B cells less efficient to undergo GC reaction and thus impact on the development of effective antibody responses and might also result in reduced survival signals. Together with the down-regulation of CCR7 and CXCR5 which also reduce the migratory capacity, down-regulation of IL-21R may be a further mechanism of immune tolerance by excluding these cells from generating high-affinity antibodies and reduce survival signal from IL-21. In support of this, human STAT3-deficiency, the canonical pathway downstream of IL-21R signaling, is associated with impaired development of antigen-specific memory B cells and plasmablasts (93). However, as our clustering analysis highlights, IL-21R is not downregulated in the entire CD21$^-$ naïve B cell compartment as subsets exist in chronic HIV-1 infection that expressing high levels of IL-21R and thus should have the potential to undergo IL-21 dependent affinity maturation (Figure 5A-D).

The increase of IL-21R levels we observed in $CD21^-$ MZ B cells during chronic HIV infection is intriguing (Figure 3C-D and Supplementary figure 5A and B). IL-21 has been reported to have divergent effects on MZ B cells and was found to be associated with cell death in mice and increased affinity maturation in humans (94-96). Decreased peripheral MZ B cell frequencies in STAT-3 deficient humans highlighted the importance of IL-21 for MZ B cell homeostasis (95). An increased expression of IL-21R as we observed in HIV infection, therefore possibility suggests that these $CD21^-$ MZ B cells may have gained improved sensitivity to IL-21 which likely impacts on subsequent affinity maturation and class-switch recombination in HIV infection. As IL-21 concentrations are decreased in chronic HIV infection (97, 98), up-regulation of IL-21R might potentially serve as a compensation to receive sufficient signals for survival and activation. Future studies that resolve the causal relationship of increased IL-21R expression on the quality of antibody responses and the functional properties of the $IL\text{-}21R^{high}$ $CD21^-$ naïve B cell subsets will thus be of high interest.

HIV-1 infection is associated with impaired antibody responses against other pathogens and vaccines (24-34). Interestingly, a recent study revealed that HIV-infected patients with CD4 counts less than 350/µl lack IgM responses to Influenza vaccine whereas IgG responses could be induced, however at lower magnitude (99, 100). IgG responses may in part stem from reactivation of memory B cells, while early IgM responses are elicited *de novo* and therefore suggesting an intrinsic defect of naïve B cells in mounting IgM responses (99, 101). Indeed as we show here, a large pool of naïve B cells is anergic and therefore likely to show impaired antigen responses (Figure 7A-C).

Of note, immune responses against bacterial polysaccharides are in most cases dependent on marginal zone B cells as well as secreted IgM (102, 103) and splenectomy has been linked with higher risk of infections with bacterial pathogens such as *Streptococcus pneumoniae* (102-104). Infections associated with dramatic alterations of the B cell compartment such as HIV-1 are known to show reduced responses against polysaccharide-based vaccines and are associated with increased risk of bacterial co-infections, however, the reasons for this defect have thus far been unclear (28, 29, 32, 105-107). The extensive emergence of non-responsive $CD21^-$ MZ B cells that we demonstrate here may be a plausible explanation for these impaired responses.

To elucidate the phenotypic diversity within $CD21^-$ naïve B cells we employed the clustering algorithm SPADE combined with hierarchical clustering using the Ward method which revealed 10 distinct $CD21^-$ naïve B cell clusters in healthy and HIV-1 infected donors (5A-C and Supplementary figure 6A and B). While the functional properties of these clusters need to be determined, their differential expression profiles raise the possibility that for certain clusters also a functional heterogeneity may exist. More closely related clusters may however

rather represent CD21$^-$ naïve B cell at different developmental stages and thus rather display the gradual loss/gain of certain receptor without a directly linked change in functionality. Dissection of potential functional differences and developmental pathways will be important future avenues of research leading to an improved understanding of the role of CD21$^-$ naïve B cell in immune responses. Importantly, judging from the receptor expression of the diverse CD21$^-$ naïve B cell clusters CD21$^-$ naïve B cells exist which maintained the capacity to migrate towards diverse inflamed tissues and preserved IL-21R to retain responsiveness to IL-21 mediated signaling. Of further note, the enriched subsets during chronic HIV-1 infection were widely characterized by high levels of CXCR4 and CD19 in combination with low or no levels of CCR7.

Interestingly, poly- and autoreactive BCR have been described to be enriched within CD21$^-$ B cells in healthy controls and patients with autoimmune diseases (59, 76) and moreover were described to be in an anergic state (58, 59, 76). The frequency of polyreactive BCR within CD21$^-$ naïve B cells in HIV infection needs to be determined. Considering that CD21$^-$ B cells in HIV-1 infection have strong phenotypic and functional similarities with B cells in autoimmune diseases raises the possibility that poly- and autoreactive BCR are also prevalent amongst CD21$^-$ B cells in HIV infection. If the HIV-associated excessive immune activation leads to elevated frequencies of polyreactive CD21$^-$ naïve B cells this could lead to alterations in immune tolerance checkpoints similar to autoimmune diseases (59, 76). In further support of such a scenario, transitional B cells, which are elevated in HIV-1 infection, are known to show high frequencies of polyreactive BCR and require peripheral immune tolerance mechanism to silence these cells before developing into naïve B cells (57, 108-110). IL-7 and BAFF, two important factors supporting B cell survival during B cell development and maintenance, are elevated in HIV-1 infected individuals (57, 111, 112). IL-7 in particular supports the egress of transitional B cells from bone marrow (57, 113, 114) and both, the increased levels of IL-7 and BAFF are thus likely to support survival of autoreactive B cell clones in the periphery (115, 116).

Of particular relevance in HIV-1 infection, poly- and/or autoreactivity is a common feature of many neutralizing antibodies and bnAbs in HIV-1 infection (62, 117-121). For some, e.g., the MPER-directed bnAbs 2F5 and 4E10 autoreactivity appears to be in part linked with their neutralization activity (63, 118, 122). Polyreactivity has been suggested to aid the development of neutralizing antibody responses as it promotes heteroligation and increased affinity of HIV-1 envelope specific antibodies (63). However, elicitation of polyreactive bnAbs requires a concerted action of immune tolerance mechanisms and may thus be rare (123-128). Recent reports of co-evolution of viral diversification, autologous antibody response and development of bnAbs showed that polyreactivity developed during affinity maturation (8,

63) in line with the observation that many memory B cells acquire polyreactivity during GC reaction (108, 129). The potential roles of $CD21^-$ naïve and $CD21^-$ MZ B cells in the elicitation of potent HIV-specific antibody responses will thus be important to define specifically as both have a lowered responsiveness to stimulation (Figure 7). In support of potential role, a recent report from Tipton et al. demonstrates that a large fraction of plasmablasts and IgM^+ memory B cells in the periphery of SLE patients are derived from so-called activated naïve B cells with a phenotype comparable with the $CD21^-$ naïve B cells described in our study (60). These activated naïve B cells showed increased polyreactivity, a remarkable frequency of SHM and the ability to develop into large clones. Whether these activated naïve B cells participate in GC reaction or go through extrafollicular pathways has not yet been investigated. Nevertheless these observations are highly intriguing, highlighting that activated $CD21^-$ naïve B cells can undergo evolution towards B cell receptors with higher affinities as demonstrated by SHM and their ability to develop into large clusters of antibody-secreting effector cells. To explore this potential pathway in HIV-1 infection, dedicated studies will be needed to dissect whether $CD21^-$ naïve B cells in HIV-1 infection are likewise able to undergo SHM and CSR and, develop into effector cells.

The seeming dichotomy of observations with on the one hand $CD21^-$ naïve B cells exhibiting reduced response to BCR stimulation and the expansion to large clonal families observed in SLE patients remains puzzling (59, 60). The breakdown of immune tolerance checkpoints in autoimmune diseases may result in higher frequencies of polyreactive B cells in the periphery. Activation of their BCR with their cognate autoantigen may aid there survival and allow to at least partially overcome the anergic state. In line with this tonic BCR signals are known to be important to support survival of mature B cells (130). In contrast in HIV-1 the emergence of $CD21^-$ naïve B cells are most likely driven by antigen-independent bystander activation which may be less efficient than activation with a cognate antigen. The decisive factor whether $CD21^-$ naïve B cells overcome their anergic state and induce potent antibody responses might be the duration and/or quality and pathway of activation. In addition, T cell help in HIV infection is defective and therefore not capable providing sufficient help to overcome the anergic state of $CD21^-$ naïve and $CD21^-$ MZ B cells. In support of a reduced capacity to adequately respond to antigen the lower efficacy of vaccines in HIV-infected patients can be overcome by administering more series of booster vaccinations (106, 131).

In summary, our comprehensive analysis of the B cell compartment in HIV-infection revealed a number of signatures associated with chronic immune activation, most importantly anergic naïve and MZ B cells that are characterized by down-regulation of CD21 and changed chemokine and IL-21R expression pattern which have thus far not been described in HIV-1 infection. Unraveling the role of $CD21^-$ naïve and MZ B cells together with other B cell

clusters in the development of humoral immune responses will be critical for understanding pathogenic changes of the immune system in HIV-1 infection and accordingly tailor preventive and therapeutic vaccine approaches.

5.5 Methods

Clinical specimen

Cryopreserved peripheral blood mononuclear cells (PBMC) and plasma of HIV-1 infected individuals were available from samples stored in the biobank of the Zurich Primary HIV Infection Study (ZPHI). The ZPHI is an ongoing, observational, nonrandomized, single center cohort founded in 2002 that specifically enrolls patients with documented acute or recent primary HIV-1 infection (ClinicalTrials.gov identifier NCT00537966) (132). The ZPHI is approved by the ethics committee of the Kantonale Ethikkommission Zürich and written informed consent was obtained from all participants. Longitudinal samples of patients that started ART early (during the acute infection stage, n=11) and late (in the chronic infection stage, n=10) were analyzed and included samples from the untreated acute and chronic stage and after 1 year of ART (Supplementary table 1 and 2). A separate set of patients were analyzed during the chronic infection stage for functional disturbance in B cell subsets (Figure 6F and 7, Supplementary table 1 and 2). Patient and disease demographics (estimated time of infection, CD4 cell count and plasma viral load level at sampling date) were available through the ZPHI data bank.

PBMC and plasma from healthy donors (n=21) were collected in the frame of a separate clinical study (PI H. Günthard) that was approved by the ethics committee of the Kantonale Ethikkommission Zürich and written informed consent was obtained from all participants.

PBMC were isolated by density-gradient centrifugation using LymphoPrep (Axis-Shield) from whole blood drawn in EDTA vacutainer tubes (BD Biosciences). Until further processing PBMC were cryopreserved using 90% inactivated FCS (Thermo Fisher Scientific) and 10% DMSO (Sigma Aldrich) and stored in liquid nitrogen. Plasma was heat-inactivated for 1h at 56°C and stored at -80°C for further analysis.

Flow cytometry

To monitor B cell populations by flow cytometry PBMC were stained using a 16-parameter panel as described *(Liechti, T. et al. manuscript in preparation, Chapter 4)*. Briefly, cells were thawed and washed with FACS buffer containing PBS (Thermo Fisher Scientific), 2% heat-inactivated FCS (Thermo Fisher Scientific), 2mM EDTA (Sigma Aldrich) and 20µg/ml DNase (Sigma Aldrich), stained with a cocktail of antibodies directed against surface markers encompassing CD3 APC-Cy7 (clone SK7, Biolegend), CD14 APC-Cy7 (clone HCD14, Biolegend), CD16 APC-Cy7 (clone 3G8, Biolegend), CD10 BV650 (clone HI10a, BD

Pharmingen), CD19 BV786 (clone SJ25C1, BD Pharmingen), CD21 BV711 (clone B-ly4m BD Pharmingen), CD27 PE-CF594 (clone M-T271, BD Pharmingen), CD38 AF700 (clone HIT2, Biolegend), IgG1 PE (clone HP6001, Southern Biotech), IgG3 FITC (polyclonal sheep IgG, AbD Serotec), IgA APC (polyclonal goat IgG, Jackson Immuno), CCR7 BV605 (clone G043H7, Biolegend), CXCR3 PE-Cy7 (clone G025H7, Biolegend), CXCR5 BV510 (clone RF8B2, BD Pharmingen), IL-21R BV421 (clone 2G1-K12, Biolegend) and Live/dead near-infrared dye (Life Technologies). IgD (clone IA6-2, Biolegend) and CXCR4 (clone 12G5, Biolegend) were labelled in-house with labeling kits for PE-Cy5 (Innova Biosciences) and PE-Cy5.5 (Innova Biosciences), respectively, according to the manufacturer's instructions. Each new batch of labeled antibodies was titrated in parallel with and adjusted to the old batch to ascertain comparable staining intensities. Cells were afterwards fixed and permeabilized with the FoxP3 staining kit (eBioscience) according to manufacturer's instructions to stain for Ki-67 PerCP-eFluor710 (clone 20Raj1, eBioscience). Data was acquired on a BD Fortessa calibrated daily using the CS&T module. Staining intensity QC was conducted as recommended (133) and individual stainings with markers that did not fulfil requirements excluded when comparative analysis of intensities was performed (Supplementary figure 1). To further limit the possibility of influences due to day-to-day variability in the flow cytometry analysis, all longitudinally time points of a given patient were analyzed at the same day. In addition patients assigned to the early and late ART group were included in all experiments to exclude batch effects.

The staining to analyze IgM, CD95 and FcRL4 expression was performed with the same protocol but with a smaller panel including Live/dead near-infrared dye (Life Technologies), CD19 BV510 (clone SJ25C1, BD Pharmingen), IgM FITC (polyclonal goat, Caltag), CD95 BV421 (clone DX2, Biolegend), FcRL4 PE (clone 413D12, Biolegend), IgD APC (clone IA6-2, Biolegend), CD21 BV711 (clone B-ly4, BD Pharmingen), CD27 PE-CF594 (clone M-T271, BD Pharmingen), IgG PE-Cy7 (clone G18-145, BD Pharmingen), CD10 BV650 (clone HI10a, BD Pharmingen) and CD38 AF700 (clone HIT2, Biolegend).

Clustering analysis

The diversity of $CD21^-$ naïve B cells was assessed using the clustering algorithm SPADE (spanning-tree progression analysis of density-normalized events) integrated into the cytometry analysis platform Cytobank (134). 17 of the 21 analyzed HIV-infected patients were included in the clustering analysis. Two patients had to be excluded as no sample from the acute time point was available, two patients were excluded due to staining patterns resulting in unusual clustering results. As reference 15 healthy controls were included in the

analysis. Clustering was done using pre-gated CD21$^-$ naïve B cells including all recorded events. Target number of expected nodes was set to 200 and down-sampling to 2%. In order to analyze total longitudinal changes of CD21$^-$ naïve B cells the flow cytometry files of the individual time points or the control group were concatenated and integrated into the clustering. Clustering was based on the markers CCR7, CXCR3, CXCR5 and IL-21R. CD19 was not included due its unimodal expression profile. CXCR4 was not included due to variability in staining intensity.

We chose a setting of over-clustering, by allowing for 200 different clusters as this allows to build separate clusters of very rare cell populations. As a consequence frequent cell populations can separate into different clusters despite sharing phenotypic properties. Therefore, clusters created by SPADE were further clustered using hierarchical clustering with the Ward method in R and visualized with the hetmap.2 function. For Ward clustering and visualization, the SPADE output (z-transformed arcsinh median fluorescence intensities of individual clusters) of the concatenated chronic 2 year samples was used due to the fact that this measurement encompassed the highest frequency of CD21$^-$ naïve B cells and therefore all SPADE clusters should contain cell events. Importantly, Ward clustering is based on the same markers used for SPADE clustering. CXCR4 and CD19 expression of the SPADE clusters was visualized to investigate the expression profile of these two markers on SPADE and Ward clusters. Based on the hierarchical tree generated by Ward clustering a total of 10 main clusters could be defined. For manual analysis, the SPADE clusters of the concatenated chronic 2 year samples were again concatenated according to the Ward cluster classification. The cell events of these Ward clusters were further analyzed in FlowJo version 10 (Treestar) to assess the unique expression profile of the Ward clusters.

IgG ELISA

Total immunoglobulin concentrations in heat-inactivated plasma from the HIV-1 infected patients (Supplementary table 2) were measured by enzyme-linked immunosorbent assay (ELISA) as described previously (135). Briefly, 96 well immunosorbent plates (Thermo Fisher Scientific) were coated with polyclonal goat anti-human IgG (2µg/ml; Southern Biotech) in sodium carbonate buffer pH8.2 for 2 hours at room temperature. PBS/2% BSA (Sigma Aldrich) was used as a blocking reagent for 30 minutes at 37°C. Serial dilutions of the plasma samples were applied to the plates and incubated for 2 hours at room temperature. Plasma IgG was detected using a biotinylated polyclonal goat anti-human IgG (southern Biotech; 2 ng/ml) followed by streptavidin-alkaline phosphatase (Sigma Aldrich, 40ng/ml) each diluted in PBS/2% BSA and incubated for 1 hour at room temperature. CDP-Star

system (Applied Biosystems) was used as alkaline phosphatase substrate and luminescence was measured after 30min with a Dynex luminometer (Magellan Biosciences). Human IgG (Sigma Aldrich) was used as a standard to determine the concentration of plasma IgG.

Expression of apoptosis markers

Cryopreserved PBMC from 10 healthy controls and 10 chronically infected patients were analyzed for the frequency of apoptotic cells within the different B cell subsets (Supplementary table 2). Cells were stained with antibodies CD19 biotin (clone HIB19, BD Pharmingen), CD21 PE (clone B-ly4, BD Pharmingen), CD27 PE-CF594 (clone M-T271, BD Pharmingen), IgD PE-Cy7 (clone IA6-2, Biolegend) and Live/Dead near-infrared (Life Technologies). CD19 was detected by using BV421-conjugated streptavidin (Biolegend). The apoptosis markers cleaved caspase 3 inhibitor FITC-C6-DEVD-FMK (AAT Bioquest) and Annexin V APC (BD Pharmingen) stainings were performed according to the manufacturer's protocol. Samples were analyzed either on a FACS Aria III or a BD FACS Verse immediately after staining and analyzed with FlowJo version 10. Apoptotic cells were defined as double positive for Annexin V and FITC-C6-DEVD-FMK (136).

Phosflow analysis

PBMC were rested after thawing for 4 hours in RPMI medium without supplements and incubated in RPMI containing Live/Dead near-infrared dye (Life Technologies) for 20 minutes at room temperature. Cells were washed and split in two wells and resuspended in either only RPMI for the unstimulated sample or in RPMI containing 10µg/ml goat anti-human IgG/IgA/IgM f(ab)2 (Jackson Immuno). Stimulation was done for 5 minutes including a 2 minute centrifugation step to remove the medium followed by addition of the fixation and permeabilization solution of the Foxp3 staining kit according to manufacturer's instructions (eBiosciences). Cells were fixed and permeabilized for 45 minutes at 4°C and afterwards stained with CD3 APC-Cy7 (clone SK7, Biolegend), CD14 APC-Cy7 (clone HCD14, Biolegend), CD16 APC-Cy7 (clone 2G8, Biolegend), CD10 PE-Cy5 (clone HI10a, BD Pharmingen), CD19 BV510 (clone SJ25C1, BD Pharmingen), CD21 BV711 (clone B-ly4, BD Pharmingen), CD27 PE-CF594 (clone M-T271, BD Pharmingen), IgD APC (clone IA6-2, Biolegend) and PE-labeled antibody specific for intracellular phosphorylated tyrosine motifs (clone PY20, BD Pharmingen) for 30 minutes at room temperature. Cells were extensively washed and measured using a BD Fortessa. Analysis was done with with FlowJo 10 (TreeStar).

Statistical analysis

B cell subset frequencies of HIV-1 infected individuals at different disease stages and healthy donors were compared with unpaired one-way ANOVA (Kruskal-Wallis test) and Dunn's multiple testing correction (Figures 1A-C; 4, 5, 6C, Supplementary table 3 and Supplementary Figure 8). For comparison of longitudinal phenotypic changes non-parametric matched Friedman test and Dunn's multiple testing correction test was used to compare time points within the study groups (Figures 1A-C, 5D, 6B and Supplementary Figure 8). Correlation analysis of infected patients and healthy controls was done by Spearman correlation (Figure 1A-C). Linear regression was used to analyze correlation of $CD21^-$ and $CD21^+$ naïve and $CD21^-$ and $CD21^+$ MZ B cells with clinical parameters (Figure 2). Phenotypic comparisons between $CD21^-$ and $CD21^+$ naïve or $CD21^-$ and $CD21^+$ MZ B cell subsets within the same patients was done by Wilcoxon matched-pairs signed rank test (Figure 3B, 6C-G and 7C) and between healthy donors and HIV-1 infected patients using the Mann-Whitney test (Figure 3C-E, 6C-G, 7D). Friedman test and Dunn's multiple testing correction test was used to compare different memory B cell subsets from the same donor in Figure 7C. Statistical analysis was done with Prism (GraphPad) and P values less than 0.05 were considered statistically significant. Heatmaps and hierarchical clustering were generated with heatmap.2 function in R version 3.3.1 (https://r-project.org/) and the interface R studio. SPADE clustering analysis was performed using Cytobank.

5.6 Figure legends

Figure 1: *B cell subset changes during HIV infection.*

(A) Frequencies of main B cell subsets, **(B)** memory B cell subsets and **(C)** $CD21^-$ naïve and $CD21^-$ MZ B cells from healthy donors (n=29) and HIV-1 infected patients (n=19) at acute and chronic (2 years of continuous virus replication) disease stage and after 1 year of ART are shown. **(D)** Spearman correlation of healthy donors (n=29) and chronically infected patients (n=21) based on subset frequencies shown in figure 1A-C is depicted. The dendrogram is colored according to the cut-off used to define patient clsuters. **(E)** Comparison of clinical parameters from the patient clusters (Healthy, Chronic and Intermediate) identified with hierarchical clustering of spearman correlation in Figure 1D was performed. Non-parametric unpaired Kruskal-Wallis test was used to compare healthy controls and HIV-1 infected patients and comparison of patient clusters. Longitudinal analysis of HIV-1 infected patients was done using non-paramtetric paired Friedman's test. Dunn's multiple comparison test was performed to correct for multiple testing. $P<0.05$ was considered statistically significant. *p<0.05, **p<0.01, ***p<0.001, ****p<0.0001.

Figure 2: Correlation of $CD21^-$ naïve and $CD21^-$ MZ B cells

Linear regression analysis of $CD21^-$ naïve and MZ B with CD4 counts, viral load and plasma IgG concentration in acute (n=19; n for correlation with CD4=11) and chronic HIV-1 infection (2 years of continuous virus replication; n=21; n for correlation with CD4=20) is shown. Regression coefficient r^2 and p-values are indicated. $P<0.05$ was considered statistically significant.

Figure 3: Phenotype of $CD21^-$ naïve and $CD21^-$ MZ B cells

(A) Histogram overlays from flow cytometric analysis of CCR7, CXCR3, CXCR4, CXCR5, CD19 and IL-21R expression on $CD21^-$ and $CD21^+$ naïve (darkred and red, respectively) and MZ B cells (darkblue and blue, respectively) from a chronic HIV-1 infected patient. Where applied FMO controls (grey) are shown. **(B)** Comparison of frequencies of $CD21^-$ (grey open circle) and $CD21^+$ (black circle) naïve and MZ B cells expressing CCR7, CXCR3, CXCR4, CXCR5 and IL-21R in healthy controls (n=29) and chronically (2 years of continuous virus replication) HIV-1 infected patients (n=21) is depicted. **(C)** Differences of the same markers

between healthy (n=29) and chronically HIV-1 infected patients (n=21) are shown. ND; comparison not performed due to irregular staining as depicted in supplementary figure 1 and described in the methods part. Median fluorescence intensity (MFI) fold change for **(D)** CCR7, CXCR3, CXCR4, CXCR5 and IL-21R and **(E)** CD19 between $CD21^-$ and $CD21^+$ naïve or $CD21^-$ and $CD21^+$ MZ B cells compared between healthy controls (n=29) and chronically HIV-1 infected patients (n=21) are shown. Comparison of $CD21^-$ and $CD21^+$ naïve and MZ B cells within the same individual was done by Wilcoxon matched-pairs signed rank test. Mann-Whitney T test was used to test differences between healthy controls and chronically HIV-1 infected patients. $P<0.05$ was considered statistically significant. *p<0.05, **p<0.01, ***p<0.001, ****p<0.0001.

Figure 4: Longitudinal analysis of phenotypic markers on $CD21^-$ naïve and $CD21^-$ MZ B cells

Longitudinal analysis of median fluorescence intensities of phenotypic marker expressed on $CD21^-$ naïve and MZ B cells are shown. HIV-1 infected patients were split in early ART group (closed circles; n=11) and late ART group (open circles, n=8). Matched-pair non-parametric one-way ANOVA Friedman test was used to compare MFI values within the study groups and non-paired non-parametric ANOVA Kruskal-Wallis test was used to compare MFI values between study groups. Dunn's multiple comparison test was performed to correct for multiple testing. $P<0.05$ was considered statistically significant. *p<0.05, **p<0.01, ***p<0.001.

Figure 5: Computational clustering algorithm SPADE reveals heterogeneity of $CD21^-$ naïve B cells in chronic HIV infection

(A) SPADE analysis of $CD21^-$ naïve B cells is shown from combined data of chronically HIV-1 infected patients (n=17; chronic 2 years). The marker expression levels of the defined cluster are depicted as a gradient with yellow showing highest expression. Dot sizes correspond to cell counts of the individual clusters. **(B)** Expression of markers not used for clustering (CXCR4 and CD19) are shown within the SPADE tree. **(C)** Heatmap with expression profile of SPADE clusters ordered using Ward's hierarchical clustering I shown. Similar SPADE clusters are merged in 10 Ward clusters and named 1-10 as shown in the heatmap. Dendrogram is colored according to the cut-off used to define Ward clusters. **(D)** Comparison of Ward cluster frequencies between healthy donors (black dots) and the different time points acute (blue), chronic 1 year (light red), chronic 2 years (dark red) and ART 1 year (grey) of HIV-1 infected patients are depicted. The latter were separated based on the study groups in early (closed dots) and late ART group (open circles). Matched-pair

non-parametric one-way ANOVA Friedman test was used to compare cluster frequencies within the study groups and non-paired non-parametric ANOVA Kruskal-Wallis test was used to compare frequencies between study groups and to healthy controls. Dunn's multiple comparison test was used to perform multiple testing corrections. P values are shown. P<0.05 was considered statistically significant. *p<0.05, **p<0.01, ***p<0.001.

Figure 6: $CD21^-$ naïve $CD21^-$ MZ B cells express high levels of IgM and activation markers and contain increased frequencies of proliferating and apoptotic cells.

(A) Example of flow cytometry data for IgM, CD95 and FcRL4 staining on $CD21^+$ and $CD21^-$ naïve and $CD21^+$ and $CD21^-$ MZ B cells of a chronic (2 years of active infection) HIV-1 infected patient. Overlay of $CD21^-$ naïve and $CD21^-$ MZ B cells (red) and total B cells are shown in the top row. **(B)** IgM, CD95 and FcRL4 expression dynamics in $CD21^-$ and $CD21^+$ naïve and $CD21^-$ and $CD21^+$ MZ B cells are shown in percent negative and positive events in case of IgM and CD95 and FcRL4, respectively. Healthy controls (n=29) and HIV infected patients (n=6) are shown. Longitudinal changes in Figure 6B of HIV-1 infected patients were performed using matched-pair non-parametric one-way ANOVA Friedman test. To compare healthy controls with HIV-1 infected patients non-paired non-parametric ANOVA Kruskal-Wallis test was used. To correct for multiple testing Dunn's multiple comparison test was performed. **(C)** Direct comparison of IgM, CD95 and FcRL4 expression on $CD21^-$ and $CD21^+$ naïve and $CD21^-$ and $CD21^+$ MZ B cells in healthy subjects (n=29) and chronic HIV-infected patients (n=7) are shown. **(D)** Flow cytometry dot plots of Ki-67 expression on $CD21^-$ and $CD21^+$ naïve and $CD21^-$ and $CD21^+$ MZ B cells from a chronic (2 years of active infection) HIV-1 infected patient are depicted. **(E)** Comparison of the intracellular expression of proliferation marker Ki-67 in $CD21^-$ and $CD21^+$ naïve and $CD21^-$ and $CD21^+$ MZ B cells in healthy controls (n=29) and chronic HIV-infected patients (n=21) is shown. **(F)** Example of flow cytometry dot plots of FITC labeled caspase 3 inhibitor FITC-C6-DEVD-FMK and Annexin V staining from a chronic (2 years of active infection) HIV-1 infected patient to determine the frequency of double-positive apoptotic $CD21^-$ and $CD21^+$ naïve and $CD21^-$ and $CD21^+$ MZ B cells. **(G)** Frequency of apoptotic $CD21^-$ and $CD21^+$ naïve and MZ B cells are quantified in healthy controls (n=10) and chronic HIV-infected patients (n=10). Comparison of $CD21^-$ and $CD21^+$ naïve or $CD21^-$ and $CD21^+$ MZ B cells in Figure 6C, 6E and 6G were done using matched-pair non-parametric Wilcoxon signed rank test and comparison between healthy controls and HIV-infected patients by using unpaired non-parametric Mann-Whitney test. P<0.05 was considered statistically significant. *p<0.05, **p<0.01, ***p<0.001, ****p<0.0001.

Figure 7: $CD21^-$ naïve and $CD21^-$ MZ B cells show impaired phosphorylation upon BCR-dependent stimulation highlighting their anergic state.

(A) Histogram overlays of flow cytometric phosflow analysis in unstimulated (black) and BCR cross-linking stimulated (blue) $CD21^-$ and $CD21^+$ naïve and $CD21^-$ and $CD21^+$ MZ B cells are shown from a healthy control. **(B)** Tyrosine phosphorylation was analyzed before and upon stimulation with anti-IgG/IgA/IgM in healthy subjects (n=10) and chronic HIV-1 infected patients (n=10) and visualized as a heatmap for $CD21^-$ and $CD21^+$ naïve and $CD21^-$ and $CD21^+$ MZ B cells and the four memory B cell subsets based on CD21 and CD27 expression, namely intermediate (IM; $CD21^+CD27^-$), resting (RM; $CD21^+CD27^+$), activated (AM; $CD21^-CD27^+$) and tissue-like (TLM; $CD21^-CD27^-$) memory B cells. The color gradient indicates the log-transformed MFI values with yellow as highest phosphorylated tyrosine levels. **(C)** Total tyrosine phosphorylation MFI between $CD21^-$ naïve and $CD21^-$ MZ B cells at basal levels and upon stimulation are depicted for healthy subjects (n=10; grey dots) and chronic HIV-1 infected patients (n=10; red dots). Memory B cell subsets are included as a control. **(D)** Direct comparison of total tyrosine phosphorylation MFI of $CD21^-$ and $CD21^+$ naïve, $CD21^-$ and $CD21^+$ MZ B cells and memory B cell subsets upon stimulation between healthy controls and chronic HIV-1 infected patients are depicted. Wilcoxon matched-pairs signed rank test was used to compare $CD21^-$ and $CD21^+$ naïve and $CD21^-$ and $CD21^+$ MZ B cells within healthy subjects and chronic HIV-1 infected patients. For the comparison between memory B cell subsets Kruskal-Wallis one-way ANOVA with Dunn's multiple testing correction was used. To compare phosphorylation levels between healthy subjects and chronic HIV-1 infected patients Mann-Whitney T test was applied. $P<0.05$ was considered statistically significant. *$p<0.05$, **$p<0.01$, ***$p<0.001$, ****$p<0.0001$.

5.7 Figures

Figure 1

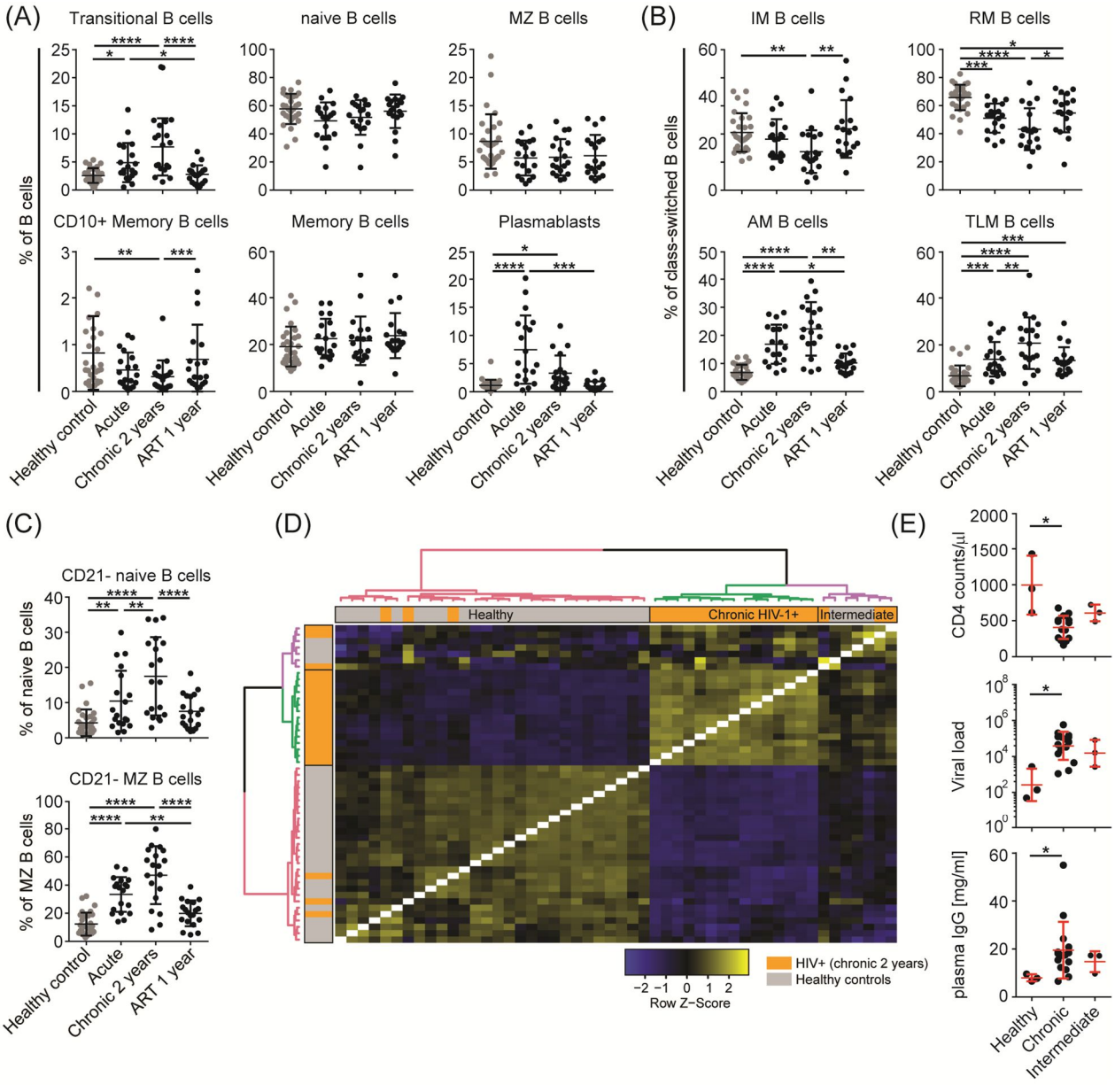

Figure 2

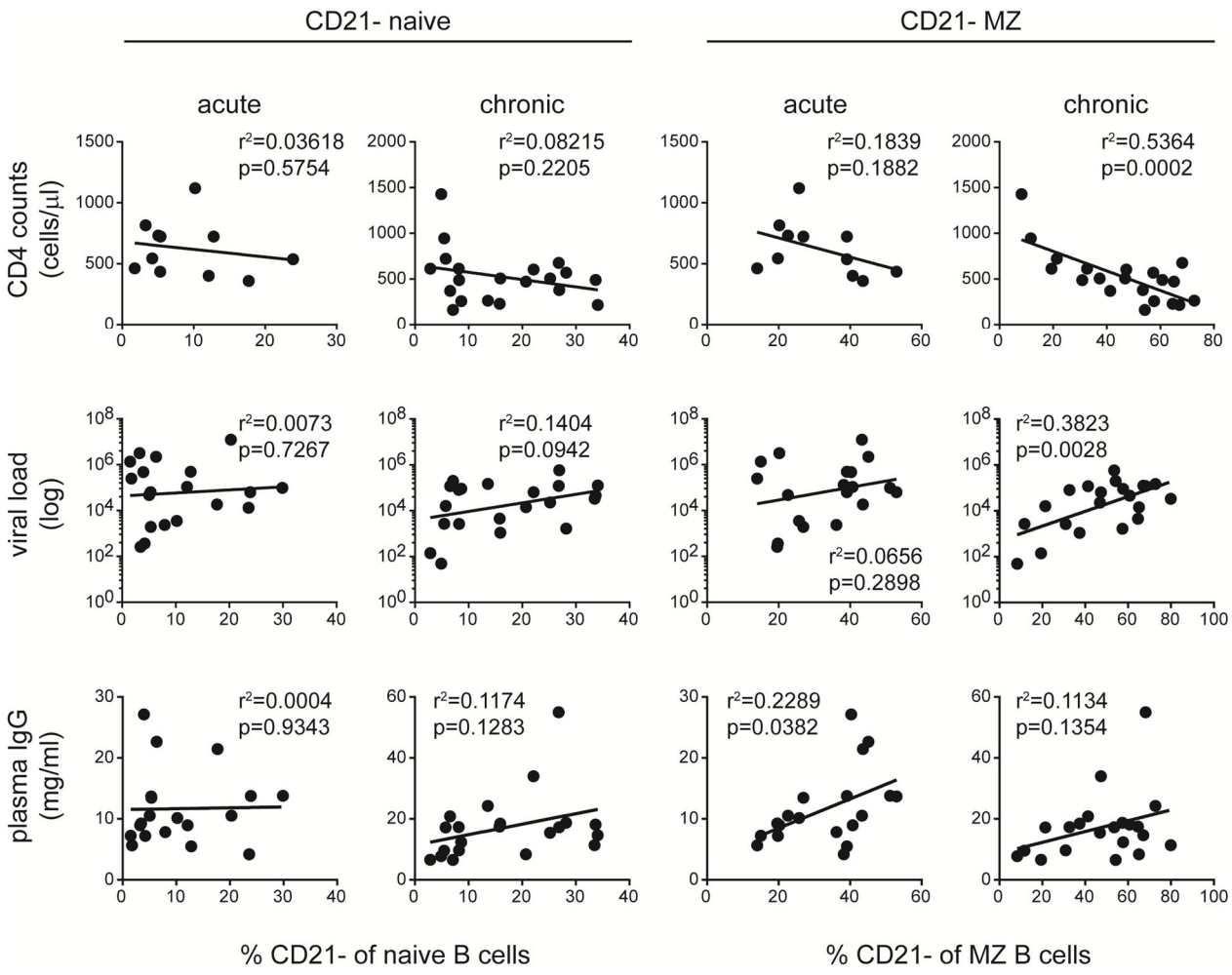
CD21- naive
CD21- MZ
acute
chronic
acute
chronic
CD4 counts (cells/µl)
r²=0.03618
p=0.5754
r²=0.08215
p=0.2205
r²=0.1839
p=0.1882
r²=0.5364
p=0.0002
viral load (log)
r²=0.0073
p=0.7267
r²=0.1404
p=0.0942
r²=0.0656
p=0.2898
r²=0.3823
p=0.0028
plasma IgG (mg/ml)
r²=0.0004
p=0.9343
r²=0.1174
p=0.1283
r²=0.2289
p=0.0382
r²=0.1134
p=0.1354
% CD21- of naive B cells
% CD21- of MZ B cells

Figure 3

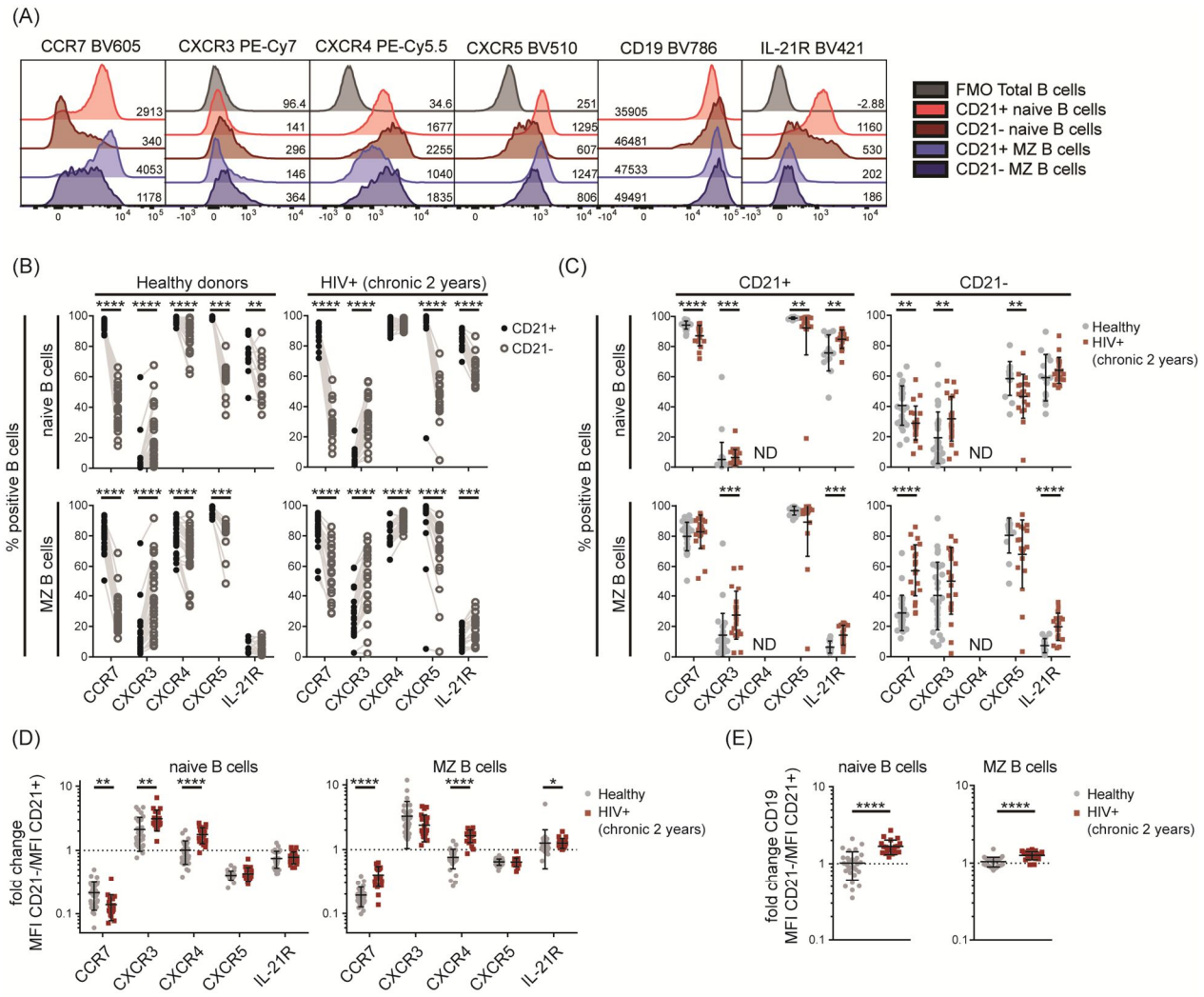
(A)
CCR7 BV605
CXCR3 PE-Cy7
CXCR4 PE-Cy5.5
CXCR5 BV510
CD19 BV786
IL-21R BV421
FMO Total B cells
CD21+ naive B cells
CD21- naive B cells
CD21+ MZ B cells
CD21- MZ B cells
(B)
Healthy donors
HIV+ (chronic 2 years)
CD21+
CD21-
% positive B cells
naive B cells
MZ B cells
CCR7
CXCR3
CXCR4
CXCR5
IL-21R
(C)
CD21+
CD21-
ND
Healthy
HIV+
(chronic 2 years)
(D)
naive B cells
MZ B cells
fold change
MFI CD21-/MFI CD21+)
(E)
fold change CD19
MFI CD21-/MFI CD21+)

Figure 4

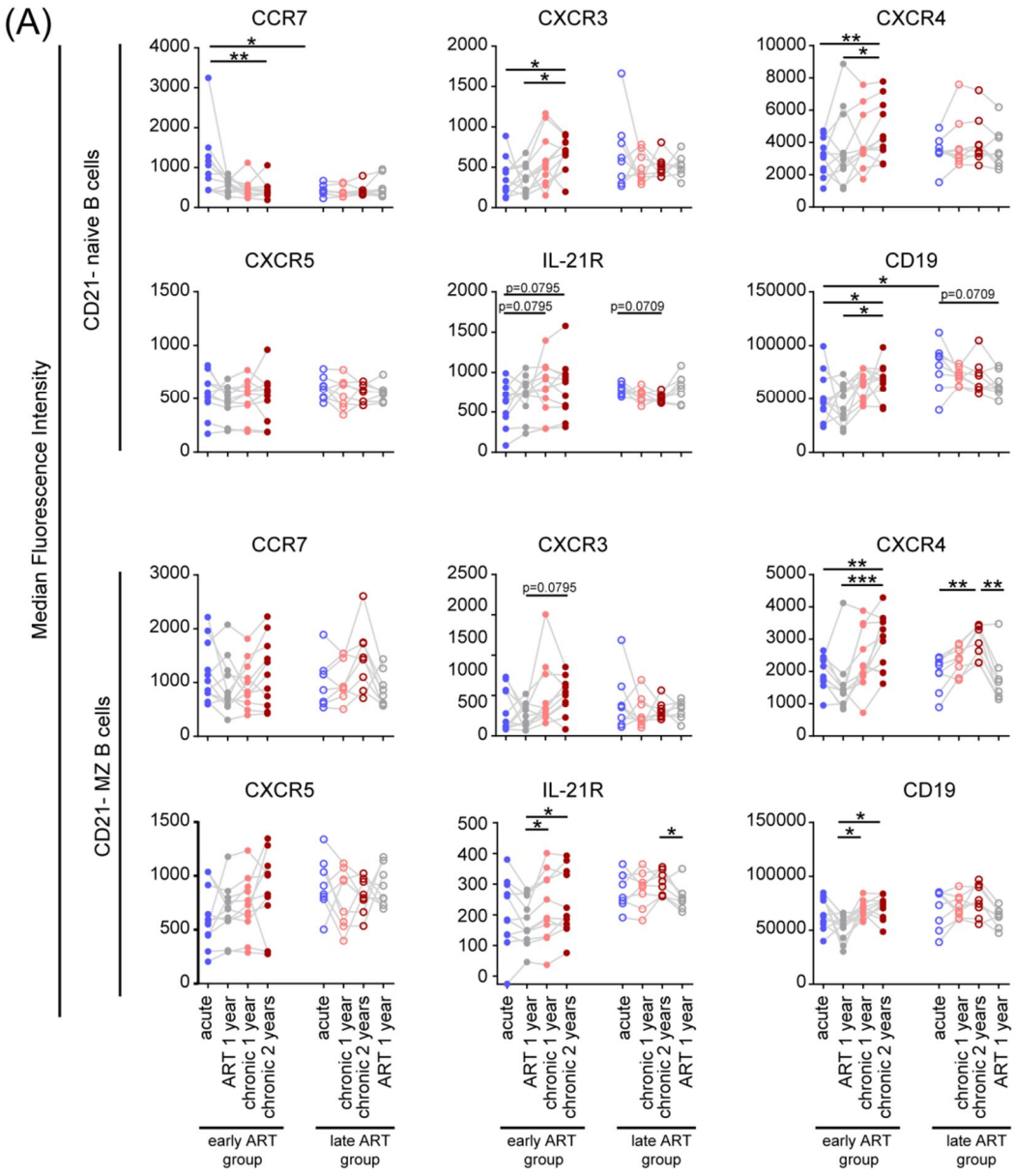
(A)
Median Fluorescence Intensity
CD21- naive B cells
CD21- MZ B cells
CCR7
CXCR3
CXCR4
CXCR5
IL-21R
CD19
p=0.0795
p=0.0709
acute
ART 1 year
chronic 1 year
chronic 2 years
early ART group
late ART group

Figure 5

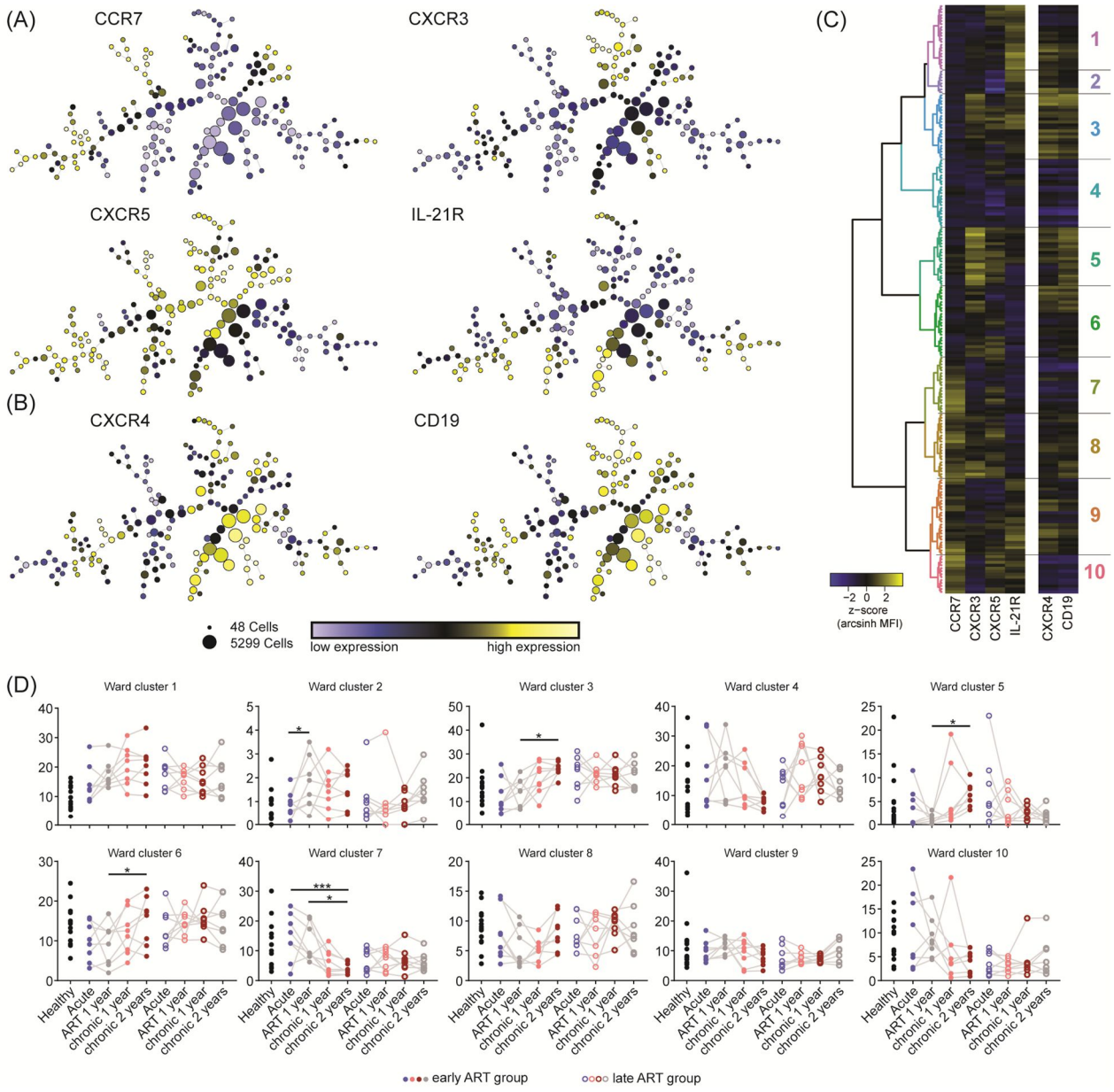
(A)
CCR7
CXCR3
CXCR5
IL-21R
(B)
CXCR4
CD19
48 Cells
5299 Cells
low expression
high expression
(C)
1
2
3
4
5
6
7
8
9
10
−2 0 2
z−score
(arcsinh MFI)
CCR7
CXCR3
CXCR5
IL-21R
CXCR4
CD19
(D)
Ward cluster 1
Ward cluster 2
Ward cluster 3
Ward cluster 4
Ward cluster 5
Ward cluster 6
Ward cluster 7
Ward cluster 8
Ward cluster 9
Ward cluster 10
Healthy
Acute
ART 1 year
chronic 1 year
chronic 2 years
early ART group
late ART group

Figure 6

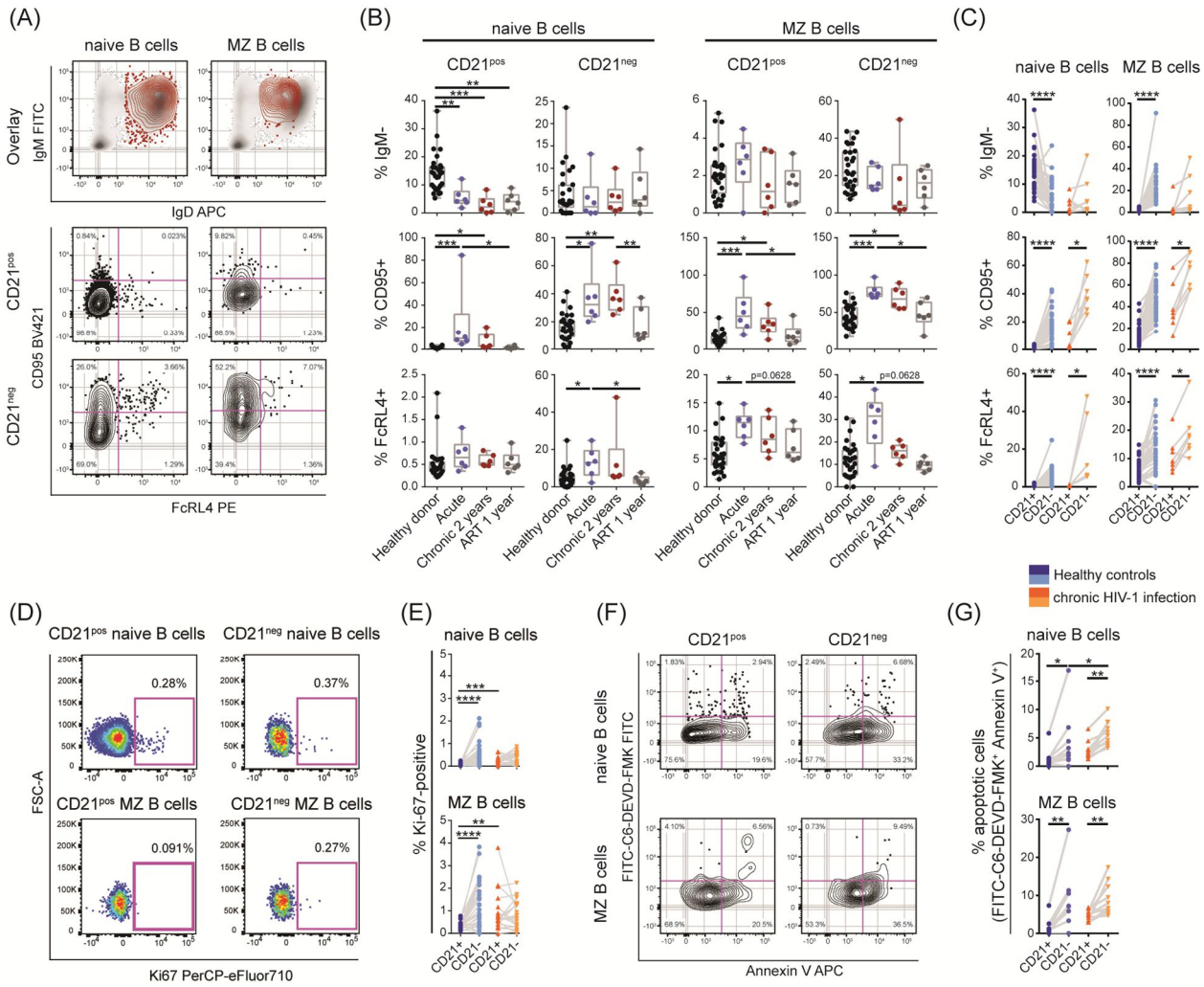
(A)
naive B cells
MZ B cells
Overlay
IgM FITC
IgD APC
CD21pos
CD95 BV421
CD21neg
FcRL4 PE
(B)
naive B cells
MZ B cells
CD21pos
CD21neg
% IgM-
% CD95+
% FcRL4+
p=0.0628
Healthy donor
Acute
Chronic 2 years
ART 1 year
(C)
naive B cells
MZ B cells
% IgM-
% CD95+
% FcRL4+
CD21+
CD21-
Healthy controls
chronic HIV-1 infection
(D)
CD21pos naive B cells
CD21neg naive B cells
CD21pos MZ B cells
CD21neg MZ B cells
0.28%
0.37%
0.091%
0.27%
FSC-A
Ki67 PerCP-eFluor710
(E)
naive B cells
MZ B cells
% Ki-67-positive
(F)
CD21pos
CD21neg
naive B cells
MZ B cells
FITC-C6-DEVD-FMK FITC
Annexin V APC
(G)
naive B cells
MZ B cells
% apoptotic cells
(FITC-C6-DEVD-FMK+ Annexin V+)

Figure 7

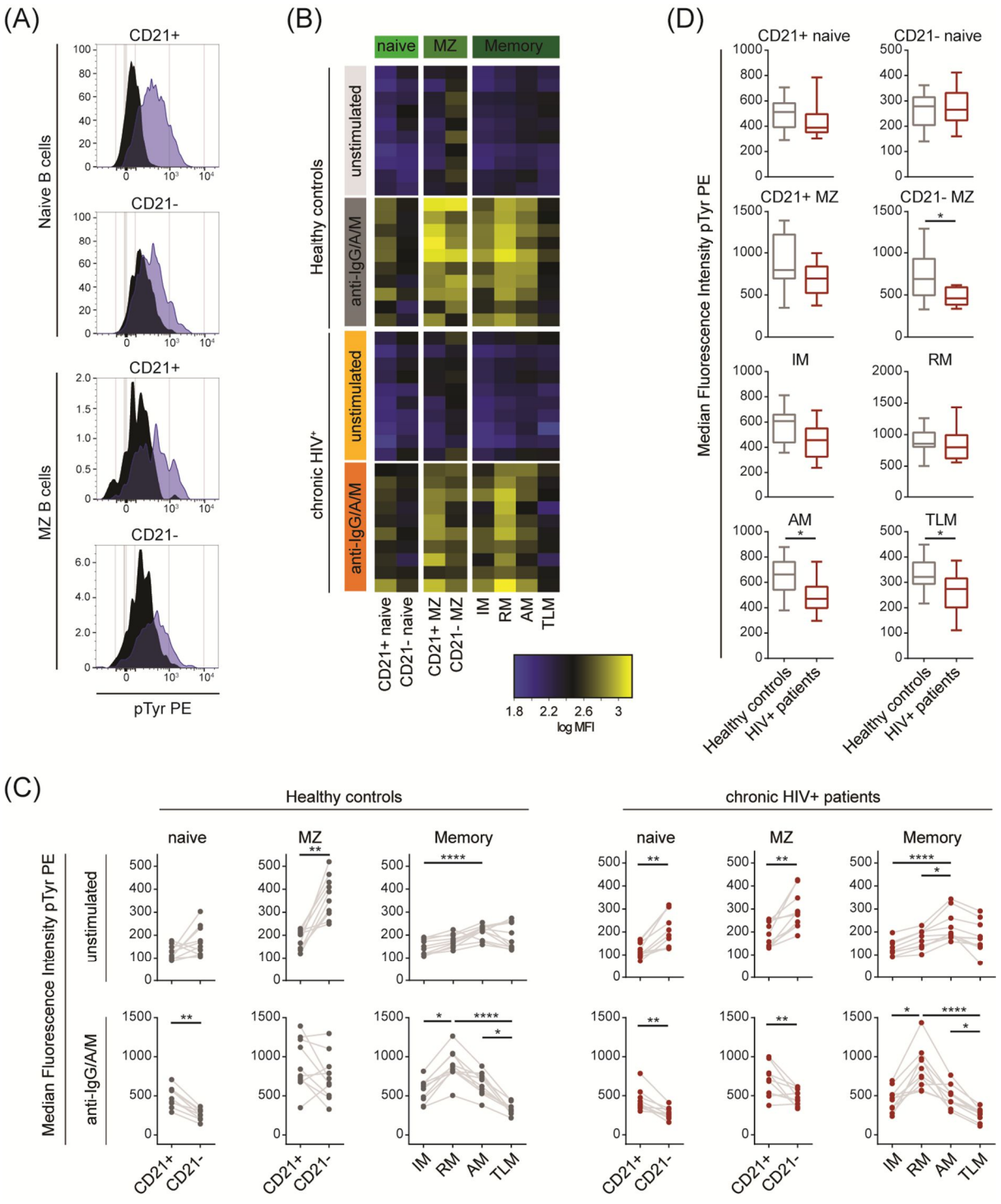
(A)
CD21+
CD21-
CD21+
CD21-
Naive B cells
MZ B cells
pTyr PE
(B)
naive
MZ
Memory
Healthy controls
chronic HIV+
unstimulated
anti-IgG/A/M
unstimulated
anti-IgG/A/M
CD21+ naive
CD21- naive
CD21+ MZ
CD21- MZ
IM
RM
AM
TLM
log MFI
(D)
CD21+ naive
CD21- naive
CD21+ MZ
CD21- MZ
IM
RM
AM
TLM
Median Fluorescence Intensity pTyr PE
Healthy controls
HIV+ patients
(C)
Healthy controls
chronic HIV+ patients
naive
MZ
Memory
Median Fluorescence Intensity pTyr PE
unstimulated
anti-IgG/A/M
CD21+
CD21-
IM
RM
AM
TLM

5.8 References

1. Tomaras, G.D., and Haynes, B.F. 2009. HIV-1-specific antibody responses during acute and chronic HIV-1 infection. *Curr Opin HIV AIDS* 4:373-379.

2. Tomaras, G.D., Yates, N.L., Liu, P., Qin, L., Fouda, G.G., Chavez, L.L., Decamp, A.C., Parks, R.J., Ashley, V.C., Lucas, J.T., et al. 2008. Initial B-cell responses to transmitted human immunodeficiency virus type 1: virion-binding immunoglobulin M (IgM) and IgG antibodies followed by plasma anti-gp41 antibodies with ineffective control of initial viremia. *J Virol* 82:12449-12463.

3. Overbaugh, J., and Morris, L. 2012. The Antibody Response against HIV-1. *Cold Spring Harb Perspect Med* 2:a007039.

4. Wei, X., Decker, J.M., Wang, S., Hui, H., Kappes, J.C., Wu, X., Salazar-Gonzalez, J.F., Salazar, M.G., Kilby, J.M., Saag, M.S., et al. 2003. Antibody neutralization and escape by HIV-1. *Nature* 422:307-312.

5. Bunnik, E.M., Pisas, L., van Nuenen, A.C., and Schuitemaker, H. 2008. Autologous neutralizing humoral immunity and evolution of the viral envelope in the course of subtype B human immunodeficiency virus type 1 infection. *J Virol* 82:7932-7941.

6. Gray, E.S., Moore, P.L., Choge, I.A., Decker, J.M., Bibollet-Ruche, F., Li, H., Leseka, N., Treurnicht, F., Mlisana, K., Shaw, G.M., et al. 2007. Neutralizing antibody responses in acute human immunodeficiency virus type 1 subtype C infection. *J Virol* 81:6187-6196.

7. Richman, D.D., Wrin, T., Little, S.J., and Petropoulos, C.J. 2003. Rapid evolution of the neutralizing antibody response to HIV type 1 infection. *Proc Natl Acad Sci U S A* 100:4144-4149.

8. Liao, H.X., Lynch, R., Zhou, T.Q., Gao, F., Alam, S.M., Boyd, S.D., Fire, A.Z., Roskin, K.M., Schramm, C.A., Zhang, Z.H., et al. 2013. Co-evolution of a broadly neutralizing HIV-1 antibody and founder virus. *Nature* 496:469-+.

9. Wibmer, C.K., Bhiman, J.N., Gray, E.S., Tumba, N., Karim, S.S.A., Williamson, C., Morris, L., and Moore, P.L. 2013. Viral Escape from HIV-1 Neutralizing Antibodies Drives Increased Plasma Neutralization Breadth through Sequential Recognition of Multiple Epitopes and Immunotypes. *Plos Pathogens* 9.

10. Moore, P.L., Gray, E.S., Wibmer, C.K., Bhiman, J.N., Nonyane, M., Sheward, D.J., Hermanus, T., Bajimaya, S., Tumba, N.L., Abrahams, M.R., et al. 2012. Evolution of an HIV glycan-dependent broadly neutralizing antibody epitope through immune escape. *Nat Med* 18:1688-1692.

11. Doria-Rose, N.A., Schramm, C.A., Gorman, J., Moore, P.L., Bhiman, J.N., DeKosky, B.J., Ernandes, M.J., Georgiev, I.S., Kim, H.J., Pancera, M., et al. 2014. Developmental pathway for potent V1V2-directed HIV-neutralizing antibodies. *Nature* 509:55-62.

12. Moore, P.L., Sheward, D., Nonyane, M., Ranchobe, N., Hermanus, T., Gray, E.S., Abdool Karim, S.S., Williamson, C., and Morris, L. 2013. Multiple pathways of escape from HIV broadly cross-neutralizing V2-dependent antibodies. *J Virol*.

13. Lynch, R.M., Wong, P., Tran, L., O'Dell, S., Nason, M.C., Li, Y., Wu, X., and Mascola, J.R. 2015. HIV-1 fitness cost associated with escape from the VRC01 class of CD4 binding site neutralizing antibodies. *J Virol* 89:4201-4213.

14. Wu, X., Wang, C., O'Dell, S., Li, Y., Keele, B.F., Yang, Z., Imamichi, H., Doria-Rose, N., Hoxie, J.A., Connors, M., et al. 2012. Selection Pressure on HIV-1 Envelope by Broadly Neutralizing Antibodies to the Conserved CD4-Binding Site. *J Virol*.

15. Huang, K.H., Bonsall, D., Katzourakis, A., Thomson, E.C., Fidler, S.J., Main, J., Muir, D., Weber, J.N., Frater, A.J., Phillips, R.E., et al. 2010. B-cell depletion reveals a role for antibodies in the control of chronic HIV-1 infection. *Nat Commun* 1:102.

16. Derdeyn, C.A., Moore, P.L., and Morris, L. 2014. Development of broadly neutralizing antibodies from autologous neutralizing antibody responses in HIV infection. *Curr Opin HIV AIDS* 9:210-216.

17. Meffre, E., Louie, A., Bannock, J., Kim, L.J., Ho, J., Frear, C.C., Kardava, L., Wang, W., Buckner, C.M., Wang, Y., et al. 2016. Maturational characteristics of HIV-specific antibodies in viremic individuals. *JCI Insight* 1.

18. Bosch, K.A., Rainwater, S., Jaoko, W., and Overbaugh, J. 2010. Temporal analysis of HIV envelope sequence evolution and antibody escape in a subtype A-infected individual with a broad neutralizing antibody response. *Virology* 398:115-124.

19. Moore, P.L., Williamson, C., and Morris, L. 2015. Virological features associated with the development of broadly neutralizing antibodies to HIV-1. *Trends in Microbiology* 23:204-211.

20. Rusert, P., Kouyos, R.D., Kadelka, C., Ebner, H., Schanz, M., Huber, M., Braun, D.L., Hoze, N., Scherrer, A., Magnus, C., et al. 2016. Determinants of HIV-1 broadly neutralizing antibody induction. *Nat Med* 22:1260-1267.

21. Doria-Rose, N.A., Klein, R.M., Daniels, M.G., O'Dell, S., Nason, M., Lapedes, A., Bhattacharya, T., Migueles, S.A., Wyatt, R.T., Korber, B.T., et al. 2010. Breadth of human immunodeficiency virus-specific neutralizing activity in sera: clustering analysis and association with clinical variables. *J Virol* 84:1631-1636.

22. Boliar, S., Murphy, M.K., Tran, T.C., Carnathan, D.G., Armstrong, W.S., Silvestri, G., and Derdeyn, C.A. 2012. B-lymphocyte Dysfunction in Chronic HIV-1 Infection Does Not Prevent Cross-clade Neutralization Breadth. *J Virol*.

23. Ferreira, C.B., Merino-Mansilla, A., Llano, A., Perez, I., Crespo, I., Llinas, L., Garcia, F., Gatell, J.M., Yuste, E., and Sanchez-Merino, V. 2013. Evolution of Broadly Cross-Reactive HIV-1-Neutralizing Activity: Therapy-Associated Decline, Positive Association with Detectable Viremia, and Partial Restoration of B-Cell Subpopulations. *Journal of Virology* 87:12227-12236.

24. Hasang, W., Dembo, E.G., Wijesinghe, R., Molyneux, M.E., Kublin, J.G., and Rogerson, S. 2014. HIV-1 infection and antibodies to Plasmodium falciparum in adults. *J Infect Dis* 210:1407-1414.

25. Titanji, K., De Milito, A., Cagigi, A., Thorstensson, R., Grutzmeier, S., Atlas, A., Hejdeman, B., Kroon, F.P., Lopalco, L., Nilsson, A., et al. 2006. Loss of memory B cells impairs maintenance of long-term serologic memory during HIV-1 infection. *Blood* 108:1580-1587.

26. Chang, C.C., Crane, M., Zhou, J., Mina, M., Post, J.J., Cameron, B.A., Lloyd, A.R., Jaworowski, A., French, M.A., and Lewin, S.R. 2013. HIV and co-infections. *Immunol Rev* 254:114-142.

27. Ballet, J.J., Sulcebe, G., Couderc, L.J., Danon, F., Rabian, C., Lathrop, M., Clauvel, J.P., and Seligmann, M. 1987. Impaired anti-pneumococcal antibody response in patients with AIDS-related persistent generalized lymphadenopathy. *Clin Exp Immunol* 68:479-487.

28. Kroon, F.P., van Dissel, J.T., Rijkers, G.T., Labadie, J., and van Furth, R. 1997. Antibody response to Haemophilus influenzae type b vaccine in relation to the number of CD4+ T lymphocytes in adults infected with human immunodeficiency virus. *Clin Infect Dis* 25:600-606.

29. Kroon, F.P., Vandissel, J.T., Dejong, J.C., and Vanfurth, R. 1994. Antibody-Response to Influenza, Tetanus and Pneumococcal Vaccines in Hiv-Seropositive Individuals in Relation to the Number of Cd4+ Lymphocytes. *AIDS* 8:469-476.

30. Crum-Cianflone, N.F., and Wallace, M.R. 2014. Vaccination in HIV-infected adults. *AIDS Patient Care STDS* 28:397-410.

31. Mena, G., Garcia-Basteiro, A.L., and Bayas, J.M. 2015. Hepatitis B and A vaccination in HIV-infected adults: A review. *Hum Vaccin Immunother* 11:2582-2598.

32. Kerneis, S., Launay, O., Turbelin, C., Batteux, F., Hanslik, T., and Boelle, P.Y. 2014. Long-term immune responses to vaccination in HIV-infected patients: a systematic review and meta-analysis. *Clin Infect Dis* 58:1130-1139.

33. Wheatley, A.K., Kristensen, A.B., Lay, W.N., and Kent, S.J. 2016. HIV-dependent depletion of influenza-specific memory B cells impacts B cell responsiveness to seasonal influenza immunisation. *Sci Rep* 6:26478.

34. MacLennan, C.A., Gilchrist, J.J., Gordon, M.A., Cunningham, A.F., Cobbold, M., Goodall, M., Kingsley, R.A., van Oosterhout, J.J., Msefula, C.L., Mandala, W.L., et al. 2010. Dysregulated humoral immunity to nontyphoidal Salmonella in HIV-infected African adults. *Science* 328:508-512.

35. Haas, A., Zimmermann, K., and Oxenius, A. 2011. Antigen-dependent and -independent mechanisms of T and B cell hyperactivation during chronic HIV-1 infection. *J Virol* 85:12102-12113.

36. Bangs, S.C., McMichael, A.J., and Xu, X.N. 2006. Bystander T cell activation - implications for HIV infection and other diseases. *Trends in Immunology* 27:518-524.

37. Manches, O., Frleta, D., and Bhardwaj, N. 2014. Dendritic cells in progression and pathology of HIV infection. *Trends in Immunology* 35:114-122.

38. Moir, S., and Fauci, A.S. 2009. B cells in HIV infection and disease. *Nat Rev Immunol* 9:235-245.

39. Moir, S., and Fauci, A.S. 2013. Insights into B cells and HIV-specific B-cell responses in HIV-infected individuals. *Immunol Rev* 254:207-224.

40. Moir, S., and Fauci, A.S. 2014. B-cell exhaustion in HIV infection: the role of immune activation. *Curr Opin HIV AIDS* 9:472-477.

41. Moir, S., Ho, J., Malaspina, A., Wang, W., DiPoto, A.C., O'Shea, M.A., Roby, G., Kottilil, S., Arthos, J., Proschan, M.A., et al. 2008. Evidence for HIV-associated B cell exhaustion in a dysfunctional memory B cell compartment in HIV-infected viremic individuals. *J Exp Med* 205:1797-1805.

42. Moir, S., Buckner, C.M., Ho, J., Wang, W., Chen, J., Waldner, A.J., Posada, J.G., Kardava, L., O'Shea, M.A., Kottilil, S., et al. 2010. B cells in early and chronic HIV infection: evidence for preservation of immune function associated with early initiation of antiretroviral therapy. *Blood*.

43. Portugal, S., Tipton, C.M., Sohn, H., Kone, Y., Wang, J., Li, S., Skinner, J., Virtaneva, K., Sturdevant, D.E., Porcella, S.F., et al. 2015. Malaria-associated atypical memory B cells exhibit markedly reduced B cell receptor signaling and effector function. *Elife* 4.

44. Weiss, G.E., Crompton, P.D., Li, S.P., Walsh, L.A., Moir, S., Traore, B., Kayentao, K., Ongoiba, A., Doumbo, O.K., and Pierce, S.K. 2009. Atypical Memory B Cells Are Greatly Expanded in Individuals Living in a Malaria-Endemic Area. *Journal of Immunology* 183:2176-2182.

45. Cherukuri, A., Cheng, P.C., Sohn, H.W., and Pierce, S.K. 2001. The CD19/CD21 complex functions to prolong B cell antigen receptor signaling from lipid rafts. *Immunity* 14:169-179.

46. Poe, J.C., Hasegawa, M., and Tedder, T.F. 2001. CD19, CD21, and CD22: multifaceted response regulators of B lymphocyte signal transduction. *Int Rev Immunol* 20:739-762.

47. Roozendaal, R., and Carroll, M.C. 2007. Complement receptors CD21 and CD35 in humoral immunity. *Immunol Rev* 219:157-166.

48. de Bree, G.J., and Lynch, R.M. 2016. B cells in HIV pathogenesis. *Curr Opin Infect Dis* 29:23-30.

49. Griffith, J.W., Sokol, C.L., and Luster, A.D. 2014. Chemokines and chemokine receptors: positioning cells for host defense and immunity. *Annu Rev Immunol* 32:659-702.

50. von Andrian, U.H., and Mempel, T.R. 2003. Homing and cellular traffic in lymph nodes. *Nat Rev Immunol* 3:867-878.

51. Coelho, F.M., Natale, D., Soriano, S.F., Hons, M., Swoger, J., Mayer, J., Danuser, R., Scandella, E., Pieczyk, M., Zerwes, H.G., et al. 2013. Naive B-cell trafficking is shaped by local chemokine availability and LFA-1-independent stromal interactions. *Blood* 121:4101-4109.

52. Ansel, K.M., Ngo, V.N., Hyman, P.L., Luther, S.A., Forster, R., Sedgwick, J.D., Browning, J.L., Lipp, M., and Cyster, J.G. 2000. A chemokine-driven positive feedback loop organizes lymphoid follicles. *Nature* 406:309-314.

53. Cyster, J.G. 2010. B cell follicles and antigen encounters of the third kind. *Nat Immunol* 11:989-996.

54. Cagigi, A., Mowafi, F., Phuong Dang, L.V., Tenner-Racz, K., Atlas, A., Grutzmeier, S., Racz, P., Chiodi, F., and Nilsson, A. 2008. Altered expression of the receptor-ligand pair CXCR5/CXCL13 in B cells during chronic HIV-1 infection. *Blood* 112:4401-4410.

55. Henneken, M., Dorner, T., Burmester, G.R., and Berek, C. 2005. Differential expression of chemokine receptors on peripheral blood B cells from patients with rheumatoid arthritis and systemic lupus erythematosus. *Arthritis Res Ther* 7:R1001-1013.

56. Moir, S., Malaspina, A., Ho, J., Wang, W., Dipoto, A.C., O'Shea, M.A., Roby, G., Mican, J.M., Kottilil, S., Chun, T.W., et al. 2008. Normalization of B cell counts and subpopulations after antiretroviral therapy in chronic HIV disease. *J Infect Dis* 197:572-579.

57. Malaspina, A., Moir, S., Ho, J., Wang, W., Howell, M.L., O'Shea, M.A., Roby, G.A., Rehm, C.A., Mican, J.M., Chun, T.W., et al. 2006. Appearance of immature/transitional B cells in HIV-infected individuals with advanced disease: correlation with increased IL-7. *Proc Natl Acad Sci U S A* 103:2262-2267.

58. Rakhmanov, M., Keller, B., Gutenberger, S., Foerster, C., Hoenig, M., Driessen, G., van der Burg, M., van Dongen, J.J., Wiech, E., Visentini, M., et al. 2009. Circulating CD21low B cells in common variable immunodeficiency resemble tissue homing, innate-like B cells. *Proc Natl Acad Sci U S A* 106:13451-13456.

59. Isnardi, I., Ng, Y.S., Menard, L., Meyers, G., Saadoun, D., Srdanovic, I., Samuels, J., Berman, J., Buckner, J.H., Cunningham-Rundles, C., et al. 2010. Complement receptor 2/CD21-human naive B cells contain mostly autoreactive unresponsive clones. *Blood* 115:5026-5036.

60. Tipton, C.M., Fucile, C.F., Darce, J., Chida, A., Ichikawa, T., Gregoretti, I., Schieferl, S., Hom, J., Jenks, S., Feldman, R.J., et al. 2015. Diversity, cellular origin and autoreactivity of antibody-secreting cell population expansions in acute systemic lupus erythematosus. *Nat Immunol* 16:755-765.

61. Flint, S.M., Gibson, A., Lucas, G., Nandigam, R., Taylor, L., Provan, D., Newland, A.C., Savage, C.O., and Henderson, R.B. 2016. A distinct plasmablast and naive B-cell phenotype in primary immune thrombocytopenia. *Haematologica* 101:698-706.

62. Liu, M., Yang, G., Wiehe, K., Nicely, N.I., Vandergrift, N.A., Rountree, W., Bonsignori, M., Alam, S.M., Gao, J., Haynes, B.F., et al. 2015. Polyreactivity and autoreactivity among HIV-1 antibodies. *J Virol* 89:784-798.

63. Mouquet, H., Scheid, J.F., Zoller, M.J., Krogsgaard, M., Ott, R.G., Shukair, S., Artyomov, M.N., Pietzsch, J., Connors, M., Pereyra, F., et al. 2010. Polyreactivity increases the apparent affinity of anti-HIV antibodies by heteroligation. *Nature* 467:591-595.

64. Mouquet, H., Warncke, M., Scheid, J.F., Seaman, M.S., and Nussenzweig, M.C. 2012. Enhanced HIV-1 neutralization by antibody heteroligation. *Proc Natl Acad Sci U S A*.

65. Bohnhorst, J.O., Bjorgan, M.B., Thoen, J.E., Natvig, J.B., and Thompson, K.M. 2001. Bm1-Bm5 classification of peripheral blood B cells reveals circulating germinal center founder cells in healthy individuals and disturbance in the B cell subpopulations in patients with primary Sjogren's syndrome. *J Immunol* 167:3610-3618.

66. Sims, G.P., Ettinger, R., Shirota, Y., Yarboro, C.H., Illei, G.G., and Lipsky, P.E. 2005. Identification and characterization of circulating human transitional B cells. *Blood* 105:4390-4398.

67. Przekopowitz, M., Kuppers, R., and Weniger, M.A. 2015. A large fraction of human tonsillar B cells expressing CD27 are germinal center B cells. *Immunol Cell Biol* 93:429-430.

68. Kolar, G.R., Mehta, D., Pelayo, R., and Capra, J.D. 2007. A novel human B cell subpopulation representing the initial germinal center population to express AID. *Blood* 109:2545-2552.

69. Jackson, S.M., Harp, N., Patel, D., Wulf, J., Spaeth, E.D., Dike, U.K., James, J.A., and Capra, J.D. 2009. Key developmental transitions in human germinal center B cells are revealed by differential CD45RB expression. *Blood* 113:3999-4007.

70. Moir, S., Malaspina, A., Ogwaro, K.M., Donoghue, E.T., Hallahan, C.W., Ehler, L.A., Liu, S., Adelsberger, J., Lapointe, R., Hwu, P., et al. 2001. HIV-1 induces phenotypic and functional perturbations of B cells in chronically infected individuals. *Proc Natl Acad Sci U S A* 98:10362-10367.

71. Masilamani, M., Kassahn, D., Mikkat, S., Glocker, M.O., and Illges, H. 2003. B cell activation leads to shedding of complement receptor type II (CR2/CD21). *Eur J Immunol* 33:2391-2397.

72. Wehr, C., Eibel, H., Masilamani, M., Illges, H., Schlesier, M., Peter, H.H., and Warnatz, K. 2004. A new CD21low B cell population in the peripheral blood of patients with SLE. *Clin Immunol* 113:161-171.

73. Fearon, D.T., and Carroll, M.C. 2000. Regulation of B lymphocyte responses to foreign and self-antigens by the CD19/CD21 complex. *Annu Rev Immunol* 18:393-422.

74. Terrier, B., Joly, F., Vazquez, T., Benech, P., Rosenzwajg, M., Carpentier, W., Garrido, M., Ghillani-Dalbin, P., Klatzmann, D., Cacoub, P., et al. 2011. Expansion of functionally anergic CD21-/low marginal zone-like B cell clones in hepatitis C virus infection-related autoimmunity. *J Immunol* 187:6550-6563.

75. Charles, E.D., Brunetti, C., Marukian, S., Ritola, K.D., Talal, A.H., Marks, K., Jacobson, I.M., Rice, C.M., and Dustin, L.B. 2011. Clonal B cells in patients with hepatitis C virus-associated mixed cryoglobulinemia contain an expanded anergic CD21low B-cell subset. *Blood* 117:5425-5437.

76. Saadoun, D., Terrier, B., Bannock, J., Vazquez, T., Massad, C., Kang, I., Joly, F., Rosenzwajg, M., Sene, D., Benech, P., et al. 2013. Expansion of autoreactive unresponsive CD21-/low B cells in Sjogren's syndrome-associated lymphoproliferation. *Arthritis Rheum* 65:1085-1096.

77. Anchang, B., Hart, T.D., Bendall, S.C., Qiu, P., Bjornson, Z., Linderman, M., Nolan, G.P., and Plevritis, S.K. 2016. Visualization and cellular hierarchy inference of single-cell data using SPADE. *Nat Protoc* 11:1264-1279.

78. Qiu, P., Simonds, E.F., Bendall, S.C., Gibbs, K.D., Jr., Bruggner, R.V., Linderman, M.D., Sachs, K., Nolan, G.P., and Plevritis, S.K. 2011. Extracting a cellular hierarchy from high-dimensional cytometry data with SPADE. *Nat Biotechnol* 29:886-891.

79. Ward, J.H. 1963. Hierarchical Grouping to Optimize an Objective Function. *Journal of the American Statistical Association* 58:236-&.

80. Duty, J.A., Szodoray, P., Zheng, N.Y., Koelsch, K.A., Zhang, Q., Swiatkowski, M., Mathias, M., Garman, L., Helms, C., Nakken, B., et al. 2009. Functional anergy in a subpopulation of naive B cells from healthy humans that express autoreactive immunoglobulin receptors. *J Exp Med* 206:139-151.

81. Hao, Z.Y., Duncan, G.S., Seagal, J., Su, Y.W., Hong, C., Haight, J., Chen, N.J., Elia, A., Wakeham, A., Li, W.Y., et al. 2008. Fas Receptor Expression in Germinal-Center B Cells Is Essential for T and B Lymphocyte Homeostasis. *Immunity* 29:615-627.

82. Sciaranghella, G., Tong, N., Mahan, A.E., Suscovich, T.J., and Alter, G. 2012. Decoupling activation and exhaustion of B cells in spontaneous controllers of HIV infection. *AIDS*.

83. Schulz, K.R., Danna, E.A., Krutzik, P.O., and Nolan, G.P. 2012. Single-cell phospho-protein analysis by flow cytometry. *Curr Protoc Immunol* Chapter 8:Unit 8 17 11-20.

84. Moir, S., Malaspina, A., Pickeral, O.K., Donoghue, E.T., Vasquez, J., Miller, N.J., Krishnan, S.R., Planta, M.A., Turney, J.F., Justement, J.S., et al. 2004. Decreased survival of B cells of HIV-viremic patients mediated by altered expression of receptors of the TNF superfamily. *J Exp Med* 200:587-599.

85. Moir, S., and Fauci, A.S. 2008. Pathogenic mechanisms of B-lymphocyte dysfunction in HIV disease. *J Allergy Clin Immunol* 122:12-19; quiz 20-11.

86. Pensieroso, S., Galli, L., Nozza, S., Ruffin, N., Castagna, A., Tambussi, G., Hejdeman, B., Misciagna, D., Riva, A., Malnati, M., et al. 2013. B-cell subset alterations and correlated factors in HIV-1 infection. *AIDS* 27:1209-1217.

87. Deenick, E.K., Avery, D.T., Chan, A., Berglund, L.J., Ives, M.L., Moens, L., Stoddard, J.L., Bustamante, J., Boisson-Dupuis, S., Tsumura, M., et al. 2013. Naive and memory human B cells have distinct requirements for STAT3 activation to differentiate into antibody-secreting plasma cells. *J Exp Med* 210:2739-2753.

88. Ettinger, R., Kuchen, S., and Lipsky, P.E. 2008. The role of IL-21 in regulating B-cell function in health and disease. *Immunol Rev* 223:60-86.

89. Ettinger, R., Sims, G.P., Fairhurst, A.M., Robbins, R., da Silva, Y.S., Spolski, R., Leonard, W.J., and Lipsky, P.E. 2005. IL-21 induces differentiation of human naive and memory B cells into antibody-secreting plasma cells. *J Immunol* 175:7867-7879.

90. Spolski, R., and Leonard, W.J. 2014. Interleukin-21: a double-edged sword with therapeutic potential. *Nat Rev Drug Discov* 13:379-395.

91. Tangye, S.G. 2015. Advances in IL-21 biology - enhancing our understanding of human disease. *Curr Opin Immunol* 34:107-115.

92. Zotos, D., Coquet, J.M., Zhang, Y., Light, A., D'Costa, K., Kallies, A., Corcoran, L.M., Godfrey, D.I., Toellner, K.M., Smyth, M.J., et al. 2010. IL-21 regulates germinal center B cell differentiation and proliferation through a B cell-intrinsic mechanism. *J Exp Med* 207:365-378.

93. Avery, D.T., Deenick, E.K., Ma, C.S., Suryani, S., Simpson, N., Chew, G.Y., Chan, T.D., Palendira, U., Bustamante, J., Boisson-Dupuis, S., et al. 2010. B cell-intrinsic signaling through IL-21 receptor and STAT3 is required for establishing long-lived antibody responses in humans. *J Exp Med* 207:155-171.

94. Tortola, L., Yadava, K., Bachmann, M.F., Muller, C., Kisielow, J., and Kopf, M. 2010. IL-21 induces death of marginal zone B cells during chronic inflammation. *Blood* 116:5200-5207.

95. Puga, I., Cols, M., Barra, C.M., He, B., Cassis, L., Gentile, M., Comerma, L., Chorny, A., Shan, M., Xu, W., et al. 2012. B cell-helper neutrophils stimulate the diversification and production of immunoglobulin in the marginal zone of the spleen. *Nat Immunol* 13:170-180.

96. Cerutti, A., Cols, M., and Puga, I. 2013. Marginal zone B cells: virtues of innate-like antibody-producing lymphocytes. *Nat Rev Immunol* 13:118-132.

97. Iannello, A., Boulassel, M.R., Samarani, S., Debbeche, O., Tremblay, C., Toma, E., Routy, J.P., and Ahmad, A. 2010. Dynamics and Consequences of IL-21 Production in HIV-Infected Individuals: A Longitudinal and Cross-Sectional Study. *Journal of Immunology* 184:114-126.

98. Iannello, A., Tremblay, C., Routy, J.P., Boulassel, M.R., Toma, E., and Ahmad, A. 2008. Decreased levels of circulating IL-21 in HIV-infected AIDS patients: correlation with CD4+ T-cell counts. *Viral Immunol* 21:385-388.

99. Fritz, S., Mossdorf, E., Durovic, B., Zenhaeusern, G., Conen, A., Steffen, I., Battegay, M., Nuesch, R., and Hess, C. 2010. Virosomal influenza-vaccine induced immunity in HIV-infected individuals with high versus low CD4+ T-cell counts: clues towards a rational vaccination strategy. *AIDS* 24:2287-2289.

100. Malaspina, A., Moir, S., Orsega, S.M., Vasquez, J., Miller, N.J., Donoghue, E.T., Kottilil, S., Gezmu, M., Follmann, D., Vodeiko, G.M., et al. 2005. Compromised B cell responses to influenza vaccination in HIV-infected individuals. *J Infect Dis* 191:1442-1450.

101. Pape, K.A., Taylor, J.J., Maul, R.W., Gearhart, P.J., and Jenkins, M.K. 2011. Different B Cell Populations Mediate Early and Late Memory During an Endogenous Immune Response. *Science*.

102. Weill, J.C., Weller, S., and Reynaud, C.A. 2009. Human marginal zone B cells. *Annu Rev Immunol* 27:267-285.

103. Weller, S., Braun, M.C., Tan, B.K., Rosenwald, A., Cordier, C., Conley, M.E., Plebani, A., Kumararatne, D.S., Bonnet, D., Tournilhac, O., et al. 2004. Human blood IgM "memory" B cells are circulating splenic marginal zone B cells harboring a prediversified immunoglobulin repertoire. *Blood* 104:3647-3654.

104. Kruetzmann, S., Rosado, M.M., Weber, H., Germing, U., Tournilhac, O., Peter, H.H., Berner, R., Peters, A., Boehm, T., Plebani, A., et al. 2003. Human immunoglobulin M memory B cells controlling Streptococcus pneumoniae infections are generated in the spleen. *J Exp Med* 197:939-945.

105. Nuccitelli, A., Rinaudo, C.D., and Maione, D. 2015. Group B Streptococcus vaccine: state of the art. *Ther Adv Vaccines* 3:76-90.

106. Sadlier, C., O'Dea, S., Bennett, K., Dunne, J., Conlon, N., and Bergin, C. 2016. Immunological efficacy of pneumococcal vaccine strategies in HIV-infected adults: a randomized clinical trial. *Sci Rep* 6:32076.

107. Zhang, L., Li, Z., Wan, Z., Kilby, A., Kilby, J.M., and Jiang, W. 2015. Humoral immune responses to Streptococcus pneumoniae in the setting of HIV-1 infection. *Vaccine* 33:4430-4436.

108. Meffre, E., and Wardemann, H. 2008. B-cell tolerance checkpoints in health and autoimmunity. *Curr Opin Immunol* 20:632-638.

109. Mietzner, B., Tsuiji, M., Scheid, J., Velinzon, K., Tiller, T., Abraham, K., Gonzalez, J.B., Pascual, V., Stichweh, D., Wardemann, H., et al. 2008. Autoreactive IgG memory antibodies in patients with systemic lupus erythematosus arise from nonreactive and polyreactive precursors. *Proc Natl Acad Sci U S A* 105:9727-9732.

110. Wardemann, H., Yurasov, S., Schaefer, A., Young, J.W., Meffre, E., and Nussenzweig, M.C. 2003. Predominant autoantibody production by early human B cell precursors. *Science* 301:1374-1377.

111. Rodriguez, B., Valdez, H., Freimuth, W., Butler, T., Asaad, R., and Lederman, M.M. 2003. Plasma levels of B-lymphocyte stimulator increase with HIV disease progression. *AIDS* 17:1983-1985.

112. Fontaine, J., Chagnon-Choquet, J., Valcke, H.S., Poudrier, J., Roger, M., Montreal Primary, H.I.V.I., and Long-Term Non-Progressor Study, G. 2011. High expression levels of B lymphocyte stimulator (BLyS) by dendritic cells correlate with HIV-related B-cell disease progression in humans. *Blood* 117:145-155.

113. Sportes, C., Babb, R.R., Krumlauf, M.C., Hakim, F.T., Steinberg, S.M., Chow, C.K., Brown, M.R., Fleisher, T.A., Noel, P., Maric, I., et al. 2010. Phase I study of recombinant human interleukin-7 administration in subjects with refractory malignancy. *Clin Cancer Res* 16:727-735.

114. Lundstrom, W., Fewkes, N.M., and Mackall, C.L. 2012. IL-7 in human health and disease. *Semin Immunol* 24:218-224.

115. Sammicheli, S., Ruffin, N., Lantto, R., Vivar, N., Chiodi, F., and Rethi, B. 2012. IL-7 modulates B cells survival and activation by inducing BAFF and CD70 expression in T cells. *J Autoimmun* 38:304-314.

116. Mackay, F., and Browning, J.L. 2002. BAFF: a fundamental survival factor for B cells. *Nat Rev Immunol* 2:465-475.

117. Mouquet, H., Warncke, M., Scheid, J.F., Seaman, M.S., and Nussenzweig, M.C. 2012. Enhanced HIV-1 neutralization by antibody heteroligation. *Proc Natl Acad Sci U S A* 109:875-880.

118. Alam, S.M., McAdams, M., Boren, D., Rak, M., Scearce, R.M., Gao, F., Camacho, Z.T., Gewirth, D., Kelsoe, G., Chen, P., et al. 2007. The role of antibody polyspecificity and lipid reactivity in binding of broadly neutralizing anti-HIV-1 envelope human monoclonal antibodies 2F5 and 4E10 to glycoprotein 41 membrane proximal envelope epitopes. *J Immunol* 178:4424-4435.

119. Bonsignori, M., Wiehe, K., Grimm, S.K., Lynch, R., Yang, G., Kozink, D.M., Perrin, F., Cooper, A.J., Hwang, K.K., Chen, X., et al. 2014. An autoreactive antibody from an SLE/HIV-1 individual broadly neutralizes HIV-1. *J Clin Invest* 124:1835-1843.

120. Haynes, B.F., Fleming, J., St Clair, E.W., Katinger, H., Stiegler, G., Kunert, R., Robinson, J., Scearce, R.M., Plonk, K., Staats, H.F., et al. 2005. Cardiolipin polyspecific autoreactivity in two broadly neutralizing HIV-1 antibodies. *Science* 308:1906-1908.

121. Zhu, Z., Qin, H.R., Chen, W., Zhao, Q., Shen, X., Schutte, R., Wang, Y., Ofek, G., Streaker, E., Prabakaran, P., et al. 2011. Cross-reactive HIV-1-neutralizing human monoclonal antibodies identified from a patient with 2F5-like antibodies. *J Virol* 85:11401-11408.

122. Alam, S.M., Morelli, M., Dennison, S.M., Liao, H.X., Zhang, R., Xia, S.M., Rits-Volloch, S., Sun, L., Harrison, S.C., Haynes, B.F., et al. 2009. Role of HIV membrane in neutralization by two broadly neutralizing antibodies. *Proc Natl Acad Sci U S A* 106:20234-20239.

123. Mascola, J.R., and Haynes, B.F. 2013. HIV-1 neutralizing antibodies: understanding nature's pathways. *Immunol Rev* 254:225-244.

124. Verkoczy, L., Chen, Y., Bouton-Verville, H., Zhang, J., Diaz, M., Hutchinson, J., Ouyang, Y.B., Alam, S.M., Holl, T.M., Hwang, K.K., et al. 2011. Rescue of HIV-1 broad neutralizing antibody-expressing B cells in 2F5 VH x VL knockin mice reveals multiple tolerance controls. *Journal of Immunology* 187:3785-3797.

125. Verkoczy, L., Diaz, M., Holl, T.M., Ouyang, Y.B., Bouton-Verville, H., Alam, S.M., Liao, H.X., Kelsoe, G., and Haynes, B.F. 2010. Autoreactivity in an HIV-1 broadly reactive neutralizing antibody variable region heavy chain induces immunologic tolerance. *Proc Natl Acad Sci U S A* 107:181-186.

126. Verkoczy, L., Kelsoe, G., Moody, M.A., and Haynes, B.F. 2011. Role of immune mechanisms in induction of HIV-1 broadly neutralizing antibodies. *Curr Opin Immunol*.

127. Zhang, R., Verkoczy, L., Wiehe, K., Munir Alam, S., Nicely, N.I., Santra, S., Bradley, T., Pemble, C.W.t., Zhang, J., Gao, F., et al. 2016. Initiation of immune tolerance-controlled HIV gp41 neutralizing B cell lineages. *Sci Transl Med* 8:336ra362.

128. Verkoczy, L., Kelsoe, G., and Haynes, B.F. 2014. HIV-1 envelope gp41 broadly neutralizing antibodies: hurdles for vaccine development. *PLoS Pathog* 10:e1004073.

129. Tiller, T., Tsuiji, M., Yurasov, S., Velinzon, K., Nussenzweig, M.C., and Wardemann, H. 2007. Autoreactivity in human IgG+ memory B cells. *Immunity* 26:205-213.

130. Stadanlick, J.E., Kaileh, M., Karnell, F.G., Scholz, J.L., Miller, J.P., Quinn, W.J., 3rd, Brezski, R.J., Treml, L.S., Jordan, K.A., Monroe, J.G., et al. 2008. Tonic B cell antigen receptor signals supply an NF-kappaB substrate for prosurvival BLyS signaling. *Nat Immunol* 9:1379-1387.

131. Whitaker, J.A., Rouphael, N.G., Edupuganti, S., Lai, L., and Mulligan, M.J. 2012. Strategies to increase responsiveness to hepatitis B vaccination in adults with HIV-1. *Lancet Infect Dis* 12:966-976.

132. Rieder, P., Joos, B., Scherrer, A.U., Kuster, H., Braun, D., Grube, C., Niederost, B., Leemann, C., Gianella, S., Metzner, K.J., et al. 2011. Characterization of human immunodeficiency virus type 1 (HIV-1) diversity and tropism in 145 patients with primary HIV-1 infection. *Clin Infect Dis* 53:1271-1279.

133. Roederer, M., Quaye, L., Mangino, M., Beddall, M.H., Mahnke, Y., Chattopadhyay, P., Tosi, I., Napolitano, L., Terranova Barberio, M., Menni, C., et al. 2015. The genetic architecture of the human immune system: a bioresource for autoimmunity and disease pathogenesis. *Cell* 161:387-403.

134. Chen, T.J., and Kotecha, N. 2014. Cytobank: providing an analytics platform for community cytometry data analysis and collaboration. *Curr Top Microbiol Immunol* 377:127-157.

135. Trkola, A., Kuster, H., Leemann, C., Oxenius, A., Fagard, C., Furrer, H., Battegay, M., Vernazza, P., Bernasconi, E., Weber, R., et al. 2004. Humoral immunity to HIV-1: kinetics of antibody responses in chronic infection reflects capacity of immune system to improve viral set point. *Blood* 104:1784-1792.

136. Jayaraman, S. 2003. Intracellular determination of activated caspases (IDAC) by flow cytometry using a pancaspase inhibitor labeled with FITC. *Cytometry Part A* 56A:104-112.

5.9 Supplementary table and figure legends

Supplementary table 1: Characteristics of the early and late treatment groups

Summary of the clinical characteristics of the HIV-1 infected patients for the time points analyzed are shown. Patients are separated into the study groups based on initiation of ART early ART and late ART group. [a]Comparison was done between early ART group (weeks off ART) and late ART group (weeks of active replication) to compare the continuous period of active replication before chronic 2 year sample was collected. Differences between the study groups were calculated with Mann-Whitney test and considered statistically significant with a p value <0.05.

Supplementary table 2: Patient characteristics

Characteristics of the individual patients are shown and in addition the samples used for the different assays are depicted.

Supplementary table 3: Comparison of Ward clusters between healthy donors and HIV-1 infected patients

Statistical results of comparison of Ward cluster frequencies between healthy controls (n=15) and the different time points of HIV-1 infected individuals (n=17) of both study groups as shown in figure 5. Non-paired non-parametric ANOVA Kruskal-Wallis test was used to compare frequencies of Ward cluster between study groups and healthy controls. Dunn's multiple comparison test was used to perform multiple testing corrections. P values are shown. P<0.05 was considered statistically significant. *p<0.05, **p<0.01, ***p<0.001, ****p<0.0001.

Supplementary figure 1: Quality control of phenotypic markers for each sample.

Median fluorescence signal intensities for phenotypic markers IL-21R, CCR7, CXCR3, CXCR4, CXCR5 and Ki-67 of all samples measured in this study are shown. Samples from each experiment are concatenated. Where applied FMO control is shown. Irregular stainings as described in the method part are highlighted by blue and red background.

Supplementary figure 2: Gating strategy to identify B cell subsets.

(A) Gating strategy to define main subsets of B cells ($Dump^-CD19^+$), which are transitional ($CD10^+CD38^+IgD^+$; green gate), $CD10^+$ memory ($CD10^+CD38^{low}IgD^-$; green gate), naïve ($CD10^-IgD^+CD27^-$; blue gate), Marginal Zone (MZ) B cells ($IgD^+CD27^+CD38^{low}$, blue gate) and class-switched B cells (IgD^-CD38^{low}, orange gate) and plasmablasts (IgD^-CD38^{high}, purple gate). Gating is shown with a healthy control sample. **(B)** Gating of $CD21^-$ and $CD21^+$ naïve and MZ B cells as well as the definition of memory B cell subsets based on CD21 and CD27 expression, which includes intermediate memory (IM; $CD21^+CD27^-$), resting memory (RM; $CD21^+CD27^+$), activated memory (AM; $CD21^-CD27^+$) and tissue-like memory ($CD21^-CD27^-$) B cells, are depicted from a healthy control and a chronic HIV-1 infected patient.

Supplementary figure 3: Phenotypic characterization of $CD10^+$ memory B cells.

(A) Histogram overlay of CD27 expression on $CD10^-IgD^+$ B cells (grey) and $CD10^+$ memory B cells from a healthy control is shown. **(B)** Percentage of CD27-expressing $CD10^+$ memory B cells in healthy donors (n=29) is depicted. **(C)** Comparison of frequency of IgA+, $IgG1^+$ and $IgG3^+$ cells in $CD10^+$ memory B cells (black dots) and class-switched B cells ($CD10^-IgD^-CD38^{low}$) in healthy donors (n=29) is shown. Mann-Whitney test was used to determine differences between class-switched and $CD10^+$ memory B cells.

Supplementary figure 4: Differences between patients with ART initiated during acute or chronic phase.

(A) Comparison of main B cell subsets, **(B)** memory B cell subsets and **(C)** $CD21^-$ naïve and $CD21^-$ MZ B cells (C) between acute ART group (n=11; orange squares) and chronic ART group (n=10; blue dots) at different time points are shown. Differences were analyzed by using unpaired non-parametric Mann-Whitney test. P values are shown. **(D)** Comparison of $CD10^+$ memory B cells between healthy donors (n=29) and early (n=11) and late (n=10) ART group is shown. Comparison was done to healthy controls with unpaired non-parametric ANOVA Kruskal-Wallis. Dunn's multiple comparison test was used to perform multiple testing corrections. $P<0.05$ was considered statistically significant. *$p<0.05$, **$p<0.01$.

Supplementary figure 5: $CD21^-$ naïve and $CD21^-$ MZ B cells exhibit a unique expression pattern of chemokine receptors, Il-21R and CD19.

(A) Flow cytometry dot plots and gating to estimate the frequency of CCR7-, CXCR3-, CXCR4-, CXCR5- and IL-21R-expressing $CD21^-$ and $CD21^+$ naïve and $CD21^-$ and $CD21^+$ MZ B cells and the corresponding FMO controls where applied are shown from one healthy control as an example. **(B)** Differences median fluorescence intensity between $CD21^+$ and $CD21^-$ naïve (upper row) and $CD21^+$ and $CD21^-$ MZ B cells (lower row) in healthy controls and chronic HIV-infected patients (2 years of active infection) are shown for CCR7, CXCR3, CXCR4, CXCR5, IL-21R and CD19. Comparison within patients was done using Wilcoxon matched-pairs signed rank test. Mann-Whitney T test was used to test differences between healthy controls and chronically HIV-infected patients. $P<0.05$ was considered statistically significant. *p<0.05, **p<0.01, ***p<0.001, ****p<0.0001.

Supplementary figure 6: Backgating of Ward clusters show unique phenotypes of the individual Ward clusters.

(A) Expression levels of CCR7, CXCR3, CXCR4, CXCR5, IL-21R and CD19 on individual Ward cluster are shown as z-score of arcsinh transformed MFI values. Z-Scores <0.22 were indicates as negative (-) whereas intermediate expression levels were defined as 0.22<z-score<1 (+). Z-scores >1 are considered as high expression levels (++). **(B)** FlowJo analysis to estimate the homogeneity of marker expression on Ward clusters are shown from the combined chronic HIV-1 infected patients (2 years of active replication). The first column shows contour plots of marker expression on $CD21^-$ naïve B cells and the subsequent columns depict the overlay of Ward cluster (red colored) on top of $CD21^-$ naïve B cells (grey colored).

Supplementary figure 7: Correlation of marker expression on $CD21^-$ and $CD21^+$ naïve and $CD21^-$ and $CD21^+$ MZ B cells and clinical parameters.

Spearman correlation of expression of CCR7, CXCR3, CXCR4, CXCR5 and IL-21R and in addition log-transformed viral load, plasma IgG levels (mg/ml) and CD4 counts are visualized with heatmaps for $CD21^-$ and $CD21^+$ naïve and $CD21^-$ and $CD21^+$ MZ B cells. P-values of spearman correlation calculation are shown and considered significant when $p<0.05$ and colored orange. p-values between 0.05 and 0.06 are colored yellow and highlight possible correlation although not meeting the significance requirements whereas non-significant values are shown as blue boxes.

Supplementary figure 8: Activated and exhausted memory B cells express higher levels of activation marker CD95 and FcRL4.

(A) Flow cytometry dot plots of CD95 and FcRL4 expression on the four memory B cell subsets , intermediate (IM), resting (RM), activated (AM) and tissue-like memory (TLM) B cells, are shown from a chronic HIV-1 infected patient (2 years of active infection). **(B)** Comparison of CD95 and FcRL-4 expression on memory B cell subsets is shown. Analysis was performed on healthy controls (n=29) and different time points of HIV-infected patients (n=6). Non-parametric unpaired Kruskal-Wallis one-way ANOVA and Dunn's multiple correction test was used. $P<0.05$ was considered statistically significant. *p<0.05, **p<0.01, ***p<0.001, ****p<0.0001.

5.10 Supplementary tables and figures

Supplementary table 1

Time point	Parameter	Acute ART group (n=11)	Chronic ART group (n=10)	p-value
Acute	Weeks of infection	5 (3-8)	13 (8-24)	**<0.0001**
	Viral load	475000 (2380-12400000) (n=11)	18300 (261-107000) (n=8)	**0.0268**
	CD4 counts	724 (436-816) (n=5)	540.5 (359-1120) (n=6)	0.5368
Chronic 1 year	Weeks of active virus replication	51 (41-65)	51.5 (31-59)	0.3762
	Weeks off ART	45 (36-62)	Not available	0.6912[a]
	Viral load	6650 (0-786000)	23200 (264-103500)	0.3494
	CD4 counts	663 (457-1094)	477 (270-1099)	0.1145
Chronic 2 years	Weeks of active virus replication	112 (101-138)	122.5 (71-139)	0.7171
	Weeks off ART	109 (94-134)	Not available	0.2893[a]
	Viral load	14200 (140-122000)	86400 (49-580000)	0.0513
	CD4 counts	569 (371-945)	263 (163-1429) (n=9)	**0.0441**
ART 1 year	Weeks on ART	53 (33-68)	58.5 (20-72)	0.2273
	Viral load	0 (0-0)	0 (0-58)	0.0902
	CD4 counts	798 (460-1363)	579 (278-905)	**0.0381**

Supplementary table 2

Patients		Clinical characteristics						Samples used for individual assays							
Patient ID	study group	disease stage	viral load	CD4 counts	Weeks of replication	Weeks on ART	Weeks after ART stop	B cell subset analysis	Phenotypic analysis	Longitudinal phenotypic analysis	SPADE	IgM, CD95 and FcRL4 analysis	Phosflow	Apoptosis assay	Plasma used for IgG ELISA
ZPHI-Pat02	Late ART group	Acute	63500	537	13	NA	NA	x	x	x	x				x
ZPHI-Pat07	Early ART group	Acute	2380	NA	8	NA	NA	x	x	x	x				x
ZPHI-Pat23	Late ART group	Acute	3500	1120	8	NA	NA	x	x	x	x	x			x
ZPHI-Pat31	Early ART group	Acute	495500	724	5	NA	NA	x	x	x		x			x
ZPHI-Pat32	Early ART group	Acute	248500	463	4	NA	NA	x	x	x	x				x
ZPHI-Pat38	Late ART group	Acute	363	544	13	NA	NA	x	x	x	x				x
ZPHI-Pat39	Early ART group	Acute	13200	NA	7	NA	NA	x	x	x	x				x
ZPHI-Pat40	Late ART group	Acute	98000	NA	14	NA	NA	x	x	x	x				x
ZPHI-Pat44	Early ART group	Acute	1360000	NA	3	NA	NA	x	x	x		x			x
ZPHI-Pat48	Late ART group	Acute	107000	402	24	NA	NA	x	x	x	x				x
ZPHI-Pat49	Early ART group	Acute	2220000	NA	4	NA	NA	x	x	x	x				x
ZPHI-Pat58	Early ART group	Acute	3170000	816	5	NA	NA	x	x	x	x	x			x
ZPHI-Pat59	Early ART group	Acute	475000	NA	5	NA	NA	x	x	x	x	x			x
ZPHI-Pat60	Late ART group	Acute	261	NA	10	NA	NA	x	x	x	x				x
ZPHI-Pat71	Late ART group	Acute	18300	359	8	NA	NA	x	x	x	x				x
ZPHI-Pat72	Early ART group	Acute	47300	732	6	NA	NA	x	x	x	x	x			x
ZPHI-Pat78	Late ART group	Acute	1930	723	17	NA	NA	x	x	x	x				x
ZPHI-Pat92	Early ART group	Acute	62700	436	4	NA	NA	x	x	x	x				x
ZPHI-Pat93	Early ART group	Acute	12400000	NA	3	NA	NA	x	x	x	x				x
ZPHI-Pat02	Late ART group	Chronic 1 year	44000	567	42	NA	NA			x	x				

ZPHI-Pat07	Early ART group	Chronic 1 year	1560	679	45	NA	37			x	x			
ZPHI-Pat11	Late ART group	Chronic 1 year	103500	298	55	NA	NA							
ZPHI-Pat23	Late ART group	Chronic 1 year	264	1099	59	NA	NA			x	x			
ZPHI-Pat31	Early ART group	Chronic 1 year	34300	658	57	NA	52			x				
ZPHI-Pat32	Early ART group	Chronic 1 year	154	888	47	NA	43			x	x			
ZPHI-Pat38	Late ART group	Chronic 1 year	2370	478	53	NA	NA			x	x			
ZPHI-Pat39	Early ART group	Chronic 1 year	43900	457	56	NA	51			x	x			
ZPHI-Pat40	Late ART group	Chronic 1 year	11100	331	51	NA	NA			x	x			
ZPHI-Pat44	Early ART group	Chronic 1 year	6650	746	65	NA	62			x				
ZPHI-Pat48	Late ART group	Chronic 1 year	89900	270	53	NA	NA			x	x			
ZPHI-Pat49	Early ART group	Chronic 1 year	786000	814	41	NA	36			x	x			
ZPHI-Pat58	Early ART group	Chronic 1 year	546	1094	59	NA	54			x	x			
ZPHI-Pat59	Early ART group	Chronic 1 year	110000	503	54	NA	49			x	x			
ZPHI-Pat60	Late ART group	Chronic 1 year	29000	476	52	NA	NA			x	x			
ZPHI-Pat71	Late ART group	Chronic 1 year	43400	315	31	NA	NA			x	x			
ZPHI-Pat72	Early ART group	Chronic 1 year	7200	663	51	NA	44			x	x			
ZPHI-Pat75	Late ART group	Chronic 1 year	17400	848	44	NA	NA							
ZPHI-Pat78	Late ART group	Chronic 1 year	8910	727	31	NA	NA			x	x			
ZPHI-Pat92	Early ART group	Chronic 1 year	0	621	49	NA	45			x	x			
ZPHI-Pat93	Early ART group	Chronic 1 year	3300	527	45	NA	42			x	x			
ZPHI-Pat02	Late ART group	Chronic 2 years	46362	490	96	NA	NA	x	x	x	x			x
ZPHI-Pat07	Early ART group	Chronic 2 years	14200	472	128	NA	120	x	x	x	x			x
ZPHI-Pat11	Late ART group	Chronic 2 years	149000	263	122	NA	NA	x	x			x		x
ZPHI-Pat23	Late ART group	Chronic 2 years	49	1429	108	NA	NA	x	x	x	x	x		x
ZPHI-Pat31	Early ART group	Chronic 2 years	22900	507	110	NA	105	x	x	x		x		x
ZPHI-Pat32	Early ART group	Chronic 2 years	140	613	138	NA	134	x	x	x	x			x
ZPHI-Pat38	Late ART group	Chronic 2 years	4500	229	134	NA	NA	x	x	x	x			x
ZPHI-Pat39	Early ART group	Chronic 2 years	64600	604	108	NA	102	x	x	x	x			x
ZPHI-Pat40	Late ART group	Chronic 2 years	33400	NA	123	NA	NA	x	x	x	x			x
ZPHI-Pat44	Early ART group	Chronic 2 years	16200	722	112	NA	109	x	x	x		x		x

ZPHI-Pat48	Late ART group	Chronic 2 years	91800	258	127	NA	NA	x	x	x	x			x
ZPHI-Pat49	Early ART group	Chronic 2 years	122000	677	112	NA	106	x	x	x	x			x
ZPHI-Pat58	Early ART group	Chronic 2 years	2700	945	115	NA	110	x	x	x	x	x		x
ZPHI-Pat59	Early ART group	Chronic 2 years	120000	371	123	NA	118	x	x	x	x	x		x
ZPHI-Pat60	Late ART group	Chronic 2 years	201331	163	131	NA	NA	x	x	x	x			x
ZPHI-Pat71	Late ART group	Chronic 2 years	125530	217	71	NA	NA	x	x	x	x			x
ZPHI-Pat72	Early ART group	Chronic 2 years	1100	507	101	NA	94	x	x	x	x	x		x
ZPHI-Pat75	Late ART group	Chronic 2 years	81000	614	139	NA	NA	x	x					x
ZPHI-Pat78	Late ART group	Chronic 2 years	580000	379	104	NA	NA	x	x	x	x			x
ZPHI-Pat92	Early ART group	Chronic 2 years	2650	489	122	NA	118	x	x	x	x			x
ZPHI-Pat93	Early ART group	Chronic 2 years	1651	569	102	NA	100	x	x	x	x			x
ZPHI-Pat02	Late ART group	ART 1 year	0	905	NA	72	NA	x		x	x			
ZPHI-Pat07	Early ART group	ART 1 year	0	460	NA	57	NA	x		x	x			
ZPHI-Pat11	Late ART group	ART 1 year	0	278	NA	63	NA	x				x		
ZPHI-Pat23	Late ART group	ART 1 year	0	595	NA	20	NA	x		x	x	x		
ZPHI-Pat31	Early ART group	ART 1 year	0	678	NA	59	NA	x		x		x		
ZPHI-Pat32	Early ART group	ART 1 year	0	699	NA	59	NA	x		x	x			
ZPHI-Pat38	Late ART group	ART 1 year	0	580	NA	59	NA	x		x	x			
ZPHI-Pat39	Early ART group	ART 1 year	0	844	NA	53	NA	x		x	x			
ZPHI-Pat40	Late ART group	ART 1 year	0	373	NA	58	NA	x		x	x			
ZPHI-Pat44	Early ART group	ART 1 year	0	877	NA	68	NA	x		x		x		
ZPHI-Pat48	Late ART group	ART 1 year	0	431	NA	57	NA	x		x	x			
ZPHI-Pat49	Early ART group	ART 1 year	0	994	NA	33	NA	x		x	x			
ZPHI-Pat58	Early ART group	ART 1 year	0	1363	NA	49	NA	x		x	x	x		
ZPHI-Pat59	Early ART group	ART 1 year	0	1028	NA	33	NA	x		x	x	x		
ZPHI-Pat60	Late ART group	ART 1 year	58	NA	NA	60	NA	x		x	x			
ZPHI-Pat71	Late ART group	ART 1 year	0	550	NA	53	NA	x		x	x			
ZPHI-Pat72	Early ART group	ART 1 year	0	512	NA	53	NA	x		x	x	x		
ZPHI-Pat75	Late ART group	ART 1 year	23	804	NA	52	NA	x						
ZPHI-Pat78	Late ART group	ART 1 year	1	579	NA	68	NA	x		x	x			

ZPHI-Pat92	Early ART group	ART 1 year	0	750	NA	46	NA	x	x	x		
ZPHI-Pat93	Early ART group	ART 1 year	0	798	NA	59	NA	x	x	x		
ZPHI-Pat07	Early ART group	Chronic	45508	360	145	NA	145				x	x
ZPHI-Pat23	Late ART group	Chronic	13023	530	534	NA	NA				x	x
ZPHI-Pat31	Early ART group	Chronic	52400	487	123	NA	122				x	x
ZPHI-Pat32	Early ART group	Chronic	7023	637	294	NA	294				x	x
ZPHI-Pat39	Early ART group	Chronic	90000	390	146	NA	146				x	x
ZPHI-Pat44	Early ART group	Chronic	20000	680	203	NA	203				x	x
ZPHI-Pat49	Early ART group	Chronic	59000	408	203	NA	203				x	x
ZPHI-Pat58	Early ART group	Chronic	10978	851	266	NA	266				x	x
ZPHI-Pat75	Late ART group	Chronic	69000	376	159	NA	NA				x	x
ZPHI-Pat93	Early ART group	Chronic	3682	511	223	NA	222				x	x

Supplementary table 3

	Early ART group				Late ART group			
Ward cluster	acute	ART 1 year	Chronic 1 year	Chronic 2 years	acute	Chronic 1 year	Chronic 2 years	ART 1 year
1	0.4305	**0.0006**	**0.0006**	**0.0075**	**0.0037**	**0.0142**	**0.0348**	**0.0152**
2	>0.9999	0.1031	**0.0468**	**0.0468**	>0.9999	>0.9999	>0.9999	0.0717
3	>0.9999	0.5813	**0.0256**	>0.9999	**0.0474**	0.0793	0.1662	0.3852
4	>0.9999	>0.9999	0.9542	>0.9999	>0.9999	0.632	>0.9999	>0.9999
5	>0.9999	>0.9999	0.1866	0.3437	>0.9999	>0.9999	>0.9999	>0.9999
6	0.4974	>0.9999	>0.9999	0.27	>0.9999	>0.9999	>0.9999	>0.9999
7	>0.9999	0.1184	**0.0092**	>0.9999	0.1375	0.3268	0.2153	0.1002
8	>0.9999	0.0723	>0.9999	0.0854	>0.9999	>0.9999	>0.9999	>0.9999
9	>0.9999	>0.9999	>0.9999	0.4415	>0.9999	>0.9999	>0.9999	>0.9999
10	>0.9999	0.3488	0.0556	>0.9999	**0.0207**	**0.0107**	0.0552	0.1629

Supplementary figure 1

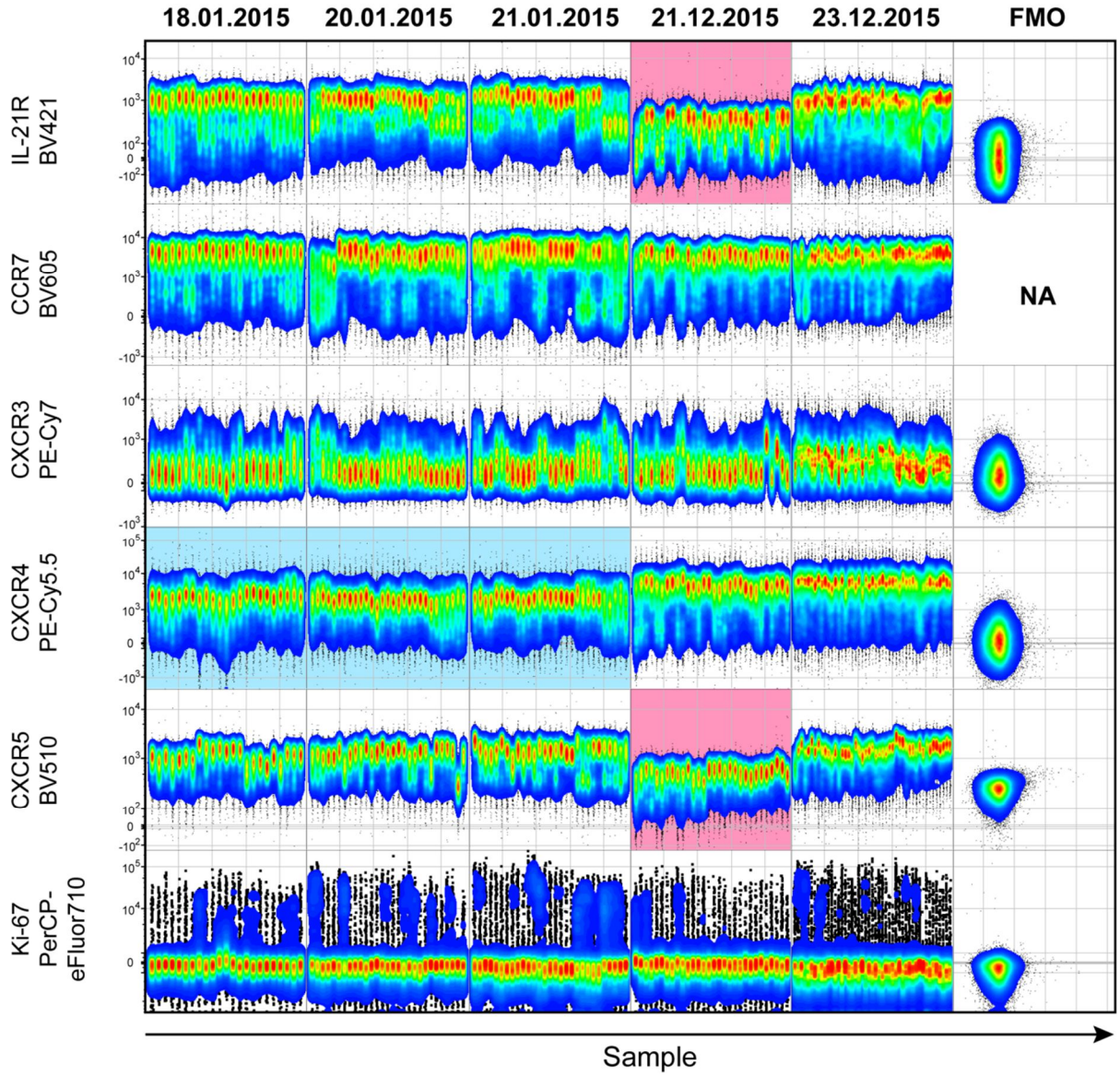

Supplementary figure 2

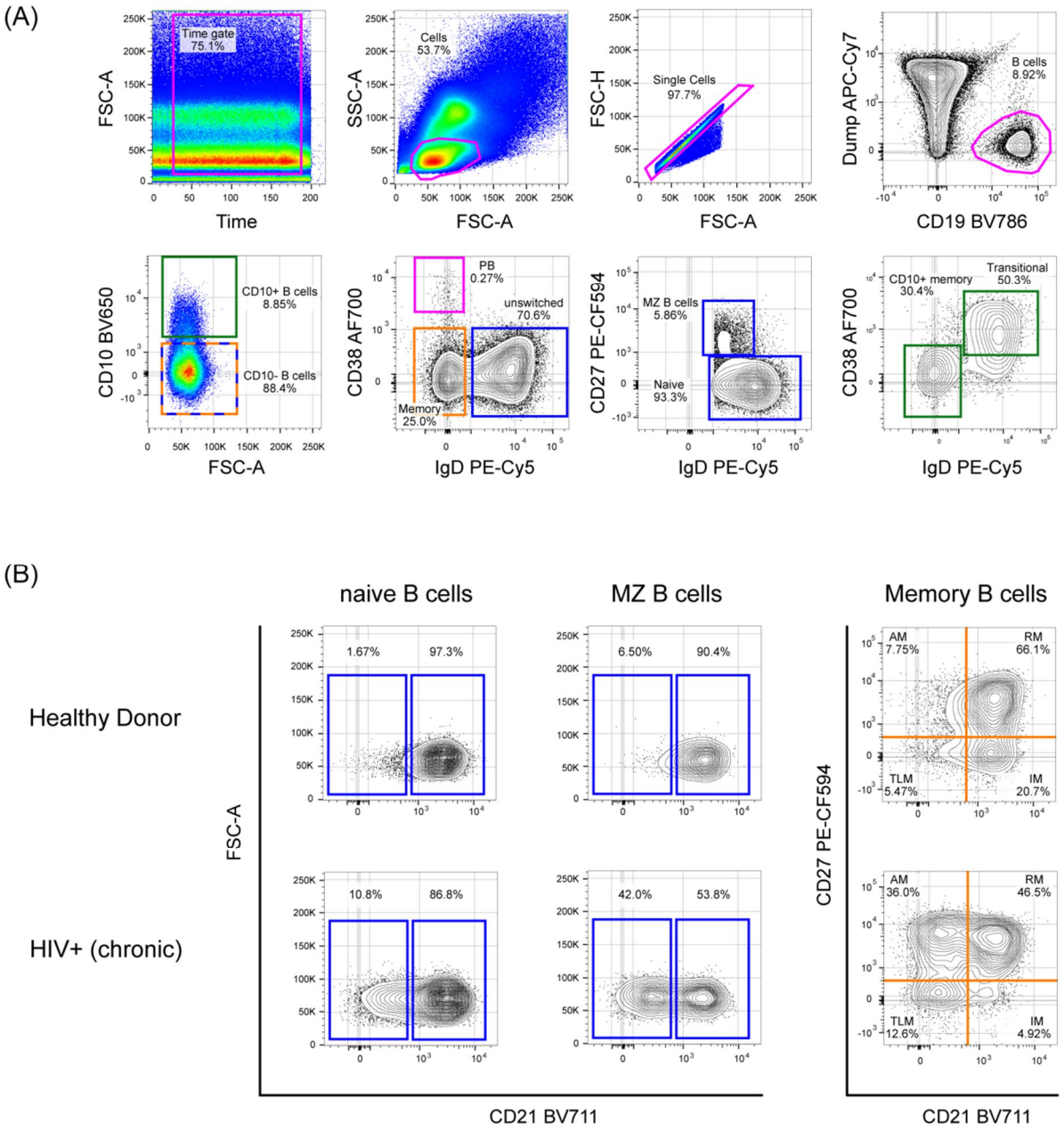

Supplementary figure 3

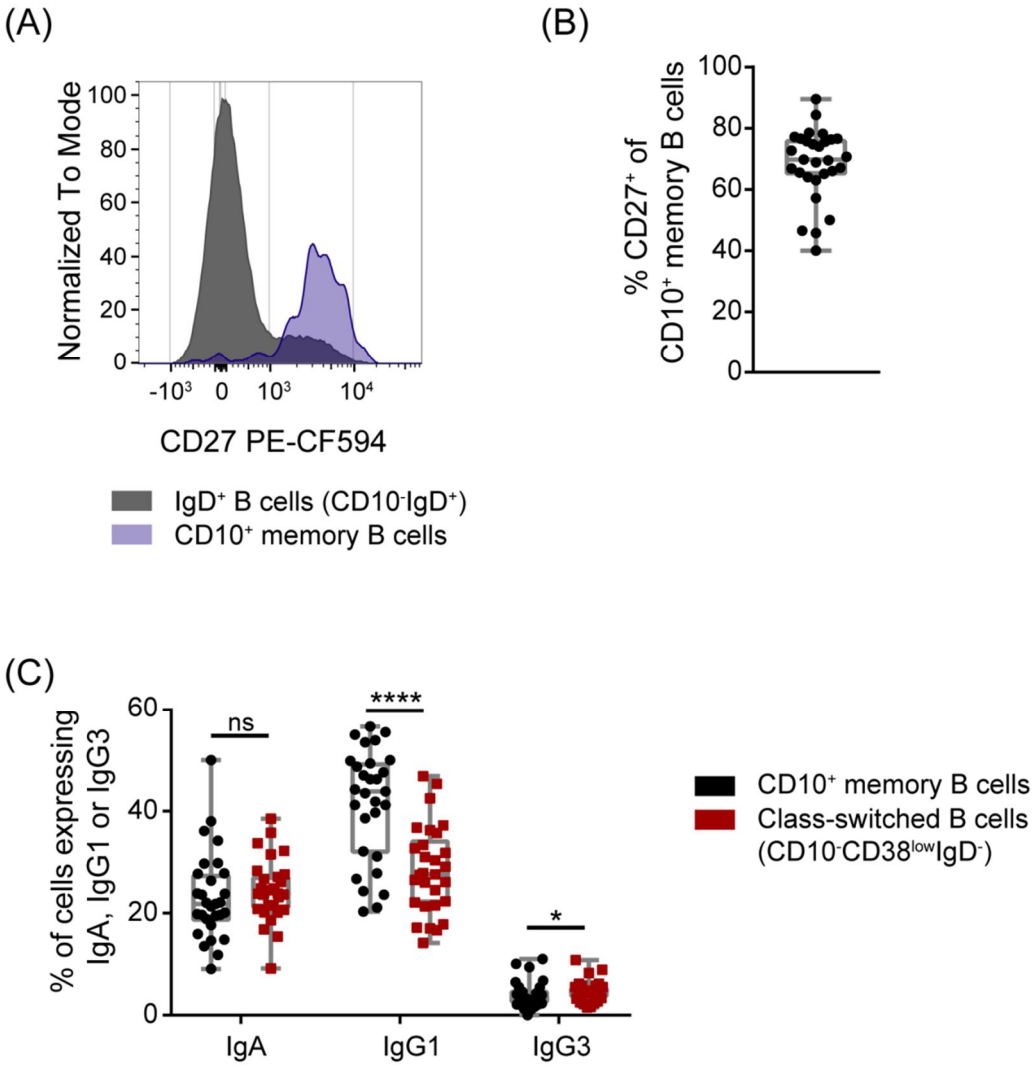

Supplementary figure 4

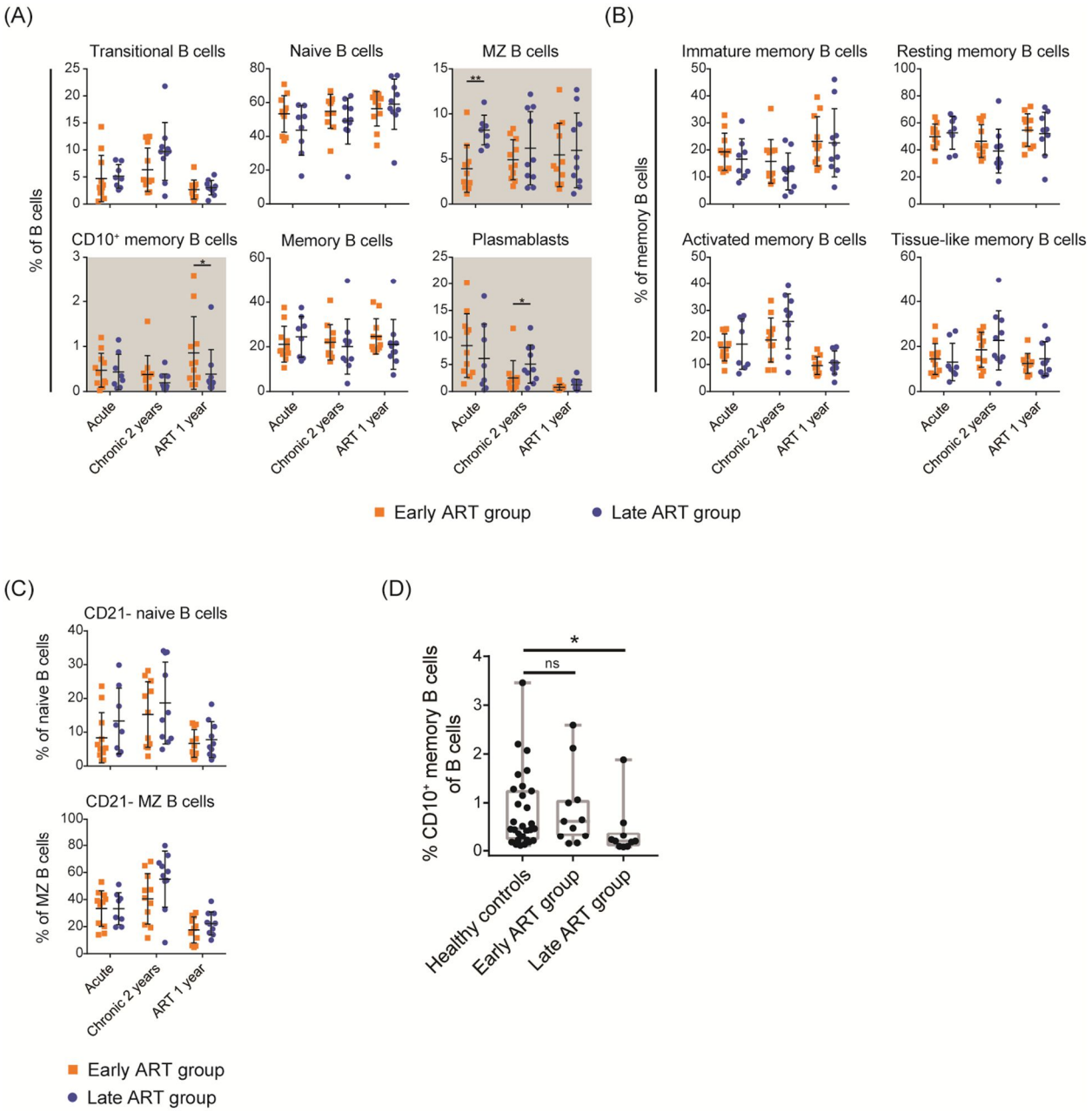

Supplementary figure 5

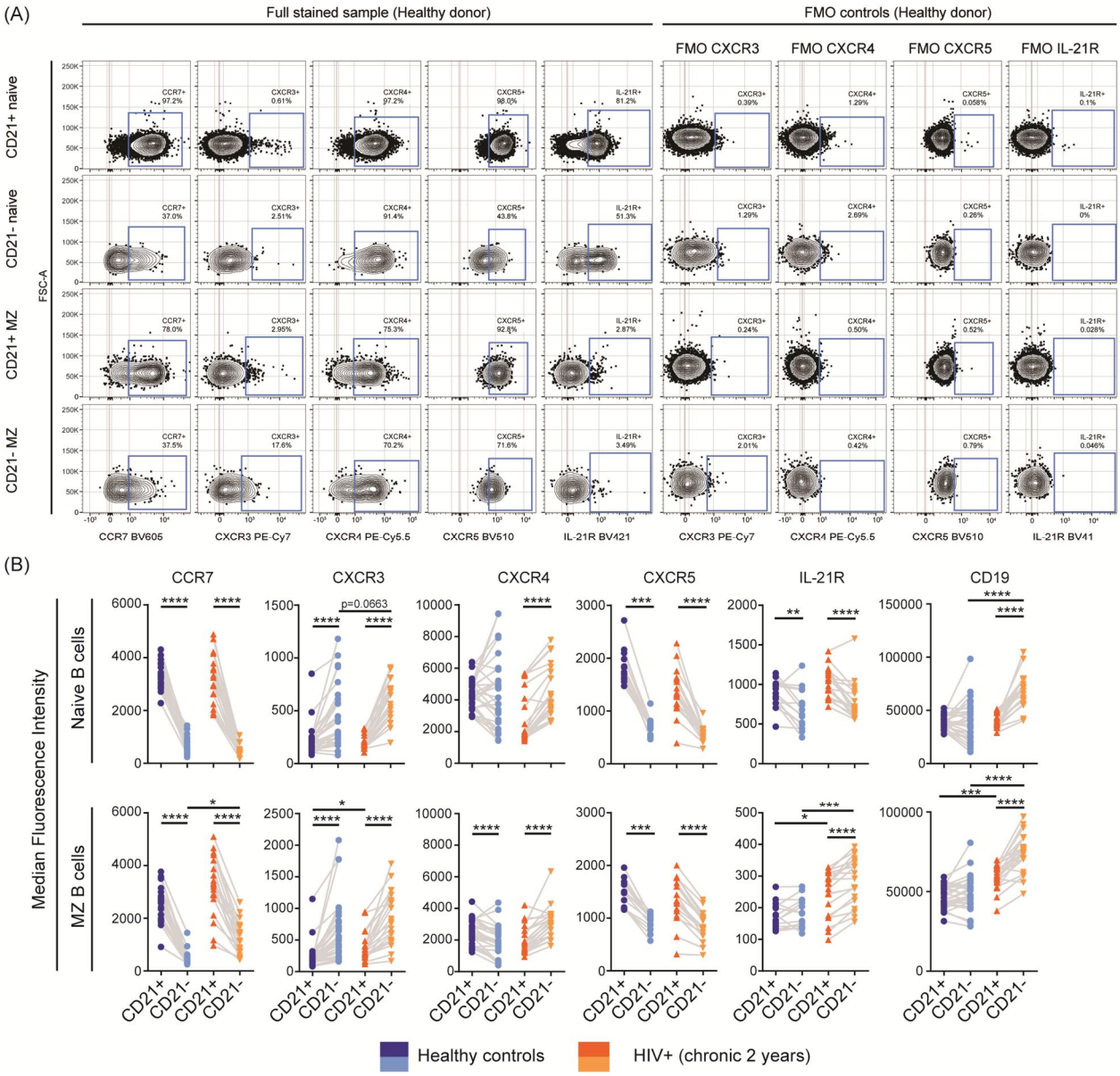

Supplementary figure 6

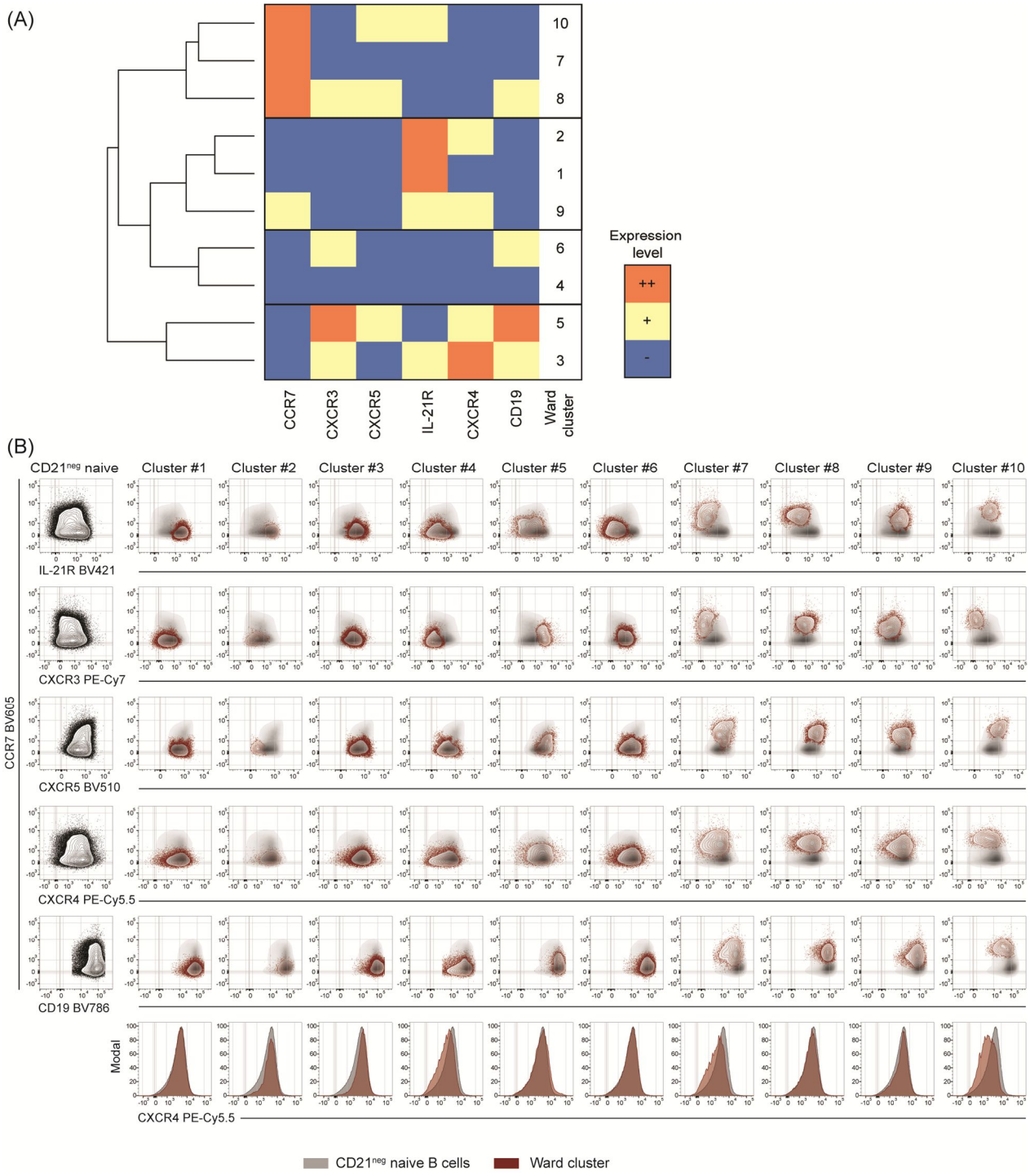

Supplementary figure 7

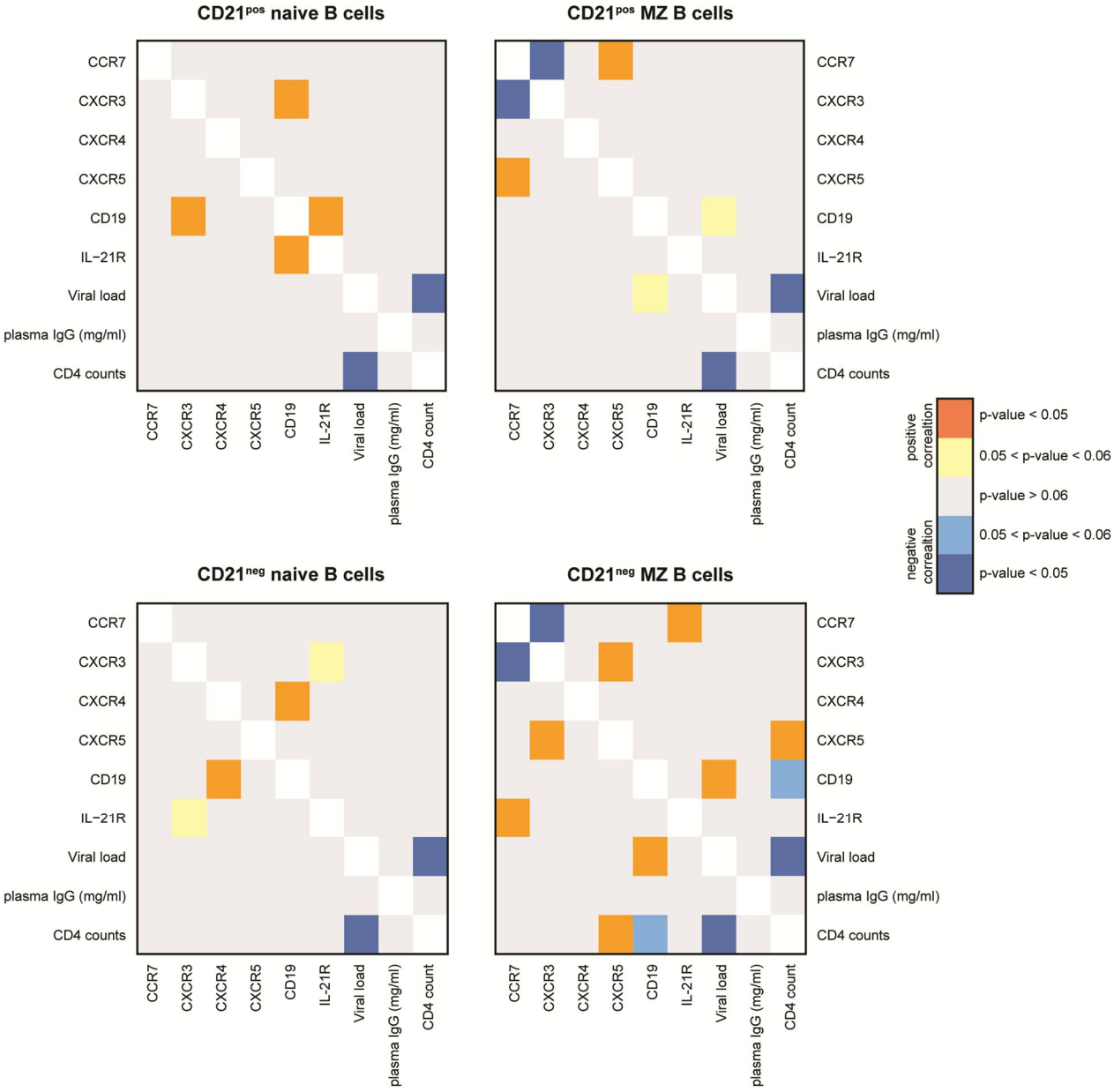

Supplementary figure 8

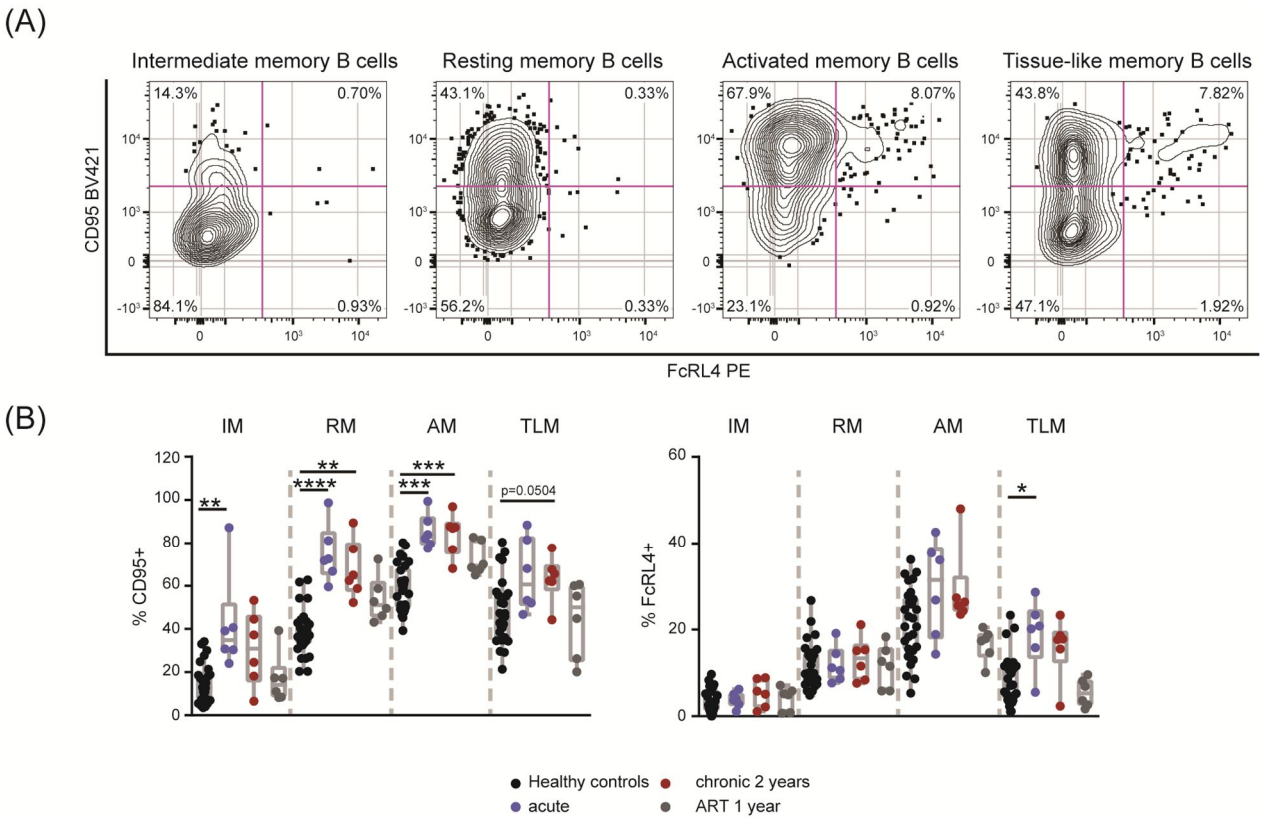

6. Unsupervised high-dimensional flow cytometric analysis of memory B cells in healthy and HIV-1 infected individuals

Manuscript in preparation. My contributions include study design, generating, analyzing and plotting all data. Significant input for computational analysis and statistical analysis as well as Figure 2C were provided by Claus Kadelka. I prepared all figures and wrote the manuscript which was commented on by the coauthors.

Unsupervised high-dimensional flow cytometric analysis of memory B cells in healthy and HIV-1 infected individuals

Thomas Liechti[1], Claus Kadelka[1,2], Dominique L. Braun[1,2], Herbert Kuster[1,2], Jürg Böni[1], Huldrych F. Günthard[1,2], Alexandra Trkola[1].

[1]Institute of Medical Virology, University of Zurich, Switzerland

[2]Division of Infectious Diseases and Hospital Epidemiology, University Hospital Zurich, Zurich, Switzerland

6.1 Abstract

HIV-1 infection induces severe perturbations of the B cell compartment foremost an increased activation and exhaustion of memory B cells and plasmablasts that are linked with impaired antibody responses against HIV-1 and co-infections. To allow resolution of mechanism underlying HIV-1 induced alteration of B cell responses and to identify B cell subsets most relevant for the induction of effective, neutralizing antibody responses against HIV-1 the phenotypical diversity and dynamics of memory B cells and plasmablasts during HIV-1 infection need to be delineated. Here we report on a comprehensive analysis of memory B cells and plasmablasts in HIV-1 infected and healthy donors using multicolor flow cytometry in combination with computational analysis tools that revealed an unprecedented diversity of subsets. Memory B cell subsets with distinct isotypes showed unique distribution of activated and exhausted cells and phenotypic differences in healthy and HIV-1 infected donors suggesting that class-switch recombination to distinct isotypes are a consequence of unique activation circumstances and can lead to divergent phenotypic characteristics. The comprehensive memory B cell landscape we established here provides essential support for further studies aiming to resolve the functional properties of memory B cell subsets in HIV-1 infection and specific targeting of subsets by vaccination.

6.2 Introduction

Neutralizing antibodies are a key component of natural immune responses against viral pathogens and play a key role in vaccine-induced antiviral immunity (1-4). As memory B cells can persist for decades in the periphery, the induction of memory B cells secreting high-affinity antibodies with the ability to neutralize pathogens and to induce Fc-mediated immune responses is a central focus of vaccine development (5-7). In HIV-1 infection, a peculiar dichotomy in respect to B cell responses exists. For one, B cell responses are generally distorted (8-18). Alteration in B cells subsets are signified by increased numbers of activated and exhausted memory B cell subsets that are linked with virus replication and disease progression (12, 14-16, 19-22). As a consequence antibody responses to HIV-1 and unrelated antigens are diminished in HIV-1 infected individuals (11, 23-30). While there is a general agreement on these dysfunctionalities, broadly neutralizing antibodies (bnAbs) that potently block HIV-1 infection, develop almost exclusively in viremic individuals after prolonged infection (31-33). Thus, while B cell responses are genuinely impaired, bnAbs paradoxically appear to require exactly this setting to emerge. Induction of bnAb responses is the ultimate goal of HIV-1 vaccine design but despite decades of intensive efforts, current candidate vaccines struggle to mount even modestly protective antibodies [reviewed in (25, 34-37)]. Unraveling the underlying causalities of B cell alterations in HIV-1 infection and the requirements for bnAb evolution is thus of high importance (25, 31, 35, 38).

Memory B cells can be phenotypically and functionally divided into four subsets based on CD21 and CD27 expression which are referred to as intermediate ($CD21^+CD27^-$; IM), resting ($CD21^+CD27^+$; RM), activated ($CD21^-CD27^+$; AM) and exhausted “tissue-like” ($CD21^-CD27^-$; TLM) memory B cells (12, 14, 16, 22). In chronic viral diseases such as HIV-1 infection activated and exhausted memory B cell subsets increase in frequency (12, 14, 16, 39) and exhaustion of memory B cells has been suggested to be a driving force of impaired antibody responses against HIV-1 and long-term memory against other pathogens (11, 16, 26, 40). While virus load, CD4 loss, immune activation and disease progression have been associated with pronounced increase of AM and TLM subsets (12, 14), the majority of AM and TLM B cells are not HIV-1 specific highlighting that these cells emerge as consequence of a bystander immune activation (9).

While the increase in activated and exhausted B cells in HIV-1 infection is well established, the dynamics and developmental pathways of the individual subsets have not yet been unraveled. It has been long appreciated that memory B cells encompass highly diverse subsets beyond the IM, RM, AM and TLM B cells based on the expression of differing markers including chemokine receptors, B cell receptor isotypes and activation markers (5).

Despite this apparent heterogeneity only few studies have thus far investigated the phenotypic diversity of memory B cells at high dimensionality (41-46). A precise definition of the memory B cell landscape will however be important to enable verification of the differences in functional properties of subsets and their impact on clearing infections (41, 43, 47).

The bystander activation of memory B cells is thought to drive terminal differentiation towards antibody-secreting plasmablasts (12, 14, 48-53). In line with this frequencies of plasmablasts upsurge in HIV-1 infection, and, similar to what has been observed for AM and TLM B cells, only a minor fraction of plasmablasts are HIV-specific underlining the participation of bystander activation processes (8, 17). Of particular note, the increase in plasmablasts correlates with elevated total plasma IgG levels in HIV-1 infection a condition referred to as hypergammaglobulinemia (8, 12, 14, 50)

Phenotypically the highly proliferating plasmablasts are defined by an high expression of CD27 and CD38, and a prototypic low CD19 expression paired with the expression of the proliferation marker Ki-67 in the vast majority of cells (54, 55). Beyond this canonical phenotype phenotypic differences of plasmablasts have been observed in a range of infectious and chronic inflammatory diseases (8, 54, 56-59). Alterations of phenotypic and functional properties of plasmablast in HIV-1 infection have however thus far not been systematically explored. Considering that these cells represent the last stage of the B cell response before developing into long-lived antibody secreting plasma cells, a detailed phenotypic evaluation of the plasmablast repertoire may provide valuable insights how the antibody repertoire is shaped during HIV-1 infection (60).

In the present study we report on a high-dimensional map of the memory B cell and plasmablast landscape in HIV-1 infected individuals and healthy subjects. The phenotypic analysis we present here provides novel insights into the diversity of memory B cells and plasmablasts and the dynamics of the individual subsets in HIV-1 infection. A detailed delineation of the memory B cell compartment as we provide here is key to allow future definition of memory B cell subsets associated with the development of potent HIV-1 specific antibodies. The latter is of particular importance for vaccination strategies to enable specific targeting of these cells to foster the development of bnAbs. By comparing B cell subsets in heathy donors and in longitudinal samples of HIV-1 infected individuals during acute and chronic infection and after antitretroviral therapy our study highlights which perturbations of the B cell response are fully reversibly by ART and which are not. As HIV-1 infected individuals under successful ART retain lower responsiveness to diverse vaccines and infections (29, 61-67), B cell alterations that persist during ART may provide important cues

for future definition of the underlying causes of the reduced humoral immune reactivity in HIV-1 infection.

6.3 Results

6.3.1 High-dimensional analysis of the phenotypic diversity of memory B cells and plasmablasts in HIV-1 infection

In the current study we sought to establish a detailed landscape of memory B cell and plasmablast alterations in HIV-1 infection as a step towards the delineation of B cell subsets that are involved in the induction of bnAbs. Fine-mapping of the B cell repertoire will provide further insights into which subsets are afflicted by HIV-1 infection and where the limitations of current ART are in reverting B cell functionality to normal levels. A specific focus of our phenotypic analysis was on exploring to what extent alterations differ depending on the BCR isotype as isotype responses to different antigens are differentially steered (68, 69). The latter is of particular interest for bnAb responses. The majority of HIV-1 Env specific and neutralizing antibodies including bnAbs are IgG1 (35, 70, 71). A striking exception are however MPER reactive bnAbs, of which all three currently isolated developed as IgG3 isotypes (35, 72). Owing to the high autoreactivity of the MPER bnAbs 2F5 and 4E10 and the ensuing need to overcome counter-selection and tolerance mechanisms in order to evolve the elicitation of these antibodies is highly restricted (73-78). What the prerequisites in HIV-1 infection are that allow MPER antibodies to evolve and if this is linked with IgG3 isotype is currently not known (79). In a first step towards resolving the underlying casualties we sought in the present study to define phenotypic alteration of IgG1, IgG3 and IgA isotypes which are the main three isotypes considered relevant in eliciting anti-HIV-1 activities (70, 79, 80).

To do this we analyzed 12 phenotypic markers on $CD19^{+}CD10^{-}IgD^{-}$ class-switched B cells from three longitudinal time points (during acute infection, after 2 years chronic infection and after 1 year of ART; Supplementary table 1 and 2) from 15 HIV-1 infected individuals that participated in the Zurich Primary HIV Infection Study (ZPHI) and compared these to the B cell repertoire of a control group of 15 healthy donors measured at a single time point.

To obtain a general overview of composition of memory B cells and plasmablasts in healthy donors and at the individual stages of HIV-1 infection, we applied t-SNE (Figure 1A. The location of pre-gated memory B cell subsets based on CD21 and CD27 expression and $CD27^{high}CD38^{high}$ plasmablasts are highlighted by individual colors in the t-SNE map (Figure 1A). As previously described frequencies of AM B cells, TLM B cells and plasmablasts are increased in HIV-1 infection as visualized by an increased density of these populations in the t-SNE map of chronically infected patients (14, 22). A global analysis of the individual memory B cell subsets reveals unique expression patterns of chemokine receptors, IL-21R and the proliferation marker Ki-67 in chronic HIV-1 infection (Figure 1B). We observed a down-regulation of CCR7 and CXCR5 during B cell transition from intermediate to tissue-like

memory B cells, whereas CXCR4 and IL-21R were upregulated. In addition, CXCR3 levels peal at the activated memory B cell stage and revert to lower levels in TLM B cells (Figure 1B). A similar pattern was observed also for proliferation which was the highest in AM B cells among the memory B cell subsets. The majority of plasmablasts showed Ki-67 expression which is in accordance with previous observations (Figure 1B and Supplementary figure 1) [reviewed in(54)]. In addition, plasmablasts expressed CXCR3, CXCR4 and IL-21R (Figure 1B) (81-83).

6.3.2 Distinct properties of IgG1, IgG3 and IgA expressing memory B cells

We next visualized the expression intensities of the different markers in the t-SNE map (Figure 2A). These expression maps revealed an astonishing heterogeneity within the B cell subsets highlighting a more complex diversity of the memory B cell compartment than anticipated (Figure 2A). Of particular note, the t-SNE map revealed that memory B cell subsets as defined by CD21/CD27 expression are differentially distributed among IgA-, IgG1- and IgG3-expressing memory B cells. IgG3-expressing memory B cells composed the highest proportion of TLM B cells, whereas IgA-expressing memory B cells mainly were restricted to the CD27 expressing RM and AM B cells (Figure 2A and Supplementary figure 2).

To verify this we manually gated class-switched B cells excluding $IgD^{-}CD38^{high}$ plasmablasts and estimated the frequency of IgA-, IgG1- and IgG3-expressing memory B cells (Figure 2B and Supplementary figure 3A). In line with what is known from the literature across both HIV-1 infected and healthy donors, IgA- and IgG1-expressing memory B cells showed similar frequencies within total B cells while IgG3-expressing memory B cells are less frequent (Supplementary figure 3A) (84). While HIV-1 infection had no effect on total levels of IgA, IgG1 and IgG3 expressing memory B cells (Supplementary figure 3B) the distribution of IM, RM, AM and TLM B cells amongst the manually gated IgA, IgG1 and IgG3 expressing memory B cells was markedly different (Figure 2C-D) confirming the results of the t-SNE analysis (Figure 2A and Supplementary figure 2). Based on the results from healthy donors peripheral IgA^{+} memory B cells are in general predominantly RM B cells, IgG3-expressing memory B cells contain the highest frequencies of IM and TLM B cells and very low levels of RM B cells, while AM B cells include higher levels of $IgG1^{+}$ and $IgG3^{+}$ than IgA^{+} memory B cells (Figure 2C and D). In sum these frequency distributions highlight that peripheral IgA-expressing memory B cells are the least activated and exhausted, followed by $IgG1^{+}$ B cells and $IgG3^{+}$ B cell subsets which intriguingly is dominated by IM and TLM memory B cells, potentially indicating a rapid transition through the activation steps to TLM B cells. We

observed a similar frequency distribution amongst HIV-1 infected patients although due to the disease-dependent B cell alterations certain distributions shifted (Figure 2C and 2D). Of particular note as IgG3 frequencies amongst IM and RM B cells dropped whereas their frequency in both AM and TLM B cells increased the frequency of memory B cell subsets within IgG3 expressing cells were more similar to $IgG1^+$ B cells in HIV-1 infection than in healthy donors. The same pattern of upregulation of AM and TLM frequencies was observed for IgA expressing B cells (Figure 2C and D).

Irrespective of the isotype expressed frequencies of RM and AM B cells in acute infection differed the most from healthy donors highlighting that they are among the earliest subsets that experience disease-dependent alterations. Although ART as previously described (14, 22) restored the frequency distribution of IM, AM , RM and TLM B cells close to healthy donor levels (Fig 2C and D), elevated levels of AM and TLM B cells and decreased levels of RM B cell persist even after 1 year of ART. This was particularly pronounced for $IgG1^+$ memory B cells suggesting possibly a more severe perturbation or reduced capacity for normalization than IgA- and IgG3-expressing B cells during therapy. This was true for both early and late initiation of ART since we could not detect any difference in frequencies of the investigated memory B cell subsets between the study groups after 1 year of ART (Supplementary figure 4).

6.3.3 Alterations of the memory B cell compartment in chronic HIV-1 infection are tightly linked with disease progression

A known major driver of immune cell activation and exhaustion during HIV-1 infection is viral replication and associated bystander effects (12, 14). We thus next performed a comprehensive correlation map analysis to explore the interrelationships between the different isotype expressing memory B cell subsets and plasmablasts amongst each other and with disease parameters (viral load, CD4 counts and plasma IgG levels; (Figure 3) during acute and chronic HIV-1 infection. An inverse association between frequencies of the activated/exhausted subsets (AM and TLM) and IM and RM B cells is already evident during the acute stage across the majority of the different isotype expressing B cell subsets. This is remarkable as a direct link with disease parameters was not yet evident for the memory B cell subsets during acute infection whereas increases in plasmablasts already in acute infection showed a clear association with viral load levels emphasizing that the differentiation to antibody-secreting cells is tightly driven by virus replication and associated immune activation (14). In chronic infection association with disease parameters became generally evident and that increases in plasmablast, AM and TLM B cells and decreases in IM and RM

B cells independent of expressed antibody isotype are driven by viral load (Figure 3). As expected from the inverse association of CD4 and viral load (85), CD4 counts negatively correlates with the emergence of memory B cell activation and exhaustion (Figure 3).

Elevated total IgG levels defined as hypergammaglobulinemia are a characteristic of B cell response perturbations in chronic HIV infection and considered a result of bystander activation of B cells and can thus be viewed as surrogate marker of immune activation in HIV-1 infection (8, 12, 14, 50). In line with this, plasma IgG levels in chronic infection correlated with the frequency of plasmablasts, total $IgG1^+$ memory B cells $IgG1^+$ AM and $IgG3^+$ AM B cells.

6.3.4 Phenotypic differences of IgG1, IgG3 and IgA expressing memory B cells in healthy donors

The high-dimensional multiparametric flow cytometry analysis we conducted allowed us to conduct a comprehensive comparison of phenotypic features of IgA, IgG1 and IgG3 isotype-expressing memory B cells focusing on IL-21R, the chemokine receptors CCR7, CXCR3, CXCR4, CXCR5 and the proliferation marker Ki-67 (Figure 4). We first performed a phenotypic characterization of the three types of isotype expressing cells in IM, RM, AM and TLM B cells in healthy donors (Figure 4A). IM and RM $IgG3^+$ B cells proved to markedly differ from IgA^+ and $IgG1^+$ cells, showing significantly lower CCR7 and CXCR5 but higher CXCR3 and IL-21R expression (Figure 4A). Lower CXCR5 and higher CXCR3 characterized also $IgG3^+$ AM and TLM B cells. CXCR4 levels interestingly were only strongly upregulated on $IgG3^+$ IM and AM B cells compared to the other isotype expressing cells (Figure 4A). For most parameters $IgG1^+$ IM and RM showed an intermediate phenotype between IgA^+ and $IgG3^+$ memory B cells.

The distinct expression pattern of $IgG3^+$ B cells could potentially be a result from a more activated phenotype compared to other isotype expressing cells as previously suggested (86). To probe directly if the isotype subsets differ in their proliferation history we analyzed the intracellular expression of the proliferation marker Ki-67 (Figure 4B) (87). Interestingly, with the exception of RM cells where all isotype expressing cells were comparable, IgA-expressing subsets proved to be the most strongly proliferating while $IgG1^+$ and $IgG3^+$ B cell subsets showed only low levels of proliferation. Thus, even though the altered receptor densities on IgG3 expressing cells suggest a somewhat higher activation this did not result in increased proliferation of these cells. The markedly higher proliferation of IgA cells may be an indication that these cells originate from different environments than IgG1 and IgG3 expressing cells (42, 88).

6.3.5 Phenotypic differences of IgG1, IgG3 and IgA expressing memory B cells in HIV-1 infection

We next analyzed the dynamics of phenotypic changes on IgA-, IgG1- and IgG3-expressing memory B cell subsets in HIV-infection comparing acute, chronic infection and the effect of ART to the status in healthy donors (Figure 5). While across all memory B cell subsets expression of CCR7, CXCR4, CXCR5, IL-21R and Ki-67 on IgA-, IgG1- and IgG3-expressing did not markedly differ (data not shown), we observed a marked upregulation of CXCR3 in chronic infection for IgG1 and IgG3 IM and RM B cells and a low level upregulation of CXCR3 on all IgA subsets (Figure 5A). Hence, the less activated subsets showed the strongest upregulation of CXCR3. Interestingly 1 year of ART does not show lower CXCR3 expression in IgA, IgG1 and IgG3 IM and RM cells compared to the chronic time point (Figure 5A). As our patient cohort included two group of patients, those who started ART early during acute infection and those who started late in chronic infection, we next explored if the differential effect of ART is linked to the stage of ART initiation (Figure 5B). Indeed, for several B cells subsets CXCR3 expression was significantly higher after late treatment highlights that CXCR3 expression is not completely normalized upon late ART and therefore memory B cells are likely to retain enhanced potential to migrate towards inflamed tissues secreting the CXCR3 ligands CXCL9-11 (89).

6.3.6 Rapid change of phenotypic markers in plasmablasts in acute HIV-1 infection

In a next step we analyzed the phenotypic changes of plasmablasts during HIV infection. In contrast to what we had observed for memory B cells the main changes for plasmablasts already occurred with acute infection and were signified by a marked downregulation of CCR7 and notable, but less pronounced upregulation of CXCR4, CXCR5 and I-21R compared to healthy donors (Figure 6A). Interestingly, with the exception of lower CCR7 expression the changes in these markers reverted to normal levels in chronic infection whereas CXCR3 levels were upregulated. In line with the generally high proliferation of plasmablasts (Supplementary figure 1) (54), we observed no HIV-1 induced alterations in Ki-67 expression (Figure 6B).

6.3.7 *Clustering algorithm defines complex heterogeneity within memory B cell subsets*

Considering the complexity of the phenotypic differences we observed in the t-SNE and the manual gating analysis we next applied the clustering algorithm SPADE (spanning-tree progression analysis of density-normalized events) to group cells with similar expression profiles into clusters. The SPADE trees allowed a rapid definition of cluster regions in chronic HIV-1 infected patients with expression patterns comparable to plasmablasts and memory B cell expressing different isotypes (Supplementary figure 5A). In line with our prior analyses memory B cells harbored distinct expression profiles according to their BCR isotype (Supplementary figure 5B).

In order to be able to define rare subsets as separate populations clustering algorithms such as SPADE perform over-clustering that resulting in a high number of clusters with similar phenotypes (Figure 5A-C). We thus performed a second hierarchical clustering based on Ward's hierarchical clustering method in order to merge similar SPADE clusters (Supplementary figure 6) which resulted in the definition of 40 differential clusters among memory B cells and plasmablasts (Figure 7A and 8A and Supplementary figure 6). We grouped these clusters manually based on their expression of CD21 and CD27 into the known IM, RM, AM and TLM B cell subsets and defined plasmablasts based on expression of Ki-67, CD27 and CD38 (Figure 7A and 8A). Clusters that were assigned to these specific subsets showed overall the known characteristics, e.g. CXCR3 was expressed on the majority of clusters defined as AM and TLM B cells whereas CXCR5 expression was mostly restricted to IM and RM B cells and TLM B cells were signified by high CXCR4 and IL-21R expression (Figure 7A). However, the Ward analysis revealed that each main memory B cell subset contained clusters with unusual expression pattern that were not revealed by our prior global expression analysis. While CXCR3 expression is generally low on RM B cells the clustering analysis highlighted that nevertheless RM B cell populations with high CXCR3 expression (Figure 7A; Ward cluster 9, 10, 13, 16 and 28) and no CCR7 expression could be observed (Figure 7A; Ward cluster16, 18 and 25) exist. Likewise, despite an overall low expression of CCR7 on AM B cells, distinct AM B cell populations express CCR7 at high levels (Figure 7A; Ward cluster 5, 8, 14, 15 and 27). Of particular note, comparing the results of the Ward and t-SNE analysis we confirmed that these unusual phenotypes can also be traced by t-SNE supporting the utility of t-SNE in revealing complex cell population heterogeneity (Figure 2A and Supplementary figure 2).

As certain ward clusters deviated from the global expression profiles of AM and RM B cells (Figure 1B) we probed whether manual gating and clustering analysis results in similar frequencies of RM and AM B cells to ascertain that both approaches have indeed

comparable capabilities to define major B cell subsets. We found that the computational clustering analysis assigns slightly lower numbers of RM B cells compared to manual gating (median difference of 8.136% ± 5.218%) but both methods retrieve identical numbers of AM B cells (Supplementary figure 7) highlighting the validity of both approaches. This was also supported when we compared the frequency of $CCR7^{high}$ cells within RM and AM B cells with both methods which confirmed that also by Ward analysis RM B cells contain higher frequency of $CCR7^{high}$ cells (49.77% ± 10.64%) than AM B cells (31.05% ± 11.86%). A limitation of the global analysis as we conducted it, is that it relies on median fluorescence intensity values. The latter is useful to estimate expression levels across larger populations but bears the caveat that markers expressed only on a minority of cells are neglected. This may have in the analysis of AM B cells lead to an underappreciation of $CCR7^{high}$ cells since less than 50% are expressing high levels of CCR7.

To further verify the validity of the Ward cluster analysis, we manually monitored the expression pattern of the individual Ward clusters and found that they formed homogenous populations. The manual re-analysis also confirmed that the assignment of the individual clusters to memory B cell subsets as defined by CD21/CD27 expression was in the majority of Ward clusters accurate and allowed to reveal subpopulations with unique characteristics. For example, re-analysis of cluster 9, which belongs to RM B cells allowed verification of the unusual high expression of CXCR3 that was not revealed by prior MFI based global expression analysis (Figure 7B). Nevertheless, few clusters showed heterogeneous CD21/CD27 expression highlighting that other markers are more decisive for the definition of these clusters.

Interestingly the dynamics of individual memory B cell clusters differed during HIV-1 infection. While total IM and RM B cell numbers decrease and AM and TLM B cells increase (Chapter 5, Figure 1B), this was not the case for all individual clusters within these subsets (Fig 7C). For instance, the IM B cell cluster with high expression of IL-21R (Ward cluster 24) was not affected whereas the $IL\text{-}21R^{-}$ clusters decreased in chronic HIV-1 infection. Likewise, three RM B cell clusters (Ward clusters 16, 17 and 28) with comparatively low CCR7 expression were not affected by HIV-1 infection. While the majority of AM B cell clusters increased during HIV infection and decreased after 1 year of ART, AM Ward cluster 15 which is signified by high Ki-67 expression showed rapid reduction during acute phase and normalized during later stages of HIV infection (Figure 7A and C).

Most ward clusters assigned to plasmablasts showed a characteristic low expression of CD19 paired with high expression of CD27, CD38 and Ki-67 (Figure 8A) (54, 90). Yet, some clusters linked with plasmablasts in our analysis, expressed only two of these canonical plasmablasts markers. One intriguing observation was a rare plasmablast population (91)

that lacked CD27 expression but maintained high levels of CD38 and Ki-67 (Figure 8A). In general the plasmablast clusters showed highly diverse expression patterns of chemokine receptors CCR7, CXCR3 and CXCR5. We again confirmed the expression profiles manually and verified that all clusters showed homogenous expression patterns as exemplified by cluster 32 (Figure 8B).

Interestingly, we observed non-proliferating plasmablast associated cell clusters expressing no or little Ki-67 expression (cluster 33 and 40) which increased levels during HIV infection (Figure 8C). Several plasmablast clusters show characteristic dynamics during HIV-1 infection with increased levels during acute and chronic phase and restored levels after 1 year of ART (clusters 31, 33, 35, 37, 39, 40) while HIV-1 infection had no or only a marginal effect on others (cluster 32, 34, 36, 38). In sum this highlights that also in plasmablasts a considerable heterogeneity exists that are differentially affected by HIV-1 infection.

6.4 Discussion

HIV-1 infection is characterized by severe immunomodulatory effects that severely impact on B cell responses (9, 10, 12, 14-16, 23, 30). Hallmarks of these alterations are hypergammaglobulinemia and an accumulation of activated and exhausted memory B cells (12, 14, 17) which are functionally linked with a decreased capacity to mount novel antibody responses against diverse antigens (11, 23-30). Despite the reduced capacity to mount effective B cell responses with progressing disease, potent HIV-1 specific broadly neutralizing antibodies develop preferentially after several years of HIV-1 infection (31-33). Definition if and which specific B cell subsets or stimulatory environments foster bnAb evolution is of high interest to guide HIV vaccine design. In a step towards this we conducted here a high-dimensional analysis of the memory B cell and plasmablast compartment in healthy donors and HIV-infected patients that is amongst the most comprehensive attempted to date (41-46, 92).

Most studies that have analyzed the dynamics of memory B cells during HIV-1 infection thus far focused solely on the canonical subdivision into intermediate ($CD21^+CD27^-$), resting ($CD21^+CD27^+$), activated ($CD21^-CD27^+$) and exhausted tissue-like ($CD21^-CD27^-$) memory B cells and a selected range of phenotypic characteristics of these four subsets (12, 14, 16, 93). With the current study we aimed for a high-dimensional analysis of the memory B cell compartment including the assessment of activation markers, BCR isotypes, chemokine receptors, proliferation marker and the cytokine receptor IL-21R in a 16-paramter flow cytometry analysis. To reveal the complexity of the memory B cell landscape we used a combination of manual examination and computational clustering algorithms.

Our analysis of the memory B cell compartment in HIV-1 infected individuals confirmed all previously observed perturbations (Chapter 5; Figure 1B) and the strong association with clinical markers of disease progression (Figure 3) (12, 14) but beyond this revealed a high complexity of subsets within the four memory B cell types (Figure 7A-D).

An important aspect of our study was the differentiation of memory B cells according to the BCR isotype. Focusing on IgA, IgG1 and IgG3, which are considered most relevant for HIV-1 specific neutralizing antibody responses (70, 80), we analyzed the distribution of the isotype expressing B cells across the different memory B cell subsets and their phenotypic differences. A precise definition of differential regulation of BCR isotypes is of particular interest in respect to HIV-1 bnAbs. bnAbs directed against gp120 like gp120 specific antibodies in general are predominantly IgG1 whereas the three MPER-specific bnAbs isolated thus far emerged as IgG3 (35, 94, 95). Whether epitope specificities steer this disparate distribution or specific co-stimulatory events are necessary to induce the

generation of the partly autoreactive MPER bnabs is a matter of extensive research efforts (25, 35, 36).

Using the t-SNE algorithm we revealed distinct distributions of IgA-, IgG1- and IgG3-expressing memory B among IM, RM, AM and TLM B cells in both healthy and HIV-1 infected donors (Figure 1A and 2C and Supplementary Figure 2). IgG3 and IgA expressing memory B cells differed the most in their phenotypic features, with IgG3 expressing cells encompassing the highest proportion of activated AM and exhausted TLM B cells whereas IgA-expressing memory B cells showed a high frequency of RM B cells (Figure 2B-D). The increased frequency of $IgG3^+$ B cells amongst activated and exhausted B cells is intriguing and agrees with previous observations (86, 96, 97). The developmental paths of these cells remain unclear but a low variable gene mutation rate of a fraction of $CD27^-IgG3^+$ B cells potentially suggests that some of the cells originate from germinal center- and T cell-independent responses or represent the first wave of antibody responses (42, 86, 97, 98). While antigens and exposure can influence CSR to induce a specific isotype (68), this can not be the sole reason for the differential distribution of BCR isotypes cross the memory B cell subsets as we observed similar patterns in healthy donors and in HIV-1 infection.

In line with their activated and exhausted profile, IM and RM $IgG3^+$ B cells showed reduced levels of CCR7 and CXCR5 and increased levels of CXCR3 and IL-21R when compared to IgA+ and IgG1+ memory B cells in healthy donors (Figure 4) suggesting that IgG3-expressing IM and RM B cells may bear a higher potential to differentiate into AM and TLM B cells. HIV-1 infection lead to a generally higher expression of CXCR3 in IM and RM memory B cell subsets across all BCR isotypes expressing cells (Figure 5A). This emphasizes that HIV induces phenotypic changes within IM, RM, AM and TLM B cells in addition to their altered distribution. As up-regulation of CXCR3 is indicative for activation processes, the phenotypic analyses highlights that differentially activated subpopulations exist within the canonical memory B cells subsets that are solely based on CD21/CD27 classification (16, 82, 99).

Activation as based on CXCR3 expression was fully reversed by early initiation of ART but not when ART was initiated late during chronic infection (Figure 5B) supporting the notion that initiation of ART in the acute phase can prevent irreversible B cell alterations (14, 22). Whether elevated levels of CXCR3 on B cells subsets amongst are an indication of long debated residual virus replication, long-term presentation of viral antigens or a result of slow turnover of these cells and/or the CXCR3 receptor remains to be determined (82, 100-102) .

To obtain a detailed overview of the memory B cell and plasma landscape we re-analyzed all data using the clustering algorithm SPADE and Ward hierarchical clustering which revealed

30 distinct memory B cell and 10 plasmablast clusters (Figure7A and 8A and Supplementary Figure 5A-D and 6). While these computational approaches highlighted the same gross changes we observed in the global analysis, they revealed a higher than previously appreciated heterogeneity within the IM, RM, AM and TLM B cells and plasmablasts of healthy individuals which were in part differentially affected by HIV-1 infection, highlighting the need to improve monitoring and our understanding of the diverse subsets within the B cell population (Figure 7A-C and 8A-C). Of particular note, some cell clusters within IM, RM and TLM B cells were not altered by HIV-1 infection. This included IM B cells expressing high levels of IL-21R which did not change in frequency, whereas IL21R$^-$ IM B cells decreased during HIV infection. Tracing the underlying causalities may be difficult as the general function of IM B cells are poorly understood but it is feasible that IL-21R signaling may contribute to their survival (103-105).

The refined analysis of plasmablasts we conducted here confirmed earlier reports that highlighted their phenotypical diversity (54). We found similar to the memory B ell landscape that HIV-1 infection afflicted plasmablast subsets differentially. Most intriguingly, we found that plasmablast subsets show a diversity in CXCR3 expression emphasizing that a fraction of plasmablasts are migrating towards inflamed tissues (82, 106). High CCR7 levels on certain plasmablast subsets emphasized that they are destined to migrate to/from lymphoid tissues. (106). Interestingly, we observed phenotypic changes amongst plasmablast subsets predominantly during acute infection where perturbations of the memory B cells were less evident possibly indicating that direct action of the cytokine storm early in the acute phase may be linked to the modulations of plasmablast rather than preceding alteration of memory B cells (107, 108).

Overall our high-dimensional analysis provides a detailed map of the memory B cell and plasmablast compartments in both healthy individuals and HIV-1 infection that provide a basis for further dissection of B cell responses to explore components of the B cell response the restrict or promote bnAb evolution.

6.5 Methods

Clinical specimen

Cryopreserved peripheral blood mononuclear cells (PBMC) and plasma of HIV-1 infected individuals (n=19) were available from samples stored in the biobank of the Zurich Primary HIV Infection Study (ZPHI). The ZPHI is an ongoing, observational, nonrandomized, single center cohort founded in 2002 that specifically enrolls patients with documented acute or recent primary HIV-1 infection (ClinicalTrials.gov identifier NCT00537966) (109). The ZPHI is approved by the ethics committee of the Kantonale Ethikkommission Zürich and written informed consent was obtained from all participants. Longitudinal samples of patients that started ART early (during the acute infection stage, n=11) and late (in the chronic infection stage, n=8), were analyzed. Longitudinal samples encompassed samples from the untreated acute and chronic stage (year 1, year 2) and after 1 year of ART (Supplementary table 1 and 2). Patient and disease demographics (estimated time of infection, CD4 cell count and plasma viral load level at sampling date) were available through the ZPHI data bank.

PBMC and plasma from healthy donors (n= 29; single time points) were collected in the frame of a separate clinical study (PI H. Günthard) that was approved by the ethics committee of the Kantonale Ethikkommission Zürich and written informed consent was obtained from all participants.

PBMC were isolated by density-gradient centrifugation using LymphoPrep (Axis-Shield) from whole blood drawn in EDTA vacutainer tubes (BD Biosciences). Until further processing PBMC were cryopreserved using 90% inactivated FCS (Thermo Fisher Scientific) and 10% DMSO (Sigma Aldrich) and stored in liquid nitrogen. Plasma was heat-inactivated for 1h at 56°C and stored at -80°C for further analysis.

Flow Cytometry

To monitor B cell populations by flow cytometry PBMC were stained using a 16-parameter panel as described *(Liechti, T. et al. manuscript in preparation, Chapter 4)*. Briefly, cells were thawed and washed with FACS buffer containing PBS (Thermo Fisher Scientific), 2% heat-inactivated FCS (Thermo Fisher Scientific), 2mM EDTA (Sigma Aldrich) and 20µg/ml DNase (Sigma Aldrich), stained with a cocktail of antibodies directed against surface markers encompassing CD3 APC-Cy7 (clone SK7, Biolegend), CD14 APC-Cy7 (clone HCD14, Biolegend), CD16 APC-Cy7 (clone 3G8, Biolegend), CD10 BV650 (clone HI10a, BD Pharmingen), CD19 BV786 (clone SJ25C1, BD Pharmingen), CD21 BV711 (clone B-ly4m

BD Pharmingen), CD27 PE-CF594 (clone M-T271, BD Pharmingen), CD38 AF700 (clone HIT2, Biolegend), IgG1 PE (clone HP6001, Southern Biotech), IgG3 FITC (polyclonal sheep IgG, AbD Serotec), IgA APC (polyclonal goat IgG, Jackson Immuno), CCR7 BV605 (clone G043H7, Biolegend), CXCR3 PE-Cy7 (clone G025H7, Biolegend), CXCR5 BV510 (clone RF8B2, BD Pharmingen), IL-21R BV421 (clone 2G1-K12, Biolegend) and Live/dead near-infrared dye (Life Technologies). IgD (clone IA6-2, Biolegend) and CXCR4 (clone 12G5, Biolegend) were labelled in-house with labeling kits for PE-Cy5 (Innova Biosciences) and PE-Cy5.5 (Innova Biosciences), respectively, according to the manufacturer's instructions. Each new batch of labeled antibodies was titrated in parallel with and adjusted to the old batch to ascertain comparable staining intensities. Cells were afterwards fixed and permeabilized with the FoxP3 staining kit (eBioscience) according to manufacturer's instructions to stain for Ki-67 PerCP-eFluor710 (clone 20Raj1, eBioscience). Data was acquired on a BD Fortessa calibrated daily using the CS&T module. Staining intensity QC was conducted as recommended (110) and individual stainings with markers that did not fulfil requirements excluded when comparative analysis of intensities was performed. To further limit the possibility of influences due to day-to day variability in the flow cytometry analysis, all longitudinally time points of a given patient were analyzed at the same day. In addition patients assigned to the early and late ART group were included in all experiments to exclude batch effects. Compensation was done for each experiment individually. Manual analysis was done with FlowJo (TreeStar).

Analysis using t-distributed stochastic neighbor embedding (t-SNE) and spanning-tree progression analysis of density-normalized events (SPADE)

Data analysis was performed using Cytobank (Cytobank Inc.), a cloud-based software that provides the integrated analysis tools SPADE and t-SNE (111-113). Class-switched $CD19^{+}CD10^{-}IgD^{-}$ B cells were pre-gated and analyzed with t-SNE and SPADE using the markers IgA, IgG1, IgG3, CD21, CD27, CD38, CCR7, CXCR3, CXCR5, IL-21R and Ki-67. In these analyses we included samples from a single time point from healthy controls (n=15) and longitudinal time points of HIV-1 infected patients (n=15) (acute infection, chronic infection after 2 years and after 1 year of ART 1 year). All measurements from a specific time point of HIV-infected individuals and from healthy donors were concatenated to visualize the global differences between control group, acute and chronic phase of HIV infection and upon 1 year of ART.

T-SNE analysis was performed using identical cell counts from each sample in order to guarantee equal contribution from each donor and time-point to the t-SNE based

dimensionality reduction. As CXCR4 staining showed some variability this marker was excluded from SPADE and t-SNE analysis but information on CXCR4 was made available for visual examination, distribution and expression profile of CXCR4 in both analyses. For CD19 the same approach was used due to marginal differences between the different subsets not providing further information on clustering and t-SNE.

We chose a setting of over-clustering, by allowing for 200 different clusters for SPADE as this allows to build separate clusters of very rare cell populations. As a consequence frequent cell populations can separate into different clusters despite sharing phenotypic properties. Therefore, clusters created by SPADE were further clustered using hierarchical clustering with the Ward method in R and visualized with the hetmap.2 function (114). SPADE clusters were ordered and grouped by Ward hierarchical clustering method based on z-score normalized data of arcsinh transformed median fluorescence intensity values from the individual SPADE clusters. By analyzing the hierarchical tree a cut-off was determined to optimally distinguish the several phenotypes resulting in 40 distinct Ward-based clusters within class-switched B cells. To categorize the expression profile of the individual Ward clusters we manually determined the z-score at which cells are positive for a given marker and defined negative (-), low expression (+), intermediated expression (++) and high expression (+++).

IgG ELISA

Total immunoglobulin concentrations in heat-inactivated plasma from the HIV-1 infected patients were measured by enzyme-linked immunosorbent assay (ELISA) as described previously (115). Briefly, 96 well immunosorbent plates (Thermo Fisher Scientific) were coated with polyclonal goat anti-human IgG (Southern Biotech) in sodium carbonate buffer pH8.2 for 2 hours at room temperature. PBS/2% BSA (Sigma Aldrich) was used as a blocking reagent for 30 minutes at 37°C. Serial dilutions of the plasma samples were applied to the plates and incubated for 2 hours at room temperature. Plasma IgG was detected using a biotinylated polyclonal goat anti-human IgG (southern Biotech; 2 ng/ml) followed by streptavidin-alkaline phosphatase (Sigma Aldrich, 40ng/ml) each diluted in PBS/2% BSA and incubated for 1 hour at room temperature. CDP-Star system (Applied Biosystems) was used as alkaline phosphatase substrate and luminescence was measured after 30min with a Dynex luminometer (Magellan Biosciences). Human IgG (Sigma Aldrich) was used as a standard to determine the concentration of plasma IgG.

Statistical analysis

Comparison of memory B cell subsets between healthy controls and HIV-1 infected patients was done using unpaired non-parametric Kruskal-Wallis one-way ANOVA and comparison between different time points of HIV-1 infected patients using paired non-parametric Friedman one-way ANOVA. Multiple comparison correction was performed using Dunn's multiple testing correction test. Comparisons in Figure 2C and 5B are done using unpaired non-parametric Mann-Whitney test without multiple testing corrections. P-values are highlighted as color gradient. Comparisons between the early and late treatment group was done with unpaired non-parametric Mann-Whitney test. $P<0.05$ was considered statistically significant. Significance levels are reported as *$p<0.05$, **$p<0.01$, ***$p<0.001$, ****$p<0.0001$. Statistical tests were calculated using Prism version 7 (GraphPad). Correlations (Figure 3) were calculated using non-parametric Spearman correlation and visualization was done using the corrplot package and heatmaps using the heatmap.2 package for R programming language (version 3.3.1, http://cran.r-project.org). Heatmaps for figure 2C were done with Matlab (MathWorks).

6.6 Figure legends

Figure 1: Dimensionality reduction analysis t-SNE reveal HIV-1 dependent dynamics of class-switched B cells.

(A) t-SNE maps of $CD19^{+}CD10^{-}IgD^{-}$ class-switched B cells from healthy (n=15) and HIV-infected individuals (n=15) at acute phase, after 2 years of chronic infection and after 1 year of ART are shown. The main memory B cell subsets and plasmablasts are overlaid and differentially colored. All events of the corresponding group are concatenated and displayed. **(B)** Median expression intensity (MFI) of phenotypic markers on main memory B cell subsets defined based on CD21 and CD27 expression and plasmablasts after 2 years of chronic infection are depicted. The MFI of fluorescence minus one (FMO) controls estimated on total $CD19^{+}$ B cells are depicted as grey dashed line where applied. Comparison of memory B cell subsets and plasmablasts are done using paired non-parametric Friedman one-way ANOVA and multiple comparison correction was performed using Dunn's multiple testing correction test. $P<0.05$ was considered statistically significant. Significance levels are reported as *p<0.05, **p<0.01, ***p<0.001, ****p<0.0001.

Figure 2: Frequency analysis of memory B cells expressing distinct isotypes.

(A) Expression intensities of phenotypic markers in the t-SNE maps are shown. Concatenated samples after 2 years of chronic infection are depicted. **(B)** Gating strategy to define IgA, IgG1 and IgG3 expressing memory B cells ($CD19^{+}CD10^{-}IgD^{-}CD38^{low}$) and the main memory B cell subsets within these isotype-expressing memory B cells based on CD21 and CD27 expression is shown from a chronic HIV-1 infected patient. **(C)** Frequency of main memory B cell subsets based on CD21/CD27 classification within IgA, IgG1 and IgG3 expressing memory B cells in healthy subjects (n=29; black dots) and HIV-infected individuals (n=17) at acute stage (blue dots), after 2 years of chronic infection (dark red dots) and after 1 year of ART (grey dots) are depicted. **(D)** The p-values from the comparisons of the frequencies of main B cell subsets plotted in Figure 2C defined based on CD21/CD27 expression within the different isotype-expressing memory B cells of healthy controls and HIV-1 infected patients at different disease stages and after 1 year of ART are visualized as a heatmap. The scale is according to the p-value in which red and blue colored boxes indicates when subsets from rows are decreased or increased, respectively, compared to the subset in columns. Pairs not compared are colored grey. Unpaired non-parametric Mann-

Whitney test without multiple testing corrections was used for the comparison. P<0.05 was considered statistically significant.

Figure 3: Spearman correlation analysis of several subsets and clinical features in acute and chronic HIV-1 disease.

Analysis with samples from the acute (n=17) and chronic (n=19) phase of HIV-1 infection are depicted. The matrices in the top row show the Spearman's Rank Coefficient. The dot size corresponds to the value of the coefficient and the color indicates positive or negative correlation if colored red or blue, respectively. Only statistically significant correlations are shown. Empty fields indicate insignificant p-values. The bottom row displays the p-values of the spearman correlations as a heatmap. P<0.05 was considered statistically significant.

Figure 4: Phenotypic differences of IgA, IgG1, and IgG3 expressing memory B cell subsets.

(A) Median expression intensity of CCR7, CXCR3, CXCR4, CXCR5 and IL-21R in healthy subjects (n=29; n=14 for CXCR5 and IL-21R) are shown for the main memory B cell subsets based on CD21 and CD27 expression within the different isotype-expressing memory B cells. **(B)** Percentage of Ki-67 expression on the same cell subsets of healthy donors (n=29) are depicted. Paired non-parametric Friedman one-way ANOVA was used to compare B cell subsets and multiple comparison correction was performed using Dunn's multiple testing correction test. P<0.05 was considered statistically significant. Significance levels are reported as *p<0.05, **p<0.01, ***p<0.001, ****p<0.0001.

Figure 5: HIV-1 infection alters the expression of CXCR3 on memory B cell subsets.

(A) The expression levels of CXCR3 on memory B cell subsets divided into the different isotype-expressing memory B cells are shown for healthy controls (n=29) and HIV-infected patients (n=17) at acute and 2 years of chronic disease stage and after 1 year of ART. Comparison of memory B cell subsets between healthy controls and HIV-1 infected patients was done using unpaired non-parametric Kruskal-Wallis one-way ANOVA and comparison between different time points of HIV-1 infected patients using paired non-parametric Friedman one-way ANOVA. Multiple comparison correction was performed using Dunn's multiple testing correction test. **(B)** CXCR3 expression levels after 1 year of ART are shown. Patients are divided in subgroups based on their initiation of therapy into early ART (n=11,

grey dots) and late ART group (n=8, black circles). Unpaired non-parametric Mann-Whitney test was used to compare early and late treatment group. P<0.05 was considered statistically significant. Significance levels are reported as *p<0.05, **p<0.01, ***p<0.001, ****p<0.0001.

Figure 6: Plasmablasts show phenotypic alterations during HIV-1 infection.

(A) Chemokine receptor and IL-21R expression levels from plasmablasts from healthy donors (n=29, n=14 for CXCR5 and IL-21R) and HIV-infected patients (n=17) at different disease stages and therapy are shown. The MFI of fluorescence minus one (FMO) controls estimated on total $CD19^+$ B cells are depicted as black dotted line where applied. **(B)** The frequency of Ki-67-positive plasmablasts were estimated for the same samples. Comparison of markers expressed on plasmablasts between healthy controls and HIV-1 infected patients was done using unpaired non-parametric Kruskal-Wallis one-way ANOVA and comparison between different time points of HIV-1 infected patients using paired non-parametric Friedman one-way ANOVA. Multiple comparison correction was performed using Dunn's multiple testing correction test. P<0.05 was considered statistically significant. Significance levels are reported as *p<0.05, **p<0.01, ***p<0.001, ****p<0.0001.

Figure 7: Memory B cells show high phenotypic diversity individually influenced by HIV-1 infection.

(A) Expression profile of Ward clusters based on SPADE/Ward hierarchical clustering of class-switched B cells from the concatenated chronic 2 year samples are depicted as a heatmap. Expression of phenotypic marker are shown as no expression (-; blue), low expression (+; yellow), medium expression (++; orange) and high expression (+++; red). Ward clusters are numbered according to Ward cluster identification in supplementary figure 6. Clusters are ordered manually according to their CD21/CD27 expression classification. **(B)** Manual inspection of Ward clusters was performed as depicted for Ward cluster #9 (red) which is overlaid on total class-switched B cells (grey). **(C)** The frequency of the individual Ward clusters in healthy control (n=15) and HIV-infected individuals (n=15) at different disease stages and ART are shown. Comparison of Ward clusters between healthy controls and HIV-1 infected patients was done using unpaired non-parametric Kruskal-Wallis one-way ANOVA and comparison between different time points of HIV-1 infected patients using paired non-parametric Friedman one-way ANOVA. Multiple comparison correction was performed using Dunn's multiple testing correction test. P<0.05 was considered statistically significant. Significance levels are reported as *p<0.05, **p<0.01, ***p<0.001, ****p<0.0001.

Figure 8: Phenotypic diversity of plasmablasts revealed with clustering analysis

(A) Expression profile of Ward cluster resembling plasmablasts is shown of the chronic disease stage. Expression of phenotypic marker is shown as no expression (-; blue), low expression (+; yellow), medium expression (++; orange) and high expression (+++; red). Ward clusters are numbered according to Ward cluster identification in supplementary figure 6. Clusters are ordered manually according to their expression of Ki-67, CD27 and CD38. **(B)** Manual validation of the individual clusters was done and cluster (#32) is shown as an example. Ward clusters (red) are overlaid on top of total class-switched B cells (grey). **(C)** Dynamics of the plasmablast clusters are shown for healthy controls (n=15) and HIV-infected patients (n=15) at different disease stages and after 1 year of ART. Comparison of Ward clusters resembling plasmablasts between healthy controls and HIV-1 infected patients was done using unpaired non-parametric Kruskal-Wallis one-way ANOVA and comparison between different time points of HIV-1 infected patients using paired non-parametric Friedman one-way ANOVA. Multiple comparison correction was performed using Dunn's multiple testing correction test. $P<0.05$ was considered statistically significant. Significance levels are reported as *$p<0.05$, **$p<0.01$, ***$p<0.001$, ****$p<0.0001$.

6.7 Figures

Figure 1

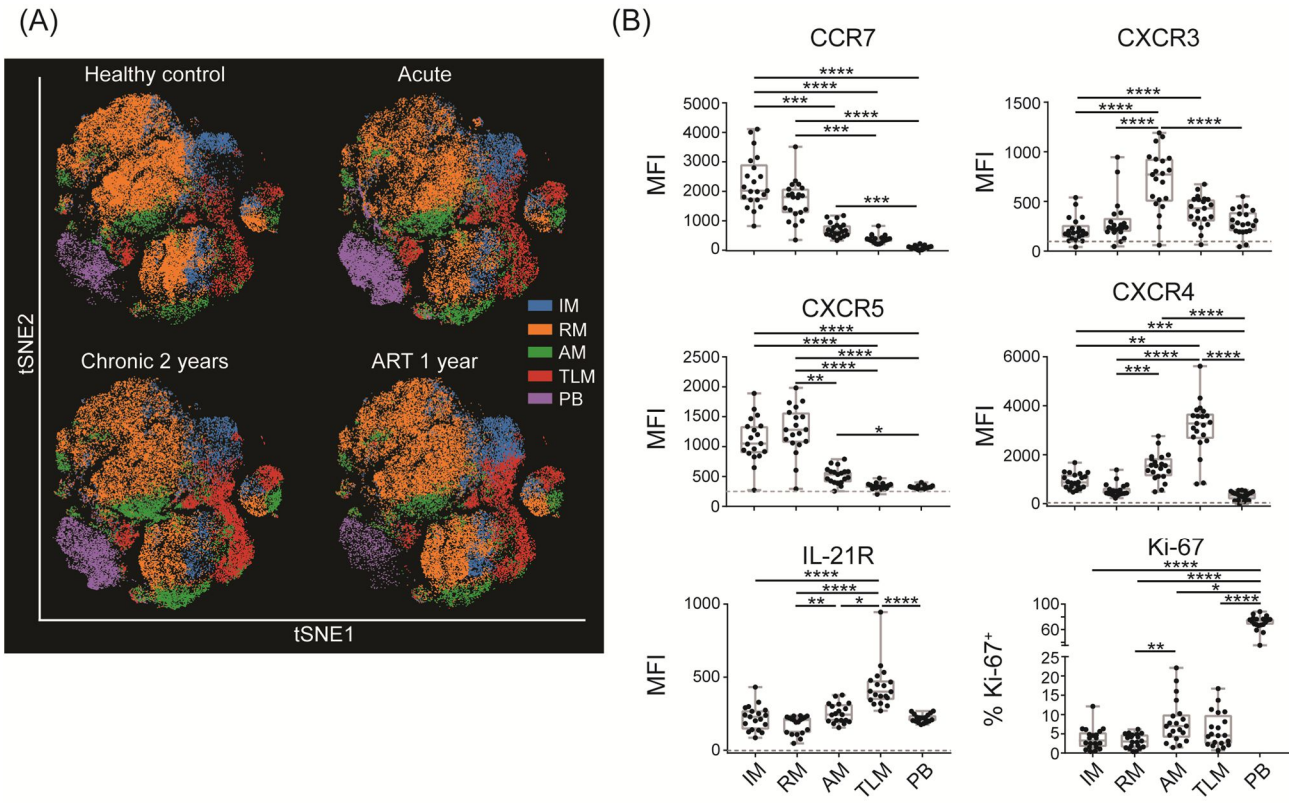

Figure 2

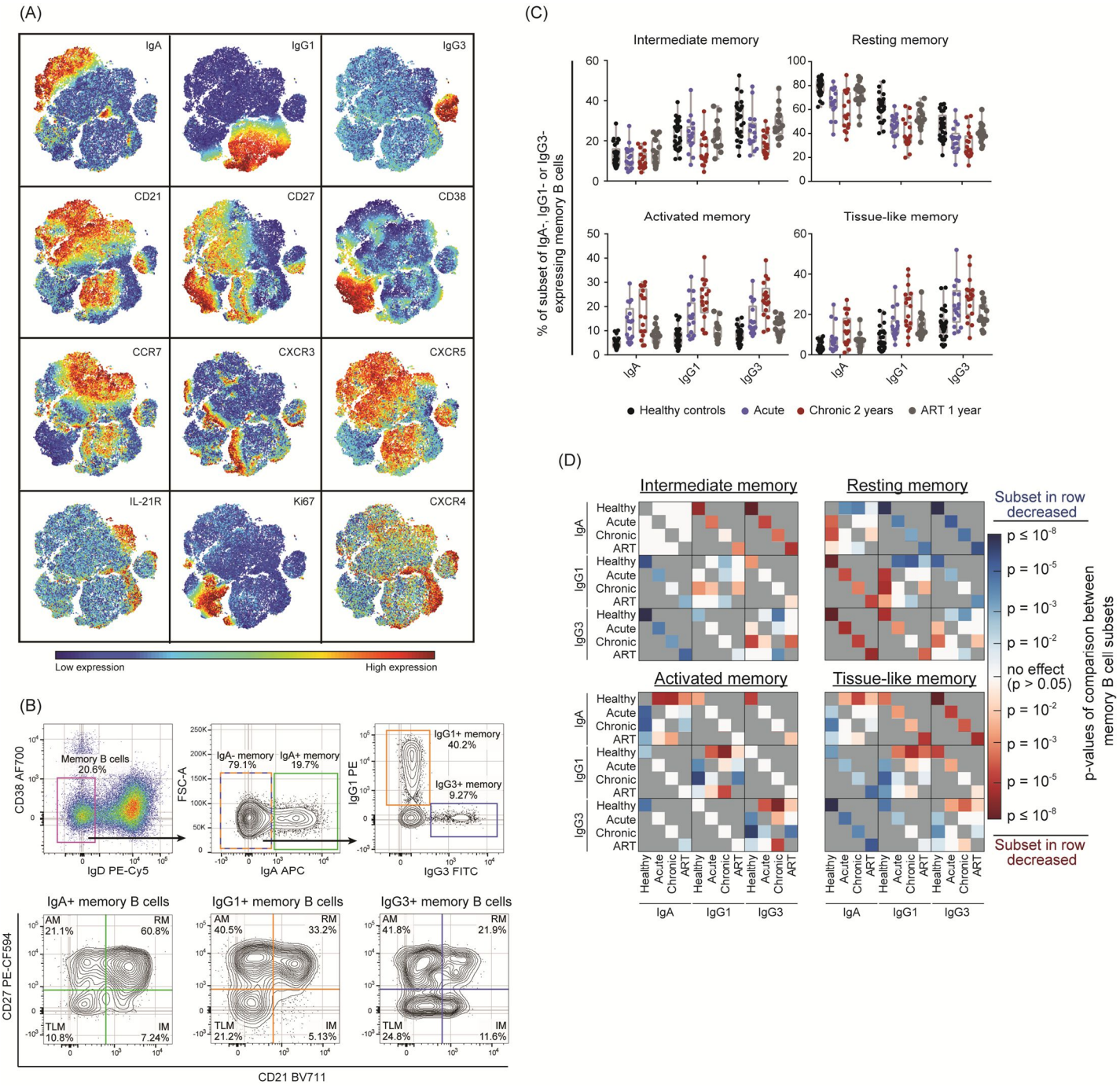
(A)
IgA
IgG1
IgG3
CD21
CD27
CD38
CCR7
CXCR3
CXCR5
IL-21R
Ki67
CXCR4
Low expression
High expression
(B)
Memory B cells 20.6%
CD38 AF700
IgD PE-Cy5
IgA- memory 79.1%
IgA+ memory 19.7%
FSC-A
IgA APC
IgG1+ memory 40.2%
IgG3+ memory 9.27%
IgG1 PE
IgG3 FITC
IgA+ memory B cells
IgG1+ memory B cells
IgG3+ memory B cells
AM 21.1%
RM 60.8%
TLM 10.8%
IM 7.24%
AM 40.5%
RM 33.2%
TLM 21.2%
IM 5.13%
AM 41.8%
RM 21.9%
TLM 24.8%
IM 11.6%
CD27 PE-CF594
CD21 BV711
(C)
Intermediate memory
Resting memory
Activated memory
Tissue-like memory
% of subset of IgA-, IgG1- or IgG3-expressing memory B cells
IgA
IgG1
IgG3
Healthy controls
Acute
Chronic 2 years
ART 1 year
(D)
Intermediate memory
Resting memory
Activated memory
Tissue-like memory
Healthy
Acute
Chronic
ART
Subset in row decreased
p ≤ 10-8
p = 10-5
p = 10-3
p = 10-2
no effect (p > 0.05)
p = 10-2
p = 10-3
p = 10-5
p ≤ 10-8
Subset in row decreased
p-values of comparison between memory B cell subsets

Figure 3

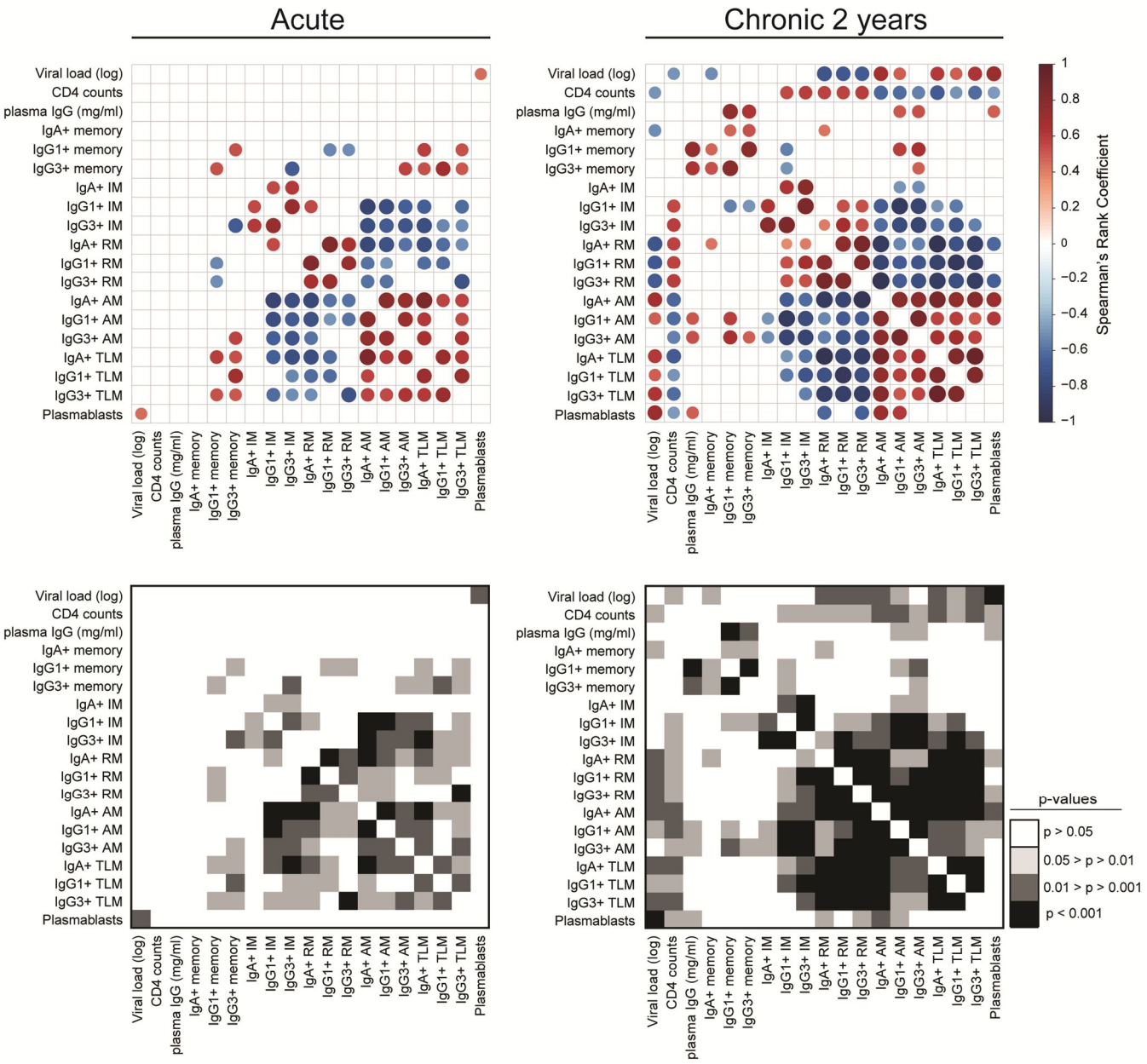
Acute
Chronic 2 years
Viral load (log)
CD4 counts
plasma IgG (mg/ml)
IgA+ memory
IgG1+ memory
IgG3+ memory
IgA+ IM
IgG1+ IM
IgG3+ IM
IgA+ RM
IgG1+ RM
IgG3+ RM
IgA+ AM
IgG1+ AM
IgG3+ AM
IgA+ TLM
IgG1+ TLM
IgG3+ TLM
Plasmablasts
Spearman's Rank Coefficient
1
0.8
0.6
0.4
0.2
0
−0.2
−0.4
−0.6
−0.8
−1
p-values
p > 0.05
0.05 > p > 0.01
0.01 > p > 0.001
p < 0.001

Figure 4

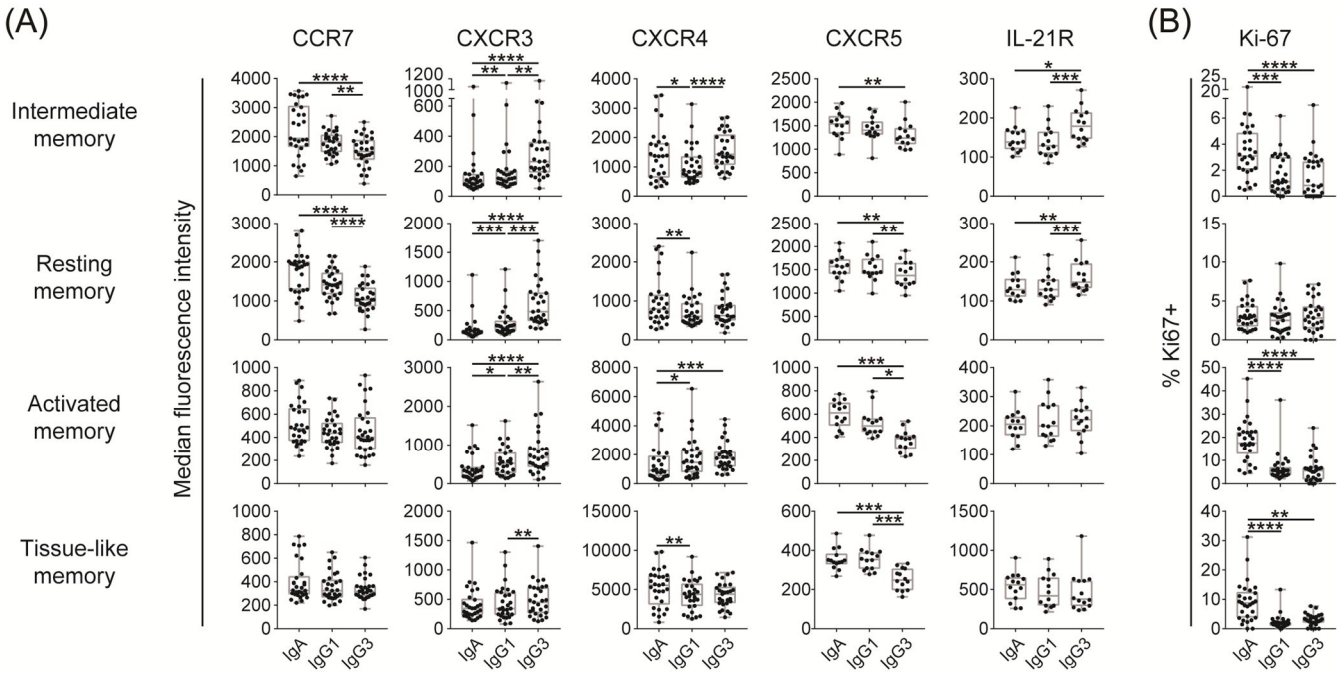
(A)
CCR7
CXCR3
CXCR4
CXCR5
IL-21R
Intermediate memory
Resting memory
Activated memory
Tissue-like memory
Median fluorescence intensity
IgA
IgG1
IgG3
(B)
Ki-67
% Ki67+

Figure 5

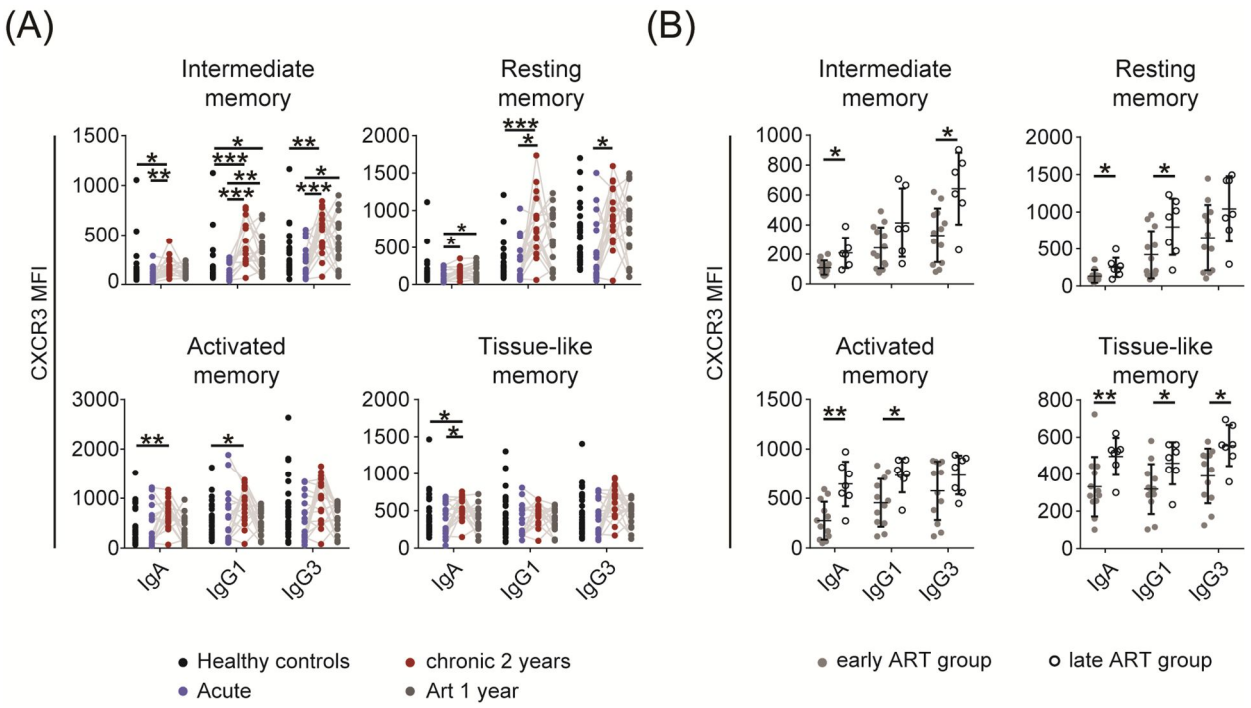
(A)
(B)
Intermediate memory
Resting memory
Activated memory
Tissue-like memory
CXCR3 MFI
IgA
IgG1
IgG3
Healthy controls
Acute
chronic 2 years
Art 1 year
early ART group
late ART group

Figure 6

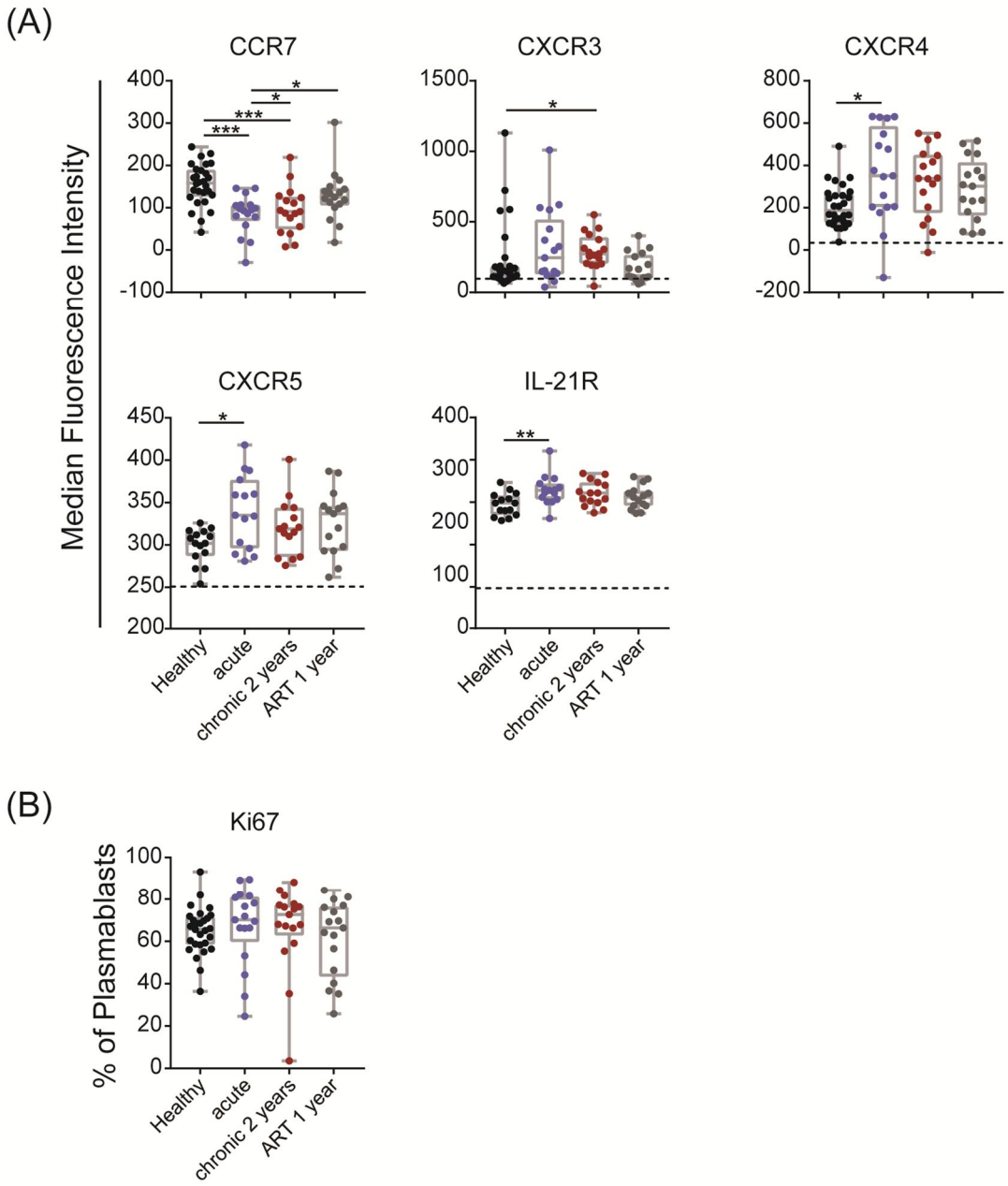
(A)
CCR7
CXCR3
CXCR4
CXCR5
IL-21R
Median Fluorescence Intensity
Healthy
acute
chronic 2 years
ART 1 year
(B)
Ki67
% of Plasmablasts

Figure 7

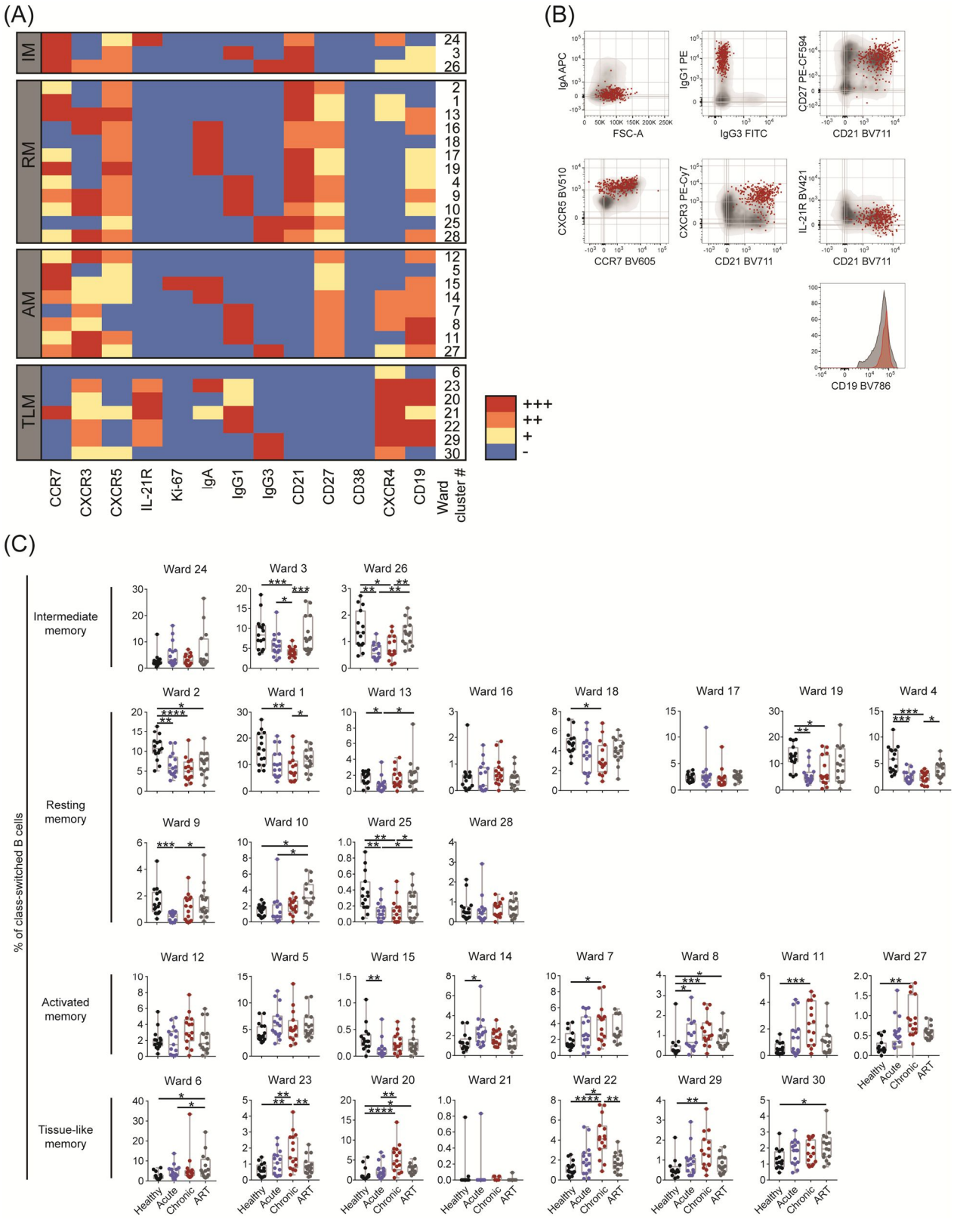
(A)
IM
RM
AM
TLM
24
3
26
2
1
13
16
18
17
19
4
9
10
25
28
12
5
15
14
7
8
11
27
6
23
20
21
22
29
30
+++
++
+
-
CCR7
CXCR3
CXCR5
IL-21R
Ki-67
IgA
IgG1
IgG3
CD21
CD27
CD38
CXCR4
CD19
Ward cluster #
(B)
IgA APC
FSC-A
IgG1 PE
IgG3 FITC
CD27 PE-CF594
CD21 BV711
CXCR5 BV510
CCR7 BV605
CXCR3 PE-Cy7
CD21 BV711
IL-21R BV421
CD21 BV711
CD19 BV786
(C)
% of class-switched B cells
Intermediate memory
Resting memory
Activated memory
Tissue-like memory
Ward 24
Ward 3
Ward 26
Ward 2
Ward 1
Ward 13
Ward 16
Ward 18
Ward 17
Ward 19
Ward 4
Ward 9
Ward 10
Ward 25
Ward 28
Ward 12
Ward 5
Ward 15
Ward 14
Ward 7
Ward 8
Ward 11
Ward 27
Ward 6
Ward 23
Ward 20
Ward 21
Ward 22
Ward 29
Ward 30
Healthy
Acute
Chronic
ART

Figure 8

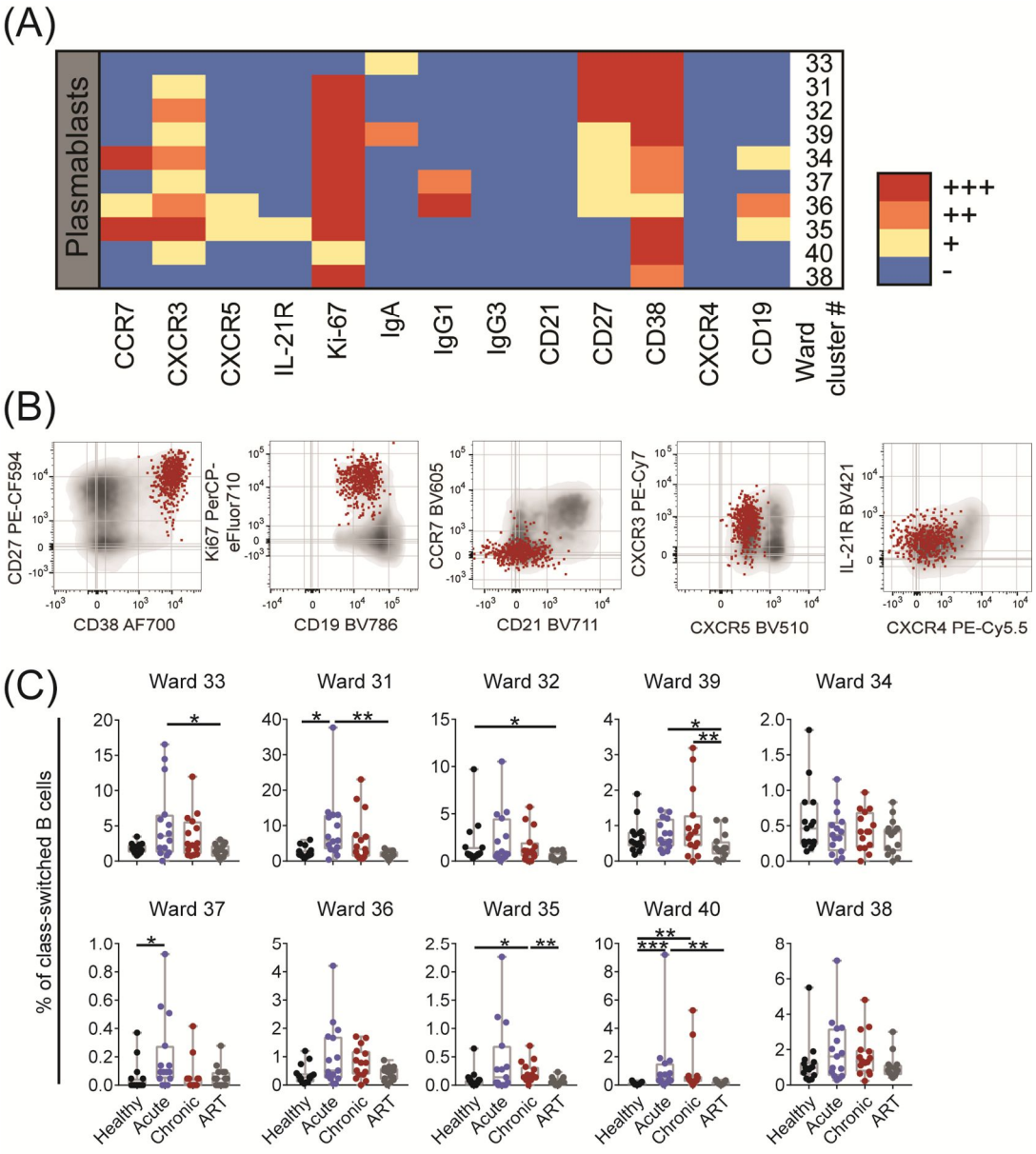
(A)
Plasmablasts
33
31
32
39
34
37
36
35
40
38
+++
++
+
-
CCR7
CXCR3
CXCR5
IL-21R
Ki-67
IgA
IgG1
IgG3
CD21
CD27
CD38
CXCR4
CD19
Ward cluster #
(B)
CD27 PE-CF594
CD38 AF700
Ki67 PerCP-eFluor710
CD19 BV786
CCR7 BV605
CD21 BV711
CXCR3 PE-Cy7
CXCR5 BV510
IL-21R BV421
CXCR4 PE-Cy5.5
(C)
% of class-switched B cells
Ward 33
Ward 31
Ward 32
Ward 39
Ward 34
Ward 37
Ward 36
Ward 35
Ward 40
Ward 38
Healthy
Acute
Chronic
ART

6.8 References

1. Dorner, T., and Radbruch, A. 2007. Antibodies and B cell memory in viral immunity. *Immunity* 27:384-392.

2. Burton, D.R. 2002. Antibodies, viruses and vaccines. *Nat Rev Immunol* 2:706-713.

3. Ball, J.K., Tarr, A.W., and McKeating, J.A. 2014. The past, present and future of neutralizing antibodies for hepatitis C virus. *Antiviral Res* 105:100-111.

4. Lanzavecchia, A., Fruhwirth, A., Perez, L., and Corti, D. 2016. Antibody-guided vaccine design: identification of protective epitopes. *Curr Opin Immunol* 41:62-67.

5. Tangye, S.G., and Tarlinton, D.M. 2009. Memory B cells: effectors of long-lived immune responses. *Eur J Immunol* 39:2065-2075.

6. Sadanand, S., Suscovich, T.J., and Alter, G. 2016. Broadly Neutralizing Antibodies Against HIV: New Insights to Inform Vaccine Design. *Annu Rev Med* 67:185-200.

7. Forthal, D., Hope, T.J., and Alter, G. 2013. New paradigms for functional HIV-specific nonneutralizing antibodies. *Curr Opin HIV AIDS* 8:393-401.

8. Buckner, C.M., Moir, S., Ho, J., Wang, W., Posada, J.G., Kardava, L., Funk, E.K., Nelson, A.K., Li, Y., Chun, T.W., et al. 2013. Characterization of plasmablasts in the blood of HIV-infected viremic individuals: evidence for nonspecific immune activation. *J Virol* 87:5800-5811.

9. Kardava, L., Moir, S., Shah, N., Wang, W., Wilson, R., Buckner, C.M., Santich, B.H., Kim, L.J., Spurlin, E.E., Nelson, A.K., et al. 2014. Abnormal B cell memory subsets dominate HIV-specific responses in infected individuals. *J Clin Invest* 124:3252-3262.

10. Malaspina, A., Moir, S., Ho, J., Wang, W., Howell, M.L., O'Shea, M.A., Roby, G.A., Rehm, C.A., Mican, J.M., Chun, T.W., et al. 2006. Appearance of immature/transitional B cells in HIV-infected individuals with advanced disease: correlation with increased IL-7. *Proc Natl Acad Sci U S A* 103:2262-2267.

11. Meffre, E., Louie, A., Bannock, J., Kim, L.J., Ho, J., Frear, C.C., Kardava, L., Wang, W., Buckner, C.M., Wang, Y., et al. 2016. Maturational characteristics of HIV-specific antibodies in viremic individuals. *JCI Insight* 1.

12. Moir, S., and Fauci, A.S. 2009. B cells in HIV infection and disease. *Nat Rev Immunol* 9:235-245.

13. Moir, S., and Fauci, A.S. 2008. Pathogenic mechanisms of B-lymphocyte dysfunction in HIV disease. *J Allergy Clin Immunol* 122:12-19; quiz 20-11.

14. Moir, S., and Fauci, A.S. 2013. Insights into B cells and HIV-specific B-cell responses in HIV-infected individuals. *Immunol Rev* 254:207-224.

15. Moir, S., and Fauci, A.S. 2014. B-cell exhaustion in HIV infection: the role of immune activation. *Curr Opin HIV AIDS* 9:472-477.

16. Moir, S., Ho, J., Malaspina, A., Wang, W., DiPoto, A.C., O'Shea, M.A., Roby, G., Kottilil, S., Arthos, J., Proschan, M.A., et al. 2008. Evidence for HIV-associated B cell exhaustion in a dysfunctional memory B cell compartment in HIV-infected viremic individuals. *J Exp Med* 205:1797-1805.

17. Moir, S., Malaspina, A., Ogwaro, K.M., Donoghue, E.T., Hallahan, C.W., Ehler, L.A., Liu, S., Adelsberger, J., Lapointe, R., Hwu, P., et al. 2001. HIV-1 induces phenotypic and functional

perturbations of B cells in chronically infected individuals. *Proc Natl Acad Sci U S A* 98:10362-10367.

18. Moir, S., Malaspina, A., Pickeral, O.K., Donoghue, E.T., Vasquez, J., Miller, N.J., Krishnan, S.R., Planta, M.A., Turney, J.F., Justement, J.S., et al. 2004. Decreased survival of B cells of HIV-viremic patients mediated by altered expression of receptors of the TNF superfamily. *J Exp Med* 200:587-599.

19. Boliar, S., Murphy, M.K., Tran, T.C., Carnathan, D.G., Armstrong, W.S., Silvestri, G., and Derdeyn, C.A. 2012. B-lymphocyte Dysfunction in Chronic HIV-1 Infection Does Not Prevent Cross-clade Neutralization Breadth. *J Virol*.

20. Pensieroso, S., Galli, L., Nozza, S., Ruffin, N., Castagna, A., Tambussi, G., Hejdeman, B., Misciagna, D., Riva, A., Malnati, M., et al. 2013. B-cell subset alterations and correlated factors in HIV-1 infection. *AIDS* 27:1209-1217.

21. Corti, D., Langedijk, J.P., Hinz, A., Seaman, M.S., Vanzetta, F., Fernandez-Rodriguez, B.M., Silacci, C., Pinna, D., Jarrossay, D., Balla-Jhagjhoorsingh, S., et al. 2010. Analysis of memory B cell responses and isolation of novel monoclonal antibodies with neutralizing breadth from HIV-1-infected individuals. *PLoS One* 5:e8805.

22. Moir, S., Buckner, C.M., Ho, J., Wang, W., Chen, J., Waldner, A.J., Posada, J.G., Kardava, L., O'Shea, M.A., Kottilil, S., et al. 2010. B cells in early and chronic HIV infection: evidence for preservation of immune function associated with early initiation of antiretroviral therapy. *Blood*.

23. Chang, C.C., Crane, M., Zhou, J., Mina, M., Post, J.J., Cameron, B.A., Lloyd, A.R., Jaworowski, A., French, M.A., and Lewin, S.R. 2013. HIV and co-infections. *Immunol Rev* 254:114-142.

24. Ferreira, C.B., Merino-Mansilla, A., Llano, A., Perez, I., Crespo, I., Llinas, L., Garcia, F., Gatell, J.M., Yuste, E., and Sanchez-Merino, V. 2013. Evolution of Broadly Cross-Reactive HIV-1-Neutralizing Activity: Therapy-Associated Decline, Positive Association with Detectable Viremia, and Partial Restoration of B-Cell Subpopulations. *Journal of Virology* 87:12227-12236.

25. Haynes, B.F., Moody, M.A., Liao, H.X., Verkoczy, L., and Tomaras, G.D. 2011. B cell responses to HIV-1 infection and vaccination: pathways to preventing infection. *Trends Mol Med* 17:108-116.

26. Titanji, K., De Milito, A., Cagigi, A., Thorstensson, R., Grutzmeier, S., Atlas, A., Hejdeman, B., Kroon, F.P., Lopalco, L., Nilsson, A., et al. 2006. Loss of memory B cells impairs maintenance of long-term serologic memory during HIV-1 infection. *Blood* 108:1580-1587.

27. Wheatley, A.K., Kristensen, A.B., Lay, W.N., and Kent, S.J. 2016. HIV-dependent depletion of influenza-specific memory B cells impacts B cell responsiveness to seasonal influenza immunisation. *Sci Rep* 6:26478.

28. MacLennan, C.A., Gilchrist, J.J., Gordon, M.A., Cunningham, A.F., Cobbold, M., Goodall, M., Kingsley, R.A., van Oosterhout, J.J., Msefula, C.L., Mandala, W.L., et al. 2010. Dysregulated humoral immunity to nontyphoidal Salmonella in HIV-infected African adults. *Science* 328:508-512.

29. Kerneis, S., Launay, O., Turbelin, C., Batteux, F., Hanslik, T., and Boelle, P.Y. 2014. Long-term immune responses to vaccination in HIV-infected patients: a systematic review and meta-analysis. *Clin Infect Dis* 58:1130-1139.

30. Malaspina, A., Moir, S., Orsega, S.M., Vasquez, J., Miller, N.J., Donoghue, E.T., Kottilil, S., Gezmu, M., Follmann, D., Vodeiko, G.M., et al. 2005. Compromised B cell responses to influenza vaccination in HIV-infected individuals. *J Infect Dis* 191:1442-1450.

31. Rusert, P., Kouyos, R.D., Kadelka, C., Ebner, H., Schanz, M., Huber, M., Braun, D.L., Hoze, N., Scherrer, A., Magnus, C., et al. 2016. Determinants of HIV-1 broadly neutralizing antibody induction. *Nat Med* 22:1260-1267.

32. Simek, M.D., Rida, W., Priddy, F.H., Pung, P., Carrow, E., Laufer, D.S., Lehrman, J.K., Boaz, M., Tarragona-Fiol, T., Miiro, G., et al. 2009. Human immunodeficiency virus type 1 elite neutralizers: individuals with broad and potent neutralizing activity identified by using a high-throughput neutralization assay together with an analytical selection algorithm. *J Virol* 83:7337-7348.

33. Doria-Rose, N.A., Klein, R.M., Daniels, M.G., O'Dell, S., Nason, M., Lapedes, A., Bhattacharya, T., Migueles, S.A., Wyatt, R.T., Korber, B.T., et al. 2010. Breadth of human immunodeficiency virus-specific neutralizing activity in sera: clustering analysis and association with clinical variables. *J Virol* 84:1631-1636.

34. Burton, D.R., and Hangartner, L. 2016. Broadly Neutralizing Antibodies to HIV and Their Role in Vaccine Design. *Annu Rev Immunol* 34:635-659.

35. Haynes, B.F., Kelsoe, G., Harrison, S.C., and Kepler, T.B. 2012. B-cell-lineage immunogen design in vaccine development with HIV-1 as a case study. *Nat Biotechnol* 30:423-433.

36. Mascola, J.R., and Haynes, B.F. 2013. HIV-1 neutralizing antibodies: understanding nature's pathways. *Immunol Rev* 254:225-244.

37. McElrath, M.J., and Haynes, B.F. 2010. Induction of immunity to human immunodeficiency virus type-1 by vaccination. *Immunity* 33:542-554.

38. Derdeyn, C.A., Moore, P.L., and Morris, L. 2014. Development of broadly neutralizing antibodies from autologous neutralizing antibody responses in HIV infection. *Curr Opin HIV AIDS* 9:210-216.

39. de Bree, G.J., and Lynch, R.M. 2016. B cells in HIV pathogenesis. *Curr Opin Infect Dis* 29:23-30.

40. Portugal, S., Tipton, C.M., Sohn, H., Kone, Y., Wang, J., Li, S., Skinner, J., Virtaneva, K., Sturdevant, D.E., Porcella, S.F., et al. 2015. Malaria-associated atypical memory B cells exhibit markedly reduced B cell receptor signaling and effector function. *Elife* 4.

41. Nair, N., Newell, E.W., Vollmers, C., Quake, S.R., Morton, J.M., Davis, M.M., He, X.S., and Greenberg, H.B. 2016. High-dimensional immune profiling of total and rotavirus VP6-specific intestinal and circulating B cells by mass cytometry. *Mucosal Immunol* 9:68-82.

42. Berkowska, M.A., Driessen, G.J., Bikos, V., Grosserichter-Wagener, C., Stamatopoulos, K., Cerutti, A., He, B., Biermann, K., Lange, J.F., van der Burg, M., et al. 2011. Human memory B cells originate from three distinct germinal center-dependent and -independent maturation pathways. *Blood* 118:2150-2158.

43. Kaminski, D.A., Wei, C., Qian, Y., Rosenberg, A.F., and Sanz, I. 2012. Advances in human B cell phenotypic profiling. *Front Immunol* 3:302.

44. Sanz, I., Wei, C., Lee, F.E., and Anolik, J. 2008. Phenotypic and functional heterogeneity of human memory B cells. *Semin Immunol* 20:67-82.

45. Wei, C., Jenks, S., and Sanz, I. 2015. Polychromatic flow cytometry in evaluating rheumatic disease patients. *Arthritis Res Ther* 17:46.

46. Pejoski, D., Tchitchek, N., Rodriguez Pozo, A., Elhmouzi-Younes, J., Yousfi-Bogniaho, R., Rogez-Kreuz, C., Clayette, P., Dereuddre-Bosquet, N., Levy, Y., Cosma, A., et al. 2016. Identification of Vaccine-Altered Circulating B Cell Phenotypes Using Mass Cytometry and a Two-Step Clustering Analysis. *J Immunol* 196:4814-4831.

47. Anolik, J.H., Looney, R.J., Lund, F.E., Randall, T.D., and Sanz, I. 2009. Insights into the heterogeneity of human B cells: diverse functions, roles in autoimmunity, and use as therapeutic targets. *Immunologic Research* 45:144-158.

48. De Milito, A., Nilsson, A., Titanji, K., Thorstensson, R., Reizenstein, E., Narita, M., Grutzmeier, S., Sonnerborg, A., and Chiodi, F. 2004. Mechanisms of hypergammaglobulinemia and impaired antigen-specific humoral immunity in HIV-1 infection. *Blood* 103:2180-2186.

49. Haas, A., Zimmermann, K., and Oxenius, A. 2011. Antigen-dependent and -independent mechanisms of T and B cell hyperactivation during chronic HIV-1 infection. *J Virol* 85:12102-12113.

50. Nagase, H., Agematsu, K., Kitano, K., Takamoto, M., Okubo, Y., Komiyama, A., and Sugane, K. 2001. Mechanism of hypergammaglobulinemia by HIV infection: circulating memory B-cell reduction with plasmacytosis. *Clin Immunol* 100:250-259.

51. Lane, H.C., Masur, H., Edgar, L.C., Whalen, G., Rook, A.H., and Fauci, A.S. 1983. Abnormalities of B-cell activation and immunoregulation in patients with the acquired immunodeficiency syndrome. *N Engl J Med* 309:453-458.

52. Morris, L., Binley, J.M., Clas, B.A., Bonhoeffer, S., Astill, T.P., Kost, R., Hurley, A., Cao, Y., Markowitz, M., Ho, D.D., et al. 1998. HIV-1 antigen-specific and -nonspecific B cell responses are sensitive to combination antiretroviral therapy. *J Exp Med* 188:233-245.

53. Shirai, A., Cosentino, M., Leitmanklinman, S.F., and Klinman, D.M. 1992. Human-Immunodeficiency-Virus Infection Induces Both Polyclonal and Virus-Specific B-Cell Activation. *Journal of Clinical Investigation* 89:561-566.

54. Fink, K. 2012. Origin and Function of Circulating Plasmablasts during Acute Viral Infections. *Front Immunol* 3:78.

55. Caraux, A., Klein, B., Paiva, B., Bret, C., Schmitz, A., Fuhler, G.M., Bos, N.A., Johnsen, H.E., Orfao, A., Perez-Andres, M., et al. 2010. Circulating human B and plasma cells. Age-associated changes in counts and detailed characterization of circulating normal CD138- and CD138+ plasma cells. *Haematologica* 95:1016-1020.

56. Tarlton, N.J., Green, C.M., Lazarus, N.H., Rott, L., Wong, A.P., Abramson, O.N., Bremer, M., Butcher, E.C., and Abramson, T. 2012. Plasmablast frequency and trafficking receptor expression are altered in pediatric ulcerative colitis. *Inflamm Bowel Dis* 18:2381-2391.

57. Flint, S.M., Gibson, A., Lucas, G., Nandigam, R., Taylor, L., Provan, D., Newland, A.C., Savage, C.O., and Henderson, R.B. 2016. A distinct plasmablast and naive B-cell phenotype in primary immune thrombocytopenia. *Haematologica* 101:698-706.

58. Hong, S., Lee, H.W., Chang, D.Y., You, S., Kim, J., Park, J.Y., Ahn, S.H., Yong, D., Han, K.H., Yoo, O.J., et al. 2013. Antibody-secreting cells with a phenotype of Ki-67low, CD138high, CD31high, and CD38high secrete nonspecific IgM during primary hepatitis A virus infection. *J Immunol* 191:127-134.

59. Odendahl, M., Mei, H., Hoyer, B.F., Jacobi, A.M., Hansen, A., Muehlinghaus, G., Berek, C., Hiepe, F., Manz, R., Radbruch, A., et al. 2005. Generation of migratory antigen-specific plasma blasts and mobilization of resident plasma cells in a secondary immune response. *Blood* 105:1614-1621.

60. Montezuma-Rusca, J.M., Moir, S., Kardava, L., Buckner, C.M., Louie, A., Kim, L.J., Santich, B.H., Wang, W., Fankuchen, O.R., Diaz, G., et al. 2015. Bone marrow plasma cells are a primary source of serum HIV-1-specific antibodies in chronically infected individuals. *J Immunol* 194:2561-2568.

61. Crum-Cianflone, N.F., and Wallace, M.R. 2014. Vaccination in HIV-infected adults. *AIDS Patient Care STDS* 28:397-410.

62. Tebas, P., Frank, I., Lewis, M., Quinn, J., Zifchak, L., Thomas, A., Kenney, T., Kappes, R., Wagner, W., Maffei, K., et al. 2010. Poor immunogenicity of the H1N1 2009 vaccine in well controlled HIV-infected individuals. *AIDS* 24:2187-2192.

63. Kroon, F.P., van Dissel, J.T., Rijkers, G.T., Labadie, J., and van Furth, R. 1997. Antibody response to Haemophilus influenzae type b vaccine in relation to the number of CD4+ T lymphocytes in adults infected with human immunodeficiency virus. *Clin Infect Dis* 25:600-606.

64. Kroon, F.P., Vandissel, J.T., Dejong, J.C., and Vanfurth, R. 1994. Antibody-Response to Influenza, Tetanus and Pneumococcal Vaccines in Hiv-Seropositive Individuals in Relation to the Number of Cd4+ Lymphocytes. *AIDS* 8:469-476.

65. Nuccitelli, A., Rinaudo, C.D., and Maione, D. 2015. Group B Streptococcus vaccine: state of the art. *Ther Adv Vaccines* 3:76-90.

66. Sadlier, C., O'Dea, S., Bennett, K., Dunne, J., Conlon, N., and Bergin, C. 2016. Immunological efficacy of pneumococcal vaccine strategies in HIV-infected adults: a randomized clinical trial. *Sci Rep* 6:32076.

67. Zhang, L., Li, Z., Wan, Z., Kilby, A., Kilby, J.M., and Jiang, W. 2015. Humoral immune responses to Streptococcus pneumoniae in the setting of HIV-1 infection. *Vaccine* 33:4430-4436.

68. Tongren, J.E., Drakeley, C.J., McDonald, S.L., Reyburn, H.G., Manjurano, A., Nkya, W.M., Lemnge, M.M., Gowda, C.D., Todd, J.E., Corran, P.H., et al. 2006. Target antigen, age, and duration of antigen exposure independently regulate immunoglobulin G subclass switching in malaria. *Infect Immun* 74:257-264.

69. Roussilhon, C., Oeuvray, C., Muller-Graf, C., Tall, A., Rogier, C., Trape, J.F., Theisen, M., Balde, A., Perignon, J.L., and Druilhe, P. 2007. Long-term clinical protection from falciparum malaria is strongly associated with IgG3 antibodies to merozoite surface protein 3. *PLoS Med* 4:e320.

70. Tomaras, G.D., and Haynes, B.F. 2009. HIV-1-specific antibody responses during acute and chronic HIV-1 infection. *Curr Opin HIV AIDS* 4:373-379.

71. Yates, N.L., Lucas, J.T., Nolen, T.L., Vandergrift, N.A., Soderberg, K.A., Seaton, K.E., Denny, T.N., Haynes, B.F., Cohen, M.S., and Tomaras, G.D. 2011. Multiple HIV-1-specific IgG3 responses decline during acute HIV-1: implications for detection of incident HIV infection. *AIDS* 25:2089-2097.

72. Huang, J., Ofek, G., Laub, L., Louder, M.K., Doria-Rose, N.A., Longo, N.S., Imamichi, H., Bailer, R.T., Chakrabarti, B., Sharma, S.K., et al. 2012. Broad and potent neutralization of HIV-1 by a gp41-specific human antibody. *Nature* 491:406-412.

73. Verkoczy, L., Chen, Y., Bouton-Verville, H., Zhang, J., Diaz, M., Hutchinson, J., Ouyang, Y.B., Alam, S.M., Holl, T.M., Hwang, K.K., et al. 2011. Rescue of HIV-1 broad neutralizing antibody-expressing B cells in 2F5 VH x VL knockin mice reveals multiple tolerance controls. *Journal of Immunology* 187:3785-3797.

74. Verkoczy, L., Diaz, M., Holl, T.M., Ouyang, Y.B., Bouton-Verville, H., Alam, S.M., Liao, H.X., Kelsoe, G., and Haynes, B.F. 2010. Autoreactivity in an HIV-1 broadly reactive neutralizing antibody variable region heavy chain induces immunologic tolerance. *Proc Natl Acad Sci U S A* 107:181-186.

75. Verkoczy, L., Kelsoe, G., and Haynes, B.F. 2014. HIV-1 envelope gp41 broadly neutralizing antibodies: hurdles for vaccine development. *PLoS Pathog* 10:e1004073.

76. Verkoczy, L., Kelsoe, G., Moody, M.A., and Haynes, B.F. 2011. Role of immune mechanisms in induction of HIV-1 broadly neutralizing antibodies. *Curr Opin Immunol*.

77. Haynes, B.F., Fleming, J., St Clair, E.W., Katinger, H., Stiegler, G., Kunert, R., Robinson, J., Scearce, R.M., Plonk, K., Staats, H.F., et al. 2005. Cardiolipin polyspecific autoreactivity in two broadly neutralizing HIV-1 antibodies. *Science* 308:1906-1908.

78. Yang, G., Holl, T.M., Liu, Y., Li, Y., Lu, X., Nicely, N.I., Kepler, T.B., Alam, S.M., Liao, H.X., Cain, D.W., et al. 2013. Identification of autoantigens recognized by the 2F5 and 4E10 broadly neutralizing HIV-1 antibodies. *J Exp Med* 210:241-256.

79. Gray, E.S., Madiga, M.C., Moore, P.L., Mlisana, K., Abdool Karim, S.S., Binley, J.M., Shaw, G.M., Mascola, J.R., and Morris, L. 2009. Broad neutralization of human immunodeficiency virus type 1 mediated by plasma antibodies against the gp41 membrane proximal external region. *J Virol* 83:11265-11274.

80. Banerjee, K., Klasse, P.J., Sanders, R.W., Pereyra, F., Michael, E., Lu, M., Walker, B.D., and Moore, J.P. 2010. IgG subclass profiles in infected HIV type 1 controllers and chronic progressors and in uninfected recipients of Env vaccines. *AIDS Res Hum Retroviruses* 26:445-458.

81. Hauser, A.E., Debes, G.F., Arce, S., Cassese, G., Hamann, A., Radbruch, A., and Manz, R.A. 2002. Chemotactic responsiveness toward ligands for CXCR3 and CXCR4 is regulated on plasma blasts during the time course of a memory immune response. *Journal of Immunology* 169:1277-1282.

82. Muehlinghaus, G., Cigliano, L., Huehn, S., Peddinghaus, A., Leyendeckers, H., Hauser, A.E., Hiepe, F., Radbruch, A., Arce, S., and Manz, R.A. 2005. Regulation of CXCR3 and CXCR4 expression during terminal differentiation of memory B cells into plasma cells. *Blood* 105:3965-3971.

83. Llinas, L., Lazaro, A., de Salort, J., Matesanz-Isabel, J., Sintes, J., and Engel, P. 2011. Expression profiles of novel cell surface molecules on B-cell subsets and plasma cells as analyzed by flow cytometry. *Immunology Letters* 134:113-121.

84. Horns, F., Vollmers, C., Croote, D., Mackey, S.F., Swan, G.E., Dekker, C.L., Davis, M.M., and Quake, S.R. 2016. Lineage tracing of human B cells reveals the in vivo landscape of human antibody class switching. *Elife* 5.

85. Govender, S., Otwombe, K., Essien, T., Panchia, R., de Bruyn, G., Mohapi, L., Gray, G., and Martinson, N. 2014. CD4 Counts and Viral Loads of Newly Diagnosed HIV-Infected Individuals: Implications for Treatment as Prevention. *Plos One* 9.

86. Fecteau, J.F., Cote, G., and Neron, S. 2006. A new memory CD27-IgG+ B cell population in peripheral blood expressing VH genes with low frequency of somatic mutation. *J Immunol* 177:3728-3736.

87. Noelle, R.J., Snow, E.C., Uhr, J.W., and Vitetta, E.S. 1983. Activation of Antigen-Specific B-Cells - Role of T-Cells, Cytokines, and Antigen in Induction of Growth and Differentiation. *Proceedings of the National Academy of Sciences of the United States of America-Biological Sciences* 80:6628-6631.

88. Berkowska, M.A., Schickel, J.N., Grosserichter-Wagener, C., de Ridder, D., Ng, Y.S., van Dongen, J.J., Meffre, E., and van Zelm, M.C. 2015. Circulating Human CD27-IgA+ Memory B Cells Recognize Bacteria with Polyreactive Igs. *J Immunol* 195:1417-1426.

89. Groom, J.R., and Luster, A.D. 2011. CXCR3 ligands: redundant, collaborative and antagonistic functions. *Immunol Cell Biol* 89:207-215.

90. Nutt, S.L., Hodgkin, P.D., Tarlinton, D.M., and Corcoran, L.M. 2015. The generation of antibody-secreting plasma cells. *Nat Rev Immunol* 15:160-171.

91. Toapanta, F.R., Simon, J.K., Barry, E.M., Pasetti, M.F., Levine, M.M., Kotloff, K.L., and Sztein, M.B. 2014. Gut-Homing Conventional Plasmablasts and CD27(-) Plasmablasts Elicited after a Short Time of Exposure to an Oral Live-Attenuated Shigella Vaccine Candidate in Humans. *Front Immunol* 5:374.

92. Hansmann, L., Blum, L., Ju, C.H., Liedtke, M., Robinson, W.H., and Davis, M.M. 2015. Mass cytometry analysis shows that a novel memory phenotype B cell is expanded in multiple myeloma. *Cancer Immunol Res* 3:650-660.

93. Ruffin, N., Lantto, R., Pensieroso, S., Sammicheli, S., Hejdeman, B., Rethi, B., and Chiodi, F. 2012. Immune activation and increased IL-21R expression are associated with the loss of memory B cells during HIV-1 infection. *J Intern Med* 272:492-503.

94. Buchacher, A., Predl, R., Strutzenberger, K., Steinfellner, W., Trkola, A., Purtscher, M., Gruber, G., Tauer, C., Steindl, F., Jungbauer, A., et al. 1994. Generation of human monoclonal antibodies against HIV-1 proteins; electrofusion and Epstein-Barr virus transformation for peripheral blood lymphocyte immortalization. *AIDS Res Hum Retroviruses* 10:359-369.

95. Huang, J., Ofek, G., Laub, L., Louder, M.K., Doria-Rose, N.A., Longo, N.S., Imamichi, H., Bailer, R.T., Chakrabarti, B., Sharma, S.K., et al. 2012. Broad and potent neutralization of HIV-1 by a gp41-specific human antibody. *Nature* 491:406-412.

96. Wei, C., Anolik, J., Cappione, A., Zheng, B., Pugh-Bernard, A., Brooks, J., Lee, E.H., Milner, E.C., and Sanz, I. 2007. A new population of cells lacking expression of CD27 represents a notable component of the B cell memory compartment in systemic lupus erythematosus. *J Immunol* 178:6624-6633.

97. Budeus, B., Schweigle de Reynoso, S., Przekopowitz, M., Hoffmann, D., Seifert, M., and Kuppers, R. 2015. Complexity of the human memory B-cell compartment is determined by the versatility of clonal diversification in germinal centers. *Proc Natl Acad Sci U S A* 112:E5281-5289.

98. Obukhanych, T.V., and Nussenzweig, M.C. 2006. T-independent type II immune responses generate memory B cells. *J Exp Med* 203:305-310.

99. Sciaranghella, G., Tong, N., Mahan, A.E., Suscovich, T.J., and Alter, G. 2013. Decoupling activation and exhaustion of B cells in spontaneous controllers of HIV infection. *AIDS* 27:175-180.

100. Banga, R., Procopio, F.A., Noto, A., Pollakis, G., Cavassini, M., Ohmiti, K., Corpataux, J.M., de Leval, L., Pantaleo, G., and Perreau, M. 2016. PD-1(+) and follicular helper T cells are responsible for persistent HIV-1 transcription in treated aviremic individuals. *Nat Med* 22:754-761.

101. Pallikkuth, S., Sharkey, M., Babic, D.Z., Gupta, S., Stone, G.W., Fischl, M.A., Stevenson, M., and Pahwa, S. 2015. Peripheral T Follicular Helper Cells Are the Major HIV Reservoir within Central Memory CD4 T Cells in Peripheral Blood from Chronically HIV-Infected Individuals on Combination Antiretroviral Therapy. *J Virol* 90:2718-2728.

102. Lorenzo-Redondo, R., Fryer, H.R., Bedford, T., Kim, E.Y., Archer, J., Kosakovsky Pond, S.L., Chung, Y.S., Penugonda, S., Chipman, J.G., Fletcher, C.V., et al. 2016. Persistent HIV-1 replication maintains the tissue reservoir during therapy. *Nature* 530:51-56.

103. Ettinger, R., Kuchen, S., and Lipsky, P.E. 2008. The role of IL-21 in regulating B-cell function in health and disease. *Immunol Rev* 223:60-86.

104. Ettinger, R., Sims, G.P., Fairhurst, A.M., Robbins, R., da Silva, Y.S., Spolski, R., Leonard, W.J., and Lipsky, P.E. 2005. IL-21 induces differentiation of human naive and memory B cells into antibody-secreting plasma cells. *J Immunol* 175:7867-7879.

105. Good, K.L., Bryant, V.L., and Tangye, S.G. 2006. Kinetics of human B cell behavior and amplification of proliferative responses following stimulation with IL-21. *J Immunol* 177:5236-5247.

106. Kunkel, E.J., and Butcher, E.C. 2003. Plasma-cell homing. *Nat Rev Immunol* 3:822-829.

107. McMichael, A.J., Borrow, P., Tomaras, G.D., Goonetilleke, N., and Haynes, B.F. 2010. The immune response during acute HIV-1 infection: clues for vaccine development. *Nat Rev Immunol* 10:11-23.

108. Stacey, A.R., Norris, P.J., Qin, L., Haygreen, E.A., Taylor, E., Heitman, J., Lebedeva, M., DeCamp, A., Li, D., Grove, D., et al. 2009. Induction of a striking systemic cytokine cascade prior to peak viremia in acute human immunodeficiency virus type 1 infection, in contrast to more modest and delayed responses in acute hepatitis B and C virus infections. *J Virol* 83:3719-3733.

109. Rieder, P., Joos, B., Scherrer, A.U., Kuster, H., Braun, D., Grube, C., Niederost, B., Leemann, C., Gianella, S., Metzner, K.J., et al. 2011. Characterization of human immunodeficiency virus type 1 (HIV-1) diversity and tropism in 145 patients with primary HIV-1 infection. *Clin Infect Dis* 53:1271-1279.

110. Roederer, M., Quaye, L., Mangino, M., Beddall, M.H., Mahnke, Y., Chattopadhyay, P., Tosi, I., Napolitano, L., Terranova Barberio, M., Menni, C., et al. 2015. The genetic architecture of the human immune system: a bioresource for autoimmunity and disease pathogenesis. *Cell* 161:387-403.

111. Qiu, P., Simonds, E.F., Bendall, S.C., Gibbs, K.D., Jr., Bruggner, R.V., Linderman, M.D., Sachs, K., Nolan, G.P., and Plevritis, S.K. 2011. Extracting a cellular hierarchy from high-dimensional cytometry data with SPADE. *Nat Biotechnol* 29:886-891.

112. Anchang, B., Hart, T.D., Bendall, S.C., Qiu, P., Bjornson, Z., Linderman, M., Nolan, G.P., and Plevritis, S.K. 2016. Visualization and cellular hierarchy inference of single-cell data using SPADE. *Nat Protoc* 11:1264-1279.

113. Amir, E.D., Davis, K.L., Tadmor, M.D., Simonds, E.F., Levine, J.H., Bendall, S.C., Shenfeld, D.K., Krishnaswamy, S., Nolan, G.P., and Pe'er, D. 2013. viSNE enables visualization of high dimensional single-cell data and reveals phenotypic heterogeneity of leukemia. *Nature Biotechnology* 31:545-+.

114. Ward, J.H. 1963. Hierarchical Grouping to Optimize an Objective Function. *Journal of the American Statistical Association* 58:236-&.

115. Trkola, A., Kuster, H., Leemann, C., Oxenius, A., Fagard, C., Furrer, H., Battegay, M., Vernazza, P., Bernasconi, E., Weber, R., et al. 2004. Humoral immunity to HIV-1: kinetics of antibody responses in chronic infection reflects capacity of immune system to improve viral set point. *Blood* 104:1784-1792.

6.9 Supplementary table and figure legends

Supplementary table 1: Characteristics of the early and late treatment groups

Summary of the clinical characteristics of the HIV-1 infected patients for the time points analyzed are shown. Patients are separated into the study groups based on initiation of ART early ART and late ART group. [a]Comparison was done between early ART group (weeks off ART) and late ART group (weeks of active replication) to compare the continuous period of active replication before chronic 2 year sample was collected. Differences between the study groups were calculated with Mann-Whitney test and considered statistically significant with a p value <0.05.

Supplementary table 2: Patient characteristics

Characteristics of the individual patients are shown and in addition the samples used for the different assays are depicted.

Supplementary figure 1: The majority of plasmablasts express high levels of the proliferation marker Ki-67.

Left plot shows manual gating of IgD^+ B cells (grey) encompassing marginal zone and naïve B cells, memory B cells (blue) and plasmablasts (red). Analysis of Ki-67 expression on these subsets is shown as overlaid histogram. The FMO control gated on plasmablasts is shown in black.

Supplementary figure 2: t-SNE plots with phenotypic marker expression levels

t-SNE plots from the concatenated samples of healthy donors (n=15) and HIV-1 infected patients (n=15) at the acute phase and after 1 year of ART are shown for the phenotypic marker IgA, IgG1, IgG3, CD21, CD27, CD38, CCR7, CXCR3, CXCR5, IL-21R, Ki-67 and CXCR4. Expression levels of arcsinh-transformed MFI values are shown as a color gradient ranging from blue to red color highlighting no to highest expression, respectively.

Supplementary figure 3: Frequency of isotype-expressing memory B cells

(A) Frequency of IgA (black dots), IgG1 (blue dots) and IgG3 (dark red dots) expressing B cells are shown for healthy controls (n=29) and HIV-1 infected individuals (n=17) at acute and 2 years of chronic phase and after 1 year of ART. Comparison of IgA, IgG1 and IgG3 expressing B cells was done using paired non-parametric Friedman one-way ANOVA. Multiple comparison correction was performed using Dunn's multiple testing correction test. **(B)** Comparison of IgA^+, $IgG1^+$ and $IgG3^+$ memory B cells between healthy (n=29) and HIV-1 infected patients (n=17) at acute and chronic phase and after 1 year of ART was performed. Comparison of B cell subsets between healthy controls and HIV-1 infected patients was done using unpaired non-parametric Kruskal-Wallis one-way ANOVA and comparison between different time points of HIV-1 infected patients using paired non-parametric Friedman one-way ANOVA. Multiple comparison correction was performed using Dunn's multiple testing correction test. $P<0.05$ was considered statistically significant. Significance levels are reported as *p<0.05, **p<0.01, ***p<0.001, ****p<0.0001.

Supplementary figure 4: Comparison of memory B cell subsets of early and late ART group.

Comparison of memory B cell subsets defined by CD21/CD27 expression among IgA, IgG1 and IgG3 expressing memory B cells between early (n=11; grey dots) and late (n=8; black circles) ART group after 1 year of ART is shown. Mann-Whitney test was used. $P<0.05$ was considered statistically significant.

Supplementary figure 5: SPADE clustering analysis to reveal phenotypic diversity of memory B cells in healthy donors and HIV-1 infection

(A) SPADE trees were generated from class-switched B cells ($CD19^+IgD^-CD38^{low}$) of healthy controls (n=15) and HIV-infected patients (n=15) at acute and chronic stage and after 1 year of ART. Shown is the SPADE tree from all 15 HIV-1 infected patients after 2 years of chronic infection concatenated. Cluster size corresponds to the frequency of cells in the cluster. Regions of the tree consisting of IgA-, IgG1-, IgG3- and other isotype-expressing memory B cells and plasmablasts are highlighted as green, red, blue and yellow areas, respectively. B cells expressing a different isotype are highlighted in the purple area. The expression intensities as arcsinh-transformed MFI values for markers **(B)** not included (CD19 and CXCR4) and **(C)** used for SPADE clustering are shown. Expression levels are depicted. Color range is from blue to yellow indicating low to high expression, respectively.

Supplementary figure 6: Ward hierarchical clustering of SPADE clusters

Heatmap based on expression of phenotypic markers from the individual SPADE clusters is shown. Ward hierarchical clustering was done with marker used for SPADE clustering, namely CCR7, CXCR4, CXCR5, IL-21R, Ki-67, IgA, IgG1, IgG3, CD21, CD27 and CD38. CXCR4 and CD19 were not used for Ward hierarchical clustering but are depicted on the heatmap. Expression is based on z-score transformed arcsinh MFI values. Clusters are ordered based on Ward hierarchical clustering and the coloring of the dendrogram shows the cut-off used to define Ward clusters. Ward clusters are numbered from 1-40 according to the ordering based on Ward hierarchical clustering.

Supplementary figure 7: Comparison of the frequency of RM or AM B cells defined based on manual and computational analysis.

(A) The frequencies of RM and AM B cells from HIV-infected patients (n=15) at the chronic stage of infection estimated with computational (black dots) and manual gating (red circles) are shown. **(B)** Frequency of total $CCR7^{high}$ cells within RM and AM B cells are compared from the same donors. $CCR7^{high}$ cells encompass cells exhibiting the highest expression levels of CCR7 (Figure 7A, red boxes) as estimated with the Ward clustering approach. Wilcoxon matched-pairs signed rank test was used to compare manual and computational analysis. $P<0.05$ was considered statistically significant. Significance levels are reported as *$p<0.05$, **$p<0.01$, ***$p<0.001$, ****$p<0.0001$.

6.10 Supplementary tables and figures

Supplementary table 1

Time point	Parameter	Early ART group (n=11)	Late ART group (n=8)	p-value
Acute	Weeks of infection	5 (3-8) (n=11)	13.5 (8-24) (n=6)	**0.0002**
	Viral load	475000 (2380-12400000) (n=11)	1930 (261-107000) (n=5)	**0.0275**
	CD4 counts	724 (436-816) (n=5)	633.5 (402-1120) (n=4)	0.5368
Chronic 2 years	Weeks of active virus replication	112 (101-138)	125 (104-139)	0.1838
	Weeks off ART	109 (94-134)	Not available	0.2627[a]
	Viral load	14200 (140-122000)	86400 (49-580000)	0.1087
	CD4 counts	569 (371-945)	263 (163-1429) (n=7)	0.0992
ART 1 year	Weeks on ART	53 (33-68)	58.5 (20-68)	0.3167
	Viral load	0 (0-0)	0 (0-58)	0.0578
	CD4 counts	798 (460-1363)	579 (278-804) (n=7)	**0.0154**

Supplementary table 2

Patients		Clinical characteristics						Samples used for individual assays						
Patient ID	study group	disease stage	viral load	CD4 counts	Weeks of replication	Weeks on ART	Weeks after ART stop	t-SNE analysis	SPADE	Manual Memory B cell subset analysis	Correlation analysis	Longitudinal CXCR3 analysis	Comparison of CXCR3 at ART 1year in study groups	Plasmablast analysis
ZPHI-Pat07	Early ART group	Acute	2380	NA	8	NA	NA	x	x	x	x	x		x
ZPHI-Pat23	Late ART group	Acute	3500	1120	8	NA	NA	x	x	x	x	x		x
ZPHI-Pat31	Early ART group	Acute	495500	724	5	NA	NA			x	x	x		x
ZPHI-Pat32	Early ART group	Acute	248500	463	4	NA	NA	x	x	x	x	x		x
ZPHI-Pat38	Late ART group	Acute	363	544	13	NA	NA	x	x	x	x	x		x
ZPHI-Pat39	Early ART group	Acute	13200	NA	7	NA	NA	x	x	x	x	x		x
ZPHI-Pat40	Late ART group	Acute	98000	NA	14	NA	NA	x	x	x	x	x		x
ZPHI-Pat44	Early ART group	Acute	1360000	NA	3	NA	NA			x	x	x		x
ZPHI-Pat48	Late ART group	Acute	107000	402	24	NA	NA	x	x	x	x	x		x
ZPHI-Pat49	Early ART group	Acute	2220000	NA	4	NA	NA	x	x	x	x	x		x
ZPHI-Pat58	Early ART group	Acute	3170000	816	5	NA	NA	x	x	x	x	x		x
ZPHI-Pat59	Early ART group	Acute	475000	NA	5	NA	NA	x	x	x	x	x		x
ZPHI-Pat60	Late ART group	Acute	261	NA	10	NA	NA	x	x	x	x	x		x
ZPHI-Pat72	Early ART group	Acute	47300	732	6	NA	NA	x	x	x	x	x		x
ZPHI-Pat78	Late ART group	Acute	1930	723	17	NA	NA	x	x	x	x	x		x
ZPHI-Pat92	Early ART group	Acute	62700	436	4	NA	NA	x	x	x	x	x		x
ZPHI-Pat93	Early ART group	Acute	12400000	NA	3	NA	NA	x	x	x	x	x		x
ZPHI-Pat07	Early ART group	Chronic 2 years	14200	472	128	NA	120	x	x	x	x	x		x
ZPHI-Pat11	Late ART group	Chronic 2 years	149000	263	122	NA	NA				x			
ZPHI-Pat23	Late ART group	Chronic 2 years	49	1429	108	NA	NA	x	x	x	x	x		x
ZPHI-Pat31	Early ART group	Chronic 2 years	22900	507	110	NA	105			x	x	x		x
ZPHI-Pat32	Early ART group	Chronic 2 years	140	613	138	NA	134	x	x	x	x	x		x
ZPHI-Pat38	Late ART group	Chronic 2 years	4500	229	134	NA	NA	x	x	x	x	x		x
ZPHI-Pat39	Early ART group	Chronic 2 years	64600	604	108	NA	102	x	x	x	x	x		x
ZPHI-Pat40	Late ART group	Chronic 2 years	33400	NA	123	NA	NA	x	x	x	x	x		x

ZPHI-Pat44	Early ART group	Chronic 2 years	16200	722	112	NA	109			x	x	x		x
ZPHI-Pat48	Late ART group	Chronic 2 years	91800	258	127	NA	NA	x	x	x	x	x		x
ZPHI-Pat49	Early ART group	Chronic 2 years	122000	677	112	NA	106	x	x	x	x	x		x
ZPHI-Pat58	Early ART group	Chronic 2 years	2700	945	115	NA	110	x	x	x	x	x		x
ZPHI-Pat59	Early ART group	Chronic 2 years	120000	371	123	NA	118	x	x	x	x	x		x
ZPHI-Pat60	Late ART group	Chronic 2 years	201331	163	131	NA	NA	x	x	x	x	x		x
ZPHI-Pat72	Early ART group	Chronic 2 years	1100	507	101	NA	94	x	x	x	x	x		x
ZPHI-Pat75	Late ART group	Chronic 2 years	81000	614	139	NA	NA				x			
ZPHI-Pat78	Late ART group	Chronic 2 years	580000	379	104	NA	NA	x	x	x	x	x		x
ZPHI-Pat92	Early ART group	Chronic 2 years	2650	489	122	NA	118	x	x	x	x	x		x
ZPHI-Pat93	Early ART group	Chronic 2 years	1651	569	102	NA	100	x	x	x	x	x		x
ZPHI-Pat07	Early ART group	ART 1 year	0	460	NA	57	NA	x	x	x	x	x	x	x
ZPHI-Pat11	Late ART group	ART 1 year	0	278	NA	63	NA				x		x	
ZPHI-Pat23	Late ART group	ART 1 year	0	595	NA	20	NA	x	x	x	x	x	x	x
ZPHI-Pat31	Early ART group	ART 1 year	0	678	NA	59	NA			x	x	x	x	x
ZPHI-Pat32	Early ART group	ART 1 year	0	699	NA	59	NA	x	x	x	x	x	x	x
ZPHI-Pat38	Late ART group	ART 1 year	0	580	NA	59	NA	x	x	x	x	x	x	x
ZPHI-Pat39	Early ART group	ART 1 year	0	844	NA	53	NA	x	x	x	x	x	x	x
ZPHI-Pat40	Late ART group	ART 1 year	0	373	NA	58	NA	x	x	x	x	x	x	x
ZPHI-Pat44	Early ART group	ART 1 year	0	877	NA	68	NA			x	x	x	x	x
ZPHI-Pat48	Late ART group	ART 1 year	0	431	NA	57	NA	x	x	x	x	x	x	x
ZPHI-Pat49	Early ART group	ART 1 year	0	994	NA	33	NA	x	x	x	x	x	x	x
ZPHI-Pat58	Early ART group	ART 1 year	0	1363	NA	49	NA	x	x	x	x	x	x	x
ZPHI-Pat59	Early ART group	ART 1 year	0	1028	NA	33	NA	x	x	x	x	x	x	x
ZPHI-Pat60	Late ART group	ART 1 year	58	NA	NA	60	NA	x	x	x	x	x	x	x
ZPHI-Pat72	Early ART group	ART 1 year	0	512	NA	53	NA	x	x	x	x	x	x	x
ZPHI-Pat75	Late ART group	ART 1 year	23	804	NA	52	NA				x		x	
ZPHI-Pat78	Late ART group	ART 1 year	1	579	NA	68	NA	x	x	x	x	x	x	x
ZPHI-Pat92	Early ART group	ART 1 year	0	750	NA	46	NA	x	x	x	x	x	x	x
ZPHI-Pat93	Early ART group	ART 1 year	0	798	NA	59	NA	x	x	x	x	x	x	x

Supplementary figure 1

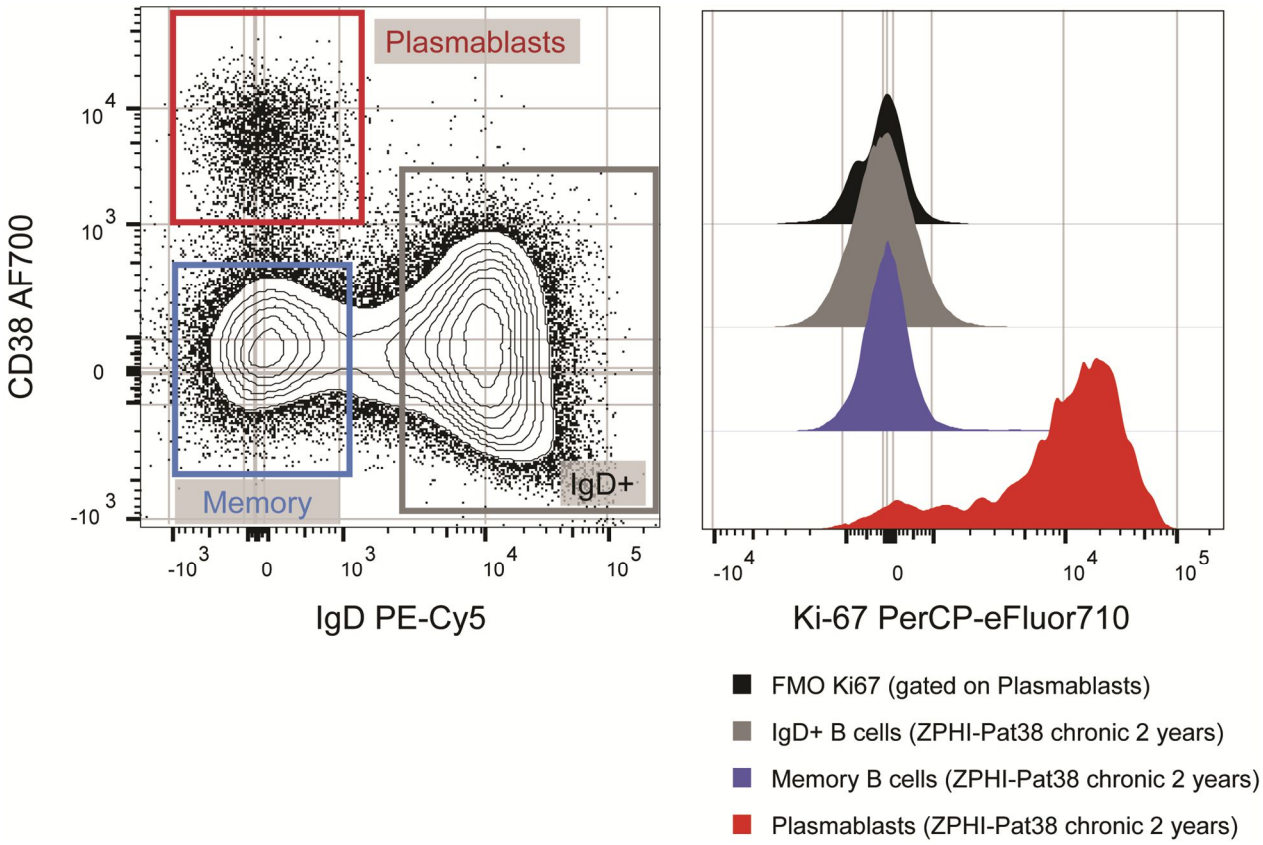

Supplementary figure 2

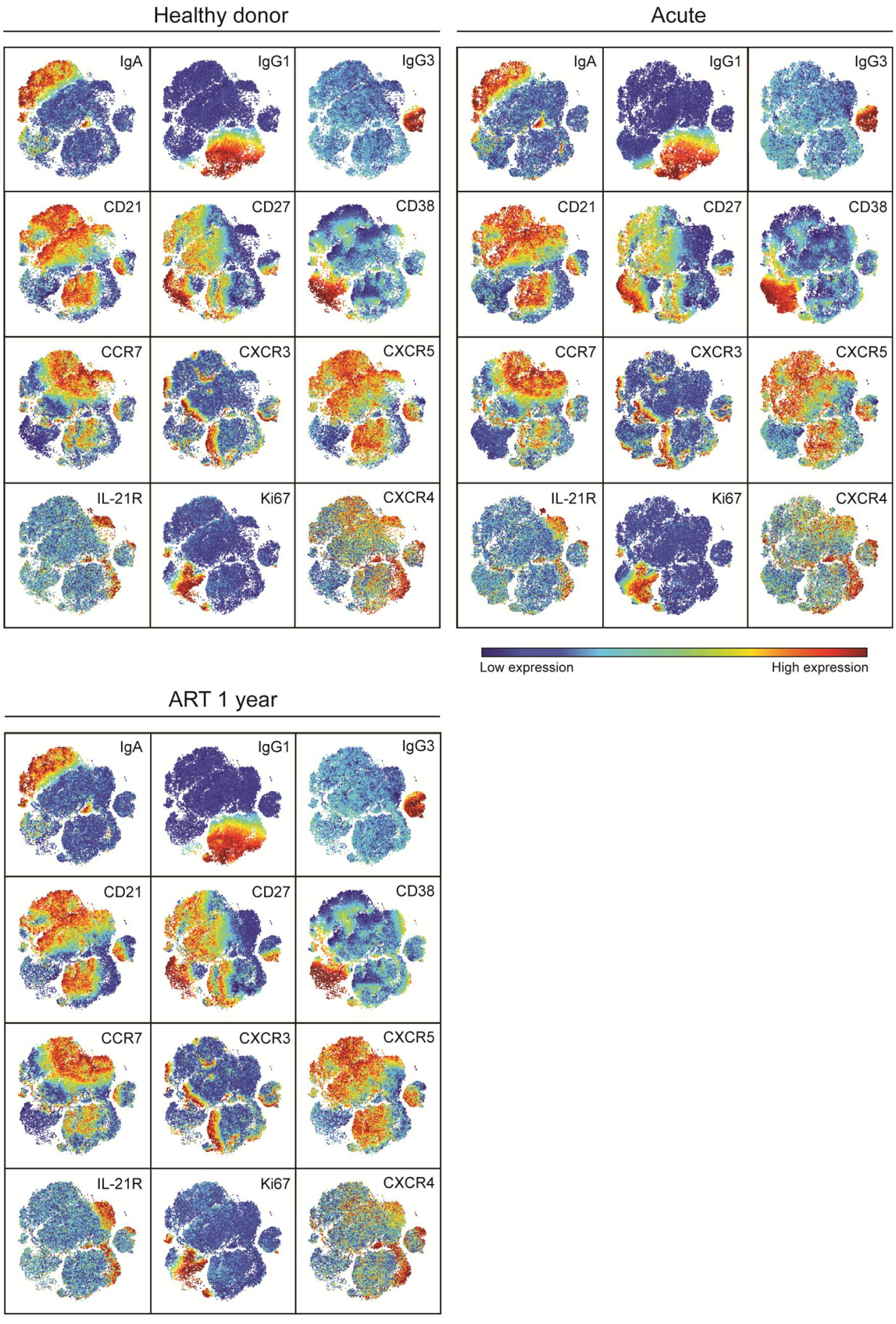

Supplementary figure 3

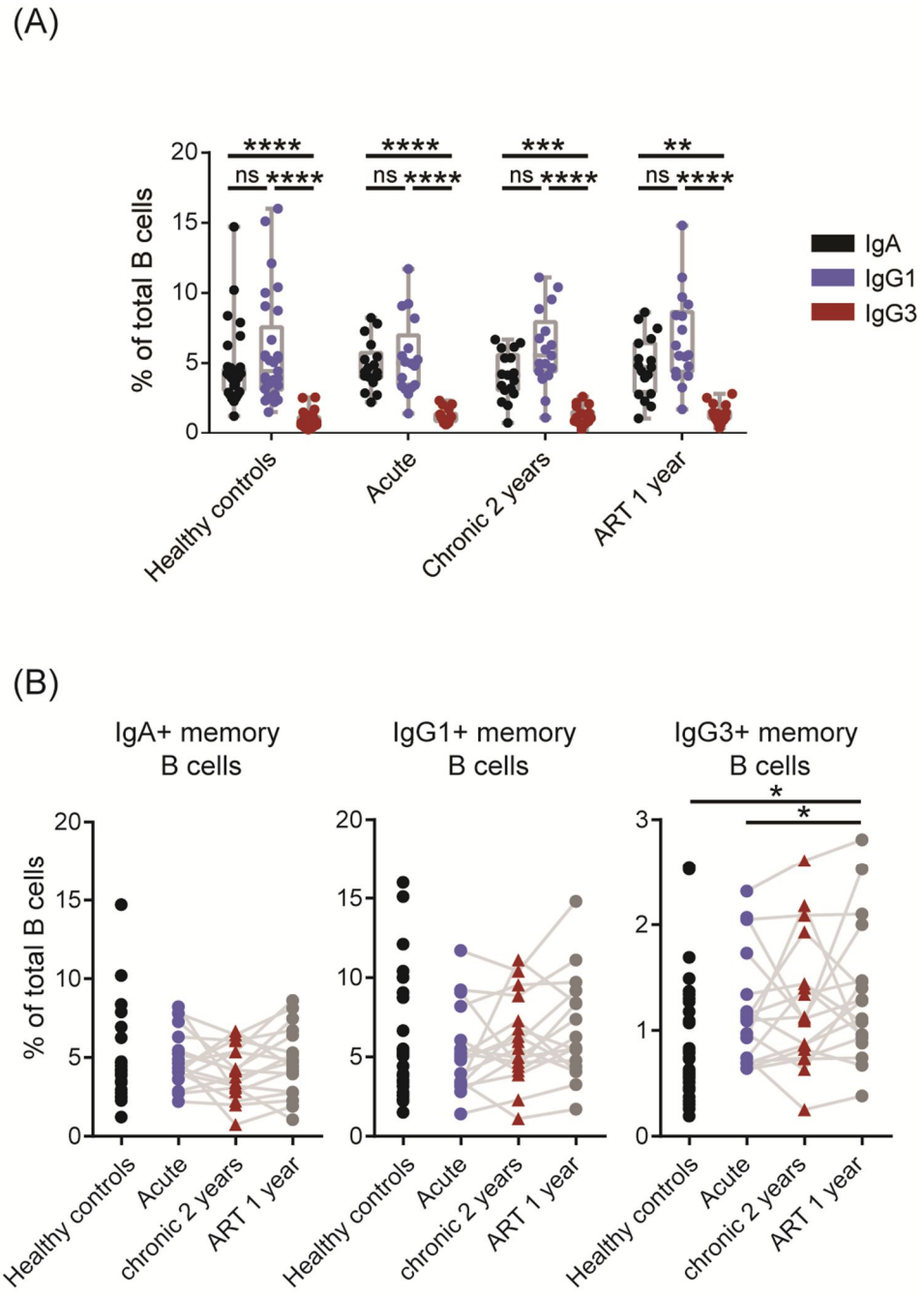

Supplementary figure 4

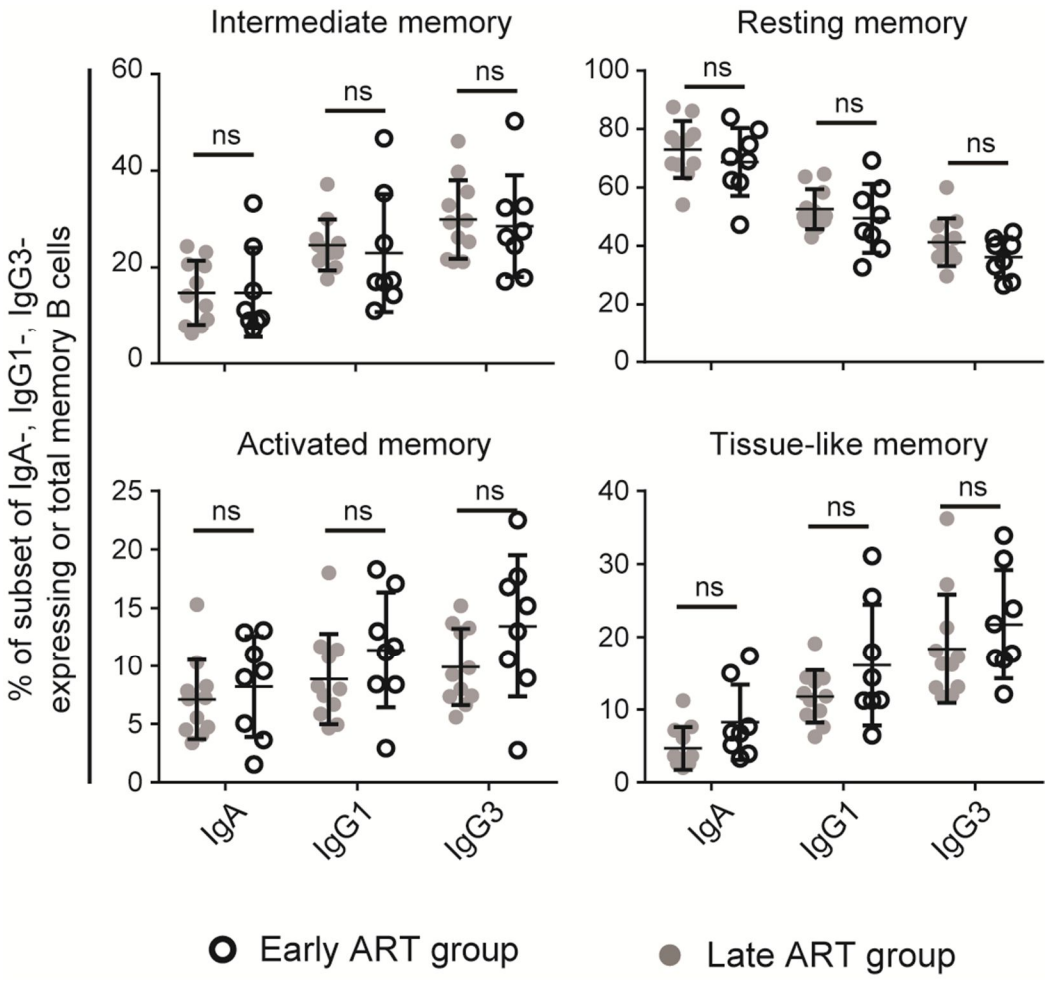

Supplementary figure 5

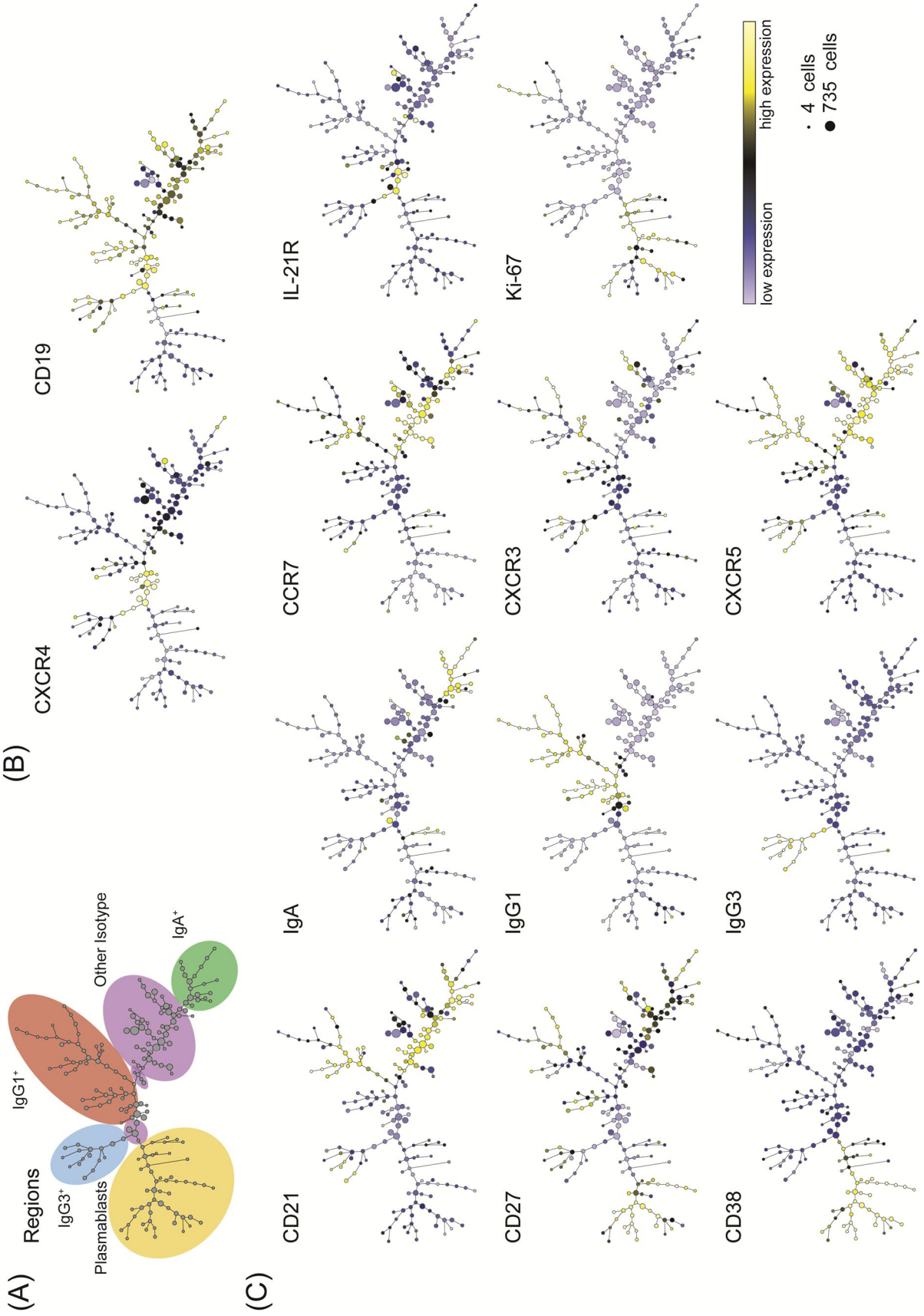

Supplementary figure 6

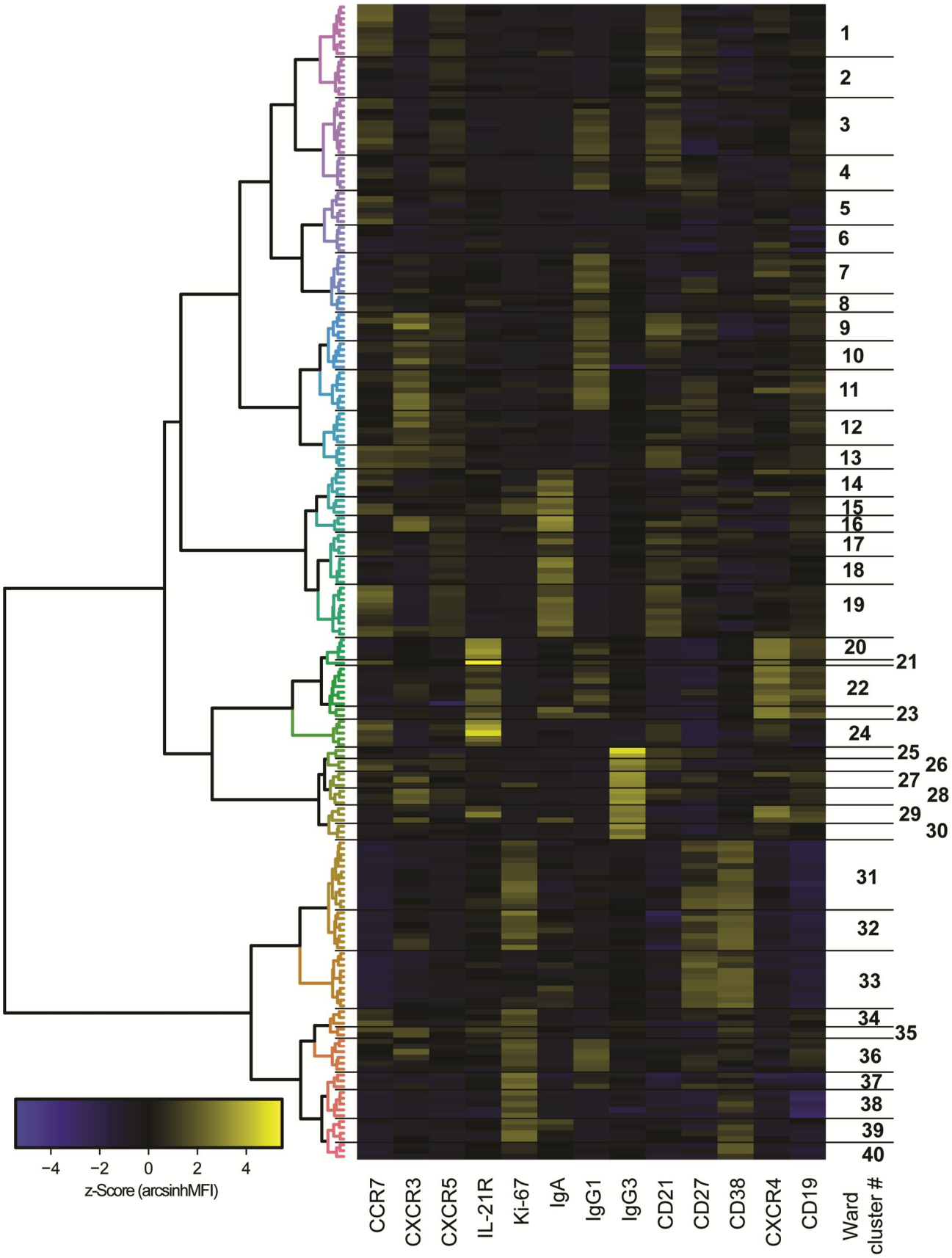

Supplementary figure 7

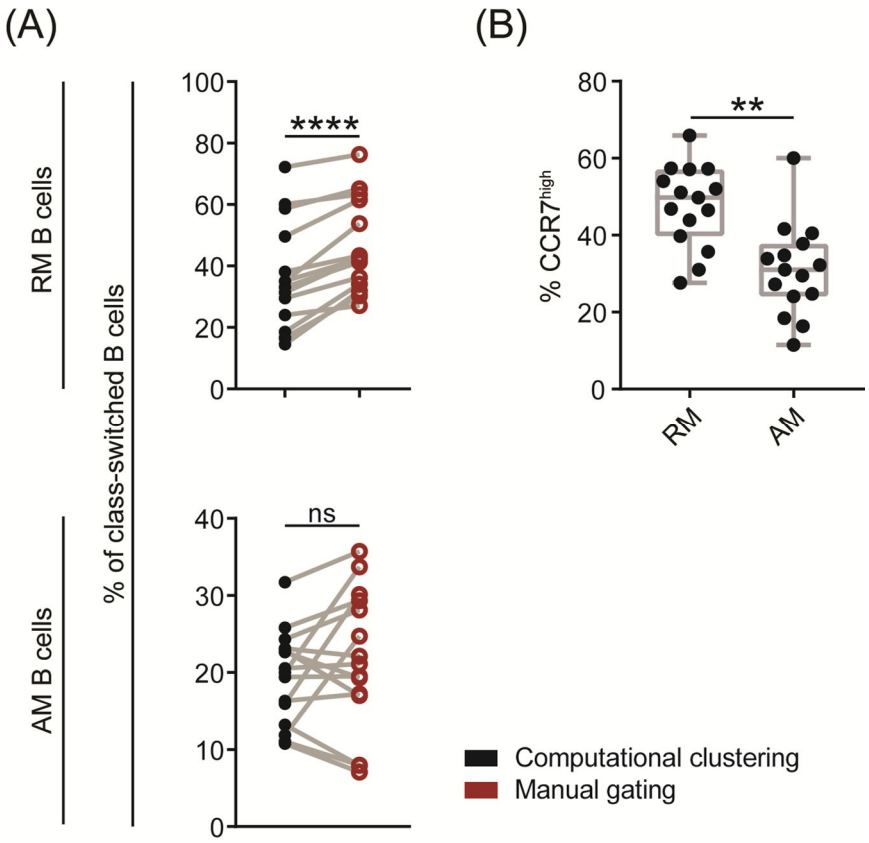

7. The Orientation of HIV-1 gp120 Binding to CD4 Receptor Differentially Modulates CD4$^+$ T cell activation

The following publication was published in the Journal of Immunology in 2014. My contributions included the determination of anti-gp120 and anti-CD4BS antibody titers in patient plasma and critical reading of the manuscript.

The Orientation of HIV-1 gp120 Binding to the CD4 Receptor Differentially Modulates CD4$^+$ T Cell Activation

Kathrin Zimmermann,* Thomas Liechti,† Anna Haas,* Manuela Rehr,* Alexandra Trkola,† Huldrych F. Günthard,‡ and Annette Oxenius*

Progressive quantitative and qualitative decline of CD4$^+$ T cell responses is one hallmark of HIV-1 infection and likely depends on several factors, including a possible contribution by the HIV-1 envelope glycoprotein gp120, which binds with high affinity to the CD4 receptor. Besides virion-associated and cell-expressed gp120, considerable amounts of soluble gp120 are found in plasma or lymphoid tissue, predominantly in the form of gp120–anti-gp120 immune complexes (ICs). Because the functional consequences of gp120 binding to CD4$^+$ T cells are controversially discussed, we investigated how gp120 affects TCR-mediated activation of human CD4$^+$ T cells by agonistic anti-CD3 mAb or by HLA class II–presented peptide Ags. We show that the spatial orientation of gp120–CD4 receptor binding relative to the site of TCR engagement differentially affects TCR signaling efficiency and hence CD4$^+$ T cell activation. Whereas spatially and temporally linked CD4 and TCR triggering at a defined site promotes CD4$^+$ T cell activation by exceeding local thresholds for signaling propagation, CD4 receptor engagement by gp120-containing ICs all around the CD4$^+$ T cell undermine its capacity in supporting proximal TCR signaling. In vitro, gp120 ICs are efficiently captured by CD4$^+$ T cells and thereby render them hyporesponsive to TCR stimulation. Consistent with these in vitro results we show that CD4$^+$ T cells isolated from HIV$^+$ individuals are covered with ICs, which at least partially contain gp120, and suggest that IC binding to CD4 receptors might contribute to the progressive decline of CD4$^+$ T cell function during HIV-1 infection. ***The Journal of Immunology*****, 2015, 194: 637–649.**

Healthy immune systems allow humans to cope lifelong with multiple persistent virus infections (1, 2). However, HIV-1 infection causes progressive deterioration of the immune system that ultimately leads to death due to opportunistic infections. Systemic immune activation as well as the continuous decline of a functional CD4$^+$ T cell response are main contributors to disease progression (3–5). The capacity of HIV-1 to progressively debilitate the immune system is multifaceted and incompletely understood. For example, the rapid evolution of HIV-1 owing to its high mutation rate (6–8), as well as its potential to establish viral reservoirs in resting memory CD4$^+$ T cells (9, 10), helps HIV-1 to evade functional immune responses. Furthermore, the HIV-1 surface envelope gp120 renders CD4$^+$ T cells prime targets for infection (11, 12) via the high-affinity gp120–CD4 receptor interaction (13) and thereby enables HIV-1 uniquely among persistent viruses to directly interfere with CD4$^+$ T cells, which are known to take a central position in adaptive immunity. Interestingly, the extent of qualitative (14) and quantitative (5, 15) defects within the CD4$^+$ T cell population in HIV-1–infected individuals is disproportionally high in comparison with the levels of infectious virus and productively infected cells (16, 17), arguing against the fact that CD4$^+$ T cell–directed viral cytopathicity is the major contributor to disease progression. However, HIV-1 replication, which is fundamental to disease progression, is not only associated with virion-associated envelope glycoprotein but also with soluble gp120 and gp160 due to shedding from the virus or from infected cells (18, 19). Consequently, soluble gp120 is present in the plasma (20–22) or lymphoid tissues of HIV$^+$ patients (23, 24), and together with the appearance of dysfunctional CD4$^+$ T cells, it is conceivable that binding of soluble gp120 to CD4$^+$ T cells may be a central parameter in HIV-1 pathogenesis that could at least partially explain the high proportion of dysfunctional CD4$^+$ T cells.

CD4 receptors play a crucial role in enhancing sensitivity of TCR-triggered T cell activation by interacting with MHC class II (MHC II) molecules on APCs (25, 26) and by their noncovalent interaction with the src family tyrosine kinase p56^{lck} whose activation initiates TCR signaling progression (26–29). In line with this, a plethora of in vitro studies provide experimental proof that gp120 binding to the CD4 receptor interferes with TCR-induced CD4$^+$ T cell activation (30–47). However, the effect of noninfectious gp120–CD4 receptor interaction on CD4$^+$ T cell activation is still a contradictory issue in the literature, and the gp120 levels measured in plasma of HIV$^+$ patients may be below those that have functional effects on cells in vitro (48). On the one hand, gp120 interaction with CD4 receptors was suggested to enhance the activation of CD4$^+$ T cells in terms of increased calcium signaling and IL-2R expression (44), transiently enhanced p56^{lck}

*Institute of Microbiology, Swiss Federal Institute of Technology Zurich, 8093 Zurich, Switzerland; †Institute of Medical Virology, University of Zurich, 8006 Zurich, Switzerland; and ‡Division of Infectious Diseases and Hospital Epidemiology, University Hospital Zurich, University of Zurich, 8091 Zurich, Switzerland

Received for publication July 21, 2014. Accepted for publication November 2, 2014.

This work was supported by Swiss Federal Institute of Technology Zurich/Swiss National Science Foundation Grant 310030_129751 (to A.O.), the University of Zurich's Clinical Research Priority Program "Viral Infectious Diseases: Zurich Primary HIV Infection Study" (to H.F.G.), and the Horten Foundation.

K.Z. and A.O. designed the experiments; K.Z., T.L., A.H., and M.R. performed experiments and analyzed data; K.Z. and A.O. discussed data; A.T. and T.L. contributed plasma samples and anti-gp120 Abs; H.F.G. enrolled patients; and K.Z. and A.O. made the figures and wrote the manuscript.

Address correspondence and reprint request to Prof. Annette Oxenius, Institute of Microbiology, Swiss Federal Institute of Technology Zurich, Vladimir-Prelog-Weg 1-5/10, HCI G401, 8093 Zurich, Switzerland. E-mail address: aoxenius@micro.biol.ethz.ch

Abbreviations used in this article: CD4BS, CD4 binding site; f.c.$_{gp120}$, final concentration of gp120; IC, immune complex; IS, immunological synapse; LAT, linker for activation of T cells; MHC II, MHC class II; MTOC, microtubule organizing center.

www.jimmunol.org/cgi/doi/10.4049/jimmunol.1401863

activity (46, 47), activation of the transcription factors AP-1 (45), and elevated proliferation (49). On the other hand, gp120 binding to CD4+ T cells was shown to reduce their activation mediated through TCR stimulation (30–43). Mechanisms to explain gp120-induced negative effects on CD4+ T cell activation are manifold: gp120-mediated cross-linking of CD4 receptors was suggested to induce CD4 receptor endocytosis (33, 35, 36, 41, 46), to prevent peptide–MHC II–CD4 receptor interaction (37, 50) through interference of gp120 with the MHC II binding site on the CD4 receptor (51), to abolish proximal TCR signaling (32, 34, 38, 40, 52), or to redistribute $p56^{lck}$ away from TCRs or from the immunological synapse (IS) (39, 53).

Based on these controversial reports and the possibility that gp120 binding to the CD4 receptor interferes with CD4+ T cell function, we investigated in detail whether and how non–virion-associated gp120 modulates TCR-induced CD4+ T cell activation. With the aim to mimic the in vivo situation as close as possible, we performed our in vitro experiments with primary CD4+ T cells and gp120–anti-gp120 immune complexes (ICs), as these are the predominant in vivo form of non–virion-associated gp120 (54, 55). To assess the impact of gp120–anti-gp120 ICs on CD4+ T cell activation, we stimulated cells either with agonistic anti-human CD3 mAb or with HLA class II–presented peptide Ags.

Our mechanistic study revealed that gp120–anti-gp120 ICs were rapidly and quantitatively transferred from APCs to CD4+ T cells. Importantly, following this process, IC-engaged CD4 receptors proved to substantially prevent subsequent TCR-mediated activation of CD4+ T cells. In contrast, CD4 and TCR cross-linking induced in vitro by immobilized gp120 and anti-human CD3 mAb on a planar substrate in close proximity promoted full CD4+ T cell activation. Thus, the microanatomical environment of how gp120 cross-links CD4 receptors appears to be crucial for the ensuing effect on CD4+ T cell activation. Our data thereby offer an explanation for the contradictory results of previous in vitro studies, reporting either enhanced or reduced CD4+ T cell activation upon gp120–CD4 receptor interaction. Furthermore, we demonstrate that CD4+ T cells from HIV-1 patients are covered with ICs that at least partly contain gp120, as also reported in Refs. 54–59, and therefore suggest that gp120-containing ICs impair CD4+ T cell activation and hence represent a crucial driving force of HIV-1 pathogenesis.

Materials and Methods

Ethics

Patients were enrolled in the Swiss HIV Cohort Study (60) or the Zurich Primary HIV Infection Study at the Division of Infectious Diseases and Hospital Epidemiology, University Hospital Zurich (http://clinicaltrials.gov, ID no. 5 NCT00537966) (61). Approval and written informed consent from patients were obtained according to the guidelines of the Ethics Committee of the University Hospital Zurich.

Cell preparation

Citrate-phosphate-dextrose anticoagulated buffy coats of healthy human adults were purchased from the Swiss Red Cross (Blutspende Zürich, Schlieren, Switzerland), and EDTA anti-coagulated blood was obtained from HIV+ and HIV− individuals from the University Hospital Zurich (Zurich, Switzerland). Viral load in HIV-1+ blood was determined at the Institute for Medical Virology at the University of Zurich (see Table I for detailed information). PBMCs were isolated by density centrifugation on lymphocyte separation media. Cells were washed in PBS and resuspended in RPMI 1640 supplemented with 10% FBS, 100 U/ml penicillin, 100 μg/ml streptomycin, and 2 mM L-glutamine (all reagents from PAA Laboratories, Pasching, Austria), which is referred to as RPMI 10 throughout. When PBMCs were not directly used for experiments, they were cryopreserved in RPMI 1640 supplemented with 20% FBS and 10% DMSO (Sigma-Aldrich Chemie, Buchs, Switzerland). Cell viability was determined by 0.4% trypan blue exclusion (Invitrogen, Basel, Switzerland) and assessed to be >90%. CD4+ T cells and CD14+ monocytes were isolated from PBMCs using anti-CD4 and anti-CD14 microbeads (Miltenyi Biotec, Bergisch Gladbach, Germany) according to the manufacturer's instructions.

Plasma samples

Plasma samples from HIV-1 patients (see Table II for detailed information) were heat inactivated at 56°C for 60 min and stored at −80°C until processing. Plasma viral loads (copies/ml), IgG anti-gp120 (JR-FL) titer, as well as IgG anti-gp120–CD4 binding site (CD4BS) titer were determined as described previously (62).

CFSE labeling

For CFSE labeling, CD4+ T cells were incubated at a concentration of 5×10^6 cells/ml in PBS supplemented with 10% FBS and 5 μM CFSE (Molecular Probes/Life Technologies Europe, Zug, Switzerland) for 11 min at 37°C. Afterward, cells were washed twice with cold RPMI 10 to quench residual CFSE and finally resuspended with RPMI 10 at an appropriate cell concentration.

IC preparation

ICs were prepared by incubating mammalian cell–derived recombinant HIV-1 gp120 JR-FL (endotoxin level < 1 endotoxin units/mg; Progenics Pharmaceuticals, Tarrytown, NY) or gp120 LAI together with non-CD4BS anti-gp120 mAbs [clone 2G12 (63) and clone 1-79 (64)] or with CD4BS anti-gp120 mAbs [clone b6 (65) and b12 (66)] at a molar gp120/anti-gp120 mAb ratio of ~4:5 (final concentration of gp120 [$f.c._{gp120}$] 5 μg/ml) to prepare gp120–anti-gp120 IC and gp120–anti-gp120–CD4BS control IC, respectively. Gp120 LAI and anti-gp120 Abs 2G12, 1-79, b6, and b12 were provided by A. Trkola. For the generation of gp120 containing ICs with plasma from HIV-1+ donors, plasma from HIV-1− and HIV-1+ donors and recombinant HIV-1 gp120 JR-FL were both diluted 1:100 and incubated for at least 2 h.

In vitro CD4+ T cell stimulation assay with plate-immobilized stimuli

CD4+ T cells (2×10^6/ml) were activated with plate-immobilized stimuli in a final volume of 100 μl RPMI 10. Plate immobilization of stimuli was done by incubating anti-human CD3 mAb (clone OKT3), anti-human CD28 mAb (clone CD28.2 or clone CD28.6), anti-human CD4 mAb (clone SK3; all from eBioscience, Vienna, Austria) recombinant gp120 JR-FL/LAI/CAAN (provided by A. Trkola) or ICs/control ICs (prepared as described previously) in a total volume of 100 μl PBS on F-bottom 96-well plates (Nunc Maxisorp; Sigma-Aldrich Chemie) for at least 18 h. Anti-human CD3 mAbs (50 ng/well) were used alone to induce subthreshold T cell activation or in combination with 0.8 μg/well gp120 or 1 μg/well anti-human CD28 mAb/CD4 mAb. To induce full T cell activation by the TCR alone, 1 μg anti-human CD3 mAb was coated on each well. For the stimulation of mouse CD4+ T cells, anti-mouse CD3ε mAb and anti-mouse CD28 mAb (both from BioLegend, Lucerna Chem AG, Lucerne, Switzerland) were used at similar concentrations as human-specific Abs. For internal assay controls, CD4+ T cells were left unstimulated or mitogenically stimulated with PMA (50 ng/ml) in combination with ionomycin (500 ng/ml, both from Sigma-Aldrich Chemie). When indicated, the gp120 binding site on the CD4 receptor was blocked by preincubation of the CD4+ T cells with anti-human CD4 mAbs (10 μg/ml, clone SK3) for 1 h at 37°C or actin polymerization was blocked by preincubation of the CD4+ T cells with cytochalasin D (50 μM, Sigma-Aldrich Chemie) for 30 min at 37°C prior to stimulation. For intracellular analysis of IL-2 expression, brefeldin A (10 μg/ml, Sigma-Aldrich Chemie) was added during the final 4 h of stimulation. Expression of CD40L, CD69, IL-2, IFN-γ, and TNF-α was analyzed after 6 h, and expression of CD25 and CD38 as well as proliferation by CFSE dilution after 5 d of stimulation at 37°C was as described below under "Flow cytometric analysis."

In vitro CD4+ T cell stimulation assay with autologous monocytes

CD4+ T cells (2×10^5) were stimulated with autologous CD14+ monocytes (1×10^5) in round-bottom 96-well cell culture plates in a final volume of 100 μl RPMI 10. Monocytes were loaded by sequential incubation of anti-human CD3 mAb (0.5–10 ng/ml, clone OKT3) for 30 min at 4°C or with CMV lysate (1:50, Virion, Rüschlikon, Switzerland) overnight at 37°C followed by incubation with ICs/control ICs ($f.c._{gp120}$ of 5 μg/ml) or gp120 containing ICs generated with plasma from HIV-1− and HIV-1+ donors (final dilution factor 100–400) (as described for IC preparation) for

Table I. Characteristics of HIV-1−infected individuals

Patient ID	Gender	Time Period of HIV-1 Infection	$CD4^+$ T Cell Count/μl	Plasma Viral Load (Copies/ml)
1	M	<5 y	20	290,000
2	M	<5 y	114	50,200
3	M	<5 y	359	257,443
4	M	<5 y	579	38,987
5	M	>10 y	314	22,558
6	M	>10 y	209	27,208

30 min at 4°C. Expression of CD69 was analyzed after 6 h, and expression of CD25 and CD38 as well as proliferation by CFSE dilution after 5 d of stimulation at 37°C was as described below under "Flow cytometric analysis."

Western blot analysis of phospho–linker for activation of T cells expression in $CD4^+$ T cells

For the analysis of levels of phosphorylated and unphosphorylated linker for activation of T cells (LAT), cells were cultured in RPMI 1640 supplemented with 10% human serum (type AB), 100 U/ml penicillin, 100 μg/ml streptomycin, and 2 mM L-glutamine (all reagents from PAA Laboratories). $CD4^+$ T cells were preactivated for 2 d with plate-immobilized anti-human CD3 mAb (50 ng/well) in combination with anti-human CD28 mAb (1 μg/well), rested for 3 d in fresh medium, and ultimately stimulated with plate-immobilized stimuli as described above under "In vitro $CD4^+$ T cell stimulation assay with plate-immobilized stimuli." Cells (6×10^5) were lysed in 30 μl cell lysis buffer (Cell Signaling Technologies/BioConcept, Allschwil, Switzerland) in the presence of phosphatase inhibitor tablets (Thermo Fisher Scientific, Reinach, Switzerland). Proteins were separated on a 10% SDS polyacrylamide gel and transferred to 0.2-μm pore size nitrocellulose transfer membranes (Schleicher and Schuel, Dassel, Germany). The amount of phosphorylated LAT was determined by polyclonal anti–phospho-LAT Ab (Tyr^{171}, 1:1000) followed by HRP-conjugated goat anti-rabbit Ab (1:5000, Jackson ImmunoResearch Laboratories, Suffolk, U.K.) using Amersham ECL technology (GE Healthcare, Glattbrugg, Switzerland). To measure the level of nonphosphorylated LAT protein, the membrane was reprobed after stripping with a polyclonal anti-LAT Ab (Cell Signaling Technology). Signal intensities were quantified by ImageJ (National Institutes of Health, Rockville, MD). After background subtraction, the signal intensity of phosphorylated LAT was normalized to the amount of nonphosphorylated LAT, and fold increase of normalized levels versus the unstimulated controls was calculated.

Microtubule organizing center polarization analysis of $CD4^+$ T cells in the context of plate and cellular stimulation by immunofluorescence confocal microscopy

For analysis of microtubule organizing center (MTOC) polarization in the context of plate stimulation, $CD4^+$ T cells were incubated for 2 h on 12-mm round coverslips (Karl Hecht Assistent, Altnau, Switzerland) that have previously been coated for at least 18 h with anti-human CD3 mAb (50 ng/ml) in combination with ICs/control ICs ($f.c._{gp120}$ of 5 μg/ml) diluted in PBS containing 0.0025% poly-L-lysine (Sigma-Aldrich Chemie). MTOC polarization analysis in the context of cellular stimulation was performed as described above under "In vitro $CD4^+$ T cell stimulation assay with autologous monocytes" except that stimulation was performed for 2 h only and cells were adhered onto poly-L-lysine (0.0025%) coated coverslips. After stimulation, cells were fixed with PBS containing 4% paraformaldehyde for 15 min at room temperature, followed by permeabilization (20% lysing solution [BD Biosciences, Allschwil, Switzerland] and 0.05% Tween 20 [National Diagnostics, Chemie Brunschwig, Basel, Switzerland]) for 10 min at room temperature. MTOC structures were visualized by staining with an anti–tubulin-β mAb (clone 9F3, Cell Signaling Technology/Bioconcept, Allschwil, Switzerland) overnight at 4°C in a humid chamber and Cy3-conjugated anti-rabbit ab (Jackson ImmunoResearch Laboratories) for 30 min at room temperature.

Analysis of IC localization by flow cytometry or immunofluorescence confocal microscopy

For the analysis of IC localization by immunofluorescence confocal microscopy, $CD14^+$ monocytes were loaded with ICs/control ICs (as described above under "In vitro $CD4^+$ T cell stimulation assay with autologous monocytes") and cocultured for 30, 60, or 120 min with $CD4^+$ T cells on poly-L-lysine (0.0025%; Sigma Aldrich Chemie)–coated coverslips. When indicated, $CD4^+$ T cells were preincubated with anti-human CD4 mAbs (10 μg/ml, clone SK3; eBioscience) for 1 h at 37°C. ICs were visualized by staining with a Cy3-conjugated anti-human IgG Ab (Jackson ImmunoResearch Laboratories) for 30 min at room temperature. For the analysis of IC localization by flow cytometry, $CD4^+$ T cells were cocultured with IC/control IC–loaded $CD14^+$ monocytes or directly with gp120 containing ICs generated with plasma from HIV-1^- and HIV-1^+ donors (final dilution of 1:100). After 6 h, IC localization was investigated by staining with an FITC-conjugated anti-human IgG (H+L) (Jackson ImmunoResearch Laboratories) as described below under "Flow cytometric analysis."

Immunofluorescence confocal microscopy

After staining, cells were fixed with PBS containing 4% paraformaldehyde for 15 min at room temperature and briefly rinsed with distilled H_2O before mounting in VectaShield (Vector Laboratories, Burlingame, CA) containing 0.1% DAPI (Sigma-Aldrich Chemie) for visualization of nuclear DNA. Confocal immunofluorescence microscopy was performed with an inverted confocal microscope (Axiovert 200, Carl Zeiss) equipped with an oil-phase contrast objective (×63 oil objective, Plan Neofluar, 1.25 numerical aperture, Carl Zeiss) and a CSU-X1 spinning-disk confocal unit (Yokogawa) and a solid-state laser unit with four laser lines (405, 488, 561, an 647 nm; Toptica). Data analysis was done with Volocity 5.0.3 (Improvision, Coventry, U.K.). Quantification of IC staining was done by evaluation of the integrated signal density by ImageJ (National Institutes of Health), with values being normalized to cell size. Analysis of MTOC polarization was done by visual scoring as described in Fig. 6B, 6E.

Flow cytometric analysis

Cells were surface stained with fluorochrome-conjugated anti-CD3 (clone UHCT-1), anti-CD4 (clone SK3), anti-CD8 (clone SK1), anti-CD14 (clone 61D3), anti-CD25 (clone BC96), anti-CD38 (clone HIT-2a), anti-CD40L (clone TRAP1), anti-CD69 (clone FN50), or anti-human IgG (H+L) (Jackson ImmunoResearch Laboratories) for 30 min at 4°C. Gp120 binding on $CD4^+$ T cells was assessed by FITC (Sigma-Aldrich Chemie)-conjugated gp120 staining for 30 min at 4°C. For the analysis of intracellular IL-2 expression, surface staining was followed by a permeabilization step of 10 min at room temperature (20% lysing solution and 0.05% Tween 20) and staining with anti–IL-2 (clone MQ1-17H12), anti–IFN-γ (clone B27), and anti–TNF-α (clone 6401.1111) for 30 min at room temperature. Abs were from BioLegend, Lucerna Chem, or BD Biosciences unless specified otherwise. When staining was performed in whole blood (Fig. 7A–C), RBCs were lysed with lysing solution directly after staining for 10 min at room temperature. For compensation, a combination of anti-mouse Igκ/negative control compensation particles (BD Biosciences) or PBMCs were used. Cells were resuspended in PBS containing 1% paraformaldehyde before acquisition. Acquisition was done on an LSR II flow cytometer (BD Biosciences) using FACSDiva software. Samples were acquired on the day of the analysis and usually $1–3 \times 10^5$ cells of interest were acquired. Doublets were excluded using side and forward scatter area and width parameters, and negative biological or fluorescence minus one controls were used to set gates. Data analysis was done with FlowJo software (Tree Star, San Carlos, CA). Cells were sequentially gated on lymphocytes, singlets, and $CD3^+CD4^+$ cells unless mentioned otherwise in the figure legend.

FACS

PBMCs were surface stained using anti-CD3 (clone UHCT-1), anti-CD4 (clone RPA-T4), anti-CD8 (clone SK1), and anti-CD14 (clone 61D3) for 30 min at 4°C. Abs were from BioLegend, Lucerna Chem, or BD Bio-

Table II. Characteristics of plasma samples from HIV-1 patients

Patient ID	IgG Anti-gp120 (JR-FL) Titer	IgG Anti–gp120-CD4BS Titer	Plasma Viral Load (Copies/ml)
1_1	15,107	6682	22,510
1_2	14,166	4926	283,140
1_3	7,342	5590	53,500
2_1	16.54	1[a]	29,700
2_2	8.23	1[a]	32,800

[a]Values < 1 indicate undetectable levels of anti–gp120-CD4BS Ab titers.

sciences. Cells were isolated on a FACSAria (BD Biosciences) using FACSDiva software.

Statistical analysis

Data were analyzed and plotted with GraphPad Prism (GraphPad Software, La Jolla, CA) and results are illustrated as means ± SEM. Statistical analysis was performed as specified in the figure legend. A p value <0.05 was considered statistically significant. In the figure legends, n values indicate individual donors unless specified otherwise.

Results

Plate-immobilized gp120 enhances TCR-induced activation of CD4+ T cells

CD4 receptors play an essential role in TCR-mediated activation of $CD4^+$ T cells through their intracellular association with the T cell–specific kinase $p56^{lck}$ (26–29). Because gp120 binds with high affinity to the CD4 receptor (13), a potential modulating capacity of TCR-driven $CD4^+$ T cell activation is attributed to gp120. Based on the importance of $CD4^+$ T cells as central players of the adaptive immune system and the high availability of soluble gp120 in the plasma or lymphoid tissue of HIV-1 patients (20–24), we set out to investigate how non–virion-associated gp120 affects TCR-induced $CD4^+$ T cell activation. In a first in vitro assay, $CD4^+$ T cells from healthy donors were stimulated with plate-immobilized recombinant gp120 in combination with low amounts (50 ng/well) of agonistic anti-human CD3 mAb, which we previously determined to induce only marginal $CD4^+$ T cell activation by itself. In combination, however, simultaneous CD4 receptor/TCR cross-linking by plate-immobilized gp120/anti-human CD3 mAb significantly enhanced $CD4^+$ T cell activation compared with gp120 and anti-CD3 stimulation alone to a similar level as CD28-induced costimulation. Activation was determined by the expression of early T cell activation markers CD69 and CD40L within 6 h (Fig. 1A–D) and levels of proliferation were measured by CFSE dilution after 5 d (Fig. 1E, 1F). Importantly, CD4 receptor cross-linking by gp120 in the absence of concomitant TCR stimulation did not have any activating capacity on $CD4^+$ T cells (Fig. 1A, 1B). Of note, a low level of $CD4^+$ T cell activation is not only enhanced by R5-tropic HIV-1 envelope glycoprotein gp120 strain JR-FL but also by gp120 originating from the R5-tropic strain CAAN, the X4-tropic strain LAI, as well as by anti-CD4 mAbs (Fig. 1C), supporting the fact that TCR-induced $CD4^+$ T cell activation is enhanced by concomitant CD4 receptor cross-linking rather than a gp120 intrinsic property. Ligation of CD4 receptors supports TCR signaling in a quantitative manner that allows the expression of activation markers and proliferation; however, cytokine expression in T cells critically depends on a qualitative, distinct costimulatory signal such as induced by the ligation by CD28 (67, 68). In line with a selective role of CD4 receptors in reinforcing proximal TCR signaling, IL-2, INF-γ, and TNF-α production was not robustly induced by gp120-mediated CD4 receptor cross-linking in contrast to CD28 costimulatory conditions (Fig. 1G, 1H). These data suggest that CD4 receptor cross-linking quantitatively supports TCR-induced signaling, yielding a high level of $CD4^+$ T cell activation when signals are provided in close temporal and spatial proximity.

Gp120-mediated increase of CD4+ T cell activation depends on gp120 binding to the CD4 receptor

The capacity of gp120 to selectively enhance TCR-induced activation of human (Fig. 1) and not mouse $CD4^+$ T cells (Fig. 2A), whose CD4 receptor does not bind gp120 (69), indicates that gp120–CD4 receptor interaction is crucial for gp120-mediated enhancement of $CD4^+$ T cell activation and also excludes the possibility that impurities of the gp120 preparation influenced the observed $CD4^+$ T cell activation. To substantiate the prerequisite of gp120–CD4 receptor interaction in promoting $CD4^+$ T cell activation, we used in a next step Abs that specifically blocked the gp120 binding site on the CD4 receptor (70). As expected, gp120 binding to $CD4^+$ T cells was reduced to background levels in the presence of the CD4 receptor blocking Ab (clone SK3) (Fig. 2B, 2C), and such blocking of the gp120 binding site on the CD4 receptor selectively abrogated anti-CD3/gp120– but not anti-CD3/anti-CD28–induced activation of $CD4^+$ T cells (Fig. 2D). Furthermore, $CD8^+CD4^+$ T cells, which are present in the blood at low frequencies (71), were efficiently activated by gp120 in the presence of low amounts of anti-human CD3 mAb, whereas this was not the case for $CD8^+CD4^-$ T cells (Fig. 2E).

The CD4 receptor–associated $p56^{lck}$ is crucial for proximal TCR signaling (26, 27, 72) by initiating a sequential cascade of tyrosine phosphorylation on signaling molecules, as for example on LAT, which is the nucleating site for multiprotein signaling complexes (73). We found that simultaneous CD4 receptor/TCR cross-linking by plate-immobilized gp120 and low amounts of plate-immobilized anti-human CD3 mAb induced slightly elevated levels of phosphorylated LAT, similar as with CD28 costimulatory conditions, in relationship to $CD4^+$ T cells that received weak TCR stimulation alone (Fig. 2F, 2G).

These experiments support the notion that gp120 binding to the CD4 receptor not only represents the first step of viral entry, but it also has the potential to significantly increase $CD4^+$ T cell activation by quantitatively supporting proximal TCR signaling.

Gp120–anti-gp120 ICs activate CD4+ T cells in a comparable manner to monomeric gp120

Because gp120 (20–24) as well as anti-gp120 Abs (74–76) are present in HIV-1 patients, gp120–anti-gp120 ICs are likely to be generated and abundant in vivo (54, 55). We therefore generated such gp120–anti-gp120 ICs by coincubating recombinant gp120 with two different human IgG anti-gp120 mAb at a molar gp120/anti-gp120 mAb ratio of ∼4:5. As schematically shown in Fig. 3A, either two different anti-gp120 mAbs that block the CD4BS [clones b6 (65) and b12 (66, 77)] or anti-gp120 mAbs that spare the CD4 binding site (non-CD4BS) [clones 2G12 (63) and 1-79 (64)] were used for the formation of gp120–anti-gp120–CD4BS control IC (*left*) or gp120–anti-gp120 IC (*right*), which are henceforth referred to as control IC or IC, respectively. Consequently, the control IC, which contains anti-gp120 Abs that target the CD4BS, does not allow any interaction with the CD4 receptor and is not expected to have any functional effect on $CD4^+$ T cells. Our results clearly showed that similarly to non–virion-associated gp120 alone, plate-immobilized IC significantly enhanced $CD4^+$ T cell activation induced by weak TCR stimulation as measured by CD69 expression (Fig. 3B, 3C) after 6 h. In contrast, the control IC failed to do so (Fig. 3B, 3C). Additionally, proliferation of $CD4^+$ T cells determined by CFSE dilution as well as the expression of late T cell activation markers CD25 and CD38 were significantly increased in the presence of IC compared with the control IC in combination with low level of TCR stimulation (Fig. 3D, 3E) after 5 d. Thus, gp120 within the context of ICs enhances a low level of TCR-driven $CD4^+$ T cell activation in a CD4 receptor–dependent manner similar to gp120 alone.

Fast transfer of monocyte-bound gp120–anti-gp120 IC to the CD4 receptor of CD4+ T cells

In a next step, we set out to investigate whether the activating potential of gp120 can be translated to a more physiological situation. To mimic a condition in which ICs made of gp120 and anti-gp120 Abs interact with CD4 receptors during TCR-induced $CD4^+$

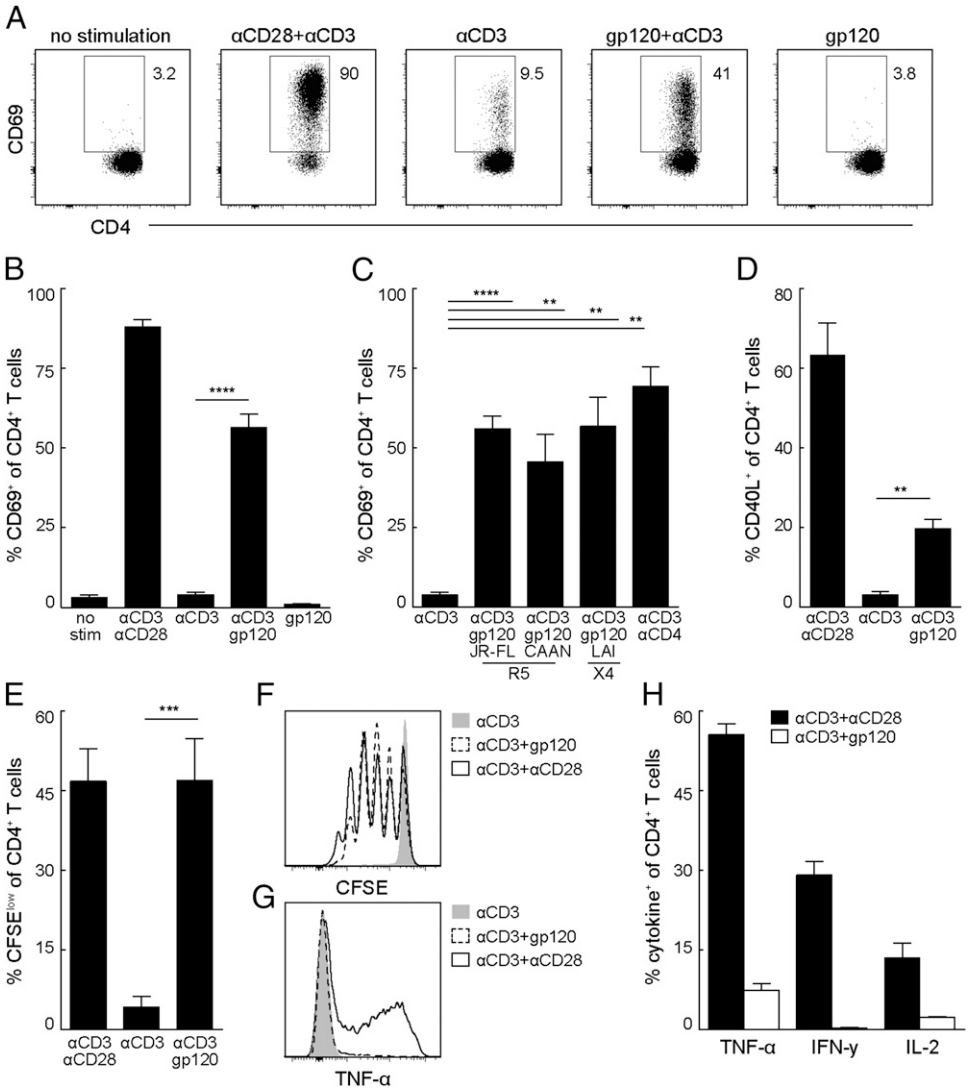

FIGURE 1. Plate-immobilized gp120 increases TCR-induced activation of $CD4^+$ T cells. $CD4^+$ T cells from healthy donors were stimulated for 6 h (**A**–**D**, **G**, and **H**) or 5 d (**E** and **F**) with subactivating amounts of plate-immobilized anti-human CD3 mAb in the presence or absence of gp120 (JR-FL, CAAN, and LAI as indicated). Gp120 JR-FL was used unless mentioned otherwise. As control, $CD4^+$ T cells were similarly stimulated with anti-human CD3 mAb in combination with anti-human CD28 mAb, with gp120 alone, or they were left untreated. (A) Dot plot of one representative experiment showing CD69 expression on $CD4^+$ T cells. (B) Bar graph depicting average expression levels of CD69 on $CD4^+$ T cells ($n = 20$, bars represent mean ± SEM, $^{****}p < 0.0001$ one-tailed paired t test). (C) Bar graph depicting average expression levels of CD69 on $CD4^+$ T cells ($n = 20$ for gp120 JR-FL, $n = 6$ for gp120 CAAN and LAI, $n = 3$ for anti-CD4 mAb; bars represent mean ± SEM; $^{**}p < 0.01$, $^{****}p < 0.0001$ one-tailed paired t test). (D) Bar graph illustrates the expression of CD40L on $CD4^+$ T cells ($n = 6$, bars represent mean ± SEM; $^{**}p < 0.01$ one-tailed paired t test). (E) Bar graph represents the average frequency of $CFSE^{low}CD4^+$ T cells ($n = 9$, bars represent mean ± SEM; $^{***}p < 0.001$ one-tailed paired t test). (F) Representative flow cytometry histogram depicts CFSE dilution profile of $CD4^+$ T cells. (G) Representative flow cytometry histogram depicts TNF-α expression in $CD4^+$ T cells. (H) Bar graph illustrates the expression of TNF-α, IFN-γ, and IL-2 on $CD4^+$ T cells ($n = 3$, bars represent mean ± SEM).

T cell stimulation by APCs, $CD4^+$ T cells from healthy donors were stimulated with autologous monocytes that had been previously incubated with gp120 containing ICs as well as anti-human CD3 mAb. Initially, flow cytometric determination of IC localization was performed by the analysis of human IgG binding after 6 h of coculture on $CD4^+$ T cells or $CD14^+$ monocytes. Control ICs were predominantly found on the $CD14^+$ monocytes whereas the IC was almost exclusively found on $CD4^+$ T cells (Fig. 4A). A similar localization pattern of control IC and IC was confirmed by the analysis of human IgG localization after 2 h by confocal microscopy (Fig. 4B). These experiments showed that only the IC and not the control IC was efficiently transferred to the $CD4^+$ T cells from monocytes on which they were initially localized. The cell–cell transfer of ICs proved to be very fast and efficient, as already after 60 min most ICs were localized on $CD4^+$ T cells (Fig. 4C). Furthermore, the transfer of ICs to $CD4^+$ T cells was abrogated in the presence of an anti-human CD4 mAb, which blocks the gp120 binding site on the CD4 receptor (Fig. 4D, 4E).

TCR-induced $CD4^+$ T cell activation is impaired in the presence of CD4 receptor cross-linking by gp120–anti-gp120 IC

We next investigated whether ICs, which were transferred from monocytes to CD4 receptors on $CD4^+$ T cells, would also reinforce responsiveness toward TCR stimulation induced by anti-human CD3 mAb–coated monocytes, as this was the case when the TCR and CD4 receptor were cross-linked in close proximity at a defined site, as for example upon immobilization of the stimuli on a plate (Figs. 1–3).

Toward this end, $CD4^+$ T cells were stimulated with monocytes that had been previously loaded with ICs that contain gp120 in

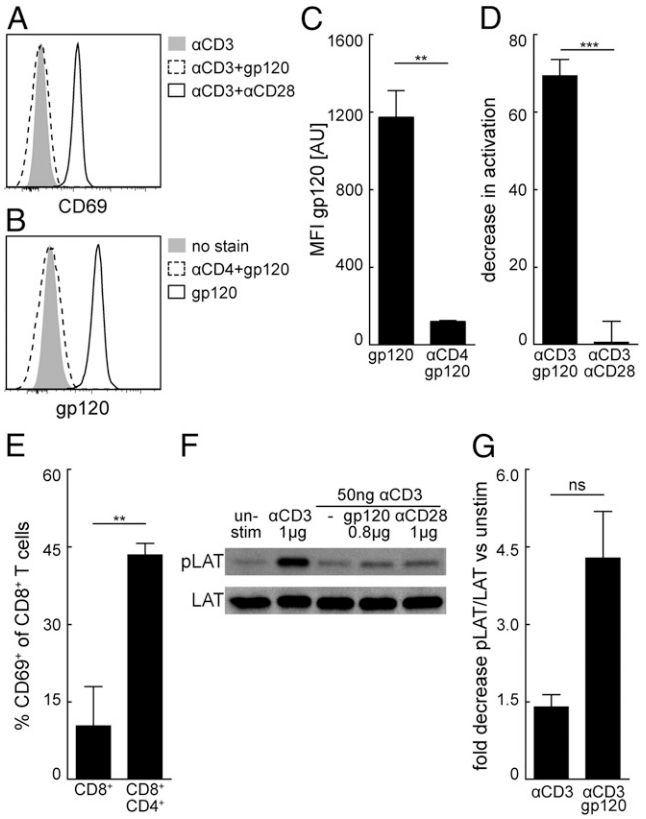

FIGURE 2. Plate-immobilized gp120 enhances TCR-mediated activation of $CD4^+$ T cells in a significant manner. (**A**) Representative flow cytometry histogram illustrates CD69 expression on mouse $CD4^+$ T cells after stimulation with plate-immobilized anti-mouse CD3 mAb alone or in combination with gp120 or anti-mouse CD28 mAb for 6 h. $CD4^+$ T cells isolated from HIV-1^- human donors were preincubated with anti-human CD4 mAb (clone SK3) to block the gp120 binding site on the CD4 receptor (**B**–**D**). (B) Representative flow cytometry histogram showing gp120 binding on $CD4^+$ T cells with and without anti-human CD4 mAb. (C) Bar graph depicting mean fluorescence intensity (MFI) signal in arbitrary units (AU) of gp120 on $CD4^+$ T cells with and without anti-human CD4 mAb (n = 3, bars represent mean ± SEM; $^{**}p < 0.01$ one-tailed paired t test). (D) Bar graph depicting the relative decrease in activation induced by stimulation with plate-immobilized anti-human CD3 mAb plus gp120 or anti-human $CD3^+$ plus anti-human CD28 in the presence versus absence of anti-human CD4 mAb (measured by CD69 expression after 6 h) (n = 9, bars represent mean ± SEM; $^{***}p < 0.001$ one-tailed paired t test). (**E**) Bar graph summarizes the expression of CD69 on human $CD8^+CD4^-$ (n = 3) or $CD8^+CD4^+$ (n = 2) T cells stimulated with plate-immobilized anti-human CD3 with and without gp120 for 6 h (cells were sequentially gated on lymphocytes, singlets, $CD3^+$, and $CD8^+CD4^-$/$CD8^+CD4^+$ cells, bars represent mean ± SEM; $^{**}p < 0.01$ one-tailed unpaired t test). $CD4^+$ T cells isolated from HIV-1^- human donors were stimulated for 2–10 min with plate-immobilized anti-human CD3 alone or in combination with gp120/anti-human CD28 or they were left unstimulated (**F** and **G**). (F) Corresponding representative immunoblot showing the levels of phosphorylated and unphosphorylated LAT. (G) Bar graph indicates the average fold increase of phospho-LAT/LAT levels (n = 3, bars represent mean ± SEM; ns, p = 0.0524 one-tailed paired t test).

combination with anti-human CD3 mAb. Gp120 within ICs either allows an interaction with the CD4 receptor (IC) or does not allow any interaction with the CD4 receptor (control IC). Interestingly, ICs that were transferred to $CD4^+$ T cells, and consequently not only cross-linked CD4 receptors at the site of TCR engagement but on the whole $CD4^+$ T cell surface, impaired $CD4^+$ T cell activation induced by anti-human CD3 mAb–loaded monocytes in comparison with control conditions with control IC–loaded monocytes. The reduction was manifested by the expression of CD69 after 6 h (Fig. 5B, 5C) or CD25 and CD38 expression as well as proliferation measured by CFSE dilution after 5 d (Fig. 5D, 5E). Importantly, the inhibitory effect of IC on TCR-induced $CD4^+$ T cell activation was not limited to polyclonal activation induced by anti-human CD3 mAb but also held true for CMV-specific $CD4^+$ T cell activation induced by HLA class II–bound CMV peptides on monocytes, as the levels of CD25 and CD38 expression as well as proliferation of CMV-specific $CD4^+$ T cells were significantly reduced in the presence of IC compared with control IC (Fig. 5F). The fact that IC-coated $CD4^+$ T cells were still susceptible to mitogenic stimulation with PMA and ionomycin (Fig. 5G) implies that IC interferes with a proximal TCR signaling event rather than rendering $CD4^+$ T cells completely incompetent to respond to activating stimuli in general.

Thus far, our data indicate that the way of CD4 receptor cross-linking by gp120 dictates in which way TCR-driven $CD4^+$ T cell is

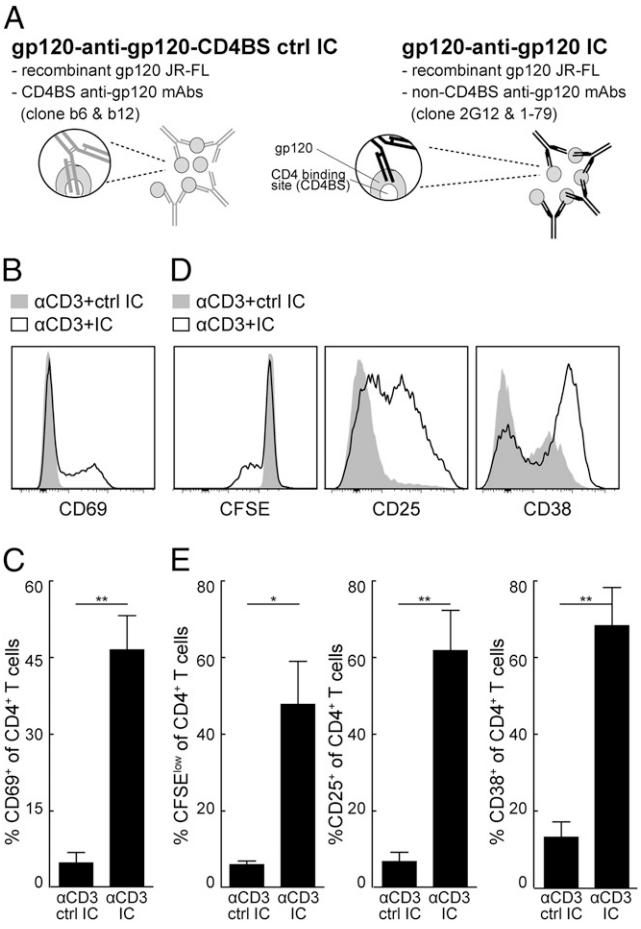

FIGURE 3. Plate-immobilized gp120–anti-gp120 ICs augment TCR-induced $CD4^+$ T cell activation in a CD4 receptor–dependent manner. (**A**) Schematic representation of gp120–anti-gp120–CD4BS control IC (ctrl IC; *left*) and gp120–anti-gp120 IC (IC; *right*) consisting of gp120 in combination with either two CD4BS anti-gp120 mAbs (clone b6 and b12) or non-CD4BS anti-gp120 mAbs (clone 2G12 and 1-79) at a molar gp120/Ab ratio of ~4:5. $CD4^+$ T cells were stimulated for 6 h (**B** and **C**) or for 5 d (**D** and **E**) with plate-immobilized control IC or IC in the presence of anti-human CD3 mAb. (B) Representative flow cytometry histogram showing CD69 expression on $CD4^+$ T cells. (C) Bar graph depicting CD69 expression on $CD4^+$ T cells (n = 4, bars represent mean ± SEM; $^{**}p < 0.01$ one-tailed paired t test). (D) Representative CFSE dilution profile and flow cytometry histogram showing CD25 and CD38 expression on $CD4^+$ T cells. (E) Bar graphs showing percentage of $CFSE^{low}$, $CD25^+$, and $CD38^+CD4^+$ T cells (n = 5, bars represent mean ± SEM; $^*p < 0.05$, $^{**}p < 0.01$ one-tailed paired t test).

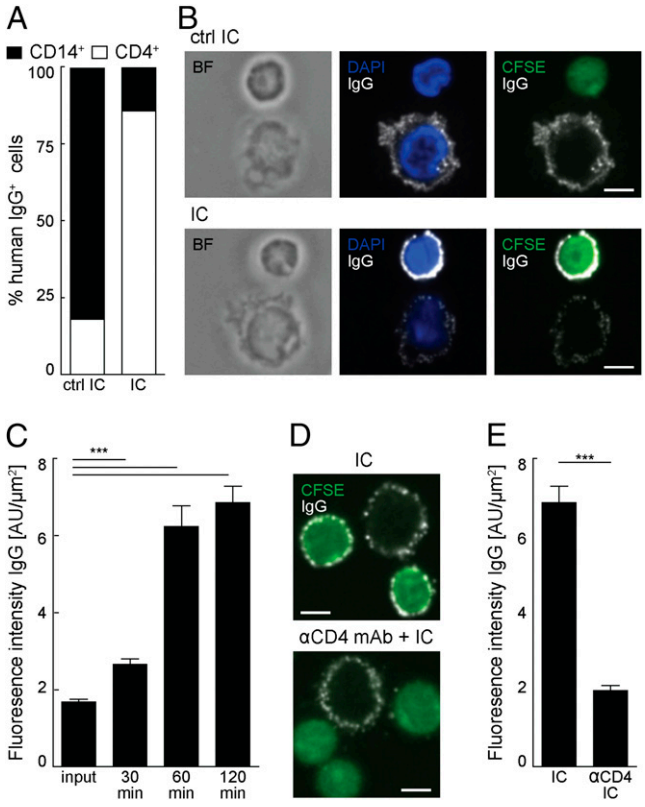

FIGURE 4. Gp120–anti-gp120 ICs are transferred from monocytes to $CD4^+$ T cells in a CD4 receptor–dependent manner. (**A**) $CD4^+$ T cells were cocultured for 6 h with control IC or IC-loaded $CD14^+$ monocytes. Bar graph represents percentage of $CD4^+$ T cells (open bar) and $CD14^+$ monocytes (filled bar) that stain for human IgG as measure for control IC and IC (as determined by flow cytometry). CFSE-labeled $CD4^+$ T cells were cocultured for 2 h (**B**, **D**, and **E**) or various time points (**C**) with control IC or IC-loaded $CD14^+$ monocytes. $CD4^+$ T cells were preincubated with an anti-human CD4 mAb (clone SK3) to block the gp120 binding site on the CD4 receptor when specified. *n*, number of individual cells. (B) Representative confocal image showing anti-human IgG for visualization of IC (white) on CFSE-labeled $CD4^+$ T cells (green) and $CD14^+$ monocytes; nuclear DNA is visualized by DAPI staining (blue). Scale bars, 5 μm. (C) Bar graph represents quantification of fluorescence intensity of anti-human IgG (in arbitrary units [AU]/μm^2) as measure of IC on $CD4^+$ T cells after 0 (input, $n = 17$), 30 ($n = 25$), 60 ($n = 12$), and 120 ($n = 24$) min of coculture with IC-loaded monocytes (bars represent mean ± SEM; $***p < 0.001$ one-tailed unpaired *t* test). (D) Representative confocal image of anti-human IgG staining (white) with and without anti-CD4. Scale bars, 5 μm. (E) Bar graph represents quantification of fluorescence intensity of anti-human IgG (in AU/μm^2) as measure for IC on $CD4^+$ T cells in the presence ($n = 24$) and absence ($n = 22$) of anti-CD4 (bars represent mean ± SEM; $***p < 0.001$ one-tailed unpaired *t* test).

affected. Whereas simultaneous TCR/CD4 receptor cross-linking confined to a specific site leads to enhanced $CD4^+$ T cell activation, CD4 receptor cross-linking by IC not only at the site of TCR engagement manifested impaired responsiveness toward TCR-induced $CD4^+$ T cell activation. We next aimed at elucidating how the manner of CD4 receptor cross-linking with respect to TCR engagement determines whether TCR signaling leads to enhanced or reduced $CD4^+$ T cell activation.

CD4 receptor cross-linking by gp120–anti-gp120 IC interferes with clustering of signaling complexes at the site of TCR engagement

TCR triggering induces a clustering of signaling complexes beyond the engaged TCRs that upon sustained signaling gives rise to the formation of IS (78–81). Such accumulation of surface and signaling molecules depends on dynamic reorganization of the actin- and tubulin-based T cell cytoskeleton (82–86), which is also reflected by the repositioning of the MTOC toward the site of stimulation (87, 88). CD4 receptors are essential in proximal TCR signaling (26–29) by recruiting $p56^{lck}$ to the establishing IS (89, 90). Because many TCR signaling molecules (e.g., the CD4 receptor) are indirectly or directly linked to the cytoskeleton (91–93), this opens the possibility that gp120 binding to the CD4 receptor interferes with IS formation. Accordingly, when cytoskeleton dynamics were abrogated by disrupting actin polymerization by cytochalasin D (94), TCR signaling induced by concomitant CD4/TCR cross-linking at a defined site did not promote full $CD4^+$ T cell activation, whereas a functional, dynamic cytoskeleton supported the accumulation of signaling complexes underneath the engaged TCRs such that local signaling strength resulted in full $CD4^+$ T cell activation (Fig. 6A). Importantly, TCR- and CD4-independent stimulation by PMA and ionomycin was not dependent on a functional, dynamic actin cytoskeleton (Fig. 6A).

We therefore speculated that spatially and temporally linked engagement of TCR and CD4 (as in the case of plate-immobilized anti-human CD3 mAb and gp120) would favor IS formation. However, when CD4 receptors are cross-linked over the entire surface of the $CD4^+$ T cell upon capturing ICs from monocytes, we suggest that the cytoskeletal dynamics that are required for IS formation might be impeded in such IC-decorated $CD4^+$ T cells. To test this hypothesis, we investigated MTOC positioning toward the growing synapse as a marker for IS formation (87, 88) by staining for β-tubulin. Fig. 6B shows representative confocal z-stack images of $CD4^+$ T cells stimulated by plate-immobilized anti-human CD3 mAb and gp120. The *left lane* shows a $CD4^+$ T cell in which the MTOC is oriented toward the stimuli (referred to as polarized), whereas the *right lane* depicts a $CD4^+$ T cell in which the MTOC is not polarized. Fig. 6E shows representative immunofluorescence images of $CD4^+$ T cells that were stimulated by anti-human CD3 mAb–loaded monocytes. On the *top*, a situation is shown in which the MTOCs of both APC-engaging $CD4^+$ T cells point toward the site of cell–cell contact (filled arrow, polarized), whereas the MTOC of the APC-engaging $CD4^+$ T cell shown in the *bottom* image points away from the cell–cell contact (open arrow, not polarized). In line with the increased $CD4^+$ T cell activation induced by plate-immobilized anti-human CD3 mAb and gp120 or IC (Figs. 1–3), MTOC polarization toward the site of TCR stimulation site was increased in the presence of IC (Fig. 6C, *bottom*, 6D) in contrast to the control IC (Fig. 6C, *top*, 6D). Note that MTOC polarization was defined as MTOC being localized in the cell hemisphere close to the planar surface. Because MTOC position is random in resting, unstimulated $CD4^+$ T cells, it will by chance point toward the site of stimulation (i.e., the planar surface) in ~50% of the cells (data not shown).

In striking contrast to the results with the plate-immobilized stimuli, reduced TCR-induced $CD4^+$ T cell activation in the presence of IC on monocytes (Fig. 5) was associated with impaired MTOC polarization toward the $CD4^+$ T cell–APC interface, whereas the presence of the control IC allowed efficient polarization of MTOCs toward the site of TCR engagement (Fig. 6F, 6G).

These data indicate that the manner of gp120/CD4 receptor cross-linking relative to the site of TCR engagement is crucial in the decision whether MTOCs can polarize to the site of engaged TCRs in a way that IS formation and hence $CD4^+$ T cell activation are supported.

$CD4^+$ T cells from HIV-1 patients are covered with ICs

Based on the fact that gp120 is present in plasma from HIV-1 patients (20–22) and that HIV-1 infection is associated with ro-

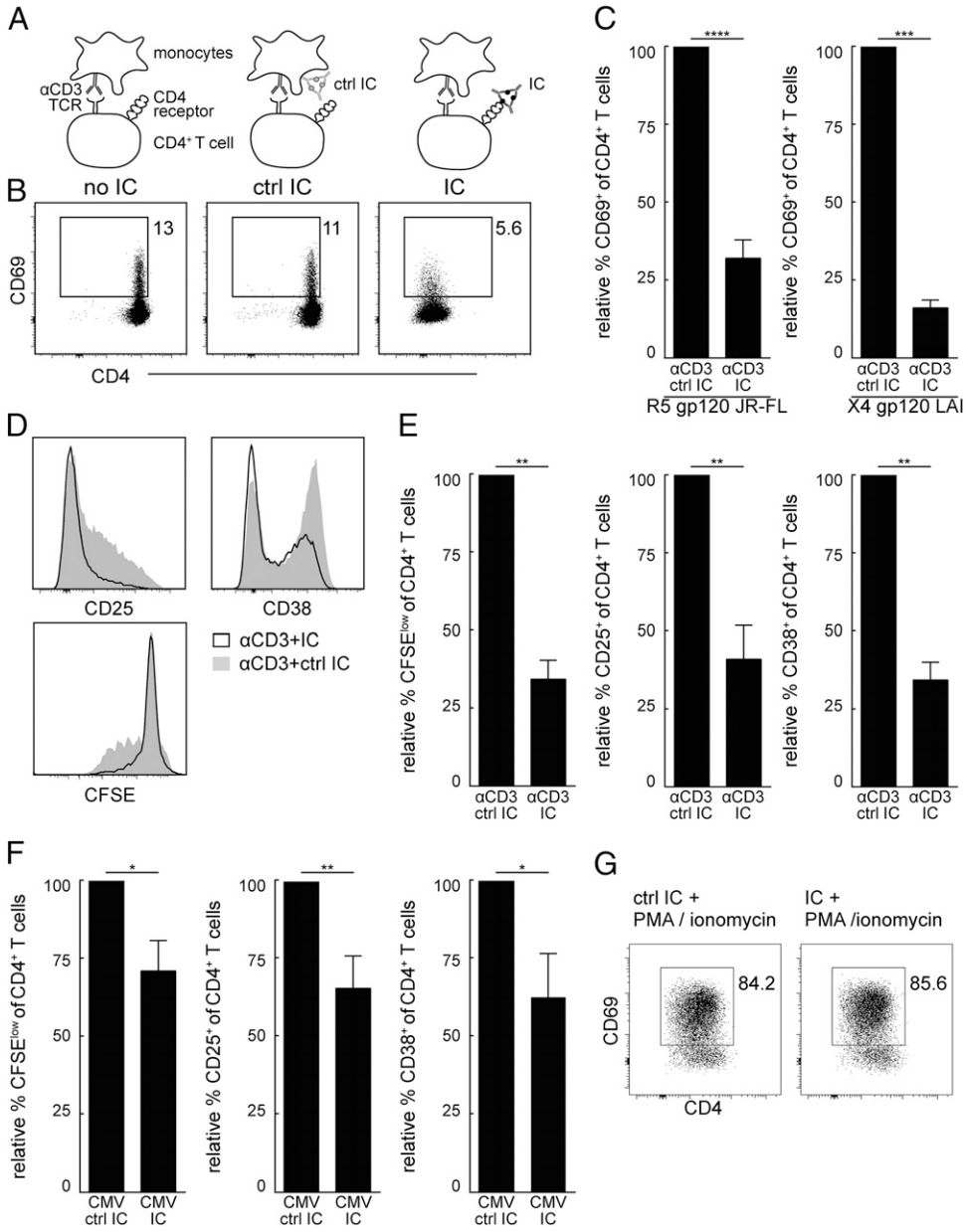

FIGURE 5. Gp120–anti-gp120 IC binding to the CD4 receptor impairs TCR-induced activation of CD4+ T cells. (**A**) Schematic illustration of CD4+ T cells stimulated with autologous monocytes that were loaded with anti-human CD3 mAb alone (no IC; *left*) or in combination with gp120–anti-gp120–CD4BS ctrl IC (ctrl IC; *middle*), as well as gp120–anti–gp120 IC (IC; *right*). ICs consist of gp120 JR-FL unless indicated otherwise in combination with either two CD4BS anti-gp120 mAbs (clone b6 and b12) or non-CD4BS anti-gp120 mAbs (clones 2G12 and 1-79) at a molar gp120/Ab ratio of ~4:5. CD4+ T cells were stimulated for 6 h (A–**C** and **G**) or for 5 d (**D**–**F**) with control IC or IC-loaded autologous monocytes in the presence of anti-human CD3 mAb or for 5 d (D and E) with control IC or IC-loaded autologous monocytes that were previously loaded with CMV lysate (F). (B) Flow cytometry dot plots of one representative experiment showing CD69 expression on CD4+ T cells. (C) Bar graphs shows relative percentage of CD69+ of CD4+ T cells normalized to anti-CD3 mAb/control IC after 6 h using ICs that contain gp120 JR-FL (*left*: $n = 9$, bars represent mean ± SEM; $^{****}p < 0.0001$ one-tailed paired *t* test) or gp120 LAI (*right*: bars represent mean ± SEM; $^{***}p < 0.001$ one-tailed paired *t* test). (D) Representative CFSE dilution profile and flow cytometry histogram showing CD25 and CD38 expression on CD4+ T cells. (E) Bar graphs showing relative percentage of CFSE^{low}, CD25+, and CD38+ of CD4+ T cells normalized to anti-CD3 mAb/control IC ($n = 3$, bars represent mean ± SEM; $^{**}p < 0.01$ one-tailed paired *t* test). (F) Bar graphs showing relative percentage of CFSE^{low}, CD25+, and CD38+ of CD4+ T cells normalized to CMV/control IC ($n = 7$, bars represent mean ± SEM; $^{*}p < 0.05$, $^{**}p < 0.01$ one-tailed paired *t* test). (G) Flow cytometry dot plot showing CD69 expression on CD4+ T cells stimulated for 6 h with PMA plus ionomycin in the presence of control IC (*left*) or IC (*right*).

bust Ab titers specific for HIV-1 surface structures (74–76, 95), gp120–anti-gp120 ICs are suggested to be the predominant form of gp120 in vivo (54, 55). Such complexes might either circulate or more likely be bound by FcR or complement receptor–expressing host cells. Based on the observation that monocyte-bound ICs were efficiently transferred to CD4+ T cells in our in vitro experiments (Fig. 4), we hypothesized that circulating CD4+ T cells from HIV-1 patients might be decorated with gp120-containing ICs. In line with this, we found that CD4+ T cells isolated from blood of HIV-1 patients (Table I) exhibited elevated anti-human IgG staining compared with CD4+ T cells isolated from blood of healthy controls (Fig. 7A–C), indicative of the presence of ICs on their surface. Because this difference was absent on CD8+ T cells (Fig. 7B), we speculated that the

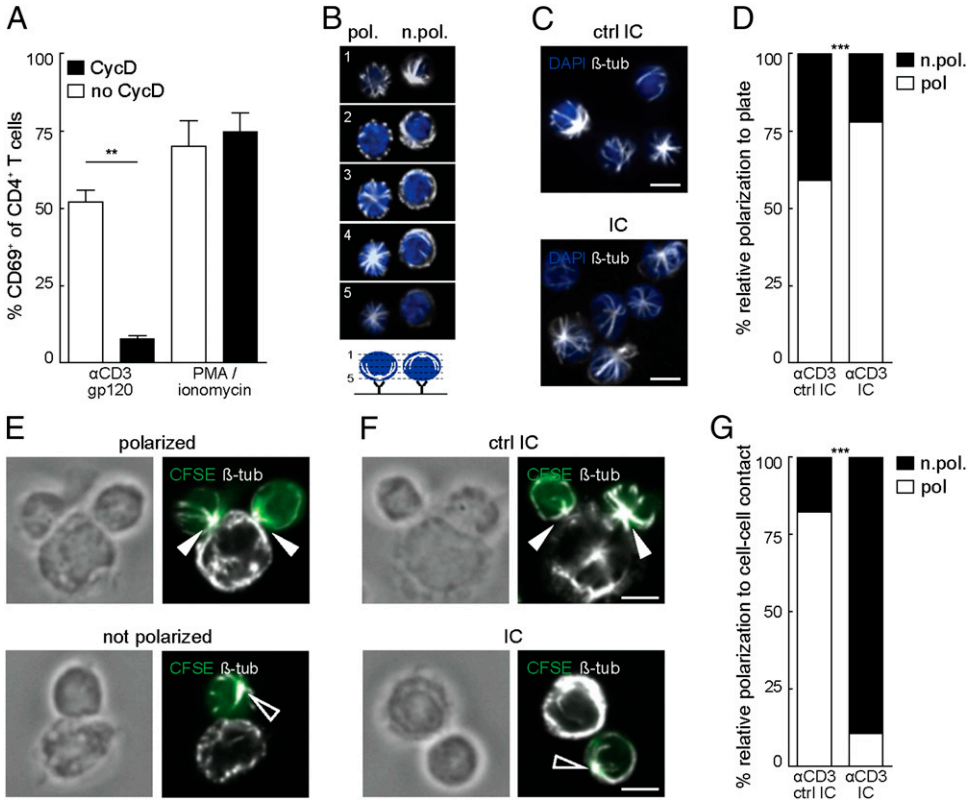

FIGURE 6. Gp120–anti-gp120 ICs interfere with the orientation of the MTOCs toward the site of TCR engagement. (**A**) Bar graphs depict the expression of CD69 on $CD4^+$ T cells stimulated for 6 h with plate-immobilized anti-CD3 plus gp120 or PMA plus ionomycin in the presence (filled bars) or absence (open bars) of cytochalasin D ($n = 3$) (bars represent mean ± SEM, $^{**}p < 0.01$ one-tailed paired t test). $CD4^+$ T cells were stimulated for 30 min with anti-human CD3 mAb in the presence of control IC or IC immobilized on coverslips showing nuclei by DAPI staining (blue) and MTOCs by β-tubulin staining (white) (**B**–**D**). (B) Exemplary z-stacks of immunofluorescence images depicting two $CD4^+$ T cells with differential MTOC polarization (*left*, polarized; *right*, not polarized), whereas MTOC polarization is referred to as MTOC positioning toward the site of TCR engagement. (C) Representative immunofluorescence images of $CD4^+$ T cells in z-stack close to the coverslip in the presence of control IC (*top*) or IC (*bottom*). (D) Bar graph summarizing MTOC polarization to the stimuli (white) and random polarization (black) in the presence of control IC ($n = 166$) and IC ($n = 180$) (n indicates number of individual cells, $^{***}p < 0.001$, χ^2 approximation). (**E**–**G**) $CD4^+$ T cells were stimulated for 2 h with monocytes loaded with anti-human CD3 mAb in the presence of control IC or IC showing nuclei by DAPI staining (blue), MTOC by β-tubulin staining (white), and CFSE-labeled $CD4^+$ T cells (green). (E) Exemplary immunofluorescence images showing MTOCs that are polarized (filled arrow) or not polarized (empty arrow) to the site of cell–cell contact or not. (F) Representative immunofluorescence images of $CD4^+$ T cells in the presence of control IC (*top*) or IC (*bottom*). (G) Bar graph summarizing MTOC polarization toward the site of cell–cell contact (white) and random polarization (black) of $CD4^+$ T cells in the presence of control IC ($n = 15$) or IC ($n = 14$)-loaded monocytes (n indicates number of individual cell–cell interactions, $^{***}p < 0.001$ Fisher exact test), Scale bar, 5 μm.

increased IgG signal on $CD4^+$ T cells, at least partially, originates from gp120-containing ICs. These ICs on the surface of $CD4^+$ T cells from HIV^+ donors might indeed contain gp120 (as also suggested in Ref. 59), because staining with two human anti-gp120 mAbs in combination with an anti-human IgG Ab yielded increased IgG staining on $CD4^+$ T cells from HIV^+ donors compared with IgG levels without the addition of the two human anti-gp120 mAbs (Fig. 7C).

The repertoire of anti-gp120 Abs in the plasma from HIV-1 patients supports the formation of gp120–anti-gp120 ICs that bind to $CD4^+$ T cells and constrain subsequent TCR-induced activation

Finally, we addressed the question whether the repertoire of polyclonal anti-gp120 Abs present in the plasma of HIV-1 patients would support the formation of gp120–anti-gp120 ICs that would interfere with TCR-mediated $CD4^+$ T cell activation. Toward this end, plasma from HIV-1 patients (Table II) was incubated with soluble gp120 to allow generation of gp120–anti-gp120 ICs, followed by adsorption to $CD4^+$ T cells from healthy donors. Staining for anti-human IgG revealed that even in plasma from HIV^+ donors with high titers of anti-gp120 Abs targeting the CD4BS, such ICs could be detected on $CD4^+$ T cells, whereas plasma from healthy controls did not lead to the formation of ICs, which specifically bound to $CD4^+$ T cells (Fig. 7D). When such gp120 ICs composed of polyclonal Abs from HIV^+ patients, in combination with anti-human CD3 mAb, were loaded on $CD14^+$ monocytes, the activation of autologous $CD4^+$ T cells was significantly impaired, as shown by the analysis of CD69 expression after 6 h (Fig. 7E).

Discussion

An exceptional peculiarity of HIV-1 is that its envelope surface glycoprotein has a very high affinity for the CD4 receptor (13), enabling HIV-1 and/or gp120 to directly interact and potentially interfere with $CD4^+$ T cell function. Such direct interference with the function of central regulators of the immune system is unique among human persistent viruses and represents a crucial factor in undermining HIV-specific and heterologous immune control. CD4 receptor binding by the HIV-1 envelope mediates not only viral infection (11, 12), but it can also amplify TCR-induced signaling by recruiting $p56^{lck}$ to the engaged TCRs (26–29, 89, 90), attributing the noninfectious interaction between gp120 and the CD4 receptor a potential role in modulating $CD4^+$ T cell responses

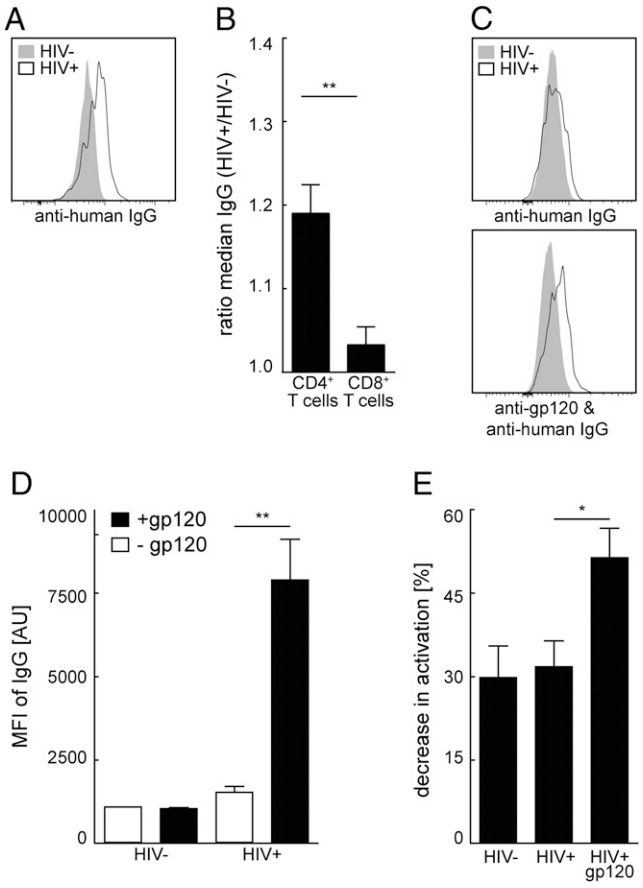

FIGURE 7. CD4+ T cells from HIV-1+ patients are covered with ICs. Anti-human IgG staining in combination with or without preincubation with human anti-gp120 mAb (clones 2G12 and 1-79) mAbs was performed on CD4+ T cells in blood from HIV-1+ and HIV-1− donors (**A**–**C**). (A) Representative FACS histogram showing anti-human IgG staining. (B) Bar graph depicting mean fluorescence intensity (MFI) in arbitrary units (AU) of human IgG on cells isolated from HIV-1+ ($n = 6$) and HIV-1− donors ($n = 6$, $^{**}p < 0.01$ two-tailed unpaired t test). (C) Representative FACS histogram showing human gp120/IgG staining and human IgG staining. (**D**) CD4+ T cells from HIV-1− donors were incubated with plasma from HIV-1− ($n = 5$) or HIV-1+ donors with and without gp120 ($n = 5$). Bar graph showing MFI of IgG in AU as measure for IC ($^{**}p < 0.01$ one-tailed paired t test). (**E**) CD4+ T cells were stimulated with monocytes loaded with anti-human CD3 mAb in combination with plasma from HIV-1− and HIV-1+ donors with and without gp120. Bar graphs represent the relative decrease in activation (measured by CD69 expression after 6 h) induced by anti-human CD3 mAb in combination with plasma from HIV-1− donors ($n = 7$), HIV-1+ donors ($n = 16$), or HIV-1+ donors plus gp120 ($n = 16$) compared with activation induced by anti-CD3 alone (n indicates number of plasma samples from five different donors in several independent experiments, $^{*}p < 0.05$ one-tailed paired t test).

(30–47). Several studies demonstrated the presence of soluble gp120 in the plasma or lymphoid tissue of HIV-1 patients (20–24), but its effect on TCR-induced CD4+ T cell activation is still a contentious issue in the literature.

Our data clearly show that the spatial orientation of CD4 receptor cross-linking by gp120 relative to the site of TCR engagement substantially affects TCR-mediated activation of CD4+ T cells. Namely, simultaneous provision of plate-immobilized agonistic anti-human CD3 mAb together with gp120 promotes CD4+ T cell activation, indicating that concomitant cross-linking of CD4 receptors and TCRs at a confined site augments the signaling of the engaged TCRs, whose cross-linking alone would not allow optimal signal propagation required for inducing full T cell activation. Gp120 provided in a simultaneous manner with TCR stimulation does not increase CD4+ T cell activation in a gp120-intrinsic manner, because CD4 cross-linking by Abs similarly enhances stimulation of CD4+ T cells in the presence of low levels of agonistic anti-CD3 mAbs, indicating that any CD4 cross-linking modality would promote CD4+ T cell activation when provided in a temporally and spatially linked manner. Conversely, ICs adsorbed to CD4 receptors all around CD4+ T cells led to substantial impairment of CD4+ T cell activation upon interaction with APCs providing TCR engagement either by agonistic anti-human CD3 mAb or antigenic HLA class II–peptide complexes.

We suggest that the basis for gp120-mediated interference with TCR-induced CD4+ T cell activation relies on the fact that CD4 receptors not only interact with the TCR–CD3 complex and $p56^{lck}$ but also with elements of the cytoskeleton (91), and consequently substantially interfere with the cytoskeletal-dependent rearrangement of signaling molecules toward the site of TCR stimulation, which ultimately regulates CD4+ T cell activation (82–86). This reasoning is supported by the observation that cross-linking of TCR–CD4 receptors in close proximity at a confined site only supports CD4+ T cell activation when the dynamics of the cytoskeleton are highly dynamic but not when actin polymerization is blocked by cytochalasin D. MTOC orientation toward the site of TCR engagement is one hallmark of a functional IS (87, 96), and our results clearly demonstrate that MTOC positioning is preferentially oriented toward plate-coimmobilized anti-human CD3 mAb and gp120. This indicates that cross-linking of CD4–TCR in close proximity allows cytoskeleton-directed accumulation of signaling molecules toward the site of engagement, thereby supporting full CD4+ T cell activation.

In contrast, IC binding to CD4 receptors of CD4+ T cells likely restricts cytoskeletal rearrangement by impairing lateral mobility of CD4 receptors and their cytoskeleton-associated framework. In line with this, we demonstrate that cross-linking of CD4 receptors by ICs not just at the site of TCR engagement hinders the accumulation of signaling units beyond the engaged TCRs, reflected by impaired MTOC orientation toward the site of TCR stimulation and hence compromised T cell activation. These results attribute gp120 a role in interfering with CD4+ T cell activation at the level of IS formation, which is in line with a previous report that describes defective recruitment of $p56^{lck}$ to the IS upon CD4 receptor engagement prior to TCR engagement (39).

Although many studies agree on a role of gp120 in negatively impacting CD4+ T cell activation (30–41, 46, 50, 52, 53), the underlying mechanism was so far not clearly elucidated. Gp120 binding to CD4 receptors was described to induce their downregulation and consequently impairing CD4–TCR complex assembly required for CD4+ T cell activation (33, 35, 36, 41, 46). Our results did not confirm CD4 receptor downregulation upon exposure to ICs within the time of analysis (data not shown). Furthermore, our data cannot confirm that gp120 prevents CD4+ T cell activation by interfering with MHC II–CD4 receptor interaction required for optimal CD4+ T cell activation (37, 50), because we observed the inhibitory effect of gp120 on CD4+ T cells activated upon MHC II–independent TCR engagement by anti-human CD3 mAb. Gp120 binding was suggested to interfere with proximal TCR signaling (32, 34, 38, 40, 52, 97), being possibly a direct consequence of impaired IS formation and consequent TCR signaling propagation, as demonstrated by our results. Moreover, we exclude that ICs manifest reduced CD4+ T cell activation due to TCRs being sterically hindered from contacting their activating ligands on the APC, because both the control IC and IC were localized comparably at the site of cell–cell contact, and only the latter ones affected CD4+ T cell activation.

HIV-1 replication is one major driving force of progressive immunodeficiency (3). One constituent of HIV-1, namely gp120, has the capacity to directly modulate $CD4^+$ T cell function, as shown previously (30–47) and in the present study. This effect has mostly been shown in vitro using relatively high concentrations of gp120, which leads to the question whether these effects might similarly operate in an in vivo scenario. Gp120 can be shed from the virion or from infected cells (18, 19) and is detectable in the plasma of HIV-1 patients, albeit there is some uncertainty about the actual gp120 concentrations (48). Levels in the plasma, however, might be much lower compared with those in lymphoid tissues where gp120 is thought to accumulate (23, 24). Thus, it is conceivable that gp120 availability in vivo might be sufficient to affect $CD4^+$ T cell function. The robust Ab response against the envelope surface structure of HIV-1 (74–76, 95, 98) results in the formation of gp120–anti-gp120 ICs, which are the most abundant form of gp120 in vivo (54, 56). Consistent with this notion, we and others (54–58) have demonstrated that $CD4^+$ T cells isolated from the blood of HIV-1 patients are covered with ICs, based on increased IgG deposition on $CD4^+$ T cells compared with healthy controls. Because no increase of IgG binding was observed on $CD8^+$ T cells, we speculate that the increased IgG signal on $CD4^+$ T cells, at least partially, originates from gp120-containing ICs. Experimental proof is provided by us and others (59) by disclosing surface staining of gp120 on a substantial proportion of $CD4^+$ T cells.

ICs that had been loaded on monocytes were rapidly and quantitatively transferred to $CD4^+$ T cells in our in vitro experiments. We suggest that this transfer is due to the different relative binding affinities of ICs to $CD4^+$ T cells or monocytes rather than on an active mechanism. Because the binding affinities between the IC and the Fc receptors on monocytes is weak compared with the high-affinity CD4–gp120 interaction (13), we speculate that ICs are captured by $CD4^+$ T cells from the monocytes in a stochastic process in which the ICs eventually localize on the cells to which they exhibit increased binding affinity. This transfer was dependent on the CD4 receptor and consequently did not occur for the control IC or in the presence of a CD4 receptor–blocking Ab, and therefore we excluded that ICs bound to the $CD4^+$ T cells in an unspecific manner. Accordingly, we suggest that ICs trapped on host cells via Fc or complement receptors as well as soluble gp120–anti-gp120 ICs might be effectively adsorbed on innocent bystander $CD4^+$ T cells. This could provoke unresponsiveness to subsequent TCR-induced activation and thereby add to $CD4^+$ T cell dysfunction during HIV-1 infection. Importantly, gp120–anti-gp120 ICs generated by the addition of gp120 to plasma from HIV-1 patients showed that the repertoire of in vivo circulating polyclonal gp120-specific Abs have the potential to generate gp120–anti-gp120 ICs that can be adsorbed by $CD4^+$ T cells. Abs that target the evolutionary conserved CD4BS (99–102) might prevent gp120-containing ICs from binding to CD4 receptors and hence could block gp120-related functional impairment of $CD4^+$ T cells similar to our control IC. Our data suggest, however, that the presence of high CD4BS Ab titers in polyclonal plasma from HIV-1^+ donors does not prevent gp120–anti-gp120 IC formation upon gp120 addition and that the thereby generated gp120-containing ICs bind to $CD4^+$ T cells and negatively affect anti-human CD3 mAb-induced $CD4^+$ T cell activation. This might be explained by the effective ratio of CD4BS versus non-CD4BS anti-gp120 Abs in the circulation, with a low ratio still allowing the formation of gp120-containing IC capable of binding to CD4 receptors. Of note, plasma in which anti-gp120 Ab titers were below the detection limit did not support the formation of gp120-containing ICs on $CD4^+$ T cells upon addition of gp120 (data not shown).

It should be considered in further studies whether gp120–anti-gp120 IC-coated $CD4^+$ T cells not only contribute to $CD4^+$ T cell dysfunction by means of impairing their TCR-induced activation but also by enhancing Ab-dependent cellular phagocytosis or Ab-dependent cellular cytotoxicity.

Overall, we demonstrate a central role of gp120–CD4 receptor interaction in impairing $CD4^+$ T cell function and consequently potential hindrance of establishing functional immune responses as one factor in the developing progressive immunodeficiency during HIV-1 infection.

The level of unresponsiveness toward TCR-induced stimulation likely depends on the extent of IC deposition on $CD4^+$ T cells. Although it is conceivable that the amounts of ICs we used in our in vitro assays might be at the upper limit or even higher compared with the average load of ICs detected on $CD4^+$ T cells isolated ex vivo in peripheral blood, the levels of gp120 and gp120-containing ICs are higher in lymphoid tissues (23, 24), and consequently we would assume that the levels of ICs on $CD4^+$ T cells might also be higher in these anatomic compartments. Beyond dispute, immune dysfunction that occurs in HIV-1–infected hosts is likely to be caused by multiple additional factors. Only very few studies compared the activation potential of $CD4^+$ T cells isolated from HIV-1 patients to $CD4^+$ T cells isolated from healthy controls, and a few of them indicated decreased in vitro lymphocyte proliferation/activation of $CD4^+$ T cells (56, 103, 104). Daniel et al. (56) revealed that this could be attributed to the presence of gp120-containing ICs on the surface of $CD4^+$ T cells. Along these lines, we demonstrate that HIV-1 gp120 directly influences $CD4^+$ T cell activation, whereby the geometry of CD4 receptor cross-linking by gp120 dictates the functional outcome of TCR-mediated $CD4^+$ T cell activation by differentially affecting IS formation. Although spatially and temporally linked engagement of CD4 receptors and TCR promote $CD4^+$ T cell activation, dispersed CD4 receptor engagement in relation to TCR triggering signals results in the opposite outcome, namely reduced propagation of TCR signaling and hence $CD4^+$ T cell activation. Our data thereby provide an explanation for the conflicting reports on gp120–CD4 receptor interaction on TCR-induced $CD4^+$ T cell activation and suggest a relevant role for the HIV-1–derived gp120 protein in mediating general downmodulation of $CD4^+$ T cell responsiveness in HIV-1–infected individuals aside the prolonged, nonphysiological activation of immune cells occurring in the context of HIV-1 infection (4, 105).

Acknowledgments

We are thankful to our patients for their commitment and specially thank C. Grube for patient care, N. Oetiker for experimental support as well as P. Rusert for providing us with anti-gp120 Abs and plasma samples from HIV-1 patients.

Disclosures

The authors have no financial conflicts of interest.

References

1. Lisco, A., C. Vanpouille, and L. Margolis. 2009. War and peace between microbes: HIV-1 interactions with coinfecting viruses. *Cell Host Microbe* 6: 403–408.
2. Virgin, H. W., E. J. Wherry, and R. Ahmed. 2009. Redefining chronic viral infection. *Cell* 138: 30–50.
3. Douek, D. C., M. Roederer, and R. A. Koup. 2009. Emerging concepts in the immunopathogenesis of AIDS. *Annu. Rev. Med.* 60: 471–484.
4. Paiardini, M., and M. Müller-Trutwin. 2013. HIV-associated chronic immune activation. *Immunol. Rev.* 254: 78–101.
5. Okoye, A. A., and L. J. Picker. 2013. $CD4^+$ T-cell depletion in HIV infection: mechanisms of immunological failure. *Immunol. Rev.* 254: 54–64.
6. Mansky, L. M., and H. M. Temin. 1995. Lower in vivo mutation rate of human immunodeficiency virus type 1 than that predicted from the fidelity of purified reverse transcriptase. *J. Virol.* 69: 5087–5094.

7. Wain-Hobson, S. 1993. The fastest genome evolution ever described: HIV variation in situ. *Curr. Opin. Genet. Dev.* 3: 878–883.
8. Bonhoeffer, S., E. C. Holmes, and M. A. Nowak. 1995. Causes of HIV diversity. *Nature* 376: 125.
9. Eisele, E., and R. F. Siliciano. 2012. Redefining the viral reservoirs that prevent HIV-1 eradication. *Immunity* 37: 377–388.
10. Finzi, D., M. Hermankova, T. Pierson, L. M. Carruth, C. Buck, R. E. Chaisson, T. C. Quinn, K. Chadwick, J. Margolick, R. Brookmeyer, et al. 1997. Identification of a reservoir for HIV-1 in patients on highly active antiretroviral therapy. *Science* 278: 1295–1300.
11. Dalgleish, A. G., P. C. Beverley, P. R. Clapham, D. H. Crawford, M. F. Greaves, and R. A. Weiss. 1984. The CD4 (T4) antigen is an essential component of the receptor for the AIDS retrovirus. *Nature* 312: 763–767.
12. Sattentau, Q. J. 1988. The role of the CD4 antigen in HIV infection and immune pathogenesis. *AIDS* 2(Suppl. 1): S11–S16.
13. Myszka, D. G., R. W. Sweet, P. Hensley, M. Brigham-Burke, P. D. Kwong, W. A. Hendrickson, R. Wyatt, J. Sodroski, and M. L. Doyle. 2000. Energetics of the HIV gp120-CD4 binding reaction. *Proc. Natl. Acad. Sci. USA* 97: 9026–9031.
14. Clerici, M., N. I. Stocks, R. A. Zajac, R. N. Boswell, D. R. Lucey, C. S. Via, and G. M. Shearer. 1989. Detection of three distinct patterns of T helper cell dysfunction in asymptomatic, human immunodeficiency virus-seropositive patients. Independence of CD4+ cell numbers and clinical staging. *J. Clin. Invest.* 84: 1892–1899.
15. McCune, J. M. 2001. The dynamics of CD4+ T-cell depletion in HIV disease. *Nature* 410: 974–979.
16. Harper, M. E., L. M. Marselle, R. C. Gallo, and F. Wong-Staal. 1986. Detection of lymphocytes expressing human T-lymphotropic virus type III in lymph nodes and peripheral blood from infected individuals by in situ hybridization. *Proc. Natl. Acad. Sci. USA* 83: 772–776.
17. Douek, D. C., L. J. Picker, and R. A. Koup. 2003. T cell dynamics in HIV-1 infection. *Annu. Rev. Immunol.* 21: 265–304.
18. Pyle, S. W., J. W. Bess, Jr., W. G. Robey, P. J. Fischinger, R. V. Gilden, and L. O. Arthur. 1987. Purification of 120,000 Dalton envelope glycoprotein from culture fluids of human immunodeficiency virus (HIV)-infected H9 cells. *AIDS Res. Hum. Retroviruses* 3: 387–400.
19. Schneider, J., O. Kaaden, T. D. Copeland, S. Oroszlan, and G. Hunsmann. 1986. Shedding and interspecies type sero-reactivity of the envelope glycopolypeptide gp120 of the human immunodeficiency virus. *J. Gen. Virol.* 67: 2533–2538.
20. Oh, S. K., W. W. Cruikshank, J. Raina, G. C. Blanchard, W. H. Adler, J. Walker, and H. Kornfeld. 1992. Identification of HIV-1 envelope glycoprotein in the serum of AIDS and ARC patients. *J. Acquir. Immune Defic. Syndr.* 5: 251–256.
21. Rychert, J., D. Strick, S. Bazner, J. Robinson, and E. Rosenberg. 2010. Detection of HIV gp120 in plasma during early HIV infection is associated with increased proinflammatory and immunoregulatory cytokines. *AIDS Res. Hum. Retroviruses* 26: 1139–1145.
22. Gilbert, M., J. Kirihara, and J. Mills. 1991. Enzyme-linked immunoassay for human immunodeficiency virus type 1 envelope glycoprotein 120. *J. Clin. Microbiol.* 29: 142–147.
23. Popovic, M., K. Tenner-Racz, C. Pelser, H. J. Stellbrink, J. van Lunzen, G. Lewis, V. S. Kalyanaraman, R. C. Gallo, and P. Racz. 2005. Persistence of HIV-1 structural proteins and glycoproteins in lymph nodes of patients under highly active antiretroviral therapy. *Proc. Natl. Acad. Sci. USA* 102: 14807–14812.
24. Santosuosso, M., E. Righi, V. Lindstrom, P. R. Leblanc, and M. C. Poznansky. 2009. HIV-1 envelope protein gp120 is present at high concentrations in secondary lymphoid organs of individuals with chronic HIV-1 infection. *J. Infect. Dis.* 200: 1050–1053.
25. Gay, D., P. Maddon, R. Sekaly, M. A. Talle, M. Godfrey, E. Long, G. Goldstein, L. Chess, R. Axel, J. Kappler, et al. 1987. Functional interaction between human T-cell protein CD4 and the major histocompatibility complex HLA-DR antigen. *Nature* 328: 626–629.
26. Glaichenhaus, N., N. Shastri, D. R. Littman, and J. M. Turner. 1991. Requirement for association of p56^{lck} with CD4 in antigen-specific signal transduction in T cells. *Cell* 64: 511–520.
27. Rudd, C. E., P. Anderson, C. Morimoto, M. Streuli, and S. F. Schlossman. 1989. Molecular interactions, T-cell subsets and a role of the CD4/CD8:p56^{lck} complex in human T-cell activation. *Immunol. Rev.* 111: 225–266.
28. Ledbetter, J. A., C. H. June, P. S. Rabinovitch, A. Grossmann, T. T. Tsu, and J. B. Imboden. 1988. Signal transduction through CD4 receptors: stimulatory vs. inhibitory activity is regulated by CD4 proximity to the CD3/T cell receptor. *Eur. J. Immunol.* 18: 525–532.
29. Veillette, A., M. A. Bookman, E. M. Horak, L. E. Samelson, and J. B. Bolen. 1989. Signal transduction through the CD4 receptor involves the activation of the internal membrane tyrosine-protein kinase p56^{lck}. *Nature* 338: 257–259.
30. Weinhold, K. J., H. K. Lyerly, S. D. Stanley, A. A. Austin, T. J. Matthews, and D. P. Bolognesi. 1989. HIV-1 GP120-mediated immune suppression and lymphocyte destruction in the absence of viral infection. *J. Immunol.* 142: 3091–3097.
31. Manca, F., J. A. Habeshaw, and A. G. Dalgleish. 1990. HIV envelope glycoprotein, antigen specific T-cell responses, and soluble CD4. *Lancet* 335: 811–815.
32. Chirmule, N., V. S. Kalyanaraman, N. Oyaizu, H. B. Slade, and S. Pahwa. 1990. Inhibition of functional properties of tetanus antigen-specific T-cell clones by envelope glycoprotein GP120 of human immunodeficiency virus. *Blood* 75: 152–159.
33. Schwartz, O., M. Alizon, J. M. Heard, and O. Danos. 1994. Impairment of T cell receptor-dependent stimulation in CD4+ lymphocytes after contact with membrane-bound HIV-1 envelope glycoprotein. *Virology* 198: 360–365.
34. Cefai, D., P. Debre, M. Kaczorek, T. Idziorek, B. Autran, and G. Bismuth. 1990. Human immunodeficiency virus-1 glycoproteins gp120 and gp160 specifically inhibit the CD3/T cell-antigen receptor phosphoinositide transduction pathway. *J. Clin. Invest.* 86: 2117–2124.
35. Cefai, D., M. Ferrer, N. Serpente, T. Idziorek, A. Dautry-Varsat, P. Debre, and G. Bismuth. 1992. Internalization of HIV glycoprotein gp120 is associated with down-modulation of membrane CD4 and p56^{lck} together with impairment of T cell activation. *J. Immunol.* 149: 285–294.
36. Chirmule, N., V. Kalyanaraman, N. Oyaizu, and S. Pahwa. 1988. Inhibitory influences of envelope glycoproteins of HIV-1 on normal immune responses. *J. Acquir. Immune Defic. Syndr.* 1: 425–430.
37. Diamond, D. C., B. P. Sleckman, T. Gregory, L. A. Lasky, J. L. Greenstein, and S. J. Burakoff. 1988. Inhibition of CD4+ T cell function by the HIV envelope protein, gp120. *J. Immunol.* 141: 3715–3717.
38. Mittler, R. S., and M. K. Hoffmann. 1989. Synergism between HIV gp120 and gp120-specific antibody in blocking human T cell activation. *Science* 245: 1380–1382.
39. Nyakeriga, A. M., C. J. Fichtenbaum, J. Goebel, S. A. Nicolaou, L. Conforti, and C. A. Chougnet. 2009. Engagement of the CD4 receptor affects the redistribution of Lck to the immunological synapse in primary T cells: implications for T-cell activation during human immunodeficiency virus type 1 infection. *J. Virol.* 83: 1193–1200.
40. Oyaizu, N., N. Chirmule, V. S. Kalyanaraman, W. W. Hall, R. Pahwa, M. Shuster, and S. Pahwa. 1990. Human immunodeficiency virus type 1 envelope glycoprotein gp120 produces immune defects in CD4+ T lymphocytes by inhibiting interleukin 2 mRNA. *Proc. Natl. Acad. Sci. USA* 87: 2379–2383.
41. Theodore, A. C., H. Kornfeld, R. P. Wallace, and W. W. Cruikshank. 1994. CD4 modulation of noninfected human T lymphocytes by HIV-1 envelope glycoprotein gp120: contribution to the immunosuppression seen in HIV-1 infection by induction of CD4 and CD3 unresponsiveness. *J. Acquir. Immune Defic. Syndr.* 7: 899–907.
42. Chirmule, N., T. W. McCloskey, R. Hu, V. S. Kalyanaraman, and S. Pahwa. 1995. HIV gp120 inhibits T cell activation by interfering with expression of costimulatory molecules CD40 ligand and CD80 (B71). *J. Immunol.* 155: 917–924.
43. Marschner, S., T. Hünig, J. C. Cambier, and T. H. Finkel. 2002. Ligation of human CD4 interferes with antigen-induced activation of primary T cells. *Immunol. Lett.* 82: 131–139.
44. Kornfeld, H., W. W. Cruikshank, S. W. Pyle, J. S. Berman, and D. M. Center. 1988. Lymphocyte activation by HIV-1 envelope glycoprotein. *Nature* 335: 445–448.
45. Chirmule, N., H. Goonewardena, S. Pahwa, R. Pasieka, V. S. Kalyanaraman, and S. Pahwa. 1995. HIV-1 envelope glycoproteins induce activation of activated protein-1 in CD4+ T cells. *J. Biol. Chem.* 270: 19364–19369.
46. Juszczak, R. J., H. Turchin, A. Truneh, J. Culp, and S. Kassis. 1991. Effect of human immunodeficiency virus gp120 glycoprotein on the association of the protein tyrosine kinase p56^{lck} with CD4 in human T lymphocytes. *J. Biol. Chem.* 266: 11176–11183.
47. Hivroz, C., F. Mazerolles, M. Soula, R. Fagard, S. Graton, S. Meloche, R. P. Sekaly, and A. Fischer. 1993. Human immunodeficiency virus gp120 and derived peptides activate protein tyrosine kinase p56^{lck} in human CD4 T lymphocytes. *Eur. J. Immunol.* 23: 600–607.
48. Klasse, P. J., and J. P. Moore. 2004. Is there enough gp120 in the body fluids of HIV-1-infected individuals to have biologically significant effects? *Virology* 323: 1–8.
49. Oravecz, T., and M. A. Norcross. 1993. Costimulatory properties of the human CD4 molecule: enhancement of CD3-induced T cell activation by human immunodeficiency virus type 1 through viral envelope glycoprotein gp120. *AIDS Res. Hum. Retroviruses* 9: 945–955.
50. Rosenstein, Y., S. J. Burakoff, and S. H. Herrmann. 1990. HIV-gp120 can block CD4-class II MHC-mediated adhesion. *J. Immunol.* 144: 526–531.
51. Piatier-Tonneau, D., L. N. Gastinel, G. Moussy, B. Bénichou, F. Amblard, P. Vaigot, and C. Auffray. 1991. Mutations in the D strand of the human CD4 V1 domain affect CD4 interactions with the human immunodeficiency virus envelope glycoprotein gp120 and HLA class II antigens similarly. *Proc. Natl. Acad. Sci. USA* 88: 6858–6862.
52. Goldman, F., W. A. Jensen, G. L. Johnson, L. Heasley, and J. C. Cambier. 1994. gp120 Ligation of CD4 induces p56^{lck} activation and TCR desensitization independent of TCR tyrosine phosphorylation. *J. Immunol.* 153: 2905–2917.
53. Goldman, F., J. Crabtree, C. Hollenback, and G. Koretzky. 1997. Sequestration of p56^{lck} by gp120, a model for TCR desensitization. *J. Immunol.* 158: 2017–2024.
54. Amadori, A., G. De Silvestro, R. Zamarchi, M. L. Veronese, M. R. Mazza, G. Schiavo, M. Panozzo, A. De Rossi, L. Ometto, J. Mous, et al. 1992. CD4 epitope masking by gp120/anti-gp120 antibody complexes. A potential mechanism for CD4+ cell function down-regulation in AIDS patients. *J. Immunol.* 148: 2709–2716.
55. Daniel, V., C. Süsal, R. Weimer, S. Zipperle, M. Kröpelin, R. Zimmermann, A. Huth-Kühne, and G. Opelz. 1996. Association of T cell dysfunction with the presence of IgG autoantibodies on CD4+ lymphocytes in haemophilia patients; results of a 10-year study. *Clin. Exp. Immunol.* 104: 4–10.
56. Daniel, V., C. Süsal, R. Weimer, R. Zimmermann, A. Huth-Kühne, and G. Opelz. 1993. Association of T cell and macrophage dysfunction with surface

gp 120-immunoglobulin-complement complexes in HIV-infected patients. *Clin. Exp. Immunol.* 93: 152–156.
57. Daniel, V., M. Sadeghi, C. Naujokat, R. Weimer, A. Huth-Kühne, R. Zimmermann, and G. Opelz. 2004. Evidence for autoantibody-induced CD4 depletion mediated by apoptotic and non-apoptotic mechanisms in HIV-positive long-term surviving haemophilia patients. *Clin. Exp. Immunol.* 135: 94–104.
58. Daniel, V., A. Melk, C. Süsal, R. Weimer, R. Zimmermann, A. Huth-Kühne, and G. Opelz. 1999. CD4 depletion in HIV-infected haemophilia patients is associated with rapid clearance of immune complex-coated $CD4^+$ lymphocytes. *Clin. Exp. Immunol.* 115: 477–484.
59. Suzuki, Y., H. Gatanaga, N. Tachikawa, and S. Oka. 2014. Slow turnover of HIV-1 receptors on quiescent $CD4^+$ T cells causes prolonged surface retention of gp120 immune complexes in vivo. *PLoS ONE* 9: e86479.
60. Schoeni-Affolter, F., B. Ledergerber, M. Rickenbach, C. Rudin, H. F. Günthard, A. Telenti, H. Furrer, S. Yerly, and P. Francioli, Swiss HIV Cohort Study. 2010. Cohort profile: the Swiss HIV Cohort study. *Int. J. Epidemiol.* 39: 1179–1189.
61. Rieder, P., B. Joos, A. U. Scherrer, H. Kuster, D. Braun, C. Grube, B. Niederost, C. Leemann, S. Gianella, K. J. Metzner, et al. 2011. Characterization of human immunodeficiency virus type 1 (HIV-1) diversity and tropism in 145 patients with primary HIV-1 infection. *Clin. Infect. Dis.* 53: 1271–1279.
62. Rusert, P., H. Kuster, B. Joos, B. Misselwitz, C. Gujer, C. Leemann, M. Fischer, G. Stiegler, H. Katinger, W. C. Olson, et al. 2005. Virus isolates during acute and chronic human immunodeficiency virus type 1 infection show distinct patterns of sensitivity to entry inhibitors. *J. Virol.* 79: 8454–8469.
63. Trkola, A., M. Purtscher, T. Muster, C. Ballaun, A. Buchacher, N. Sullivan, K. Srinivasan, J. Sodroski, J. P. Moore, and H. Katinger. 1996. Human monoclonal antibody 2G12 defines a distinctive neutralization epitope on the gp120 glycoprotein of human immunodeficiency virus type 1. *J. Virol.* 70: 1100–1108.
64. Scheid, J. F., H. Mouquet, N. Feldhahn, M. S. Seaman, K. Velinzon, J. Pietzsch, R. G. Ott, R. M. Anthony, H. Zebroski, A. Hurley, et al. 2009. Broad diversity of neutralizing antibodies isolated from memory B cells in HIV-infected individuals. *Nature* 458: 636–640.
65. Pantophlet, R., E. Ollmann Saphire, P. Poignard, P. W. Parren, I. A. Wilson, and D. R. Burton. 2003. Fine mapping of the interaction of neutralizing and non-neutralizing monoclonal antibodies with the CD4 binding site of human immunodeficiency virus type 1 gp120. *J. Virol.* 77: 642–658.
66. Barbas, C. F., III, E. Björling, F. Chiodi, N. Dunlop, D. Cababa, T. M. Jones, S. L. Zebedee, M. A. Persson, P. L. Nara, E. Norrby, et al. 1992. Recombinant human Fab fragments neutralize human type 1 immunodeficiency virus in vitro. *Proc. Natl. Acad. Sci. USA* 89: 9339–9343.
67. Schmitz, M. L., and D. Krappmann. 2006. Controlling NF-κB activation in T cells by costimulatory receptors. *Cell Death Differ.* 13: 834–842.
68. Smith-Garvin, J. E., G. A. Koretzky, and M. S. Jordan. 2009. T cell activation. *Annu. Rev. Immunol.* 27: 591–619.
69. McClure, M. O., Q. J. Sattentau, P. C. Beverley, J. P. Hearn, A. K. Fitzgerald, A. J. Zuckerman, and R. A. Weiss. 1987. HIV infection of primate lymphocytes and conservation of the CD4 receptor. *Nature* 330: 487–489.
70. Sattentau, Q. J., A. G. Dalgleish, R. A. Weiss, and P. C. Beverley. 1986. Epitopes of the CD4 antigen and HIV infection. *Science* 234: 1120–1123.
71. Kitchen, S. G., Y. D. Korin, M. D. Roth, A. Landay, and J. A. Zack. 1998. Costimulation of naive $CD8^+$ lymphocytes induces CD4 expression and allows human immunodeficiency virus type 1 infection. *J. Virol.* 72: 9054–9060.
72. Zamoyska, R., A. Basson, A. Filby, G. Legname, M. Lovatt, and B. Seddon. 2003. The influence of the src-family kinases, Lck and Fyn, on T cell differentiation, survival and activation. *Immunol. Rev.* 191: 107–118.
73. Balagopalan, L., N. P. Coussens, E. Sherman, L. E. Samelson, and C. L. Sommers. 2010. The LAT story: a tale of cooperativity, coordination, and choreography. *Cold Spring Harb. Perspect. Biol.* 2: a005512.
74. Lyerly, H. K., D. L. Reed, T. J. Matthews, A. J. Langlois, P. A. Ahearne, S. R. Petteway, Jr., and K. J. Weinhold. 1987. Anti-GP 120 antibodies from HIV seropositive individuals mediate broadly reactive anti-HIV ADCC. *AIDS Res. Hum. Retroviruses* 3: 409–422.
75. Doria-Rose, N. A., R. M. Klein, M. M. Manion, S. O'Dell, A. Phogat, B. Chakrabarti, C. W. Hallahan, S. A. Migueles, J. Wrammert, R. Ahmed, et al. 2009. Frequency and phenotype of human immunodeficiency virus envelope-specific B cells from patients with broadly cross-neutralizing antibodies. *J. Virol.* 83: 188–199.
76. McCoy, L. E., and R. A. Weiss. 2013. Neutralizing antibodies to HIV-1 induced by immunization. *J. Exp. Med.* 210: 209–223.
77. Burton, D. R., J. Pyati, R. Koduri, S. J. Sharp, G. B. Thornton, P. W. Parren, L. S. Sawyer, R. M. Hendry, N. Dunlop, P. L. Nara, et al. 1994. Efficient neutralization of primary isolates of HIV-1 by a recombinant human monoclonal antibody. *Science* 266: 1024–1027.
78. Monks, C. R., B. A. Freiberg, H. Kupfer, N. Sciaky, and A. Kupfer. 1998. Three-dimensional segregation of supramolecular activation clusters in T cells. *Nature* 395: 82–86.
79. Seminario, M. C., and S. C. Bunnell. 2008. Signal initiation in T-cell receptor microclusters. *Immunol. Rev.* 221: 90–106.
80. Dustin, M. L., and J. T. Groves. 2012. Receptor signaling clusters in the immune synapse. *Annu. Rev. Biophys.* 41: 543–556.
81. Saito, T., and T. Yokosuka. 2006. Immunological synapse and microclusters: the site for recognition and activation of T cells. *Curr. Opin. Immunol.* 18: 305–313.
82. Martín-Cófreces, N. B., B. Alarcón, and F. Sánchez-Madrid. 2011. Tubulin and actin interplay at the T cell and antigen-presenting cell interface. *Front. Immunol.* 2: 24.
83. Billadeau, D. D., J. C. Nolz, and T. S. Gomez. 2007. Regulation of T-cell activation by the cytoskeleton. *Nat. Rev. Immunol.* 7: 131–143.
84. Dustin, M. L., and J. A. Cooper. 2000. The immunological synapse and the actin cytoskeleton: molecular hardware for T cell signaling. *Nat. Immunol.* 1: 23–29.
85. Wülfing, C., and M. M. Davis. 1998. A receptor/cytoskeletal movement triggered by costimulation during T cell activation. *Science* 282: 2266–2269.
86. Sancho, D., M. Vicente-Manzanares, M. Mittelbrunn, M. C. Montoya, M. Gordón-Alonso, J. M. Serrador, and F. Sánchez-Madrid. 2002. Regulation of microtubule-organizing center orientation and actomyosin cytoskeleton rearrangement during immune interactions. *Immunol. Rev.* 189: 84–97.
87. Martín-Cófreces, N. B., J. Robles-Valero, J. R. Cabrero, M. Mittelbrunn, M. Gordón-Alonso, C. H. Sung, B. Alarcón, J. Vázquez, and F. Sánchez-Madrid. 2008. MTOC translocation modulates IS formation and controls sustained T cell signaling. *J. Cell Biol.* 182: 951–962.
88. Kupfer, A., S. L. Swain, and S. J. Singer. 1987. The specific direct interaction of helper T cells and antigen-presenting B cells. II. Reorientation of the microtubule organizing center and reorganization of the membrane-associated cytoskeleton inside the bound helper T cells. *J. Exp. Med.* 165: 1565–1580.
89. Filipp, D., B. L. Leung, J. Zhang, A. Veillette, and M. Julius. 2004. Enrichment of lck in lipid rafts regulates colocalized fyn activation and the initiation of proximal signals through TCRαβ. *J. Immunol.* 172: 4266–4274.
90. Kusumi, A., H. Ike, C. Nakada, K. Murase, and T. Fujiwara. 2005. Single-molecule tracking of membrane molecules: plasma membrane compartmentalization and dynamic assembly of raft-philic signaling molecules. *Semin. Immunol.* 17: 3–21.
91. Geppert, T. D., and P. E. Lipsky. 1991. Association of various T cell-surface molecules with the cytoskeleton. Effect of cross-linking and activation. *J. Immunol.* 146: 3298–3305.
92. Rozdzial, M. M., B. Malissen, and T. H. Finkel. 1995. Tyrosine-phosphorylated T cell receptor zeta chain associates with the actin cytoskeleton upon activation of mature T lymphocytes. *Immunity* 3: 623–633.
93. Zeyda, M., and T. M. Stulnig. 2006. Lipid Rafts & Co.: an integrated model of membrane organization in T cell activation. *Prog. Lipid Res.* 45: 187–202.
94. Valitutti, S., M. Dessing, K. Aktories, H. Gallati, and A. Lanzavecchia. 1995. Sustained signaling leading to T cell activation results from prolonged T cell receptor occupancy. Role of T cell actin cytoskeleton. *J. Exp. Med.* 181: 577–584.
95. Nara, P. L., R. R. Garrity, and J. Goudsmit. 1991. Neutralization of HIV-1: a paradox of humoral proportions. *FASEB J.* 5: 2437–2455.
96. Kupfer, A., and G. Dennert. 1984. Reorientation of the microtubule-organizing center and the Golgi apparatus in cloned cytotoxic lymphocytes triggered by binding to lysable target cells. *J. Immunol.* 133: 2762–2766.
97. Waterman, P. M., S. Marschner, E. Brandl, and J. C. Cambier. 2012. The inositol 5-phosphatase SHIP-1 and adaptors Dok-1 and 2 play central roles in CD4-mediated inhibitory signaling. *Immunol. Lett.* 143: 122–130.
98. McMichael, A. J., P. Borrow, G. D. Tomaras, N. Goonetilleke, and B. F. Haynes. 2010. The immune response during acute HIV-1 infection: clues for vaccine development. *Nat. Rev. Immunol.* 10: 11–23.
99. Scheid, J. F., H. Mouquet, B. Ueberheide, R. Diskin, F. Klein, T. Y. Oliveira, J. Pietzsch, D. Fenyo, A. Abadir, K. Velinzon, et al. 2011. Sequence and structural convergence of broad and potent HIV antibodies that mimic CD4 binding. *Science* 333: 1633–1637.
100. Kwong, P. D., and J. R. Mascola. 2012. Human antibodies that neutralize HIV-1: identification, structures, and B cell ontogenies. *Immunity* 37: 412–425.
101. Wu, X., T. Zhou, J. Zhu, B. Zhang, I. Georgiev, C. Wang, X. Chen, N. S. Longo, M. Louder, K. McKee, et al; NISC Comparative Sequencing Program. 2011. Focused evolution of HIV-1 neutralizing antibodies revealed by structures and deep sequencing. *Science* 333: 1593–1602.
102. Lynch, R. M., L. Tran, M. K. Louder, S. D. Schmidt, M. Cohen, R. Dersimonian, Z. Euler, E. S. Gray, S. Abdool Karim, J. Kirchherr, et al; CHAVI 001 Clinical Team Members. 2012. The development of CD4 binding site antibodies during HIV-1 infection. *J. Virol.* 86: 7588–7595.
103. Schnittman, S. M., H. C. Lane, J. Greenhouse, J. S. Justement, M. Baseler, and A. S. Fauci. 1990. Preferential infection of $CD4^+$ memory T cells by human immunodeficiency virus type 1: evidence for a role in the selective T-cell functional defects observed in infected individuals. *Proc. Natl. Acad. Sci. USA* 87: 6058–6062.
104. Meyaard, L., S. A. Otto, I. P. Keet, M. T. Roos, and F. Miedema. 1994. Programmed death of T cells in human immunodeficiency virus infection. No correlation with progression to disease. *J. Clin. Invest.* 93: 982–988.
105. Klatt, N. R., N. Chomont, D. C. Douek, and S. G. Deeks. 2013. Immune activation and HIV persistence: implications for curative approaches to HIV infection. *Immunol. Rev.* 254: 326–342.

8. High-Throughput Sequencing of Human Immunoglobulin Variable Regions with Subtype Identification

The following publication was published in PLoS One in 2014. During my PhD I developed a multiplex bead-based assay to investigate binding antibodies against different epitopes of HIV-1 and delineating the isotype responsible for the binding activity. In the course of this work I detected the initial MPER-specific response against MPER followed by a robust IgG3 response against the same epitope. Time points from this patient were used in Figure 3 to prove the ability to reliably detect IgG subtypes with next-generation sequencing. In addition I was involved in critical reading of the manuscript.

OPEN ACCESS Freely available online

PLOS ONE

High-Throughput Sequencing of Human Immunoglobulin Variable Regions with Subtype Identification

Merle Schanz[1], Thomas Liechti[1], Osvaldo Zagordi[1], Enkelejda Miho[2], Sai T. Reddy[2], Huldrych F. Günthard[3], Alexandra Trkola[1], Michael Huber[1]*

1 Institute of Medical Virology, University of Zurich, Zurich, Switzerland, **2** Department of Biosystems Science and Engineering, ETH Zurich, Basel, Switzerland, **3** Division of Infectious Diseases and Hospital Epidemiology, University Hospital Zurich, University of Zurich, Zurich, Switzerland

Abstract

The humoral immune response plays a critical role in controlling infection, and the rapid adaptation to a broad range of pathogens depends on a highly diverse antibody repertoire. The advent of high-throughput sequencing technologies in the past decade has enabled insights into this immense diversity. However, not only the variable, but also the constant region of antibodies determines their *in vivo* activity. Antibody isotypes differ in effector functions and are thought to play a defining role in elicitation of immune responses, both in natural infection and in vaccination. We have developed an Illumina MiSeq high-throughput sequencing protocol that allows determination of the human IgG subtype alongside sequencing full-length antibody variable heavy chain regions. We thereby took advantage of the Illumina procedure containing two additional short reads as identifiers. By performing paired-end sequencing of the variable regions and customizing one of the identifier sequences to distinguish IgG subtypes, IgG transcripts with linked information of variable regions and IgG subtype can be retrieved. We applied our new method to the analysis of the IgG variable region repertoire from PBMC of an HIV-1 infected individual confirmed to have serum antibody reactivity to the Membrane Proximal External Region (MPER) of gp41. We found that IgG3 subtype frequencies in the memory B cell compartment increased after halted treatment and coincided with increased plasma antibody reactivity against the MPER domain. The sequencing strategy we developed is not restricted to analysis of IgG. It can be adopted for any Ig subtyping and beyond that for any research question where phasing of distant regions on the same amplicon is needed.

Citation: Schanz M, Liechti T, Zagordi O, Miho E, Reddy ST, et al. (2014) High-Throughput Sequencing of Human Immunoglobulin Variable Regions with Subtype Identification. PLoS ONE 9(11): e111726. doi:10.1371/journal.pone.0111726

Editor: Shan Lu, University of Massachusetts Medical Center, United States of America

Received May 27, 2014; **Accepted** October 6, 2014; **Published** November 3, 2014

Data Availability: The authors confirm that all data underlying the findings are fully available without restriction. The raw sequencing data have been uploaded to zenodo (doi:10.5281/zenodo.10863).

Funding: Funding was provided by the Swiss National Science Foundation (www.snf.ch) grant 310000–120739 and 310030–152663 to AT, a SystemsX.ch RTD grant (AntibodyX), and the Clinical Research Priority Program Viral Infectious Diseases of the University of Zurich (http://www.viralinfectiousdiseases.uzh.ch). The funders had no role in study design, data collection and analysis, decision to publish, or preparation of the manuscript.

Competing Interests: The authors have declared that no competing interests exist.

* Email: huber.michael@virology.uzh.ch

Introduction

In the past decade, the development of high-throughput sequencing technologies (Next Generation Sequencing, NGS) has largely influenced research possibilities in immunology. Sequencing of whole antibody repertoires has become feasible and affordable, offering new approaches to quantitatively study immune responses [1,2]. For example, the search for potent neutralizing antibodies against human immunodeficiency virus type 1 (HIV-1) and ways to elicit them by vaccination has in recent years funneled extensive research that increasingly relies on NGS of the IgG variable region, which enables high-resolution profiling of antibody repertoires and the evolution of neutralizing antibodies over time [3–8].

For immune effector functions, not only the variable part of an antibody is important, but also the different isotypes of the constant region. Antibodies of the same epitope specificity can therefore elicit different effector functions depending on the isotype. Antibody-dependent cell-mediated cytotoxicity (ADCC) for instance is most active with isotype IgG1 followed by IgG3 and IgA. Subtypes of IgG differentially protect mice from bacterial infection [9] and are associated with chikungunya virus clearance and long-term clinical protection [10]. An intriguing example of the potential importance of IgG subtypes for immune reaction and antibody elicitation is the membrane-proximal external region (MPER) of gp41 of HIV-1. All of the broadly neutralizing anti-MPER antibodies identified thus far, 4E10 and 2F5 [11] and the recently identified 10E8 [12], were originally isolated as IgG3. However, in the case of 4E10, the *in vitro* neutralization potency is higher for IgG1 and absent for IgM [13]. It was suggested that this is related to the longer hinge region and greater flexibility of the IgG3 subtype [14,15]. Of note, in the recent RV144 trial [16], the first phase III trial of an HIV-1 vaccine that reported some efficacy, anti-gp120-specific isotype selection was skewed towards IgG3 [17] and anti-HIV-1 IgG3 antibodies correlated with antiviral function [18]. These examples highlight the importance

of evaluating antibody specificity alongside subtype information when studying immune responses and developing vaccines.

The Illumina MiSeq platform is rapidly becoming the dominant sequencing system for antibody repertoires due to low error rates, long read lengths, and declining costs [2]. State of the art sequencing with Illumina technology currently allows for read lengths of 2×300 nucleotides on the widely used MiSeq platform. This is sufficient to sequence an antibody variable region from both ends with an overlap allowing combination of both reads to a full-length variable region. However, the available read length might not be enough for antibodies with a long heavy chain complementary determining region 3 (HCDR3) to also include determinants of the antibody subtype in the sequences, as they are located too far downstream in the constant region. In order to overcome this limitation, we use one of the indexing reads the Illumina technology applies not in its intended function as a sample identifier, but instead as a short extra read that identifies the IgG subtype. This way, we can retrieve full-length variable regions including the IgG subtype. Of note, in the same sequencing runs light chains and other desired heavy chain isotypes can be sequenced. The second Illumina index read is not modified and used as designed to allow analysis of multiple samples in a single run.

Methods

Primers

For the heavy chain, forward primers binding to the leader sequences and reverse primers in the constant region were used [6,19]. For the kappa light chain, primers binding in the leader region [19] and in the constant region were used. Lambda light chains were amplified with primers binding in the leader/variable [19] and in the joining region [20]. Our customized protocol uses sequencing adaptors and index sequences based on the Illumina (San Diego, CA) TruSeq HT setup. Four random nucleotides were inserted between the sequencing adaptor and the specific primer to increase diversity and help cluster identification on the Illumina MiSeq flow cell. The sequences of all primers are listed in Table 1. Primers were ordered HPL-purified from Microsynth AG (Balgach, Switzerland).

Clinical specimen

PBMC from healthy donors were purified from buffy coat obtained from the Zurich Blood Transfusion Service (www.zhbsd.ch). Cryopreserved PBMC from an HIV-1 infected individual, patient ZA159, who developed strong MPER specific antibody responses during disease progression (Liechti et al, in preparation), were obtained through the Zurich primary HIV infection (ZPHI) study [21]. BioSample accession numbers for the human subjects are SAMN02911274 to SAMN02911277.

Ethics statement

Cryopreserved PBMC were obtained from an adult participant enrolled in the Zurich Primary HIV-infection (ZPHI) study (http://clinicaltrials.gov, ID 5 NCT00537966) [21]. The study was approved by the ethics committee of the canton of Zurich and written informed consent was obtained from all participating individuals. Buffy coats from healthy donors were obtained from the Zurich Blood Transfusion Service (www.zhbsd.ch) under a protocol approved by the ethics committee of the canton of Zurich.

PCR amplification

Total RNA was extracted from $10 * 10^6$ PBMC (healthy donor) or $2 * 10^6$ PBMC (patient) using the RNeasy Mini Kit (Qiagen). cDNA was synthesized in a total volume of 40 ul using 400 U SuperscriptIII, 1 ug $Oligo(dT)_{15}$ primer, 2 ul dNTP mix (10 mM each nucleotide), 2 ul 0.1 M DTT and 1–10 ug RNA. Reverse transcription was performed at 65°C for five minutes, 50°C for 60 minutes and 70°C for 15 minutes. cDNA was stored at −20°C. Ig heavy, kappa and lambda genes were amplified in separate reactions. All PCR reactions were performed in volumes of 50 ul using 0.5 ul Phusion High-Fidelity DNA Polymerase (New England Biolabs), 1 ul dNTPs (10 mM each nucleotide) and 5 ul cDNA template. The first PCR reaction was performed with the forward primer mix (0.05–0.15 uM each primer) and 0.5 uM gene specific reverse primer. The temperature protocol was adapted from [22] and consisted of once 98°C for 60 s; 4 cycles of 98°C 10 s, 45°C 30 s, 72°C 30 s; 4 cycles of 98°C 10 s, 50°C 30 s, 72°C 30 s; 17 cycles of 98°C 10 s, 68°C 30 s, 72°C 30 s; once 72°C 10 min.

The second PCR was performed with the forward index adaptor primers (TS-D501 to TS-D508, depending on the number of indices needed) and two custom reverse primers for either the IgG heavy chains (TS7IgG(int)) or the light chains and heavy chains of other isotypes (TS7icIgGcSeq). The temperature protocol was once 98°C for 60 s; 4 cycles of 98°C 10 s, 55°C 30 s, 72°C 30 s; 4 cycles of 98°C 10 s, 60°C 30 s, 72°C 30 s; 17 cycles of 98°C 10 s, 72°C 30 s; once 72°C 10 min. The four different healthy donor preparations differed in their amplification strategies: prep 4 was amplified as described above, preps 1 and 2 were amplified with 1 ul cDNA template, prep 3 with 5 ul cDNA template. Preps 1, 2 and 3 were then amplified for 12, 25 and 12 cycles in the second PCR, respectively. Samples from sorted cells were amplified for 40 cycles in the first PCR.

The amplicons were purified using the QIAquick Gel Extraction Kit (Qiagen). Samples were quantitated using Quant-iT PicoGreen (Invitrogen, Carlsbad, CA), normalized to a concentration of 4 nM (based on an average length of about 525 nucleotides for light chains and 595 nucleotides for heavy chains) and pooled equimolar for sequencing.

Sequencing strategy

In Illumina high-throughput sequencing technology, the DNA insert to be sequenced is flanked on both sides by a primer binding site, a short index and an adapter for binding to the flow cell. Conventional use allows for paired-end sequencing (forward read 1 and reverse read 2) and dual multiplexing (index read 1 and index read 2) by four independent sequencing reactions. On the MiSeq system, custom primers for read 1, read 2 and for the index read 1 can be used optionally. The priming of index read 2 cannot be customized. Further, the number of cycles can be individually chosen for all four reads, as long as the sum is not more than 25 cycles higher than the capacity of the kit used (available kits range from 50–600 cycles). We used these features of the MiSeq system to sequence the variable region of immunoglobulins in a paired-end fashion, determined the subtype of IgGs via a 12 nucleotide long identifier read and multiplexed samples by an 8 nucleotide long index read (Figure 1).

The constant region of subtype IgG1 differs from IgG2/3/4 at position 47 (AAG (K) vs. AGG (R), Figure 2). IgG1/3 and IgG2/4 differ at position 57 (TCT (S) vs. TCC (S)). By sequencing this stretch of the constant region and defining the corresponding sequences as indices, subtypes IgG1, 2/4 and 3 can be differentiated. It is not possible to distinguish IgG2 and 4 at this position; however, they can be separated based on the first triplet

Table 1. List of PCR and sequencing primers.

IGH forward	Seq5N4-VH1LA	CTTTCCCTACACGACGCTCTTCCGATCTNNNNATGGACTGGACCTGGAGGAT
	Seq5N4-VH1LB	CTTTCCCTACACGACGCTCTTCCGATCTNNNNATGGACTGGACCTGGAGCAT
	Seq5N4-VH1LC	CTTTCCCTACACGACGCTCTTCCGATCTNNNNATGGACTGGACCTGGAGAAT
	Seq5N4-VH1LD	CTTTCCCTACACGACGCTCTTCCGATCTNNNNGGTTCCTCTTTGTGGTGGC
	Seq5N4-VH1LE	CTTTCCCTACACGACGCTCTTCCGATCTNNNNATGGACTGGACCTGGAGGGT
	Seq5N4-VH1LF	CTTTCCCTACACGACGCTCTTCCGATCTNNNNATGGACTGGATTTGGAGGAT
	Seq5N4-VH1LG	CTTTCCCTACACGACGCTCTTCCGATCTNNNNAGGTTCCTCTTTGTGGTGGCAG
	Seq5N4-VH3LA	CTTTCCCTACACGACGCTCTTCCGATCTNNNNTAAAAGGTGTCCAGTGT
	Seq5N4-VH3LB	CTTTCCCTACACGACGCTCTTCCGATCTNNNNTAAGAGGTGTCCAGTGT
	Seq5N4-VH3LC	CTTTCCCTACACGACGCTCTTCCGATCTNNNNTAGAAGGTGTCCAGTGT
	Seq5N4-VH3LD	CTTTCCCTACACGACGCTCTTCCGATCTNNNNGCTATTTTTAAAGGTGTCCAGTGT
	Seq5N4-VH3LE	CTTTCCCTACACGACGCTCTTCCGATCTNNNNTACAAGGTGTCCAGTGT
	Seq5N4-VH3LF	CTTTCCCTACACGACGCTCTTCCGATCTNNNNTTAAAGCTGTCCAGTGT
	Seq5N4-VH4LA	CTTTCCCTACACGACGCTCTTCCGATCTNNNNATGAAACACCTGTGGTTCTTCC
	Seq5N4-VH4LB	CTTTCCCTACACGACGCTCTTCCGATCTNNNNATGAAACACCTGTGGTTCTT
	Seq5N4-VH4LC	CTTTCCCTACACGACGCTCTTCCGATCTNNNNATGAAGCACCTGTGGTTCTT
	Seq5N4-VH4LD	CTTTCCCTACACGACGCTCTTCCGATCTNNNNATGAAACATCTGTGGTTCTT
	Seq5N4-VH5LA	CTTTCCCTACACGACGCTCTTCCGATCTNNNNTTCTCCAAGGAGTCTGT
	Seq5N4-VH5LB	CTTTCCCTACACGACGCTCTTCCGATCTNNNNCCTCCACAGTGAGAGTCTG
	Seq5N4-VH6LA	CTTTCCCTACACGACGCTCTTCCGATCTNNNNATGTCTGTCTCCTTCCTCATC
	Seq5N4-VH7LA	CTTTCCCTACACGACGCTCTTCCGATCTNNNNGGCAGCAGCAACAGGTGCCCA
IGL forward	Seq5N4-VL1	CTTTCCCTACACGACGCTCTTCCGATCTNNNNGGTCCTGGGCCCAGTCTGTGCTG
	Seq5N4-VL2	CTTTCCCTACACGACGCTCTTCCGATCTNNNNGGTCCTGGGCCCAGTCTGCCCTG
	Seq5N4-VL3	CTTTCCCTACACGACGCTCTTCCGATCTNNNNGCTCTGTGACCTCCTATGAGCTG
	Seq5N4-VL45	CTTTCCCTACACGACGCTCTTCCGATCTNNNNGGTCTCTCTCSCAGCyTGTGCTG
	Seq5N4-VL6	CTTTCCCTACACGACGCTCTTCCGATCTNNNNGTTCTTGGGCCAATTTTATGCTG
	Seq5N4-VL7	CTTTCCCTACACGACGCTCTTCCGATCTNNNNGGTCCAATTCyCAGGCTGTGGTG
	Seq5N4-VL8	CTTTCCCTACACGACGCTCTTCCGATCTNNNNGAGTGGATTCTCAGACTGTGGTG
IGK forward	Seq5N4-VK12	CTTTCCCTACACGACGCTCTTCCGATCTNNNNATGAGGSTCCCyGCTCAGCTGCTGG
	Seq5N4-VK3	CTTTCCCTACACGACGCTCTTCCGATCTNNNNCTCTTCCTCCTGCTACTCTGGCTCCCAG
	Seq5N4-VK4	CTTTCCCTACACGACGCTCTTCCGATCTNNNNATTTCTCTGTTGCTCTGGATCTCTG
IGG reverse	TS7IgG(int)	CAAGCAGAAGACGGCATACGAGATccGTTCGGGGAAGTAGTCCTTGAC
IGL reverse	IgGcSeqhuVL1-rev	GGGAAGACCGATGGGCCCTTGGTNNNNTAGGACGGTSASCTTGGTCC
	IgGcSeqhuVL7-rev	GGGAAGACCGATGGGCCCTTGGTNNNNGAGGACGGTCAGCTGGGTGC
IGK reverse	IgGcSeqhuVKC-rev	GGGAAGACCGATGGGCCCTTGGTNNNNAGATGGTGCAGCCACAGTTC
IGM reverse	IgGcSeqhuIgM-rev	GGGAAGACCGATGGGCCCTTGGTNNNNGGTTGGGGCGGATGCACTCC
IGA reverse	IgGcSeqIgA-rev	GGGAAGACCGATGGGCCCTTGGTNNNNTTGGGGCTGGTCGGGGATGC
indexing forward	TS-D501	AATGATACGGCGACCACCGAGATCTACACTATAGCCTACACTCTTTCCCTA CACGACGCTCTTCCGATCT
	TS-D502	AATGATACGGCGACCACCGAGATCTACACATAGAGGCACACTCTTTCCCTA CACGACGCTCTTCCGATCT
	TS-D503	AATGATACGGCGACCACCGAGATCTACACCCTATCCTACACTCTTTCCCTA CACGACGCTCTTCCGATCT
	TS-D504	AATGATACGGCGACCACCGAGATCTACACGGCTCTGAACACTCTTTCCCTA CACGACGCTCTTCCGATCT
	TS-D505	AATGATACGGCGACCACCGAGATCTACACAGGCGAAGACACTCTTTCCCTA CACGACGCTCTTCCGATCT
	TS-D506	AATGATACGGCGACCACCGAGATCTACACTAATCTTAACACTCTTTCCCTA CACGACGCTCTTCCGATCT
	TS-D507	AATGATACGGCGACCACCGAGATCTACACCAGGACGTACACTCTTTCCCTA CACGACGCTCTTCCGATCT
	TS-D508	AATGATACGGCGACCACCGAGATCTACACGTACTGACACACTCTTTCCCTA CACGACGCTCTTCCGATCT

Table 1. Cont.

klMA indexing reverse	TS7icIgGcSeq	CAAGCAGAAGACGGCATACGAGATTCTCCACGAGAAGGAGGAGGGTGCCA GGGGGAAGACCGATGGGCCCTTGGT
custom sequencing	IgGcSeq	CCAGGGGGAAGACCGATGGGCCCTTGGT
	IgGcInd	CCATCGGTCTTCCCCCTGGCRCCCTSCTCC

doi:10.1371/journal.pone.0111726.t001

of the constant region (GCC (A) vs. GCT (A), Figure 2). This way, all four IgG subtypes can be called unequivocally. To make sequencing of light chains and heavy chain isotypes IgM and IgA possible in the same run, the 5′ end of the IgG constant region (nucleotides 7–45) was added into the respective reverse primers so that the same read 2 custom primer could be used for sequencing of IgG, IgA, IgM and kappa (k) and lambda (l) light chains. A separate index (klMA), which is complementary to the IgG1 index to increase base variability during sequencing, was used for those chains.

Illumina MiSeq sequencing

Pooled samples were denatured with NaOH according to the protocol (Illumina), diluted with hybridization buffer HT1 to a final dilution of 10 pM, spiked with 5% of PhiX control library and loaded into a 500 cycle version 2 reagent cartridge. Custom primers IgGcSeq and IgGcInd for the read 2 and the indexing read, respectively, were diluted to 0.5 uM in hybridization buffer HT1 and 600 ul loaded into well 19 (index read 1, IgGcInd) and well 20 (read 2, IgGcSeq) of the reagent cartridge. The sample sheet was adapted manually to allow any sequence (N_{12}) as custom index 1. Sequencing was performed for 2 * 250 cycles. The workflow was set to "GenerateFASTQ". The raw sequencing data have been uploaded to zenodo (doi:10.5281/zenodo.10863).

Data analysis

In order to obtain fastq files also for the index reads, "CreateFastqForIndexReads" in the MiSeqReporter.exe.config file was set to 1 (true). Reads were first de-multiplexed by Illumina MiSeq Reporter (version 2.4.60) based on index 2 that distinguishes the different samples. Secondly, reads were assigned to the different subtypes using a python script (available here https://gist.github.com/ozagordi/11180835) as follows: IgG1, IgG3 and light chains or heavy chains of other isotypes (klMA) were identified by their index 1; IgG2 and IgG4 were additionally discriminated based on the fourth nucleotide of the second read (IgG2 if 'G', IgG4 if 'A', read 2 is reverse complementary). For the IgG subtype indices a perfect match was required, for the klMA

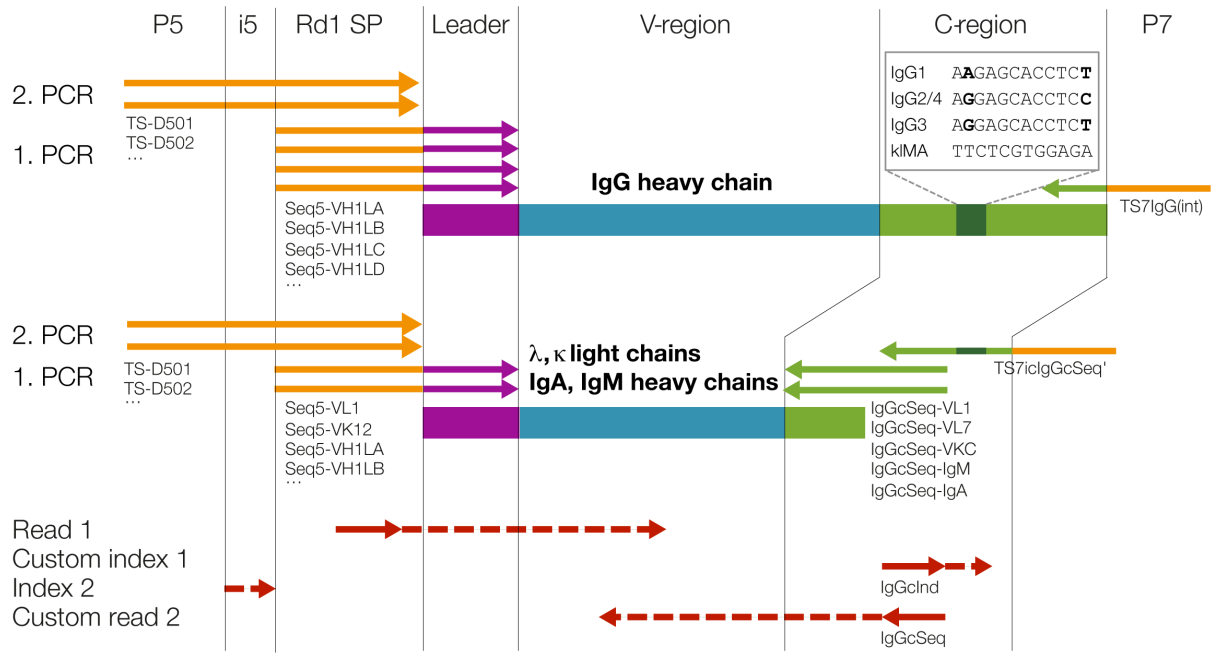

Figure 1. Amplification of Ig variable regions and high-throughput sequencing with subtype information. Antibody heavy and light chain genes are shown schematically with leader regions in purple, variable (V-) regions in blue and constant (C-) regions in green. Ig heavy, kappa and lambda light chain genes were amplified in separate reactions with family specific primers (represented by arrows) binding to leader and constant region. Primer names are indicated exemplarily below the arrows and a complete list of all primers used can be found in Table 1. Sequencing adaptors essential for the Illumina platform (flow cell binding sites P5 and P7, the index 2 region i5 and the read 1 sequencing primer binding site Rd1 SP, illustrated in orange) were added by primer extension during a second PCR reaction, except for the IgG reverse primer TS7IgG(int) which contained an adaptor and was used for both amplifications. Purified libraries were then sequenced using standard Illumina MiSeq primers for read 1 and index 2, and customized primers for index 1 and read 2 (sequencing primers are shown in red and regions sequenced with red dashed arrows).
doi:10.1371/journal.pone.0111726.g001

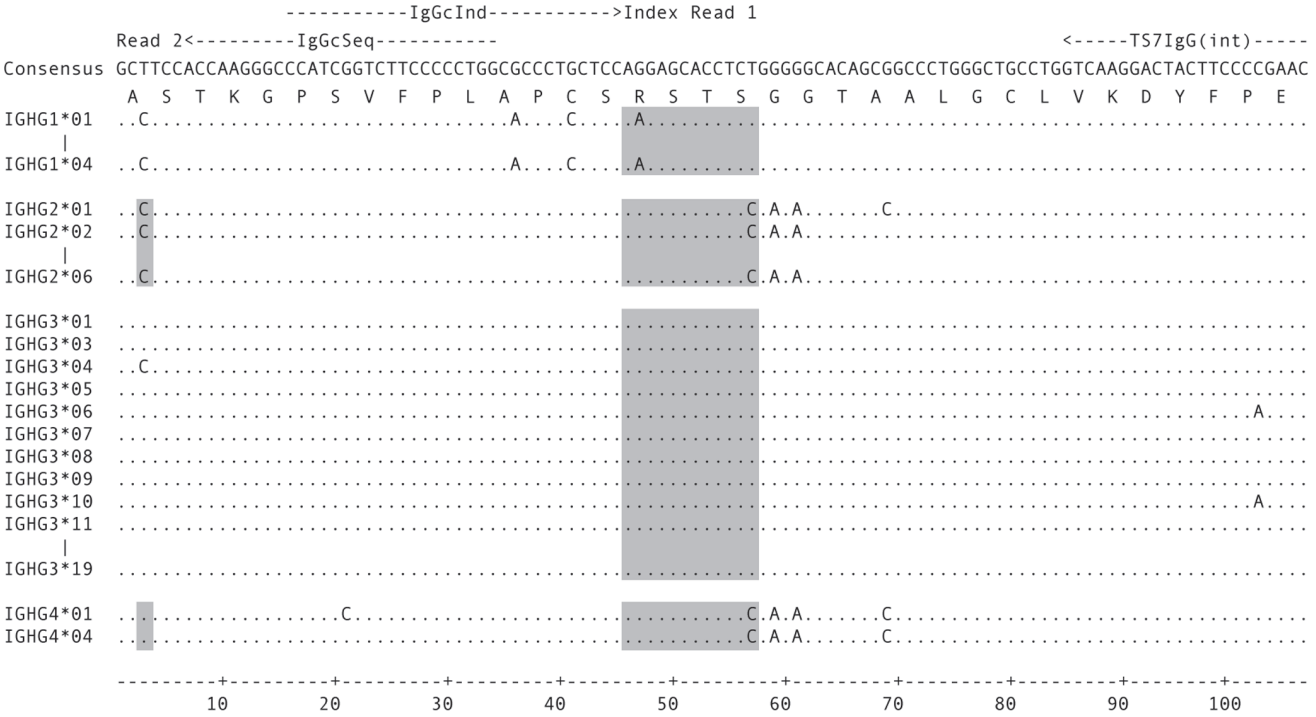

Figure 2. Determinants of IgG subtype in the constant region. IgG1 to IgG4 CH1 regions were obtained from IMGT/GENE-DB [34]. Only the first 107 nucleotides of the constant region are shown. Some alleles identical in this section have been omitted. Binding sites of the IgG reverse primer (TS7IgG(int)) used for library preparation and the custom sequencing and indexing primers (IgGcSeq and IgGcInd, respectively) are represented by dashed arrows on top. The full index 1 and the start of read 2 are indicated. Regions used for subtype assignment are shaded.
doi:10.1371/journal.pone.0111726.g002

index one mismatch was allowed. Reads not matching above criteria were classified as undetermined. Forward and reverse reads of a corresponding pair were stitched together using PANDAseq [23] with a minimal overlap of 10 nucleotides and analyzed by IMGT/HighV-QUEST [24]. Subtype frequencies were calculated as the percentage of completely indexed and full-length Ig variable region rearrangements.

Staining and cell sorting

Healthy donor PBMC were thawed, washed and split into four samples. Staining for IgG subtypes was performed in PBS/1% FCS at 4°C in the dark for 15 minutes using the following antibodies and dyes: anti-CD19 V500 (BD Horizon), anti-CD3 APC-Cy7 (BioLegend), anti-CD14 APC-Cy7 (BioLegend), LIVE/DEAD Near-IR Dead Cell Stain (Molecular Probes), anti-CD16 APC-Cy7 (BioLegend), anti-IgD PE-Cy5 (BioLegend, labeled in-house) and either anti-IgG1 PE, anti-IgG2 PE, anti-IgG3 PE or anti-IgG4 PE (all from SouthernBiotech). Cells were washed twice, re-suspended in PBS/1% FCS and cells gated for CD3/14/16/Dead$^-$ CD19$^+$ IgD$^-$ and positive for one of the IgG subtypes were sorted on a FACSAriaIII (Becton Dickinson). Sorted cells were frozen at −80°C as dry pellets prior to analysis.

Results

Validation of high-throughput immunoglobulin variable region sequencing with subtype identification

We developed a high-throughput method for the Illumina MiSeq system to sequence the full variable region of immunoglobulins in a paired-end fashion and identify at the same time the subtype of IgGs via a 12 nucleotide long custom index read (Figure 1). In order to test our sequencing strategy, we sequenced IgG heavy and light chains from PBMC from a healthy donor and an HIV-1 infected individual (ZA159 week 213, see below). The healthy donor sample was amplified in four separate reactions using different PCR conditions and cDNA input (see methods) to confirm the robustness of the IgG subtype assignment. We focused on assigning IgG subtypes and therefore did not sequence light chains for preparations 1–3. Sequencing of the five samples yielded a total of 10'249'237 passing filter reads.

19.3% (1'981'155) of the paired-end reads could not be demultiplexed to one of the five samples and were categorized as undetermined in regard of sample (Table 2). However, most of these undetermined reads (1'381'101, 13.5% of total reads) had an index identical to the TruSeq Universal primer and were confirmed to be mostly PhiX control reads (data not shown). The high number of undetermined reads therefore results from high PhiX concentrations and not from problems associated with sample preparation or library generation.

IgG subtype assignment based on index read 1 and the first triplet of the constant region sequenced in read 2 resulted in 6 categories (IgG1, IgG2, IgG3, IgG4, klMA, undetermined reads) for each sample (Table 2, column "Subtype assigned read pairs"). Of all read pairs demultiplexed to a sample, 97.5% (8'063'436) were successfully assigned to one of the IgG subtypes or the light chains.

To assemble full-length variable region sequences, corresponding paired end reads were combined with PANDAseq [23]. The overlap of reads peaked at about 100 nucleotides for heavy chains and at about 100 and 150 nucleotides for kappa and lambda light chains, respectively. 96.7% of all the read pairs overlapped (Table 2, column "Sequences after PANDAseq"). Sequences were subjected to IMGT analysis. On average, 98% of both heavy and

Table 2. Read numbers and subtype frequencies.

Sample	Subtype	Subtype assigned read pairs	Sequences after PANDAseq	Rearranged variable regions	IgG subtypes per sample
Healthy donor prep 1	IgG1	529′390	515′758	505′942	56.3%
	IgG2	369′741	360′472	354′751	39.5%
	IgG3	36′604	35′620	34′920	3.9%
	IgG4	3′785	3′645	3′572	0.4%
	klMA	nd	nd	nd	na
	Undet(b)	11′577	na	na	na
Healthy donor prep 2	IgG1	692′673	674′590	660′899	55.9%
	IgG2	488′483	475′851	467′958	39.6%
	IgG3	50′454	48′880	47′773	4.0%
	IgG4	6′191	5′968	5′859	0.5%
	klMA	nd	nd	nd	na
	Undet(b)	18′326	na	na	na
Healthy donor prep 3	IgG1	641′364	623′522	611′013	55.9%
	IgG2	453′471	441′108	433′565	39.7%
	IgG3	46′361	44′911	43′848	4.0%
	IgG4	5′386	5′155	5′030	0.5%
	klMA	nd	nd	nd	na
	Undet(b)	18′149	na	na	na
Healthy donor prep 4	IgG1	699′378	679′819	665′267	56.3%
	IgG2	481′592	468′433	460′214	39.0%
	IgG3	52′028	50′328	49′024	4.2%
	IgG4	7′199	6′900	6′695	0.6%
	klMA	1′317′918	1′257′301	1′210′698	na
	Undet(b)	84′941	na	na	na
ZA159 (week 213)	IgG1	677′787	659′884	646′977	65.8%
	IgG2	183′718	178′800	175′718	17.9%
	IgG3	163′839	158′878	155′704	15.8%
	IgG4	4′487	4′366	4′211	0.4%
	klMA	1′151′587	1′097′762	1′053′604	na
	Undet(b)	71′653	na	na	na
Undet (a)		1′981′155	na	na	na
Total reads		10′249′237	7′797′951	7′603′242	

a) Undetermined in regard of sample.
b) Undetermined in regard of subtype.
nd = not done.
na = not applicable.
doi:10.1371/journal.pone.0111726.t002

light chain sequences could be assigned to antibody variable regions. The median heavy chain variable region length in our dataset was approximately 360 nucleotides. In total, 7′603′242 subtype-assigned variable region sequences were obtained (Table 2, column "Rearranged variable regions"), showing that our strategy efficiently sequences full-length variable regions with linked subtype information.

The IgG subtype frequencies were found to be very consistent among the four preparations of healthy donor and therefore independent of PCR amplification strategies and cDNA input (Table 2, Figure 3A, average frequency ± std. deviation (%) for IgG1 equals 56.1±0.2, IgG2 39.5±0.3, IgG3 4.0±0.1, IgG4 0.5±0.1). These values correspond well to IgG subtype frequencies previously reported [25–27].

Validation of Ig subtype distribution analysis by NGS and FACS sorting

To confirm the correct calling of the IgG subtype, PBMC of a healthy donor were FACS sorted into the four different IgG subtype populations. Purity after sorting was >99% for $CD19^+$ IgG1, IgG2 and IgG3 positive cells (approximately 17000, 7000 and 4500 cells were sorted, respectively). IgG4 positive cells were not further analyzed due to the low yield (total of 82 cells sorted) and lack of possibility to assess post-sort purity by FACS. After high-throughput sequencing of these populations in a separated run and analysis by the same pipeline as described above, we found subtype frequencies of 92.8% IgG1, 97.5% IgG2 and 98.7% IgG3 for the IgG1, IgG2 and IgG3 sorted populations, respec-

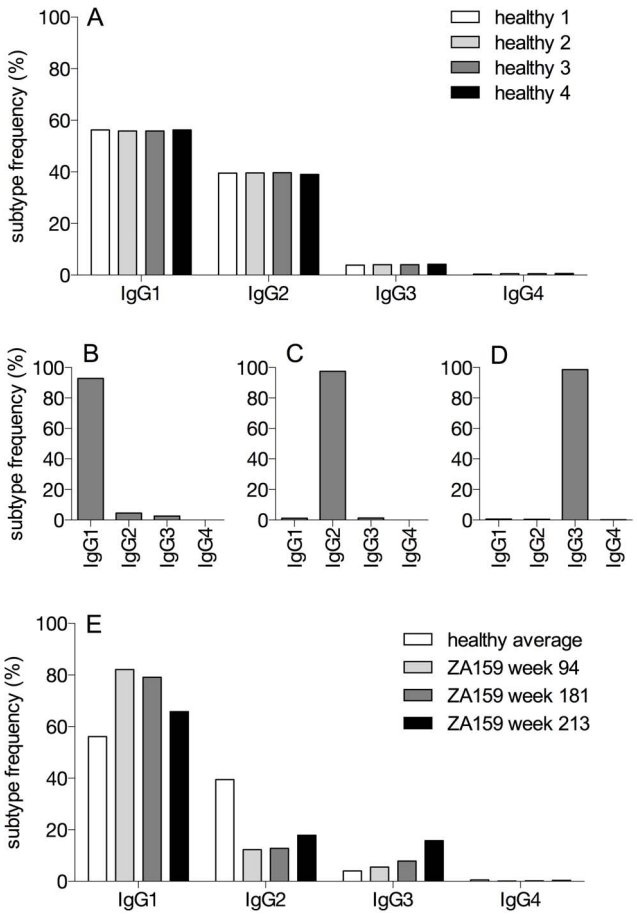

Figure 3. IgG subtypes are reliably identified. A) IgG subtype frequencies of four preparations of PBMC from one healthy donor were determined by sequencing. Different PCR protocols (prep 1 to prep 4) as described in the methods section have been applied to amplify antibody transcripts. Read numbers for the different preparations are listed in Table 2. B–D) PBMC of a healthy control were sorted by FACS into individual IgG subtype populations and sequenced. 2′221′006, 2′044′153 and 1′889′353 reads were obtained for sorted IgG1 positive cells (B), IgG2 positive cells (C) and IgG3 positive cells (D), respectively, and assigned to the IgG subtypes. E) IgG subtype frequencies of time points week 94, week 181 and week 213 (Table 2, Table S1) for patient ZA159. The average frequencies from the healthy control preparations 1–4 are shown as a comparison. Subtype frequencies in all panels were calculated as the percentage of all completely indexed and full-length variable region rearrangements.
doi:10.1371/journal.pone.0111726.g003

tively, highlighting the high specificity of our sequencing strategy (Figure 3 BCD).

IgG subtype dynamics in an HIV-1 infected patient

To get an insight if our method is applicable to monitor IgG subtype dynamics during infections, we selected an HIV-1 infected patient with pronounced IgG3-mediated anti-MPER plasma antibody response (Liechti et al. in preparation). Patient ZA159 was enrolled in the Zurich primary HIV infection study and has been followed from the acute phase of HIV-1 infection onwards [21]. The patient was on anti-retroviral treatment until week 92 post infection. Samples for NGS analysis were selected from three time points with differential IgG3-mediated MPER plasma titers: the first sample was taken 94 weeks post infection where no IgG3 MPER reactivity was apparent. Plasma from the second time point, approximately 181 weeks post infection, showed intermediate IgG3 MPER reactivity and the third, approximately 213 weeks post infection, had highest IgG3 MPER reactivity.

In addition to the wk213 sample already sequenced in the first run, frozen PBMC from the other two time points were sequenced in a second run and 732'390 and 669'244 heavy chain reads were obtained for those samples from week 94 and 181, respectively (see Table S1 for reads statistics). Assigning these reads to the IgG subtypes and comparing subtype frequencies to those from the healthy donor showed higher IgG1 and decreased IgG2 frequencies for the HIV-1 infected individual at all time points measured (Figure 3A). Of note, during viral rebound after anti-retroviral treatment cessation, IgG3 frequencies (measured by NGS) in the memory B cell compartment increased markedly (Figure 3E), which coincided with the increase in plasma IgG3 MPER reactivity.

Discussion

Repertoire analysis of antibody variable genes by NGS has become an important tool that allows unprecedented insight into antibody development pathways and holds particular promise for tailored vaccine design. Here, we describe a strategy for high-throughput sequencing of antibody heavy chains including determination of the IgG subtype. To achieve this, we adapted the Illumina MiSeq standard protocol by employing a mixed strategy of index reads and customized primers. Sequencing with custom primers and indices has been done previously [28,29], but to our knowledge our strategy of using an index read as a "third read" is novel. Different samples can still be multiplexed in the same run as the second index read remains available.

As we demonstrate here, our method determines IgG subtypes very reliably. We could successfully assign 97.5% of the reads in the demultiplexed samples to a subtype, although our identifier is 12 nucleotides long and the assignment criteria have to be very strict. Consistently, over 96% of both heavy and light chain sequences could be assigned to rearranged variable regions, demonstrating that our sequences are full-length antibody variable regions.

As the Hamming distances between the subtype identifiers are only single nucleotides, we do not allow mismatches in the subtype indices, except one mismatch in calling the klMA category. There remains a risk of misidentification of the subtype by a PCR or sequencing error, artifact recombination [30] or a mutation in the constant region. If further exclusion of misidentification by sequencing errors in the indices should become warranted for specific research questions, our analysis could be adapted to first collapse identical variable regions and then use the consensus of their index reads to determine the subtype. While this approach would decrease potential misidentifications, a full repertoire analysis of the variable domains would be required. Although this was beyond the scope of our current study, we consider this a useful and valuable modification of our analysis for future projects. Yet, despite the increased accuracy of this approach, pre-existing mutations in the constant region will not be detected and dismissed. Another possibility to empower subtype identification would be full-length sequencing of the CH1, as the difference between subtypes over the whole CH1 would increase to 6–15 nucleotides. However, the required read lengths are currently limiting for Illumina technology, as additional sequencing of the CH1 domain further downstream of our index would be necessary [27]. Even if this became possible, splitting up the available read length in several smaller reads might still be preferable, as per base sequencing quality decreases with increasing read length.

Although the purity of sorted subtype populations was higher measured by FACS than the IgG subtype frequency in the sorted samples determined by our sequencing approach, we argue that the sequencing approach serves as a quality control for the sorting and not the other way round, as even in the most controlled set up, FACS sorting will suffer from residual cross-reactivity from the staining antibodies.

No bias or cross-reactivity is expected in sequencing as this method is independent of immunoglobulin surface expression and, importantly, all subtypes are amplified with the same primer. A common primer is a key advantage compared to individual primers for each subtype. It is, however, important to note that our method, as it is presented here, is only semi-quantitative as we focused solely on subclass determination. If needed, a quantitative analysis would require a full repertoire analysis to avoid counting the same variable region multiple times. Since oversampling should be proportional for all the subtypes, distribution of subtype frequencies as shown here should not be affected.

Our method has the potential of widespread application and particularly in the antibody field the chance to fill a gap in information. So far, antibody subtypes have either only been determined in bulk in plasma samples where the information could not be linked to variable region sequences, or on the level of antibodies cloned out of single cells, where the potential for high-throughput applications is limited.

As recent data have highlighted, information on IgG subtype profiles could be very useful to study elicitation and dynamics of IgG antibodies of different subtypes, and could provide information on the quality of infection- and vaccine-induced B cell responses [18,31,32].

Our method can easily be adapted for IgA subtype discrimination. It can also be applied in other cases where priming of three reads is necessary or sequence information of a distant site is needed, e.g. in haplotype analysis used in genetics. Overall, our method combines the strength of antibody repertoire analyses by NGS with subtype information of the obtained sequences, enabling in-depth analysis of immune responses following infections or vaccinations.

Supporting Information

Table S1 Read numbers and subtype frequencies (ZA159 week 94 and 181).
(DOCX)

Acknowledgments

We thank Karin J. Metzner for critically reading the manuscript and Dagmara Lewandowska and Fabienne Desirée Geissberger for assistance with sequencing.

We thank the patient for participating in the Zurich Primary HIV Infection Study, the study nurses and physicians for excellent patient care, and the datacenter for high quality data management.

Author Contributions

Conceived and designed the experiments: MS MH. Performed the experiments: MS TL. Analyzed the data: MS TL OZ EM AT MH. Contributed reagents/materials/analysis tools: SR HG. Contributed to the writing of the manuscript: MS AT MH.

References

1. Mathonet P, Ullman CG (2013) The Application of Next Generation Sequencing to the Understanding of Antibody Repertoires. Front Immunol 4: 265.
2. Georgiou G, Ippolito GC, Beausang J, Busse CE, Wardemann H, et al. (2014) The promise and challenge of high-throughput sequencing of the antibody repertoire. Nat Biotechnol 32: 158–168.
3. Liao HX, Lynch R, Zhou T, Gao F, Alam SM, et al. (2013) Co-evolution of a broadly neutralizing HIV-1 antibody and founder virus. Nature 496: 469–476.
4. Zhu J, O'Dell S, Ofek G, Pancera M, Wu X, et al. (2012) Somatic Populations of PGT135-137 HIV-1-Neutralizing Antibodies Identified by 454 Pyrosequencing and Bioinformatics. Front Microbiol 3: 315.
5. Zhu J, Ofek G, Yang Y, Zhang B, Louder MK, et al. (2013) Mining the antibodyome for HIV-1-neutralizing antibodies with next-generation sequencing and phylogenetic pairing of heavy/light chains. Proc Natl Acad Sci U S A.
6. Scheid JF, Mouquet H, Ueberheide B, Diskin R, Klein F, et al. (2011) Sequence and structural convergence of broad and potent HIV antibodies that mimic CD4 binding. Science 333: 1633–1637.
7. Wu X, Yang ZY, Li Y, Hogerkorp CM, Schief WR, et al. (2010) Rational design of envelope identifies broadly neutralizing human monoclonal antibodies to HIV-1. Science 329: 856–861.
8. Wu X, Zhou T, Zhu J, Zhang B, Georgiev I, et al. (2011) Focused evolution of HIV-1 neutralizing antibodies revealed by structures and deep sequencing. Science 333: 1593–1602.
9. Beenhouwer DO, Yoo EM, Lai CW, Rocha MA, Morrison SL (2007) Human immunoglobulin G2 (IgG2) and IgG4, but not IgG1 or IgG3, protect mice against Cryptococcus neoformans infection. Infect Immun 75: 1424–1435.
10. Kam YW, Simarmata D, Chow A, Her Z, Teng TS, et al. (2012) Early appearance of neutralizing immunoglobulin G3 antibodies is associated with chikungunya virus clearance and long-term clinical protection. J Infect Dis 205: 1147–1154.
11. Buchacher A, Predl R, Strutzenberger K, Steinfellner W, Trkola A, et al. (1994) Generation of human monoclonal antibodies against HIV-1 proteins; electrofusion and Epstein-Barr virus transformation for peripheral blood lymphocyte immortalization. AIDS Res Hum Retroviruses 10: 359–369.
12. Huang J, Ofek G, Laub L, Louder MK, Doria-Rose NA, et al. (2012) Broad and potent neutralization of HIV-1 by a gp41-specific human antibody. Nature 491: 406–412.
13. Kunert R, Wolbank S, Stiegler G, Weik R, Katinger H (2004) Characterization of molecular features, antigen-binding, and in vitro properties of IgG and IgM variants of 4E10, an anti-HIV type 1 neutralizing monoclonal antibody. AIDS Res Hum Retroviruses 20: 755–762.
14. Roux KH, Strelets L, Michaelsen TE (1997) Flexibility of human IgG subclasses. J Immunol 159: 3372–3382.
15. Scharf O, Golding H, King LR, Eller N, Frazier D, et al. (2001) Immunoglobulin G3 from polyclonal human immunodeficiency virus (HIV) immune globulin is more potent than other subclasses in neutralizing HIV type 1. J Virol 75: 6558–6565.
16. Rerks-Ngarm S, Pitisuttithum P, Nitayaphan S, Kaewkungwal J, Chiu J, et al. (2009) Vaccination with ALVAC and AIDSVAX to prevent HIV-1 infection in Thailand. N Engl J Med 361: 2209–2220.
17. Chung AW, Ghebremichael M, Robinson H, Brown E, Choi I, et al. (2014) Polyfunctional Fc-Effector Profiles Mediated by IgG Subclass Selection Distinguish RV144 and VAX003 Vaccines. Sci Transl Med 6: 228ra238.
18. Yates NL, Liao HX, Fong Y, Decamp A, Vandergrift NA, et al. (2014) Vaccine-Induced Env V1–V2 IgG3 Correlates with Lower HIV-1 Infection Risk and Declines Soon After Vaccination. Sci Transl Med 6: 228ra239.
19. Tiller T, Meffre E, Yurasov S, Tsuiji M, Nussenzweig MC, et al. (2008) Efficient generation of monoclonal antibodies from single human B cells by single cell RT-PCR and expression vector cloning. J Immunol Methods 329: 112–124.
20. Sblattero D, Bradbury A (1998) A definitive set of oligonucleotide primers for amplifying human V regions. Immunotechnology 3: 271–278.
21. Rieder P, Joos B, Scherrer AU, Kuster H, Braun D, et al. (2011) Characterization of human immunodeficiency virus type 1 (HIV-1) diversity and tropism in 145 patients with primary HIV-1 infection. Clin Infect Dis 53: 1271–1279.
22. Menzel U, Greiff V, Khan TA, Haessler U, Hellmann I, et al. (2014) Comprehensive evaluation and optimization of amplicon library preparation methods for high-throughput antibody sequencing. PLoS One 9: e96727.
23. Bartram AK, Lynch MD, Stearns JC, Moreno-Hagelsieb G, Neufeld JD (2011) Generation of multimillion-sequence 16S rRNA gene libraries from complex microbial communities by assembling paired-end illumina reads. Appl Environ Microbiol 77: 3846–3852.
24. Alamyar E, Giudicelli V, Li S, Duroux P, Lefranc M-P (2012) IMGT/HighV-QUEST: the IMGT web portal for immunoglobulin (IG) or antibody and T cell receptor (TR) analysis from NGS high throughput and deep sequencing. Immunome research. pp. 26.
25. Berkowska MA, Driessen GJ, Bikos V, Grosserichter-Wagener C, Stamatopoulos K, et al. (2011) Human memory B cells originate from three distinct germinal center-dependent and -independent maturation pathways. Blood 118: 2150–2158.

26. Fecteau JF, Cote G, Neron S (2006) A new memory CD27-IgG+ B cell population in peripheral blood expressing VH genes with low frequency of somatic mutation. J Immunol 177: 3728–3736.
27. Maillette de Buy Wenniger LJ, Doorenspleet ME, Klarenbeek PL, Verheij J, Baas F, et al. (2013) Immunoglobulin G4+ clones identified by next-generation sequencing dominate the B cell receptor repertoire in immunoglobulin G4 associated cholangitis. Hepatology 57: 2390–2398.
28. Caporaso JG, Lauber CL, Walters WA, Berg-Lyons D, Huntley J, et al. (2012) Ultra-high-throughput microbial community analysis on the Illumina HiSeq and MiSeq platforms. ISME J 6: 1621–1624.
29. Caporaso JG, Lauber CL, Walters WA, Berg-Lyons D, Lozupone CA, et al. (2011) Global patterns of 16S rRNA diversity at a depth of millions of sequences per sample. Proc Natl Acad Sci U S A 108 Suppl 1: 4516–4522.
30. Di Giallonardo F, Zagordi O, Duport Y, Leemann C, Joos B, et al. (2013) Next-generation sequencing of HIV-1 RNA genomes: determination of error rates and minimizing artificial recombination. PLoS One 8: e74249.
31. Roussilhon C, Oeuvray C, Muller-Graf C, Tall A, Rogier C, et al. (2007) Long-term clinical protection from falciparum malaria is strongly associated with IgG3 antibodies to merozoite surface protein 3. PLoS Med 4: e320.
32. Versiani FG, Almeida ME, Melo GC, Versiani FO, Orlandi PP, et al. (2013) High levels of IgG3 anti ICB2-5 in Plasmodium vivax-infected individuals who did not develop symptoms. Malar J 12: 294.
33. Illumina (2012) Illumina Customer Sequence Letter. San Diego, Illumina, Inc: 17.
34. Giudicelli V, Chaume D, Lefranc MP (2005) IMGT/GENE-DB: a comprehensive database for human and mouse immunoglobulin and T cell receptor genes. Nucleic Acids Res 33: D256–261.

9. Discussion

HIV-1 infection induces a dramatic polyclonal immune activation of B cells that resulting in elevated frequency of antibody-secreting cells in the periphery and as a consequence thereof hypergammaglobulinemia develops (Lane, Masur et al. 1983; Schnittman, Lane et al. 1986; De Milito, Nilsson et al. 2004; Buckner, Moir et al. 2013). The perturbations in the B cell repertoire afflicted by HIV-1 are widespread. Recent bone marrow egressing transitional B cells are increased likely as direct consequence of the reduced $CD4^+$ T cell and concomitant elevated plasma IL-7 levels in HIV-1 infection (Malaspina, Moir et al. 2006; Malaspina, Moir et al. 2007). Memory B cells show a skewed differentiation profile shifting frequencies away from resting memory (RM) B cells, the dominating memory B cell subset in healthy individuals, to activated (AM) and exhausted tissue-like (TLM) memory B cells which both are characterized by down-regulation of CD21 and additionally of CD27 for TLM B cells (Moir, Ho et al. 2008; Moir and Fauci 2013).

IgG-expressing TLM B cells show increased proliferation history *in vivo* compared to RM and AM B cells highlighting that TLM B cells emerge as a consequence of activation (Meffre, Louie et al. 2016). Nevertheless TLM B cells contain less diversified variable genes of the B cell receptor (BCR) and reduced responsiveness to BCR-mediated stimulation highlighting that this subset is exhausted and excluded from further development into high-affinity B cell clones (Moir, Ho et al. 2008; Meffre, Louie et al. 2016). In addition TLM B cells are characterized by increased expression of inhibitory receptors such as CD22, FcRL4 and SIGLEC-6 known to dampen BCR-mediated activation (Moir, Ho et al. 2008; Kardava, Moir et al. 2011). Comparison of gp120 CD4 binding site-specific antibodies derived from RM and TLM B cells of HIV-1 infected individuals showed that RM B cells contained higher frequencies of clones with the potential to neutralize HIV-1 supporting that TLM B cells are impaired in developing high-affinity antibody responses (Meffre, Louie et al. 2016). In addition to the alterations observed in the B cell compartment HIV-1 induces $CD4^+$ T cell depletion and profound remodeling of lymphoid structures characterized by massive B cell proliferation, follicle hyperplasia, involution and fibrosis further impairing B cell responses (Grossman, Meier-Schellersheim et al. 2006; Brenchley and Douek 2008; Lederman and Margolis 2008; Levesque, Moody et al. 2009). As a consequence HIV-1 infection is accompanied by impaired B cell responses against co-infections and vaccines (Kroon, Vandissel et al. 1994; Kroon, van Dissel et al. 1997; Malaspina, Moir et al. 2005; Bussmann, Reiche et al. 2010; Cagigi, Nilsson et al. 2010; Tebas, Frank et al. 2010; Chang, Crane et al. 2013).

Despite this apparent impairment in mounting novel antibody responses, HIV-1 specific neutralizing antibodies continue to develop throughout the disease course (Wei, Decker et al. 2003; Tomaras and Haynes 2009; Overbaugh and Morris 2012; Liao, Lynch et al. 2013). In a fraction of individuals exceptionally potent and broadly neutralizing antibodies (bnAbs) develop after several years of untreated HIV-1 infection (Simek, Rida et al. 2009; Doria-Rose, Klein et al. 2010; Rusert, Kouyos et al. 2016). The length of the infection and antigen loads have been shown to be driving factors of bnAb development (Gray, Moore et al. 2007; Sather, Armann et al. 2009; Moore, Williamson et al. 2015; Rusert, Kouyos et al. 2016). Hence, the very factors that drive the distortion of the B cell response are linked to successful bnAb elicitation. Which components of the B cell response are required to mount bnAb responses is a subject of intense research efforts to guide bnAb elicitation by vaccines [reviewed in (Haynes, Moody et al. 2011; Haynes, Kelsoe et al. 2012; Mascola and Haynes 2013)].

A number of bnAbs have been isolated over the years and intensively characterized to understand how they gain such neutralization breadth and potency (Haynes and Montefiori 2006; Haynes, Moody et al. 2011; Burton, Poignard et al. 2012; Haynes, Kelsoe et al. 2012; Burton and Hangartner 2016). Interestingly, many bnAbs show unusual features such as high rates of somatic hypermutation (SHM) of the variable and framework regions, long third complementary determining regions of the heavy chain (CDRH3) and polyreactivity [reviewed in (Mascola and Haynes 2013; West, Scharf et al. 2014)]. In sum these results suggest that functional B cell subsets exist that maintained the ability to undergo extensive maturation and selection despite the profound B cell alterations in HIV-1 infection [reviewed in (Haynes, Kelsoe et al. 2012; Mascola and Haynes 2013)].

Although B cell alterations in HIV-1 infection have been intensively studied, we still lack a high-dimensional analysis of the B cell compartment in HIV-1 infected individuals that has sufficient depth to fine-map phenotypic differences within B cell subsets.. Such information would be crucial to define immune signatures associated with either the lack or the induction of potent immune responses against HIV-1 or co-infections and vaccines. The potential of multi-dimensional flow cytometry has been highlighted by the recent reports defining protective T cell responses associated with clinical outcome of HIV-1 infection and vaccine efficacy (Aghaeepour, Chattopadhyay et al. 2012; Lin, Finak et al. 2015). The aim of this thesis was to study the B cell compartment in HIV-1 infection using multidimensional flow cytometry in combination with unsupervised computational analysis tools to elucidate B cell subset alterations in HIV-1 infection.

In the first part of this thesis the development of a multicolor flow cytometry panel to dissect B cell subsets is described. The panel includes markers to distinguish the main B cell subsets according to their developmental stage (transitional B cells, naïve B cells, marginal

zone (MZ) B cells, memory B cells and plasmablasts) based on the expression of CD10, CD19, CD27, CD38 and IgD. A central goal of our analysis was to distinguish memory B cell subsets further based on the expression of different BCR isotypes (IgA, IgG1 and IgG3), CD21 and CD27. The CD21/CD27 expression pattern allows to distinguish intermediate (IM; $CD21^{+}CD27^{-}$), resting (RM; $CD21^{+}CD27^{+}$), activated (AM; $CD21^{-}CD27^{+}$) and tissue-like (TLM; $CD21^{-}CD27^{-}$) memory B cells (Kardava, Moir et al. 2014; Meffre, Louie et al. 2016).

Since chemokine receptors define the migratory potential of immune cells, we assessed expression of CCR7, CXCR3, CXCR4 and CXCR5 with our panel. CCR7 and CXCR5 are important for B cells to enter the T cell area and B cell follicle, respectively [reviewed in (Griffith, Sokol et al. 2014)]. CXCR4 can attract B cells to several sites but is mainly known for its function of migration towards and homeostasis of the cellular compartment in the bone marrow (Sugiyama, Kohara et al. 2006; Chu and Berek 2013). In addition CXCR4 has been shown to be important for GC reaction, lymph node entry and migration to inflammatory sites (Okada, Ngo et al. 2002; Dotan, Werner et al. 2010; Victora, Schwickert et al. 2010; Werner, Guzner-Gur et al. 2013). The ligands of CXCR3, namely CXCL9-11, are expressed at inflammatory sites and attract CXCR3-bearing immune cells to sites of active inflammation [reviewed in (Groom and Luster 2011; Griffith, Sokol et al. 2014)]. By monitoring expression of these chemokine receptors, our panel provides insight on the possible target destinations of B cell subsets.

The cytokine IL-21 plays a crucial role in germinal center reaction and plasmablast differentiation (Ettinger, Sims et al. 2005; Ettinger, Kuchen et al. 2008; Avery, Deenick et al. 2010; Linterman, Beaton et al. 2010; Zotos, Coquet et al. 2010; Crotty 2011; Deenick, Avery et al. 2013; Spolski and Leonard 2014; Tangye 2015). We thus included an analysis of IL-21R expression on B cell subsets to obtain insights on their responsiveness to IL-21 (Ettinger, Sims et al. 2005; Ettinger, Kuchen et al. 2008; Linterman, Beaton et al. 2010; Zotos, Coquet et al. 2010). As a further parameter we monitored intracellular staining of Ki-67, a classical proliferation marker, that allows the determination of proliferating and therefore recently activated B cells [reviewed in (Scholzen and Gerdes 2000; Harwood and Batista 2010)].

To analyze all markers on the same cell subset a 16 color flow cytometry panel was developed following recent guidelines (Perfetto, Chattopadhyay et al. 2004; Mahnke and Roederer 2007). We used a progressive approach increasing from a 11 to a 16 colors panel to obtain a panel with sufficient resolution that allows to define the desired B cell subsets and their phenotypic characteristics (Chapter 4; Figure 1 and online table 6). Nevertheless, several iterations in changing fluorochrome combinations were necessary in order to attain sufficient staining resolution despite fluorescence spill-over.

In chapter 5, we applied the final 16 color B cell panel to study the B cell repertoire in 21 patients enrolled in the Zurich Primary HIV Infection (ZPHI) cohort study longitudinally. We included samples from the acute and chronic infection phase and after 1 year of highly active antiretroviral therapy (ART). The patients were stratified into two groups based on the initiation of ART. The "early treatment group" initiated ART during the acute phase and stopped ART after ≥ 1 year and then progressed. Patients in the "late ART treatment" group initiated ART in the chronic phase. B cell populations at the different longitudinal time points of HIV-1 infection were then compared to data from 29 healthy individuals.

In a first step flow cytometry data were analyzed manually by defining main B cell populations and comparing their frequencies at different disease and treatment stages in comparison with healthy individuals. The analysis confirmed previously described increased levels of transitional B cells and plasmablasts as well as the skewing of the memory B cell compartment towards AM and TLM B cells with reduced levels of RM B cells in viremic patients (Chapter 5; Figure 1A and B) (Lane, Masur et al. 1983; Malaspina, Moir et al. 2006; Moir, Ho et al. 2008; Buckner, Moir et al. 2013).

Activation of memory B cells results in loss of CD21 expression as a consequence of transcriptional down-regulation of CD21 and potentially CD21 shedding (Moir, Malaspina et al. 2001; Masilamani, Kassahn et al. 2003). Based on these prior findings CD21 has become a canonical marker to discriminate activated and exhausted from resting memory B cells. In the current study I explored CD21 expression on naïve (IgD^+CD27^-) and MZ (IgD^+CD27^+) B cells. Surprisingly, HIV-1 infection lead to increased frequencies of $CD21^{neg}$ naïve and $CD21^{neg}$ MZ B cells which reverted to normal levels upon initiation of ART (Chapter 5; Figure 1C). $CD21^{neg}$ naïve B cells have been described in the context of autoimmune diseases and reported to show an exhausted phenotype, lower responsiveness to BCR-mediated stimulation and increased frequencies of autoreactive clones (Rakhmanov, Keller et al. 2009; Isnardi, Ng et al. 2010; Tipton, Fucile et al. 2015; Flint, Gibson et al. 2016). Furthermore $CD21^{neg}$ naïve B cells in autoimmune disease have altered chemokine receptor expression profiles that matched the expression pattern observed in $CD21^{neg}$ naïve and MZ cells described in our study and were signified by reduced levels of CCR7 and CXCR5 an elevated expression of CXCR3 (Chapter 5; Figure 3B). Based on the chemokine expression patterns it is likely that these altered subsets shift their migratory pattern from entering lymph nodes and B cell follicles to reach sites of inflammation (Griffith, Sokol et al. 2014; Moir and Fauci 2014).

I used spanning-tree progression analysis of density-normalized events (SPADE), a recently developed clustering algorithm to cluster multidimensional single cell data, to explore diverse phenotypes within $CD21^{neg}$ naïve B cells in HIV-1-infected patients (Chapter 5; Figure 5A)

(Qiu, Simonds et al. 2011). CD21^{neg} MZ B cell frequencies in the cryo-preserved PBMC samples that were available for these studies were not sufficient for yield reliable results in the SPADE analysis and were therefore not included. We found that CXCR3-expressing CD21^{neg} naïve B cells express high levels of CXCR4 and CD19 and low levels of CCR7, a signature associated with activation and exhaustion (cluster #3 and #5; Chapter 5; Figure 5C) (Moir, Ho et al. 2008; Rakhmanov, Keller et al. 2009; Isnardi, Ng et al. 2010; Tipton, Fucile et al. 2015). In contrast, within subsets expressing CCR7 only few cells show high levels of CXCR3, CD19 and CXCR4 and therefore resemble conventional naïve B cells (Chapter 5; Figure 5C). CXCR5- and IL-21R are expressed on diverse subsets with no clear pattern of co-expressing markers (Chapter 5; Figure 5C). Most strikingly, the cluster analysis revealed that several phenotypically divergent CD21^{neg} naïve B cell subsets can be defined and that the expression signature of some CD21^{neg} naïve B cell subsets are more associated with exhaustion whereas other signatures are similar to the quiescent state observed in conventional naïve B cells. Therefore the transition of subsets within CD21^{neg} naïve B cells to a distinct phenotype could be associated with differentiation, functional changes or activation and exhaustion. It will be interesting to dissect in forthcoming studies, if and how these subpopulations differ in their function, developmental or activation stage.

CD21^{neg} naïve B cells described in autoimmune diseases and CVID are characterized by impaired responsiveness to stimulation and increased apoptosis (Rakhmanov, Keller et al. 2009; Isnardi, Ng et al. 2010). In addition these cells express high levels of the activation and exhaustion markers CD95 and FcRL4, respectively (Rakhmanov, Keller et al. 2009). The phenotypic analysis I performed in my thesis showed strong similarities between CD21^{neg} naïve and CD21^{neg} MZ B cells in healthy and HIV-1-infected individuals and the naïve CD21^{neg} B cells subset described in autoimmune diseases and CVID. I thus investigated the functional properties of these subsets in healthy and HIV-1 infected individuals. Indeed, CD21^{neg} naïve and CD21^{neg} MZ B cells up-regulate CD95 and FcRL4 in healthy and chronically HIV-1 infected individuals and HIV-1 infection results in further up-regulation of these markers (Chapter 5; Figure 6A-C) (Moir, Ho et al. 2008; Sciaranghella, Tong et al. 2012). CD95 is highly up-regulated in activated GC B cells and the CD95/CD95L-axis plays an important role in B cell homeostasis and elimination of autoreactive B cells in GC of mice (Hao, Duncan et al. 2008). Therefore CD95 is likely to be essential for the elimination of activated low-affinity B cells which do not receive sufficient T cell help during GC reaction. In line with this, CD21^{neg} naïve and CD21^{neg} MZ B cells showed increased frequencies of apoptotic cells compared to CD21^{pos} cells both in healthy and chronically HIV-1 infected individuals which could be a result of CD95/CD95L-dependent mechanisms (Chapter 5; Figure 6E and F) (Medina, Segundo et al. 1997; Sciaranghella, Tong et al. 2012).

In order to investigate the responsiveness of CD21^{neg} naïve B cells to BCR-mediated stimulation in healthy and chronically HIV-1 infected individuals I used a flow cytometry-based method to determine to magnitude of phosphorylated tyrosine motifs since phosphorylation is an early and crucial event in B cell activation (Harwood and Batista 2010; Schulz, Danna et al. 2012). Elevated basal phosphorylation levels in CD21^{neg} naïve and CD21^{neg} MZ B cells were observed in chronically HIV-1-infected individuals while in healthy subjects only CD21^{neg} MZ showed significantly elevated phosphorylation compared to CD21^{pos} MZ B cells (Chapter 5; Figure 7C). Upon BCR cross-linking phosphorylation levels were higher in CD21^{pos} naïve and CD21^{pos} MZ B cells compared to their CD21^{neg} cells highlighting that the responsiveness of CD21^{neg} naïve and CD21^{neg} MZ B cells to BCR-mediated stimulation is impaired. Interestingly though, no difference between CD21^{pos} and CD21^{neg} MZ B cells could be observed in healthy individuals (Chapter 5; Figure 7C). Collectively our data suggest that CD21^{neg} naïve and CD21^{neg} MZ B cells are impaired in their responsiveness to BCR-mediated stimulation. However the elevated phosphorylation levels *ex vivo* observed in healthy and HIV-1 infected individuals support that CD21^{neg} naïve and MZ B cells resemble an activated phenotype. Our functional analysis support the notion that CD21^{neg} naïve and CD21^{neg} MZ B cells that emerge during HIV-1 infection show highly similar phenotypical and functional properties with CD21^{neg} naïve B cells observed in autoimmune diseases and common variable immunodeficiency (CVID).

HIV-1 infection results in loss of memory B cells and diminished B cell responses to co-infections and vaccines (Ballet, Sulcebe et al. 1987; Kroon, Vandissel et al. 1994; Kroon, van Dissel et al. 1997; Malaspina, Moir et al. 2005; Titanji, De Milito et al. 2006; Chang, Crane et al. 2013; Crum-Cianflone and Wallace 2014; Mena, Garcia-Basteiro et al. 2015). Since the results presented in this study highlight that a high proportion of naïve and MZ B cells show loss of CD21 and are characterized by an activated and exhausted phenotype during chronic HIV-1 infection these cells are likely to be impaired in reacting to these pathogens. MZ B cells are known to be important for polysaccharide-directed responses and therefore the reduced efficacy of pneumococcal vaccines could be a consequence of the impaired MZ B cell compartment (Kroon, Vandissel et al. 1994; Kruetzmann, Rosado et al. 2003; Weill, Weller et al. 2009; Crum-Cianflone and Wallace 2014).

Autoreactive B cell clones are enriched within CD21^{neg} naïve B cells in autoimmune diseases and CVID (Rakhmanov, Keller et al. 2009; Isnardi, Ng et al. 2010). The phenotypical and functional similarities of CD21^{neg} naïve B cells in HIV-1 infection, autoimmune diseases and CVID raise the possibility that these cells may harbor a similar potential to express polyreactive BCR irrespective of the disease setting. It would thus be of importance to proof experimentally if this indeed is the case for CD21^{neg} naïve B cells in HIV-1 infection in

forthcoming studies. It has long been known that HIV-1 infected patients show increased frequencies of autoreactive B cells (Kobie, Alcena et al. 2012). In addition, the bnAbs 2F5 and 4E10 targeting the membrane proximal region (MPER) of gp41 as well as several other gp120 targeting bnAbs are known to be polyreactive (Muster, Steindl et al. 1993; Buchacher, Predl et al. 1994; Zwick, Labrijn et al. 2001; Haynes, Fleming et al. 2005; Yang, Holl et al. 2013). For 2F5 and 4E10 it has been shown that their polyreactivity contributes to their activity (Haynes, Fleming et al. 2005; Alam, McAdams et al. 2007; Dennison, Anasti et al. 2011; Yang, Holl et al. 2013; Verkoczy, Kelsoe et al. 2014). While adding to their HIV inhibitory potential, the polyreactivity of MPER directed bnAbs is an impediment for their elicitation as immune tolerance mechanism need to be overcome (Verkoczy, Diaz et al. 2010; Verkoczy, Chen et al. 2011).

Polyreactivity was suggested beneficial in inducing HIV-1 specific antibodies as it may provide enhanced affinity binding to the virus surface which harbors only low amounts of the actual target protein the HIV envelope trimer (Mouquet, Scheid et al. 2010). In favor of this possibility two recent studies showed that autoreactive anergic naïve B cells can enter the GC and are selected for mutations reducing polyreactivity but maintaining and increasing affinity to the foreign antigen (Sabouri, Schofield et al. 2014). This could be observed in two monoclonal antibodies elicited during vaccinia immunization, however the loss of polyreactivity was in one antibody accompanied by reduced affinity to the foreign antigen highlighting the contribution of polyreactivity to the affinity (Reed, Jackson et al. 2016). Autoreactive naïve B cells are excluded from GC in healthy individuals, however in SLE these cells showed increased entry into GC with the potential to result in the elicitation of autoantibodies (Cappione, Anolik et al. 2005). Whether the same mechanisms occur in HIV-1 is not known. However, if HIV-1 infection results in the emergence of polyreactive anergic naïve B cells as observed in autoimmune diseases and CVID the co-operation between antigen-specificity and polyreactivity of naïve B cells might indeed contribute to the induction of HIV-specific antibody responses through synergistic activation signals. Noteworthy, the search for germline Ig sequences with the ability to bind HIV-1 envelope proteins has been largely unsuccessful highlighting the potential or co-operative mechanisms including polyreactivity to facilitate the induction of HIV-1 Env antibody responses (Hoot, McGuire et al. 2013; McGuire, Hoot et al. 2013). A particular interest of future studies will be the investigation whether $CD21^{neg}$ naïve B cells contain increased frequencies of polyreactive/autoreactive clones and whether the emergence of these cells is exploited by the immune system to induce HIV-specific antibodies.

In chapter 6 of my thesis I studied the complexity of the memory B cell and plasmablast compartment as recent studies highlight that peripheral and tissue-resident class-switched B

cells are phenotypically more diverse than anticipated (Nair, Newell et al. 2016). My studies focused on the same longitudinally HIV-1 patient cohort described in chapter 5 that was followed through periods of acute, Chronic infection and ART and healthy donors. To derive a comprehensive map of the memory B cell and plasmablast repertoire I assessed expression of 16 markers by flow cytometry as described in chapter 4. This was followed by a thorough analysis of the flow cytometry data using conventional manual gating, and several computational approaches.

Non-linear dimensionality reduction analysis using t-Distributed Stochastic Neighbor Embedding (t-SNE) algorithm allowed a projection of individual cells in two dimensions where similar cells are mapped closer together and most dissimilar cells are projected with the maximum distance (Chapter 6; Figure 1A and 2A and Supplementary figure 2) (Amir, Davis et al. 2013). The t-SNE analysis revealed that in healthy individuals the distribution of IM, RM, AM and TLM B cells differs within B cells expressing different isotypes with $IgG3^+$ memory B cells showing the highest frequency of AM and TLM B cells whereas IgA^+ memory B cells contained the highest frequency of RM B cells (Chapter 6; Figure 2C and D). $IgG1^+$ memory B cells showed an intermediate distribution of memory B cell subsets. The skewed distribution of memory B cell subsets was also evident in HIV-1 infected individuals. However, as HIV-1 infection results in accumulation of AM and TLM B cells some of the patterns were less pronounced (Chapter 6; Figure 2C and D) (Moir, Ho et al. 2008; Kardava, Moir et al. 2014). I further observed that $IgG3^+$ resting memory B cells have a phenotype associated with progression towards activated and exhausted memory B cells as characterized by reduced levels of CCR7 and CXCR5 and elevated levels of CXCR3 and IL-21R compared to IgA^+ and $IgG1^+$ RM B cells (Chapter 6; Figure 1B and 4A). Collectively these results highlight that $IgG3^+$ memory B cells show a phenotypic signature associated with activation that is already apparent in resting memory B cells and is paired with a skewed accumulation of $IgG3^+$ AM and TLM B cells. It will be of importance to resolve the underlying causes of this skewed distribution and memory B cell subsets and activated immune signature amongst $IgG3^+$ memory B cells to understand the developmental paths of these cells. Higher frequencies of $IgG3^+$ memory B cells have been observed among $CD27^-$ naïve B cells and are characterized by a low mutation rate which lead to the hypothesis that these cells are derived from T cell-independent immune responses or have left GC reaction early as a part of the early antibody response (Fecteau, Cote et al. 2006; Berkowska, Driessen et al. 2011). This scenario is however challenged by a recent study showing that the majority of $CD27^-$ $IgG3^+$ memory B cells have undergone somatic hypermutation (SHM) suggesting that $IgG3^+$ memory B cells do originate from GC-dependent responses (Budeus, Schweigle de Reynoso et al. 2015). Preferentially induced IgG3 responses were observed for certain epitopes of malaria-derived antigens emphasizing that IgG3 CSR might be guided by the physical

properties of the epitope (Tongren, Drakeley et al. 2006). In addition, IgG3 responses against malaria antigens are elevated in endemic regions suggesting that repeated antigen challenging can skew responses towards IgG3 (Tongren, Drakeley et al. 2006). Therefore IgG3 responses can potentially be shaped by persisting antigens and the properties of the antigen. Interestingly, the three isolated bnAbs specific for the MPER region were originally IgG3 whereas most gp120-specific bnAbs were isolated as IgG1 highlighting that HIV-1 contains epitopes which might be associated with preferential induction of IgG3 bnAbs (Buchacher, Predl et al. 1994; Haynes, Kelsoe et al. 2012; Huang, Ofek et al. 2012).

Our analysis highlights that HIV-1 infection results in increased CXCR3 expression on IM and RM memory B cells irrespective of the isotype expressed (Chapter 6; Figure 5A). We observed no disease-dependent alterations of CXCR3 of AM and TLM B cells likely as these cells are already activated and generally have up-regulated levels of CXCR3. Of particular note we found that only early ART successfully reduced CXCR3 levels, which stayed significantly elevated when ART was initiated during the chronic infection stage (Chapter 6; Figure 5B). This observation is a further addition to reports that show that despite effective ART activation and exhaustion of immune cells persist which potentially may be due to low levels HIV-1 replication in lymph nodes (Hatano, Jain et al. 2013; Pallikkuth, Sharkey et al. 2015; Banga, Procopio et al. 2016; Cobos Jimenez, Wit et al. 2016; Fromentin, Bakeman et al. 2016; Lorenzo-Redondo, Fryer et al. 2016). Likewise, despite ART damage of the lymphoid organs are irreversible and skewed memory B cell subset frequencies such as elevated TLM B cells cannot be completely restored (Moir, Buckner et al. 2010; Estes 2013). The elevated CXCR3 expression after prolonged period of ART in the late treatment group we defined in the present study indicates that phenotypic alterations persist despite prolonged period of therapy when ART is initiated at advanced disease stages and these persisting phenotypic alterations could have functional consequences for memory B cells. As a consequence early initiation of ART must be viewed as beneficial for the B cell compartment (Moir, Buckner et al. 2010; Moir and Fauci 2013).

The analysis of the plasmablast population we conducted revealed increased levels of almost all chemokine receptors and IL-21R except for CCR7 on plasmablasts during HIV-1 infection and highlighted a substantial phenotypic diversity of plasmablasts (Chapter 6; Figure 6). Plasmablasts and plasma cells are known to have an altered expression of chemokine receptors in chronic inflammation (Tarlton, Green et al. 2012; Buckner, Moir et al. 2014). In addition, CXCR3 and CXCR4 expression can be observed after stimulation of memory B cells and plasmablast formation *in vitro* and upon vaccination (Muehlinghaus, Cigliano et al. 2005; Odendahl, Mei et al. 2005). Interestingly, steady-state plasmablasts originate from mucosal tissues expressing IgA and mucosa-associated chemokine receptors

such as CCR10 whereas upon vaccination IgG-expressing plasmablasts emerge with a distinct expression pattern of chemokine receptors (Mei, Yoshida et al. 2009). These observations provided a first indication on the phenotypic diversity of plasmablasts and plasma cells and show that plasmablast phenotypes can be associated with unique immune states such as steady-state, vaccination or inflammation.

To further explore the diversity within memory B cells and plasmablasts revealed by the t-SNE analysis I used SPADE in combination with Ward's hierarchical clustering (Chapter 6; Figure 1A, 2A, 7 and Supplementary figure 5 and 6). This approach identified 30 memory B cell and 10 plasmablast clusters (Chapter 6; Figure 7A). The recent advent of mass cytometry and new computational analysis tools provided unprecedented insight into the diversity of B cells in periphery and tissues (Hansmann, Blum et al. 2015; Nair, Newell et al. 2016; Pejoski, Tchitchek et al. 2016). The study presented in chapter 6 of this thesis contributes to these results by showing that memory B cell populations classified by the expression pattern of CD21 and CD27 contain highly diverse subsets (chapter 6; Figure 7 and Supplementary figure 5 and 6). Clustering analysis do not always result in clearly defined populations based on CD21 and CD27 expression emphasizing that the definition of some clusters relies on distinct markers. However, in general the clustering analysis resulted in accurate definition of memory B cell subsets defined by CD21/CD27 expression. Our results suggest that memory B cells consist of phenotypically variable subsets beyond isotype and CD21/CD27 expression. Nevertheless memory B cell subsets defined based on CD21/CD27 can be associated with specific expression pattern such as IL-21R, which was observed mainly in clusters within TLM B cells (Chapter 6; figure 7A). It will be interesting to explore the functional characteristics of these subsets in future studies.

Interestingly, memory B cell subpopulations show divergent dynamics in HIV-1 infection highlighting that HIV-1 dependent memory B cell alterations are complex. For IM B cells only subsets characterized by low IL-21R expression are decreased in acute and chronic HIV-1 infection (Ward cluster #3 and #26; Chapter 6; Figure 7A and C). Interestingly, these subsets show different kinetics with Ward cluster #3 gradually decrease during the course of infection while Ward cluster #26 show the lowest frequency already at the acute stage (Chapter 6; Figure 7A and C). Within clusters showing a CD21/CD27 expression pattern consistent with TLM B cells only cells expressing CXCR3, IL-21R, CXCR4 and high levels of CD19 are elevated. However, as only few cells were assigned to Ward cluster #21 this low-frequent subset has to be re-evaluated in independent studies.

Evaluation of plasmablasts by the clustering analysis revealed classical plasmablasts defined by high expression of CD27, CD38 and Ki-67 (Chapter 6; Figure 8A) [reviewed in (Fink 2012)] and in addition $CD38^{high}Ki\text{-}67^{high}$ plasmablasts that lack CD27. Functional properties of this

plasmablast type that was recently also described to emerge in response to an oral vaccine against *Shigella* are not yet known (Toapanta, Simon et al. 2014). Interestingly, chemokine receptors CCR7, CXC3 and CXCR5 were differently expressed on the distinct plasmablast clusters (Chapter 6; Figure 8A). This is in agreement with prior reports that found that plasmablasts and plasma cells express a variety of chemokine receptors which determine their migratory potential (Kunkel and Butcher 2003; Muehlinghaus, Cigliano et al. 2005; Odendahl, Mei et al. 2005; Buckner, Moir et al. 2014; Toapanta, Simon et al. 2014). The majority of plasmablast clusters we defined expressed CXCR3 which allows these cells to migrate to inflamed tissue while only few clusters expressed CCR7 and thus might possess the potential to enter lymphoid organs (Hauser, Debes et al. 2002; Kunkel and Butcher 2003; Nakayama, Hieshima et al. 2003; Muehlinghaus, Cigliano et al. 2005; Griffith, Sokol et al. 2014).

Collectively the results obtained by the high-dimensional mapping of the B cell repertoire in Chapters 5 and 6, provides in-depth insight into the dynamics of the B cell compartment in healthy and HIV-1 infected individuals. The definition of subpopulations that go beyond the conventional B cell subsets not only illustrate the heterogeneity of the B cell repertoire but also provide means for future studies to dissect functional properties of B cell sub-species in shaping immune responses and in particular bnAb responses to HIV-1.

10. References

Aghaeepour, N., P. K. Chattopadhyay, et al. (2012). "Early immunologic correlates of HIV protection can be identified from computational analysis of complex multivariate T-cell flow cytometry assays(*)." Bioinformatics **28**(7): 1009-1016.

Alam, S. M., M. McAdams, et al. (2007). "The role of antibody polyspecificity and lipid reactivity in binding of broadly neutralizing anti-HIV-1 envelope human monoclonal antibodies 2F5 and 4E10 to glycoprotein 41 membrane proximal envelope epitopes." J Immunol **178**(7): 4424-4435.

Amanna, I. J., N. E. Carlson, et al. (2007). "Duration of humoral immunity to common viral and vaccine antigens." N Engl J Med **357**(19): 1903-1915.

Amir, E. D., K. L. Davis, et al. (2013). "viSNE enables visualization of high dimensional single-cell data and reveals phenotypic heterogeneity of leukemia." Nature Biotechnology **31**(6): 545-+.

Anchang, B., T. D. Hart, et al. (2016). "Visualization and cellular hierarchy inference of single-cell data using SPADE." Nat Protoc **11**(7): 1264-1279.

Ansel, K. M., V. N. Ngo, et al. (2000). "A chemokine-driven positive feedback loop organizes lymphoid follicles." Nature **406**(6793): 309-314.

Avci, F. Y. and D. L. Kasper (2010). "How Bacterial Carbohydrates Influence the Adaptive Immune System." Annual Review of Immunology, Vol 28 **28**: 107-130.

Avery, D. T., E. K. Deenick, et al. (2010). "B cell-intrinsic signaling through IL-21 receptor and STAT3 is required for establishing long-lived antibody responses in humans." J Exp Med **207**(1): 155-171.

Bacher, P. and A. Scheffold (2013). "Flow-cytometric analysis of rare antigen-specific T cells." Cytometry A **83**(8): 692-701.

Bachmann, M. F., U. H. Rohrer, et al. (1993). "The influence of antigen organization on B cell responsiveness." Science **262**(5138): 1448-1451.

Ballet, J. J., G. Sulcebe, et al. (1987). "Impaired anti-pneumococcal antibody response in patients with AIDS-related persistent generalized lymphadenopathy." Clin Exp Immunol **68**(3): 479-487.

Banga, R., F. A. Procopio, et al. (2016). "PD-1(+) and follicular helper T cells are responsible for persistent HIV-1 transcription in treated aviremic individuals." Nat Med **22**(7): 754-761.

Batista, F. D. and N. E. Harwood (2009). "The who, how and where of antigen presentation to B cells." Nature Reviews Immunology **9**(1): 15-27.

Baumgarth, N. (2013). "Innate-Like B Cells and Their Rules of Engagement." Crossroads between Innate and Adaptive Immunity Iv **785**: 57-66.

Bendall, S. C., G. P. Nolan, et al. (2012). "A deep profiler's guide to cytometry." Trends Immunol **33**(7): 323-332.

Bende, R. J., F. van Maldegem, et al. (2007). "Germinal centers in human lymph nodes contain reactivated memory B cells." Journal of Experimental Medicine **204**(11): 2655-2665.

Benedetto, A., A. Di Caro, et al. (1992). "Identification of a CD21 receptor-deficient, non-Ig-secreting peripheral B lymphocyte subset in HIV-seropositive drug abusers." Clin Immunol Immunopathol **62**(2): 139-147.

Berberian, L., L. Goodglick, et al. (1993). "Immunoglobulin VH3 gene products: natural ligands for HIV gp120." Science **261**(5128): 1588-1591.

Bergtold, A., D. D. Desai, et al. (2005). "Cell surface recycling of internalized antigen permits dendritic cell priming of B cells." Immunity **23**(5): 503-514.

Berkowska, M. A., G. J. Driessen, et al. (2011). "Human memory B cells originate from three distinct germinal center-dependent and -independent maturation pathways." Blood **118**(8): 2150-2158.

Bradley, L. M., L. Haynes, et al. (2005). "IL-7: maintaining T-cell memory and achieving homeostasis." Trends Immunol **26**(3): 172-176.

Brenchley, J. M. and D. C. Douek (2008). "HIV infection and the gastrointestinal immune system." Mucosal Immunol **1**(1): 23-30.

Bruggner, R. V., B. Bodenmiller, et al. (2014). "Automated identification of stratifying signatures in cellular subpopulations." Proceedings of the National Academy of Sciences of the United States of America **111**(26): E2770-E2777.

Buchacher, A., R. Predl, et al. (1994). "Generation of human monoclonal antibodies against HIV-1 proteins; electrofusion and Epstein-Barr virus transformation for peripheral blood lymphocyte immortalization." AIDS Res Hum Retroviruses **10**(4): 359-369.

Buckner, C. M., S. Moir, et al. (2013). "Characterization of plasmablasts in the blood of HIV-infected viremic individuals: evidence for nonspecific immune activation." J Virol **87**(10): 5800-5811.

Buckner, C. M., S. Moir, et al. (2014). "CXCR4/IgG-expressing plasma cells are associated with human gastrointestinal tissue inflammation." J Allergy Clin Immunol **133**(6): 1676-1685 e1675.

Bucy, R. P., R. D. Hockett, et al. (1999). "Initial increase in blood CD4(+) lymphocytes after HIV antiretroviral therapy reflects redistribution from lymphoid tissues." J Clin Invest **103**(10): 1391-1398.

Budeus, B., S. Schweigle de Reynoso, et al. (2015). "Complexity of the human memory B-cell compartment is determined by the versatility of clonal diversification in germinal centers." Proc Natl Acad Sci U S A **112**(38): E5281-5289.

Bunnik, E. M., L. Pisas, et al. (2008). "Autologous neutralizing humoral immunity and evolution of the viral envelope in the course of subtype B human immunodeficiency virus type 1 infection." J Virol **82**(16): 7932-7941.

Buri, C., M. Korner, et al. (2001). "CC chemokines and the receptors CCR3 and CCR5 are differentially expressed in the nonneoplastic leukocytic infiltrates of Hodgkin disease." Blood **97**(6): 1543-1548.

Burleigh, L., P. Y. Lozach, et al. (2006). "Infection of dendritic cells (DCs), not DC-SIGN-mediated internalization of human immunodeficiency virus, is required for long-term transfer of virus to T cells." J Virol **80**(6): 2949-2957.

Burton, D. R. and L. Hangartner (2016). "Broadly Neutralizing Antibodies to HIV and Their Role in Vaccine Design." Annu Rev Immunol **34**: 635-659.

Burton, D. R., P. Poignard, et al. (2012). "Broadly neutralizing antibodies present new prospects to counter highly antigenically diverse viruses." Science **337**(6091): 183-186.

Bussmann, B. M., S. Reiche, et al. (2010). "Loss of HIV-specific memory B-cells as a potential mechanism for the dysfunction of the humoral immune response against HIV." Virology **397**(1): 7-13.

Cagigi, A., A. Nilsson, et al. (2010). "Dysfunctional B-cell responses during HIV-1 infection: implication for influenza vaccination and highly active antiretroviral therapy." Lancet Infect Dis **10**(7): 499-503.

Cappione, A., 3rd, J. H. Anolik, et al. (2005). "Germinal center exclusion of autoreactive B cells is defective in human systemic lupus erythematosus." J Clin Invest **115**(11): 3205-3216.

Cerutti, A., M. Cols, et al. (2013). "Marginal zone B cells: virtues of innate-like antibody-producing lymphocytes." Nat Rev Immunol **13**(2): 118-132.

Chang, C. C., M. Crane, et al. (2013). "HIV and co-infections." Immunol Rev **254**(1): 114-142.

Chattopadhyay, P. K., T. M. Gierahn, et al. (2014). "Single-cell technologies for monitoring immune systems." Nat Immunol **15**(2): 128-135.

Cherukuri, A., P. C. Cheng, et al. (2001). "The CD19/CD21 complex functions to prolong B cell antigen receptor signaling from lipid rafts." Immunity **14**(2): 169-179.

Chu, V. T. and C. Berek (2013). "The establishment of the plasma cell survival niche in the bone marrow." Immunol Rev **251**(1): 177-188.

Chung, J. B., M. Silverman, et al. (2003). "Transitional B cells: step by step towards immune competence." Trends Immunol **24**(6): 343-349.

Cinamon, G., M. A. Zachariah, et al. (2008). "Follicular shuttling of marginal zone B cells facilitates antigen transport." Nature Immunology **9**(1): 54-62.

Cobos Jimenez, V., F. W. Wit, et al. (2016). "T-Cell Activation Independently Associates With Immune Senescence in HIV-Infected Recipients of Long-term Antiretroviral Treatment." J Infect Dis **214**(2): 216-225.

Coelho, F. M., D. Natale, et al. (2013). "Naive B-cell trafficking is shaped by local chemokine availability and LFA-1-independent stromal interactions." Blood **121**(20): 4101-4109.

Connick, E., T. Mattila, et al. (2007). "CTL fail to accumulate at sites of HIV-1 replication in lymphoid tissue." Journal of Immunology **178**(11): 6975-6983.

Corbeau, P. and J. Reynes (2011). "Immune reconstitution under antiretroviral therapy: the new challenge in HIV-1 infection." Blood **117**(21): 5582-5590.

Corcione, A., G. Tortolina, et al. (2002). "Chemotaxis of human tonsil B lymphocytes to CC chemokine receptor (CCR) 1, CCR2 and CCR4 ligands is restricted to non-germinal center cells." Int Immunol **14**(8): 883-892.

Cossarizza, A., S. De Biasi, et al. (2013). "Cytometry, immunology, and HIV infection: three decades of strong interactions." Cytometry A **83**(8): 680-691.

Coulter, W. H. (1956). High Speed Automatic Blood Cell Counter and Cell Size Analyzer. Preliminary draft presented at the National Electronics Conference. Chicago.

Covens, K., B. Verbinnen, et al. (2013). "Characterization of proposed human B-1 cells reveals pre-plasmablast phenotype." Blood **121**(26): 5176-5183.

Crotty, S. (2011). "Follicular helper CD4 T cells (TFH)." Annu Rev Immunol **29**: 621-663.

Crum-Cianflone, N. F. and M. R. Wallace (2014). "Vaccination in HIV-infected adults." AIDS Patient Care STDS **28**(8): 397-410.

Cyster, J. G. (2010). "B cell follicles and antigen encounters of the third kind." Nature Immunology **11**(11): 989-996.

Dauby, N., C. Kummert, et al. (2014). "Primary human cytomegalovirus infection induces the expansion of virus-specific activated and atypical memory B cells." J Infect Dis **210**(8): 1275-1285.

Davis, K. L., E. S. Gray, et al. (2009). "High titer HIV-1 V3-specific antibodies with broad reactivity but low neutralizing potency in acute infection and following vaccination." Virology **387**(2): 414-426.

De Milito, A., A. Nilsson, et al. (2004). "Mechanisms of hypergammaglobulinemia and impaired antigen-specific humoral immunity in HIV-1 infection." Blood **103**(6): 2180-2186.

De Silva, N. S. and U. Klein (2015). "Dynamics of B cells in germinal centres." Nat Rev Immunol **15**(3): 137-148.

Deeks, S. G. and B. D. Walker (2007). "Human immunodeficiency virus controllers: mechanisms of durable virus control in the absence of antiretroviral therapy." Immunity **27**(3): 406-416.

Deenick, E. K., D. T. Avery, et al. (2013). "Naive and memory human B cells have distinct requirements for STAT3 activation to differentiate into antibody-secreting plasma cells." J Exp Med **210**(12): 2739-2753.

Dennison, S. M., K. Anasti, et al. (2011). "Nonneutralizing HIV-1 gp41 envelope cluster II human monoclonal antibodies show polyreactivity for binding to phospholipids and protein autoantigens." J Virol **85**(3): 1340-1347.

Derdeyn, C. A., P. L. Moore, et al. (2014). "Development of broadly neutralizing antibodies from autologous neutralizing antibody responses in HIV infection." Curr Opin HIV AIDS **9**(3): 210-216.

Descatoire, M., J. C. Weill, et al. (2011). "A human equivalent of mouse B-1 cells?" J Exp Med **208**(13): 2563-2564.

Di Niro, R., S. J. Lee, et al. (2015). "Salmonella Infection Drives Promiscuous B Cell Activation Followed by Extrafollicular Affinity Maturation." Immunity **43**(1): 120-131.

Doepper, S., H. Stoiber, et al. (2000). "B cell-mediated infection of stimulated and unstimulated autologous T lymphocytes with HIV-1: Role of complement." Immunobiology **202**(3): 293-305.

Doepper, S., D. Wilflingseder, et al. (2003). "Mechanism(s) promoting HIV-1 infection of primary unstimulated T lymphocytes in autologous B cell/T cell co-cultures." Eur J Immunol **33**(8): 2098-2107.

Doria-Rose, N. A., R. M. Klein, et al. (2010). "Breadth of human immunodeficiency virus-specific neutralizing activity in sera: clustering analysis and association with clinical variables." J Virol **84**(3): 1631-1636.

Dotan, I., L. Werner, et al. (2010). "CXCL12 Is a Constitutive and Inflammatory Chemokine in the Intestinal Immune System." Inflammatory Bowel Diseases **16**(4): 583-592.

Ebenbichler, C. F., N. M. Thielens, et al. (1991). "Human-Immunodeficiency-Virus Type-1 Activates the Classical Pathway of Complement by Direct C1-Binding through Specific Sites in the Transmembrane Glycoprotein-Gp41." Journal of Experimental Medicine **174**(6): 1417-1424.

Ehrhardt, G. R., R. S. Davis, et al. (2003). "The inhibitory potential of Fc receptor homolog 4 on memory B cells." Proc Natl Acad Sci U S A **100**(23): 13489-13494.

Ehrhardt, G. R., J. T. Hsu, et al. (2005). "Expression of the immunoregulatory molecule FcRH4 defines a distinctive tissue-based population of memory B cells." J Exp Med **202**(6): 783-791.

Escolano, A., J. M. Steichen, et al. (2016). "Sequential Immunization Elicits Broadly Neutralizing Anti-HIV-1 Antibodies in Ig Knockin Mice." Cell **166**(6): 1445-1458 e1412.

Estes, J. D. (2013). "Pathobiology of HIV/SIV-associated changes in secondary lymphoid tissues." Immunol Rev **254**(1): 65-77.

Estes, J. D., A. T. Haase, et al. (2008). "The role of collagen deposition in depleting CD4+T cells and limiting reconstitution in HIV-1 and SIV infections through damage to the secondary lymphoid organ niche." Semin Immunol **20**(3): 181-186.

Eto, D., C. Lao, et al. (2011). "IL-21 and IL-6 are critical for different aspects of B cell immunity and redundantly induce optimal follicular helper CD4 T cell (Tfh) differentiation." PLoS One **6**(3): e17739.

Ettinger, R., S. Kuchen, et al. (2008). "The role of IL-21 in regulating B-cell function in health and disease." Immunol Rev **223**: 60-86.

Ettinger, R., G. P. Sims, et al. (2005). "IL-21 induces differentiation of human naive and memory B cells into antibody-secreting plasma cells." J Immunol **175**(12): 7867-7879.

Fecteau, J. F., G. Cote, et al. (2006). "A new memory CD27-IgG+ B cell population in peripheral blood expressing VH genes with low frequency of somatic mutation." J Immunol **177**(6): 3728-3736.

Ferreira, C. B., A. Merino-Mansilla, et al. (2013). "Evolution of Broadly Cross-Reactive HIV-1-Neutralizing Activity: Therapy-Associated Decline, Positive Association with Detectable Viremia, and Partial Restoration of B-Cell Subpopulations." Journal of Virology **87**(22): 12227-12236.

Finak, G., M. Langweiler, et al. (2016). "Standardizing Flow Cytometry Immunophenotyping Analysis from the Human ImmunoPhenotyping Consortium." Sci Rep **6**: 20686.

Fink, K. (2012). "Origin and Function of Circulating Plasmablasts during Acute Viral Infections." Front Immunol **3**: 78.

Fletcher, A. L., S. E. Acton, et al. (2015). "Lymph node fibroblastic reticular cells in health and disease." Nat Rev Immunol **15**(6): 350-361.

Flint, S. M., A. Gibson, et al. (2016). "A distinct plasmablast and naive B-cell phenotype in primary immune thrombocytopenia." Haematologica **101**(6): 698-706.

Fromentin, R., W. Bakeman, et al. (2016). "CD4+ T Cells Expressing PD-1, TIGIT and LAG-3 Contribute to HIV Persistence during ART." PLoS Pathog **12**(7): e1005761.

Fukazawa, Y., R. Lum, et al. (2015). "B cell follicle sanctuary permits persistent productive simian immunodeficiency virus infection in elite controllers." Nat Med **21**(2): 132-139.

Fulwyler, M. J. (1965). "Electronic separation of biological cells by volume." Science **150**(3698): 910-911.

Gattinoni, L., E. Lugli, et al. (2011). "A human memory T cell subset with stem cell-like properties." Nat Med **17**(10): 1290-1297.

Gaudilliere, B., G. K. Fragiadakis, et al. (2014). "Clinical recovery from surgery correlates with single-cell immune signatures." Sci Transl Med **6**(255): 255ra131.

Gawad, C., W. Koh, et al. (2016). "Single-cell genome sequencing: current state of the science." Nat Rev Genet **17**(3): 175-188.

Geijtenbeek, T. B. H., D. S. Kwon, et al. (2000). "DC-SIGN, a dendritic cell-specific HIV-1-binding protein that enhances trans-infection of T cells." Cell **100**(5): 587-597.

Gitlin, A. D., C. T. Mayer, et al. (2015). "HUMORAL IMMUNITY. T cell help controls the speed of the cell cycle in germinal center B cells." Science **349**(6248): 643-646.

Gonzalez, S. F., S. E. Degn, et al. (2011). "Trafficking of B cell antigen in lymph nodes." Annu Rev Immunol **29**: 215-233.

Good-Jacobson, K. L. and M. J. Shlomchik (2010). "Plasticity and heterogeneity in the generation of memory B cells and long-lived plasma cells: the influence of germinal center interactions and dynamics." Journal of Immunology **185**(6): 3117-3125.

Good, K. L., V. L. Bryant, et al. (2006). "Kinetics of human B cell behavior and amplification of proliferative responses following stimulation with IL-21." J Immunol **177**(8): 5236-5247.

Goodglick, L., N. Zevit, et al. (1995). "Mapping the Ig superantigen-binding site of HIV-1 gp120." J Immunol **155**(11): 5151-5159.

Gray, E. S., P. L. Moore, et al. (2007). "Neutralizing antibody responses in acute human immunodeficiency virus type 1 subtype C infection." J Virol **81**(12): 6187-6196.

Gray, E. S., P. L. Moore, et al. (2007). "Neutralizing antibody responses in acute human immunodeficiency virus type 1 subtype C infection." J Virol **81**(12): 6187-6196.

Griffin, D. O., N. E. Holodick, et al. (2011). "Human B1 cells are CD3-: A reply to "A human equivalent of mouse B-1 cells?" and "The nature of circulating CD27+CD43+ B cells"." J Exp Med **208**(13): 2566-2569.

Griffin, D. O., N. E. Holodick, et al. (2011). "Human B1 cells in umbilical cord and adult peripheral blood express the novel phenotype CD20+ CD27+ CD43+ CD70." J Exp Med **208**(1): 67-80.

Griffith, J. W., C. L. Sokol, et al. (2014). "Chemokines and chemokine receptors: positioning cells for host defense and immunity." Annu Rev Immunol **32**: 659-702.

Groom, J. R. and A. D. Luster (2011). "CXCR3 ligands: redundant, collaborative and antagonistic functions." Immunol Cell Biol **89**(2): 207-215.

Grossman, Z., M. Meier-Schellersheim, et al. (2006). "Pathogenesis of HIV infection: what the virus spares is as important as what it destroys." Nat Med **12**(3): 289-295.

Gunthard, H. F., M. S. Saag, et al. (2016). "Antiretroviral Drugs for Treatment and Prevention of HIV Infection in Adults: 2016 Recommendations of the International Antiviral Society-USA Panel." JAMA **316**(2): 191-210.

Haas, A., K. Zimmermann, et al. (2011). "Antigen-dependent and -independent mechanisms of T and B cell hyperactivation during chronic HIV-1 infection." J Virol **85**(23): 12102-12113.

Halverson, R., R. M. Torres, et al. (2004). "Receptor editing is the main mechanism of B cell tolerance toward membrane antigens." Nature Immunology **5**(6): 645-650.

Hangartner, L., R. M. Zinkernagel, et al. (2006). "Antiviral antibody responses: the two extremes of a wide spectrum." Nat Rev Immunol **6**(3): 231-243.

Hansmann, L., L. Blum, et al. (2015). "Mass cytometry analysis shows that a novel memory phenotype B cell is expanded in multiple myeloma." Cancer Immunol Res **3**(6): 650-660.

Hao, Z. Y., G. S. Duncan, et al. (2008). "Fas Receptor Expression in Germinal-Center B Cells Is Essential for T and B Lymphocyte Homeostasis." Immunity **29**(4): 615-627.

Harwood, N. E. and F. D. Batista (2010). "Early events in B cell activation." Annu Rev Immunol **28**: 185-210.

Hasbold, J., L. M. Corcoran, et al. (2004). "Evidence from the generation of immunoglobulin G-secreting cells that stochastic mechanisms regulate lymphocyte differentiation." Nat Immunol **5**(1): 55-63.

Hatano, H., V. Jain, et al. (2013). "Cell-based measures of viral persistence are associated with immune activation and programmed cell death protein 1 (PD-1)-expressing CD4+ T cells." J Infect Dis **208**(1): 50-56.

Hauser, A. E., G. F. Debes, et al. (2002). "Chemotactic responsiveness toward ligands for CXCR3 and CXCR4 is regulated on plasma blasts during the time course of a memory immune response." Journal of Immunology **169**(3): 1277-1282.

Haynes, B. F., J. Fleming, et al. (2005). "Cardiolipin polyspecific autoreactivity in two broadly neutralizing HIV-1 antibodies." Science **308**(5730): 1906-1908.

Haynes, B. F., G. Kelsoe, et al. (2012). "B-cell-lineage immunogen design in vaccine development with HIV-1 as a case study." Nat Biotechnol **30**(5): 423-433.

Haynes, B. F. and D. C. Montefiori (2006). "Aiming to induce broadly reactive neutralizing antibody responses with HIV-1 vaccine candidates." Expert Rev Vaccines **5**(4): 579-595.

Haynes, B. F., M. A. Moody, et al. (2011). "B cell responses to HIV-1 infection and vaccination: pathways to preventing infection." Trends Mol Med **17**(2): 108-116.

He, R., S. Hou, et al. (2016). "Follicular CXCR5-expressing CD8+ T cells curtail chronic viral infection." Nature **537**(7620): 412-428.

Heesters, B. A., P. Chatterjee, et al. (2013). "Endocytosis and recycling of immune complexes by follicular dendritic cells enhances B cell antigen binding and activation." Immunity **38**(6): 1164-1175.

Heesters, B. A., R. C. Myers, et al. (2014). "Follicular dendritic cells: dynamic antigen libraries." Nat Rev Immunol **14**(7): 495-504.

Henneken, M., T. Dorner, et al. (2005). "Differential expression of chemokine receptors on peripheral blood B cells from patients with rheumatoid arthritis and systemic lupus erythematosus." Arthritis Res Ther **7**(5): R1001-1013.

Herzenberg, L. A., D. Parks, et al. (2002). "The history and future of the fluorescence activated cell sorter and flow cytometry: a view from Stanford." Clin Chem **48**(10): 1819-1827.

Hoot, S., A. T. McGuire, et al. (2013). "Recombinant HIV Envelope Proteins Fail to Engage Germline Versions of Anti-CD4bs bNAbs." PLoS Pathog **9**(1): e1003106.

Huang, J., G. Ofek, et al. (2012). "Broad and potent neutralization of HIV-1 by a gp41-specific human antibody." Nature **491**(7424): 406-412.

Hulett, H. R., W. A. Bonner, et al. (1969). "Cell Sorting - Automated Separation of Mammalian Cells as a Function of Intracellular Fluorescence." Science **166**(3906): 747-&.

Isnardi, I., Y. S. Ng, et al. (2010). "Complement receptor 2/CD21- human naive B cells contain mostly autoreactive unresponsive clones." Blood **115**(24): 5026-5036.

Jakubik, J. J., M. Saifuddin, et al. (1999). "B lymphocytes in lymph nodes and peripheral blood are important for binding immune complexes containing HIV-1." Immunology **96**(4): 612-619.

Jakubik, J. J., M. Saifuddin, et al. (2000). "Immune complexes containing human immunodeficiency virus type 1 primary isolates bind to lymphoid tissue B lymphocytes and are infectious for T lymphocytes." J Virol **74**(1): 552-555.

Jelicic, K., R. Cimbro, et al. (2013). "The HIV-1 envelope protein gp120 impairs B cell proliferation by inducing TGF-beta1 production and FcRL4 expression." Nat Immunol **14**(12): 1256-1265.

Jesus, A. A., A. J. Duarte, et al. (2008). "Autoimmunity in hyper-IgM syndrome." J Clin Immunol **28 Suppl 1**: S62-66.

Ji, X., H. Gewurz, et al. (2005). "Mannose binding lectin (MBL) and HIV." Mol Immunol **42**(2): 145-152.

Junt, T., E. A. Moseman, et al. (2007). "Subcapsular sinus macrophages in lymph nodes clear lymph-borne viruses and present them to antiviral B cells." Nature **450**(7166): 110.

Kalina, T., J. Flores-Montero, et al. (2015). "Quality assessment program for EuroFlow protocols: summary results of four-year (2010-2013) quality assurance rounds." Cytometry A **87**(2): 145-156.

Kalina, T., J. Flores-Montero, et al. (2012). "EuroFlow standardization of flow cytometer instrument settings and immunophenotyping protocols." Leukemia **26**(9): 1986-2010.

Kardava, L., S. Moir, et al. (2014). "Abnormal B cell memory subsets dominate HIV-specific responses in infected individuals." J Clin Invest **124**(7): 3252-3262.

Kardava, L., S. Moir, et al. (2011). "Attenuation of HIV-associated human B cell exhaustion by siRNA downregulation of inhibitory receptors." J Clin Invest **121**(7): 2614-2624.

Kerneis, S., O. Launay, et al. (2014). "Long-term immune responses to vaccination in HIV-infected patients: a systematic review and meta-analysis." Clin Infect Dis **58**(8): 1130-1139.

Kestens, L. and F. Mandy (2016). "Thirty-five years of CD4 T-Cell counting in HIV infection: From flow cytometry in the lab to point-of-care testing in the field." Cytometry B Clin Cytom.

Kitamura, D., A. Kudo, et al. (1992). "A critical role of lambda 5 protein in B cell development." Cell **69**(5): 823-831.

Klein, U., S. Casola, et al. (2006). "Transcription factor IRF4 controls plasma cell differentiation and class-switch recombination." Nat Immunol **7**(7): 773-782.

Kobie, J. J., D. C. Alcena, et al. (2012). "9G4 autoreactivity is increased in HIV-infected patients and correlates with HIV broadly neutralizing serum activity." PLoS One **7**(4): e35356.

Kolodziejczyk, A. A., J. K. Kim, et al. (2015). "The Technology and Biology of Single-Cell RNA Sequencing." Molecular Cell **58**(4): 610-620.

Kroon, F. P., J. T. van Dissel, et al. (1997). "Antibody response to Haemophilus influenzae type b vaccine in relation to the number of CD4+ T lymphocytes in adults infected with human immunodeficiency virus." Clin Infect Dis **25**(3): 600-606.

Kroon, F. P., J. T. Vandissel, et al. (1994). "Antibody-Response to Influenza, Tetanus and Pneumococcal Vaccines in Hiv-Seropositive Individuals in Relation to the Number of Cd4+ Lymphocytes." AIDS **8**(4): 469-476.

Kruetzmann, S., M. M. Rosado, et al. (2003). "Human immunoglobulin M memory B cells controlling Streptococcus pneumoniae infections are generated in the spleen." J Exp Med **197**(7): 939-945.

Kuka, M. and M. Iannacone (2014). "The role of lymph node sinus macrophages in host defense." Ann N Y Acad Sci **1319**: 38-46.

Kunkel, E. J. and E. C. Butcher (2003). "Plasma-cell homing." Nat Rev Immunol **3**(10): 822-829.

Kurosaki, T., K. Kometani, et al. (2015). "Memory B cells." Nat Rev Immunol **15**(3): 149-159.

Kwon, D. S., G. Gregorio, et al. (2002). "DC-SIGN-mediated internalization of HIV is required for trans-enhancement of T cell infection." Immunity **16**(1): 135-144.

Lane, H. C., H. Masur, et al. (1983). "Abnormalities of B-cell activation and immunoregulation in patients with the acquired immunodeficiency syndrome." N Engl J Med **309**(8): 453-458.

Lang, J., M. Jackson, et al. (1996). "B cells are exquisitely sensitive to central tolerance and receptor editing induced by ultralow affinity, membrane-bound antigen." J Exp Med **184**(5): 1685-1697.

LeBien, T. W. (2000). "Fates of human B-cell precursors." Blood **96**(1): 9-23.

LeBien, T. W. and T. F. Tedder (2008). "B lymphocytes: how they develop and function." Blood **112**(5): 1570-1580.

Lederman, M. M. and L. Margolis (2008). "The lymph node in HIV pathogenesis." Semin Immunol **20**(3): 187-195.

Lee, S. K., R. J. Rigby, et al. (2011). "B cell priming for extrafollicular antibody responses requires Bcl-6 expression by T cells." J Exp Med **208**(7): 1377-1388.

Lefevre, E. A., R. Krzysiek, et al. (1999). "Cutting edge: HIV-1 tat protein differentially modulates the B cell response of naive, memory, and germinal center B cells." J Immunol **163**(3): 1119-1122.

Lefranc, M. P. (2001). "Nomenclature of the human immunoglobulin genes." Curr Protoc Immunol **Appendix 1**: Appendix 1P.

Levesque, M. C., M. A. Moody, et al. (2009). "Polyclonal B cell differentiation and loss of gastrointestinal tract germinal centers in the earliest stages of HIV-1 infection." PLoS Med **6**(7): e1000107.

Liao, H. X., X. Chen, et al. (2011). "Initial antibodies binding to HIV-1 gp41 in acutely infected subjects are polyreactive and highly mutated." J Exp Med.

Liao, H. X., R. Lynch, et al. (2013). "Co-evolution of a broadly neutralizing HIV-1 antibody and founder virus." Nature **496**(7446): 469.

Lin, L., G. Finak, et al. (2015). "COMPASS identifies T-cell subsets correlated with clinical outcomes." Nat Biotechnol **33**(6): 610-616.

Link, A., T. K. Vogt, et al. (2007). "Fibroblastic reticular cells in lymph nodes regulate the homeostasis of naive T cells." Nat Immunol **8**(11): 1255-1265.

Linterman, M. A., L. Beaton, et al. (2010). "IL-21 acts directly on B cells to regulate Bcl-6 expression and germinal center responses." J Exp Med **207**(2): 353-363.

Liu, Y. J., J. Zhang, et al. (1991). "Sites of specific B cell activation in primary and secondary responses to T cell-dependent and T cell-independent antigens." Eur J Immunol **21**(12): 2951-2962.

Lorenzo-Redondo, R., H. R. Fryer, et al. (2016). "Persistent HIV-1 replication maintains the tissue reservoir during therapy." Nature **530**(7588): 51-56.

MacLennan, C. A., J. J. Gilchrist, et al. (2010). "Dysregulated humoral immunity to nontyphoidal Salmonella in HIV-infected African adults." Science **328**(5977): 508-512.

MacLennan, I. C., K. M. Toellner, et al. (2003). "Extrafollicular antibody responses." Immunol Rev **194**: 8-18.

Maecker, H. T., J. P. McCoy, et al. (2012). "Standardizing immunophenotyping for the Human Immunology Project." Nature Reviews Immunology **12**(3): 191-200.

Maecker, H. T., A. Rinfret, et al. (2005). "Standardization of cytokine flow cytometry assays." BMC Immunol **6**: 13.

Mahnke, Y. D. and M. Roederer (2007). "Optimizing a multicolor immunophenotyping assay." Clin Lab Med **27**(3): 469-485, v.

Mair, F., F. J. Hartmann, et al. (2016). "The end of gating? An introduction to automated analysis of high dimensional cytometry data." Eur J Immunol **46**(1): 34-43.

Malaspina, A., S. Moir, et al. (2007). "Idiopathic CD4(+) T lymphocytopenia is associated with increases in immature/transitional B cells and serum levels of IL-7." Blood **109**(5): 2086-2088.

Malaspina, A., S. Moir, et al. (2006). "Appearance of immature/transitional B cells in HIV-infected individuals with advanced disease: correlation with increased IL-7." Proc Natl Acad Sci U S A **103**(7): 2262-2267.

Malaspina, A., S. Moir, et al. (2005). "Compromised B cell responses to influenza vaccination in HIV-infected individuals." J Infect Dis **191**(9): 1442-1450.

Martin, F., A. M. Oliver, et al. (2001). "Marginal zone and B1 B cells unite in the early response against T-independent blood-borne particulate antigens." Immunity **14**(5): 617-629.

Martinez-Maza, O., E. Crabb, et al. (1987). "Infection with the human immunodeficiency virus (HIV) is associated with an in vivo increase in B lymphocyte activation and immaturity." J Immunol **138**(11): 3720-3724.

Mascola, J. R. and B. F. Haynes (2013). "HIV-1 neutralizing antibodies: understanding nature's pathways." Immunol Rev **254**(1): 225-244.

Masilamani, M., D. Kassahn, et al. (2003). "B cell activation leads to shedding of complement receptor type II (CR2/CD21)." Eur J Immunol **33**(9): 2391-2397.

McGuire, A. T., S. Hoot, et al. (2013). "Engineering HIV envelope protein to activate germline B cell receptors of broadly neutralizing anti-CD4 binding site antibodies." J Exp Med.

McHeyzer-Williams, L. J., P. J. Milpied, et al. (2015). "Class-switched memory B cells remodel BCRs within secondary germinal centers." Nat Immunol **16**(3): 296-305.

McMichael, A. J., P. Borrow, et al. (2010). "The immune response during acute HIV-1 infection: clues for vaccine development." Nat Rev Immunol **10**(1): 11-23.

Mebius, R. E. and G. Kraal (2005). "Structure and function of the spleen." Nat Rev Immunol **5**(8): 606-616.

Medina, F., C. Segundo, et al. (1997). "Regulatory role of CD95 ligation on human B cells induced in vivo capable of spontaneous and high-rate Ig secretion." Eur J Immunol **27**(3): 700-706.

Meffre, E. (2011). "The establishment of early B cell tolerance in humans: lessons from primary immunodeficiency diseases." Ann N Y Acad Sci **1246**: 1-10.

Meffre, E., A. Louie, et al. (2016). "Maturational characteristics of HIV-specific antibodies in viremic individuals." JCI Insight **1**(3).

Meffre, E. and H. Wardemann (2008). "B-cell tolerance checkpoints in health and autoimmunity." Curr Opin Immunol **20**(6): 632-638.

Mei, H. E., T. Yoshida, et al. (2009). "Blood-borne human plasma cells in steady state are derived from mucosal immune responses." Blood **113**(11): 2461-2469.

Melchers, F. (2015). "Checkpoints that control B cell development." Journal of Clinical Investigation **125**(6): 2203-2210.

Mena, G., A. L. Garcia-Basteiro, et al. (2015). "Hepatitis B and A vaccination in HIV-infected adults: A review." Hum Vaccin Immunother **11**(11): 2582-2598.

Mesin, L., J. Ersching, et al. (2016). "Germinal Center B Cell Dynamics." Immunity **45**(3): 471-482.

Mills, D. M. and J. C. Cambier (2003). "B lymphocyte activation during cognate interactions with CD4+ T lymphocytes: molecular dynamics and immunologic consequences." Semin Immunol **15**(6): 325-329.

Minnich, M., H. Tagoh, et al. (2016). "Multifunctional role of the transcription factor Blimp-1 in coordinating plasma cell differentiation." Nat Immunol **17**(3): 331-343.

Moens, L. and S. G. Tangye (2014). "Cytokine-Mediated Regulation of Plasma Cell Generation: IL-21 Takes Center Stage." Front Immunol **5**: 65.

Moir, S., C. M. Buckner, et al. (2010). "B cells in early and chronic HIV infection: evidence for preservation of immune function associated with early initiation of antiretroviral therapy." Blood.

Moir, S. and A. S. Fauci (2008). "Pathogenic mechanisms of B-lymphocyte dysfunction in HIV disease." J Allergy Clin Immunol **122**(1): 12-19; quiz 20-11.

Moir, S. and A. S. Fauci (2009). "B cells in HIV infection and disease." Nat Rev Immunol **9**(4): 235-245.

Moir, S. and A. S. Fauci (2013). "Insights into B cells and HIV-specific B-cell responses in HIV-infected individuals." Immunol Rev **254**(1): 207-224.

Moir, S. and A. S. Fauci (2014). "B-cell exhaustion in HIV infection: the role of immune activation." Curr Opin HIV AIDS **9**(5): 472-477.

Moir, S., J. Ho, et al. (2008). "Evidence for HIV-associated B cell exhaustion in a dysfunctional memory B cell compartment in HIV-infected viremic individuals." J Exp Med **205**(8): 1797-1805.

Moir, S., A. Malaspina, et al. (2008). "Normalization of B cell counts and subpopulations after antiretroviral therapy in chronic HIV disease." J Infect Dis **197**(4): 572-579.

Moir, S., A. Malaspina, et al. (2000). "B cells of HIV-1-infected patients bind virions through CD21-complement interactions and transmit infectious virus to activated T cells." Journal of Experimental Medicine **192**(5): 637-645.

Moir, S., A. Malaspina, et al. (2001). "HIV-1 induces phenotypic and functional perturbations of B cells in chronically infected individuals." Proc Natl Acad Sci U S A **98**(18): 10362-10367.

Moir, S., A. Malaspina, et al. (2004). "Decreased survival of B cells of HIV-viremic patients mediated by altered expression of receptors of the TNF superfamily." J Exp Med **200**(7): 587-599.

Mond, J. J. and M. Brunswick (2003). "Proliferative assays for B cell function." Curr Protoc Immunol **Chapter 3**: Unit 3 10.

Mond, J. J., A. Lees, et al. (1995). "T cell-independent antigens type 2." Annu Rev Immunol **13**: 655-692.

Monroe, J. G. (2006). "ITAM-mediated tonic signalling through pre-BCR and BCR complexes." Nature Reviews Immunology **6**(4): 283-294.

Moore, P. L., C. Williamson, et al. (2015). "Virological features associated with the development of broadly neutralizing antibodies to HIV-1." Trends in Microbiology **23**(4): 204-211.

Morris, L., J. M. Binley, et al. (1998). "HIV-1 antigen-specific and -nonspecific B cell responses are sensitive to combination antiretroviral therapy." J Exp Med **188**(2): 233-245.

Morris, L., J. M. Binley, et al. (1998). "HIV-1 antigen-specific and -nonspecific B cell responses are sensitive to combination antiretroviral therapy." Journal of Experimental Medicine **188**(2): 233-245.

Mouquet, H., J. F. Scheid, et al. (2010). "Polyreactivity increases the apparent affinity of anti-HIV antibodies by heteroligation." Nature **467**(7315): 591-595.

Muehlinghaus, G., L. Cigliano, et al. (2005). "Regulation of CXCR3 and CXCR4 expression during terminal differentiation of memory B cells into plasma cells." Blood **105**(10): 3965-3971.

Muster, T., F. Steindl, et al. (1993). "A conserved neutralizing epitope on gp41 of human immunodeficiency virus type 1." J Virol **67**(11): 6642-6647.

Nair, N., E. W. Newell, et al. (2016). "High-dimensional immune profiling of total and rotavirus VP6-specific intestinal and circulating B cells by mass cytometry." Mucosal Immunol **9**(1): 68-82.

Nakayama, T., K. Hieshima, et al. (2003). "Cutting edge: Profile of chemokine receptor expression on human plasma cells accounts for their efficient recruitment to target tissues." Journal of Immunology **170**(3): 1136-1140.

Napolitano, L. A., R. M. Grant, et al. (2001). "Increased production of IL-7 accompanies HIV-1-mediated T-cell depletion: implications for T-cell homeostasis." Nat Med **7**(1): 73-79.

Nemazee, D. (2006). "Receptor editing in lymphocyte development and central tolerance." Nat Rev Immunol **6**(10): 728-740.

Neshat, M. N., L. Goodglick, et al. (2000). "Mapping the B cell superantigen binding site for HIV-1 gp120 on a V(H)3 Ig." Int Immunol **12**(3): 305-312.

Newell, E. W., N. Sigal, et al. (2012). "Cytometry by time-of-flight shows combinatorial cytokine expression and virus-specific cell niches within a continuum of CD8+ T cell phenotypes." Immunity **36**(1): 142-152.

Nitschke, L. (2005). "The role of CD22 and other inhibitory co-receptors in B-cell activation." Curr Opin Immunol **17**(3): 290-297.

Nuccitelli, A., C. D. Rinaudo, et al. (2015). "Group B Streptococcus vaccine: state of the art." Ther Adv Vaccines **3**(3): 76-90.

Nutt, S. L., P. D. Hodgkin, et al. (2015). "The generation of antibody-secreting plasma cells." Nat Rev Immunol **15**(3): 160-171.

Odendahl, M., H. Mei, et al. (2005). "Generation of migratory antigen-specific plasma blasts and mobilization of resident plasma cells in a secondary immune response." Blood **105**(4): 1614-1621.

Okada, T., M. J. Miller, et al. (2005). "Antigen-engaged B cells undergo chemotaxis toward the T zone and form motile conjugates with helper T cells." PLoS Biol **3**(6): e150.

Okada, T., V. N. Ngo, et al. (2002). "Chemokine requirements for B cell entry to lymph nodes and Peyer's patches." J Exp Med **196**(1): 65-75.

Oliviero, B., S. Mantovani, et al. (2015). "Skewed B cells in chronic hepatitis C virus infection maintain their ability to respond to virus-induced activation." Journal of Viral Hepatitis **22**(4): 391-398.

Overbaugh, J. and L. Morris (2012). "The Antibody Response against HIV-1." Cold Spring Harb Perspect Med **2**(1): a007039.

Pallikkuth, S., M. Sharkey, et al. (2015). "Peripheral T Follicular Helper Cells Are the Major HIV Reservoir within Central Memory CD4 T Cells in Peripheral Blood from Chronically HIV-Infected Individuals on Combination Antiretroviral Therapy." J Virol **90**(6): 2718-2728.

Pallikkuth, S., M. Sharkey, et al. (2016). "Peripheral T Follicular Helper Cells Are the Major HIV Reservoir within Central Memory CD4 T Cells in Peripheral Blood from Chronically HIV-

Infected Individuals on Combination Antiretroviral Therapy." Journal of Virology **90**(6): 2718-2728.

Park, C., I. Y. Hwang, et al. (2012). "Lymph node B lymphocyte trafficking is constrained by anatomy and highly dependent upon chemoattractant desensitization." Blood **119**(4): 978-989.

Parker, D. C. (1993). "T cell-dependent B cell activation." Annu Rev Immunol **11**: 331-360.

Patke, C. L. and W. T. Shearer (2000). "gp120- and TNF-alpha-induced modulation of human B cell function: proliferation, cyclic AMP generation, Ig production, and B-cell receptor expression." J Allergy Clin Immunol **105**(5): 975-982.

Paus, D., T. G. Phan, et al. (2006). "Antigen recognition strength regulates the choice between extrafollicular plasma cell and germinal center B cell diff erentiation." Journal of Experimental Medicine **203**(4): 1081-1091.

Pejoski, D., N. Tchitchek, et al. (2016). "Identification of Vaccine-Altered Circulating B Cell Phenotypes Using Mass Cytometry and a Two-Step Clustering Analysis." J Immunol **196**(11): 4814-4831.

Perfetto, S. P., P. K. Chattopadhyay, et al. (2004). "Seventeen-colour flow cytometry: unravelling the immune system." Nat Rev Immunol **4**(8): 648-655.

Perreau, M., A. L. Savoye, et al. (2013). "Follicular helper T cells serve as the major CD4 T cell compartment for HIV-1 infection, replication, and production." Journal of Experimental Medicine **210**(1): 143-156.

Phan, T. G., I. Grigorova, et al. (2007). "Subcapsular encounter and complement-dependent transport of immune complexes by lymph node B cells." Nature Immunology **8**(9): 992-1000.

Pillai, S., H. Mattoo, et al. (2011). "B cells and autoimmunity." Curr Opin Immunol **23**(6): 721-731.

Portugal, S., C. M. Tipton, et al. (2015). "Malaria-associated atypical memory B cells exhibit markedly reduced B cell receptor signaling and effector function." Elife **4**.

Qiu, P., E. F. Simonds, et al. (2011). "Extracting a cellular hierarchy from high-dimensional cytometry data with SPADE." Nat Biotechnol **29**(10): 886-891.

Rakhmanov, M., B. Keller, et al. (2009). "Circulating CD21low B cells in common variable immunodeficiency resemble tissue homing, innate-like B cells." Proc Natl Acad Sci U S A **106**(32): 13451-13456.

Rappocciolo, G., P. Piazza, et al. (2006). "DC-SIGN on B lymphocytes is required for transmission of HIV-1 to T lymphocytes." Plos Pathogens **2**(7): 691-704.

Reed, J. H., J. Jackson, et al. (2016). "Clonal redemption of autoantibodies by somatic hypermutation away from self-reactivity during human immunization." J Exp Med **213**(7): 1255-1265.

Roederer, M. (2002). "Multiparameter FACS analysis." Curr Protoc Immunol **Chapter 5**: Unit 5 8.

Roozendaal, R. and M. C. Carroll (2007). "Complement receptors CD21 and CD35 in humoral immunity." Immunol Rev **219**: 157-166.

Roozendaal, R., T. R. Mempel, et al. (2009). "Conduits mediate transport of low-molecular-weight antigen to lymph node follicles." Immunity **30**(2): 264-276.

Rusert, P., R. D. Kouyos, et al. (2016). "Determinants of HIV-1 broadly neutralizing antibody induction." Nat Med **22**(11): 1260-1267.

Saadoun, D., B. Terrier, et al. (2012). "Expansion of Autoreactive Unresponsive CD21(-/Low) B Cells in Sjogren's Syndrome Associated Lymphoproliferation." Arthritis Rheum **64**(10): S757-S757.

Saadoun, D., B. Terrier, et al. (2013). "Expansion of autoreactive unresponsive CD21-/low B cells in Sjogren's syndrome-associated lymphoproliferation." Arthritis Rheum **65**(4): 1085-1096.

Sabouri, Z., P. Schofield, et al. (2014). "Redemption of autoantibodies on anergic B cells by variable-region glycosylation and mutation away from self-reactivity." Proc Natl Acad Sci U S A **111**(25): E2567-2575.

Saeys, Y., S. Van Gassen, et al. (2016). "Computational flow cytometry: helping to make sense of high-dimensional immunology data." Nature Reviews Immunology **16**(7): 449-462.

Sather, D. N., J. Armann, et al. (2009). "Factors associated with the development of cross-reactive neutralizing antibodies during human immunodeficiency virus type 1 infection." J Virol **83**(2): 757-769.

Schacker, T. W., P. L. Nguyen, et al. (2002). "Persistent abnormalities in lymphoid tissues of human immunodeficiency virus-infected patients successfully treated with highly active antiretroviral therapy." Journal of Infectious Diseases **186**(8): 1092-1097.

Schall, T. J., K. Bacon, et al. (1993). "Human Macrophage Inflammatory Protein-Alpha (Mip-1-Alpha) and Mip-1-Beta Chemokines Attract Distinct Populations of Lymphocytes." Journal of Experimental Medicine **177**(6): 1821-1825.

Schatz, D. G. and Y. Ji (2011). "Recombination centres and the orchestration of V(D)J recombination." Nature Reviews Immunology **11**(4): 251-263.

Schatz, D. G. and P. C. Swanson (2011). "V(D)J Recombination: Mechanisms of Initiation." Annual Review of Genetics, Vol 45 **45**: 167-202.

Schnittman, S. M., H. C. Lane, et al. (1986). "Direct polyclonal activation of human B lymphocytes by the acquired immune deficiency syndrome virus." Science **233**(4768): 1084-1086.

Scholzen, T. and J. Gerdes (2000). "The Ki-67 protein: from the known and the unknown." J Cell Physiol **182**(3): 311-322.

Schulz, K. R., E. A. Danna, et al. (2012). "Single-cell phospho-protein analysis by flow cytometry." Curr Protoc Immunol **Chapter 8**: Unit 8 17 11-20.

Schwickert, T. A., G. D. Victora, et al. (2011). "A dynamic T cell-limited checkpoint regulates affinity-dependent B cell entry into the germinal center." Journal of Experimental Medicine **208**(6): 1243-1252.

Sciaranghella, G., N. Tong, et al. (2012). "Decoupling activation and exhaustion of B cells in spontaneous controllers of HIV infection." AIDS.

Seder, R. A., P. A. Darrah, et al. (2008). "T-cell quality in memory and protection: implications for vaccine design." Nature Reviews Immunology **8**(4): 247-258.

Seifert, M. and R. Kuppers (2009). "Molecular footprints of a germinal center derivation of human IgM+(IgD+)CD27+ B cells and the dynamics of memory B cell generation." J Exp Med **206**(12): 2659-2669.

Seifert, M., M. Przekopowitz, et al. (2015). "Functional capacities of human IgM memory B cells in early inflammatory responses and secondary germinal center reactions." Proc Natl Acad Sci U S A **112**(6): E546-555.

Setty, M., M. D. Tadmor, et al. (2016). "Wishbone identifies bifurcating developmental trajectories from single-cell data." Nat Biotechnol **34**(6): 637-645.

Shirai, A., M. Cosentino, et al. (1992). "Human-Immunodeficiency-Virus Infection Induces Both Polyclonal and Virus-Specific B-Cell Activation." Journal of Clinical Investigation **89**(2): 561-566.

Shlomchik, M. J. and F. Weisel (2012). "Germinal center selection and the development of memory B and plasma cells." Immunol Rev **247**(1): 52-63.

Simek, M. D., W. Rida, et al. (2009). "Human immunodeficiency virus type 1 elite neutralizers: individuals with broad and potent neutralizing activity identified by using a high-throughput neutralization assay together with an analytical selection algorithm." J Virol **83**(14): 7337-7348.

Sims, G. P., R. Ettinger, et al. (2005). "Identification and characterization of circulating human transitional B cells." Blood **105**(11): 4390-4398.

Solder, B. M., T. F. Schulz, et al. (1989). "HIV and HIV-infected cells differentially activate the human complement system independent of antibody." Immunol Lett **22**(2): 135-145.

Spear, G. T., H. X. Jiang, et al. (1991). "Direct binding of complement component C1q to human immunodeficiency virus (HIV) and human T lymphotrophic virus-I (HTLV-I) coinfected cells." AIDS Res Hum Retroviruses **7**(7): 579-585.

Spolski, R. and W. J. Leonard (2014). "Interleukin-21: a double-edged sword with therapeutic potential." Nat Rev Drug Discov **13**(5): 379-395.

Stoiber, H. (2009). "Complement, Fc receptors and antibodies: a Trojan horse in HIV infection?" Current Opinion in Hiv and Aids **4**(5): 394-399.

Stoiber, H., N. M. Thielens, et al. (1994). "The envelope glycoprotein of HIV-1 gp120 and human complement protein C1q bind to the same peptides derived from three different regions of gp41, the transmembrane glycoprotein of HIV-1, and share antigenic homology." Eur J Immunol **24**(2): 294-300.

Sugiyama, T., H. Kohara, et al. (2006). "Maintenance of the hematopoietic stem cell pool by CXCL12-CXCR4 chemokine signaling in bone marrow stromal cell niches." Immunity **25**(6): 977-988.

Sullivan, R. T., C. C. Kim, et al. (2015). "FCRL5 Delineates Functionally Impaired Memory B Cells Associated with Plasmodium falciparum Exposure." PLoS Pathog **11**(5): e1004894.

Svajger, U., M. Anderluh, et al. (2010). "C-type lectin DC-SIGN: An adhesion, signalling and antigen-uptake molecule that guides dendritic cells in immunity." Cellular Signalling **22**(10): 1397-1405.

Swingler, S., A. Mann, et al. (1999). "HIV-1 Nef mediates lymphocyte chemotaxis and activation by infected macrophages." Nature Medicine **5**(9): 997-1003.

Swingler, S., J. Zhou, et al. (2008). "Evidence for a pathogenic determinant in HIV-1 Nef involved in B cell dysfunction in HIV/AIDS." Cell Host Microbe **4**(1): 63-76.

Tang, H., J. E. Robinson, et al. (2011). "Epitopes Immediately Below the Base of the V3 Loop of gp120 as Targets for the Initial Autologous Neutralizing Antibody Response in Two HIV-1 Subtype B-Infected Individuals." J Virol.

Tangye, S. G. (2013). "To B1 or not to B1: that really is still the question!" Blood **121**(26): 5109-5110.

Tangye, S. G. (2015). "Advances in IL-21 biology - enhancing our understanding of human disease." Curr Opin Immunol **34**: 107-115.

Tangye, S. G. and K. L. Good (2007). "Human IgM+CD27+ B cells: memory B cells or "memory" B cells?" J Immunol **179**(1): 13-19.

Tarlton, N. J., C. M. Green, et al. (2012). "Plasmablast frequency and trafficking receptor expression are altered in pediatric ulcerative colitis." Inflamm Bowel Dis **18**(12): 2381-2391.

Tas, J. M., L. Mesin, et al. (2016). "Visualizing antibody affinity maturation in germinal centers." Science **351**(6277): 1048-1054.

Taylor, J. J., K. A. Pape, et al. (2015). "Apoptosis and antigen affinity limit effector cell differentiation of a single naive B cell." Science **347**(6223): 784-787.

Tebas, P., I. Frank, et al. (2010). "Poor immunogenicity of the H1N1 2009 vaccine in well controlled HIV-infected individuals." AIDS **24**(14): 2187-2192.

Tipton, C. M., C. F. Fucile, et al. (2015). "Diversity, cellular origin and autoreactivity of antibody-secreting cell population expansions in acute systemic lupus erythematosus." Nat Immunol **16**(7): 755-765.

Titanji, K., A. De Milito, et al. (2006). "Loss of memory B cells impairs maintenance of long-term serologic memory during HIV-1 infection." Blood **108**(5): 1580-1587.

Tjernlund, A., J. Zhu, et al. (2010). "In situ detection of Gag-specific CD8(+) cells in the GI tract of SIV infected Rhesus macaques." Retrovirology **7**.

Toapanta, F. R., J. K. Simon, et al. (2014). "Gut-Homing Conventional Plasmablasts and CD27(-) Plasmablasts Elicited after a Short Time of Exposure to an Oral Live-Attenuated Shigella Vaccine Candidate in Humans." Front Immunol **5**: 374.

Todd, D. J., L. J. McHeyzer-Williams, et al. (2009). "XBP1 governs late events in plasma cell differentiation and is not required for antigen-specific memory B cell development." Journal of Experimental Medicine **206**(10): 2151-2159.

Toellner, K. M., A. Gulbranson-Judge, et al. (1996). "Immunoglobulin switch transcript production in vivo related to the site and time of antigen-specific B cell activation." J Exp Med **183**(5): 2303-2312.

Toellner, K. M., W. E. Jenkinson, et al. (2002). "Low-level hypermutation in T cell-independent germinal centers compared with high mutation rates associated with T cell-dependent germinal centers." J Exp Med **195**(3): 383-389.

Toellner, K. M., S. A. Luther, et al. (1998). "T helper 1 (Th1) and Th2 characteristics start to develop during T cell priming and are associated with an immediate ability to induce immunoglobulin class switching." J Exp Med **187**(8): 1193-1204.

Tomaras, G. D. and B. F. Haynes (2009). "HIV-1-specific antibody responses during acute and chronic HIV-1 infection." Curr Opin HIV AIDS **4**(5): 373-379.

Tomaras, G. D., N. L. Yates, et al. (2008). "Initial B-cell responses to transmitted human immunodeficiency virus type 1: virion-binding immunoglobulin M (IgM) and IgG antibodies followed by plasma anti-gp41 antibodies with ineffective control of initial viremia." J Virol **82**(24): 12449-12463.

Tongren, J. E., C. J. Drakeley, et al. (2006). "Target antigen, age, and duration of antigen exposure independently regulate immunoglobulin G subclass switching in malaria." Infect Immun **74**(1): 257-264.

Trama, A. M., M. A. Moody, et al. (2014). "HIV-1 Envelope gp41 Antibodies Can Originate from Terminal Ileum B Cells that Share Cross-Reactivity with Commensal Bacteria." Cell Host & Microbe **16**(2): 215-226.

Trentin, L., A. Cabrelle, et al. (2004). "Homeostatic chemokines drive migration of malignant B cells in patients with non-Hodgkin lymphomas." Blood **104**(2): 502-508.

Verkoczy, L., Y. Chen, et al. (2011). "Rescue of HIV-1 broad neutralizing antibody-expressing B cells in 2F5 VH x VL knockin mice reveals multiple tolerance controls." Journal of Immunology **187**(7): 3785-3797.

Verkoczy, L., M. Diaz, et al. (2010). "Autoreactivity in an HIV-1 broadly reactive neutralizing antibody variable region heavy chain induces immunologic tolerance." Proc Natl Acad Sci U S A **107**(1): 181-186.

Verkoczy, L., G. Kelsoe, et al. (2014). "HIV-1 envelope gp41 broadly neutralizing antibodies: hurdles for vaccine development." PLoS Pathog **10**(5): e1004073.

Verschoor, C. P., A. Lelic, et al. (2015). "An introduction to automated flow cytometry gating tools and their implementation." Frontiers in Immunology **6**.

Victora, G. D., D. Dominguez-Sola, et al. (2012). "Identification of human germinal center light and dark zone cells and their relationship to human B-cell lymphomas." Blood **120**(11): 2240-2248.

Victora, G. D. and L. Mesin (2014). "Clonal and cellular dynamics in germinal centers." Curr Opin Immunol **28**: 90-96.

Victora, G. D. and M. C. Nussenzweig (2012). "Germinal centers." Annu Rev Immunol **30**: 429-457.

Victora, G. D., T. A. Schwickert, et al. (2010). "Germinal center dynamics revealed by multiphoton microscopy with a photoactivatable fluorescent reporter." Cell **143**(4): 592-605.

Vinuesa, C. G., M. A. Linterman, et al. (2016). "Follicular Helper T Cells." Annual Review of Immunology, Vol 28 **34**: 335-368.

von Andrian, U. H. and T. R. Mempel (2003). "Homing and cellular traffic in lymph nodes." Nat Rev Immunol **3**(11): 867-878.

Vos, Q., A. Lees, et al. (2000). "B-cell activation by T-cell-independent type 2 antigens as an integral part of the humoral immune response to pathogenic microorganisms." Immunol Rev **176**: 154-170.

Walker, B. D. and X. G. Yu (2013). "Unravelling the mechanisms of durable control of HIV-1." Nat Rev Immunol **13**(7): 487-498.

Watson, C. T., K. M. Steinberg, et al. (2013). "Complete haplotype sequence of the human immunoglobulin heavy-chain variable, diversity, and joining genes and characterization of allelic and copy-number variation." Am J Hum Genet **92**(4): 530-546.

Wei, X., J. M. Decker, et al. (2003). "Antibody neutralization and escape by HIV-1." Nature **422**(6929): 307-312.

Wei, Y., J. Feng, et al. (2015). "Flow cytometric analysis of circulating follicular helper T (Tfh) and follicular regulatory T (Tfr) populations in human blood." Methods Mol Biol **1291**: 199-207.

Weill, J. C., S. Weller, et al. (2009). "Human marginal zone B cells." Annu Rev Immunol **27**: 267-285.

Weisel, F. J., G. V. Zuccarino-Catania, et al. (2016). "A Temporal Switch in the Germinal Center Determines Differential Output of Memory B and Plasma Cells." Immunity **44**(1): 116-130.

Weiss, G. E., P. D. Crompton, et al. (2009). "Atypical Memory B Cells Are Greatly Expanded in Individuals Living in a Malaria-Endemic Area." Journal of Immunology **183**(3): 2176-2182.

Weller, S., M. C. Braun, et al. (2004). "Human blood IgM "memory" B cells are circulating splenic marginal zone B cells harboring a prediversified immunoglobulin repertoire." Blood **104**(12): 3647-3654.

Weller, S., A. Faili, et al. (2001). "CD40-CD40L independent Ig gene hypermutation suggests a second B cell diversification pathway in humans." Proc Natl Acad Sci U S A **98**(3): 1166-1170.

Weller, S., M. Mamani-Matsuda, et al. (2008). "Somatic diversification in the absence of antigen-driven responses is the hallmark of the IgM(+)IgD(+)CD27(+) B cell repertoire in infants." Journal of Experimental Medicine **205**(6): 1331-1342.

Werner, L., H. Guzner-Gur, et al. (2013). "Involvement of CXCR4/CXCR7/CXCL12 Interactions in Inflammatory bowel disease." Theranostics **3**(1): 40-46.

West, A. P., Jr., L. Scharf, et al. (2014). "Structural insights on the role of antibodies in HIV-1 vaccine and therapy." Cell **156**(4): 633-648.

Wheatley, A. K., A. B. Kristensen, et al. (2016). "HIV-dependent depletion of influenza-specific memory B cells impacts B cell responsiveness to seasonal influenza immunisation." Sci Rep **6**: 26478.

Wherry, E. J. (2011). "T cell exhaustion." Nat Immunol **131**(6): 492-499.

Wherry, E. J. and M. Kurachi (2015). "Molecular and cellular insights into T cell exhaustion." Nature Reviews Immunology **15**(8): 486-499.

Wilson, E. M. and I. Sereti (2013). "Immune restoration after antiretroviral therapy: the pitfalls of hasty or incomplete repairs." Immunological Reviews **254**(1): 343-354.

Wilson, T. J., A. Fuchs, et al. (2012). "Cutting Edge: Human FcRL4 and FcRL5 Are Receptors for IgA and IgG." J Immunol **188**(10): 4741-4745.

Wu, Y. C., D. Kipling, et al. (2010). "High-throughput immunoglobulin repertoire analysis distinguishes between human IgM memory and switched memory B-cell populations." Blood **116**(7): 1070-1078.

Xu, W., P. A. Santini, et al. (2009). "HIV-1 evades virus-specific IgG2 and IgA responses by targeting systemic and intestinal B cells via long-range intercellular conduits." Nat Immunol **10**(9): 1008-1017.

Yang, G., T. M. Holl, et al. (2013). "Identification of autoantigens recognized by the 2F5 and 4E10 broadly neutralizing HIV-1 antibodies." J Exp Med **210**(2): 241-256.

Yarchoan, R., R. R. Redfield, et al. (1986). "Mechanisms of B cell activation in patients with acquired immunodeficiency syndrome and related disorders. Contribution of antibody-producing B cells, of Epstein-Barr virus-infected B cells, and of immunoglobulin production induced by human T cell lymphotropic virus, type III/lymphadenopathy-associated virus." J Clin Invest **78**(2): 439-447.

Zhang, Y., L. Garcia-Ibanez, et al. (2016). "Regulation of germinal center B-cell differentiation." Immunol Rev **270**(1): 8-19.

Zinkernagel, R. M. (1996). "Immunology taught by viruses." Science **271**(5246): 173-178.

Zonios, D., V. Sheikh, et al. (2012). "Idiopathic CD4 lymphocytopenia: a case of missing, wandering or ineffective T cells." Arthritis Res Ther **14**(4): 222.

Zotos, D., J. M. Coquet, et al. (2010). "IL-21 regulates germinal center B cell differentiation and proliferation through a B cell-intrinsic mechanism." J Exp Med **207**(2): 365-378.

Zwick, M. B., A. F. Labrijn, et al. (2001). "Broadly neutralizing antibodies targeted to the membrane-proximal external region of human immunodeficiency virus type 1 glycoprotein gp41." J Virol **75**(22): 10892-10905.

11. Acknowledgements

I would like to thank my supervisor Prof. Dr. Alexandra Trkola for the opportunity to pursue my PhD in her laboratory and for her great support during these 5 years. My PhD went very unexpected paths but opened the exciting world of multi-dimensional single cell analysis and computational analysis to me. I am very thankful for the freedom and the encouraging support I got from Prof. Dr. Alexandra Trkola to go this path and find the passion for flow cytometry.

I thank Claus Kadelka for his support in Statistics and all the interesting discussions about high-dimensional analysis. Your curiosity is a remarkable attitude and I enjoyed working with you.

Much time has passed since I started my PhD. Many people left, new people started and it becomes hard to keep track. I would like to thank Lucy Reynell. You introduced my very well into the lab work 5 years ago and I felt very welcome.
In addition, I would like to thank all the members of the lab for the great working atmosphere. I had the joy to work with some of you in the lab and I would like to mention and thank Therese, Jacqueline, Nikolas and Emanuel for the great support.

In addition, I would like to thank Huldrych, Dominique, Christina and Herbert from the University Hospital. Your uncomplicated support, work and the access to very valuable patient samples improved my studies a lot. Thank you! In this respect, I would also like to thank the patients. Your contribution is essential for our work!

Spending so much time together brings people together. In this respect I would like to thank especially David, Emanuel, Matteo, Olli, Matthias and Nikolas for the great time and the many good memories including Applesnail, Movie nights, board games and many more… I hope to keep in touch with you!

I had the pleasure to work in the Flow Cytometry Facility of the University of Zurich. I would like to thank Cornelius, Flo, Vinko, Christina, Philipp and Claudia for the great atmosphere. With you I could share my interest in Flow cytometry and many more.

A big “thank you” goes to my parents. Your almost infinite support made this thesis possible. I hope that we can be as good parents for Anna as you were and are for me.

I would like to thank my wife Andrea. Your support, patience and understanding was beyond everything what I could expect. You are the best! Thank you so much!

Ultimately, I would like to thank my daughter Anna. I never thought that something wonderful like you will happen during my PhD. I have the joy to be a part of your life which makes me happier than anything else. You are my sunshine and seeing you laughing and growing up fulfills my life with pure joy (…except when you want to play at 3 o’clock in the morning…).

12. Curriculum Vitae

GENERAL INFORMATION

Surname:	Liechti
Name:	Thomas Andreas
Date of birth:	24.07.1985
Place of origin:	Landiswil, Switzerland

EDUCATION

2001-2004	Trainee as laboratory technician Institute of Medical Virology, University of Berne, Switzerland
2005	Federal Vocational Baccalaureate Berne, Switzerland
2006-2009	Bachelor of Science in Pharmaceutical Biotechnology University of Applied Sciences Zürich, Wädenswil, Switzerland
2009-2011	Master of Science in Microbiology and Immunology University of Berne, Switzerland Master thesis: The impact of IgD on allergy Supervised by Prof. Dr. Clemens Dahinden
2011-present	Ph.D. in Microbiology and Immunology Institute of Medical Virology, University of Zürich, Switzerland Supervised by Prof. Dr. Alexandra Trkola

RELATED EXPERIENCE

2014-2016	Operator Fluorescence-activated cell sorting, (workload 10%)
	Flow Cytometry Facility, University of Zürich

POSTER AND ORAL PRESENTATIONS

2013	*Poster*, Swiss Virology Meeting, Thun, Switzerland
2015	*Poster and talk*, Keystone Meeting HIV Vaccines, Banff, Canada
2015	*Talk*, xMAP Connect Luminex Meeting, Amsterdam, Netherlands
2016	*Poster*, CYTO Meeting, Seattle, USA

PUBLICATIONS

Zimmermann K, **Liechti T**, Haas , Rehr M, Trkola A, Günthard HF, Oxenius A. (2015) The orientation of HIV1 gp120 binding to the CD4 receptor differentially modulates CD4+ T cell activation. J Immunol, 194(2):637-49

Schanz M, **Liechti T**, Zagordi O, Miho E, Reddy ST, Günthard HF, Trkola A, Huber M. (2014) High-throughput sequencing of human immunoglobulin variable regions with subtype identification. PLOS One, 9(11):e111726